Dissertations, Theses, and Masters Projects   Theses, Dissertations, & Master Projects

1994

Physical and mechanical behavior of amorphous poly(arylene ether-co-imidazole)s and poly(arylene ether-co-imidazole) modified epoxies

Patricia D. Roberts-McDaniel

College of William & Mary - Arts & Sciences

Recommended Citation

Roberts-McDaniel, Patricia D., "Physical and mechanical behavior of amorphous poly(arylene ether-co-imidazole)s and poly(arylene ether-co-imidazole) modified epoxies" (1994). *Dissertations, Theses, and Masters Projects.* Paper 1539623850.
https://dx.doi.org/doi:10.21220/s2-aebd-6g98

INFORMATION TO USERS

This manuscript has been reproduced from the microfilm master. UMI films the text directly from the original or copy submitted. Thus, some thesis and dissertation copies are in typewriter face, while others may be from any type of computer printer.

The quality of this reproduction is dependent upon the quality of the copy submitted. Broken or indistinct print, colored or poor quality illustrations and photographs, print bleedthrough, substandard margins, and improper alignment can adversely affect reproduction.

In the unlikely event that the author did not send UMI a complete manuscript and there are missing pages, these will be noted. Also, if unauthorized copyright material had to be removed, a note will indicate the deletion.

Oversize materials (e.g., maps, drawings, charts) are reproduced by sectioning the original, beginning at the upper left-hand corner and continuing from left to right in equal sections with small overlaps. Each original is also photographed in one exposure and is included in reduced form at the back of the book.

Photographs included in the original manuscript have been reproduced xerographically in this copy. Higher quality 6" x 9" black and white photographic prints are available for any photographs or illustrations appearing in this copy for an additional charge. Contact UMI directly to order.

Physical and mechanical behavior of amorphous poly(arylene ether-*co*-imidazole)s and poly(arylene ether-*co*-imidazole) modified epoxies

Roberts-McDaniel, Patricia D., Ph.D.

The College of William and Mary, 1994

Physical and Mechanical Behavior

of Amorphous Poly(arylene ether-co-imidazole)s

and

Poly(arylene ether-co-imidazole)

Modified Epoxies

A Dissertation

Presented to the Program of

Applied Science

The College of William and Mary in Virginia

In Partial Fullfillment

Of the Requirements for the Degree of

Doctor of Philosophy

---

by

Patricia D. Roberts-McDaniel

1994

Approval Sheet

This dissertation is submitted in partial fulfillment of

the requirements for the degree of

Doctor of Philosophy

Patricia D. Roberts - McDaniel

Patricia D. Roberts-McDaniel
Author

Approved, May 1994

R. A. Orwoll, Director of Dissertation

J. W. Connell, Director of Research

T. L. St. Clair, Adjunct Faculty of Applied Science

D. M. Manos, Director of Applied Science

D. W. Thompson, Professor of Chemistry

ii

Table of Contents

List of Tables

List of Figures

.

Abstract

Due to the high crosslink density of cured epoxy resins they generally lack damage tolerance. A significant amount of research has been expended to improve the toughness of epoxies. Research into the area of thermoplastic epoxy modifiers has begun to overcome some of the limitations of early methods of epoxy toughening (i.e. lower modulus and thermal stability).

This study examines the physical and mechanical properties of random poly(arylene ether-co-imidazole) (PAE-co-Is) and the characterization of epoxies modified with poly(arylene ether-co-imidazole)s.

Poly(arylene ether-co-imidazole)s exhibited the highest solubility in N,N,N',N',-tetraglycidyl-4,4'diaminodiphenyl methane (TGMDA) based resins. The high molecular weight polymers caused significant decreases in melt flow behavior of the modified systems. Modification of TGMDA resins with PAE-co-Is significantly decreased the tetrahydrofuran sensitivity of the cured system and did not significantly affect the moisture absorption properties. One system modified with 10% w/w polymer exhibited increases in fracture toughness 1.7 times that of the unmodified system.

Physical and Mechanical Behavior

of Amorphous Poly(arylene ether-co-imidazole)s

and

Poly(arylene ether-co-imidazole)

Modified Epoxies

Chapter 1: Introduction

Thermosetting materials based on epoxy chemistry were among the first synthetic resin systems developed for use as coatings, adhesives and composite matrices[1]. Epoxies offer certain advantages over other materials such as low density, tack, drape, processability, low cost and, once cured, high glass transition temperatures (Tg), and good mechanical properties. Epoxy chemistry is based on the reaction of an oxirane (epoxy) group with a nucleophile (curing agent) such as an amine. The reaction of a diepoxy compound and a primary diamine leads to the formation of a complex highly-crosslinked polymer network.

One area of interest is the use of thermosetting materials in composites. Fiber reinforced organic composites for aerospace structural applications offer advantages over metals, such as higher strength-to-weight ratios, improved fatigue characteristics, corrosion resistance and higher stiffness (modulus). As a result newly constructed commercial and military aerospace vehicles contain ever increasing amounts of composites. The use of advanced composites is expected to grow to about 45-million kg (100 million lb) by the year 2000, with 80% of the total matrix resin systems being comprised of epoxy resins[2].

In the cured state, epoxy resins are highly crosslinked, amorphous thermoset polymers which possess excellent thermal and dimensional stability,

high modulus and strength, and outstanding adhesive properties[3,4]. However, due to the high crosslink density of the cured epoxies they generally lack damage tolerance, (i.e., they are brittle).   A significant amount of research has been expended to improve the toughness of epoxies.   Several methods have been proposed to improve the toughness of modified epoxy resins, the most common is incorporation of a second phase component such as a rubber. The toughness of a modified epoxy resin is dependent on the original resin matrix, second phase particle size, particle volume fraction, interfacial bonding, and the properties of the rubbery component. Modification of epoxy resins by incorporation of functionalized rubbers is the most widely used method to improve damage tolerance. The rubbery particles become dispersed in and bonded to the epoxy matrix. However, the inherently low Tg of the rubber often lowers both the use temperatures and some of the mechanical properties of the resulting network. The resin modulus is most notably sacrificed when rubber-toughening is employed.

Research into the area of thermoplastic epoxy modifiers has begun to overcome some of the limitations of rubber modified systems. Thermoplastic modifiers offer good thermal stability, toughness, and high glass transition temperatures. Incorporation of thermoplastic oligomers with functionalized groups has led to systems with increased fracture toughness without sacrificing the high-modulus or thermal stability of the network[5,6].

1.1 References

1. Lee, H.; Neville, K.; in, Ency. of Polym. Sci. and Tech., *6*, 209-271, **1967**.

2. Kubel Jr., E. J.; *Adv. Materials & Processes*, *136*(2) **1989**.

3. Potter, W. G., Epoxide Resins, Springer-Verlag, New York, **1970**.

4. May, C. A. and Tanaka, G. Y., Eds. Epoxy Resin Chemistry and Technology, Marcel Dekker, New York, **1973**.

5. Diamont, J.; Moulton, R. J., *SAMPE Quarterly*, *16*(1), 13-21, **1984**.

6. Bauer, R. S.; Stenzenberger, H. D.; Romer, W., *SAMPE*, April 2-5, 395-407, **1990**.

Chapter 2: Statement of Research

The goals of this research are to examine the physical and mechanical properties of random poly(arylene ether-co-imidazole)s (PAE-co-I) and the characterization of epoxies modified with PAE-co-I oligomers and polymers. These systems should possess the advantages over the commercial resins of increased fracture toughness and the possibility of combining the high rigidity and ease of processing of the epoxy with the toughness of the PAE-co-I.

The work required to meet the research goal included the synthesis and chemical characterization of a variety of PAE-co-I polymers and oligomers of differing chemical structures, molding, curing and fabrication into test specimens, and finally physical and mechanical characterization of the resulting thermoplastics and thermosets.

A great deal of research has been reported on poly(arylene ether)s (PAE)[1-21] and poly(arylene ether)s containing imidazole groups in the polymer backbone[22-25]. Nucleophilic aromatic displacement of bis(imidazole phenolates) with an activated aromatic dihalide was utilized to synthesize a variety of high molecular weight poly(arylene ether-co-imidazole)s.

The highly aromatic rigid and highly polar structure of the poly(arylene ether imidazole) lead to inherently high glass transition temperature, thermal stability,

mechanical properties and good processability. The arylene ether unit should impart toughness to the blends while the reactivity of the imidazole moiety with the oxirane ring of the epoxy allows for control of the distance between crosslinks of the modified system. The effective distance between crosslinks is lessened than when using shorter reactive thermoplastic oligomers. Therefore, it is postulated that if the PAE and PAEI could be combined properly, the new material could serve as an epoxy resin toughening agent that would impart toughness and improved mechanical properties to the thermoset without decreasing its Tg or thermal stability.

The literature review presented below summarizes some of the basic principles of mechanics of materials as well as the theories behind mechanical behavior of polymers. Background information on epoxy resin chemistry is also included in the literature review as well as reviews on epoxy resin tougheners, and poly(arylene ether imidazole)s (PAEI).

2.1 References

1.	Kreuchmas, A., U.S. Patent 2,2822,351 **1958.**

2.	Bonner, W. H., U.S. Patent 3,065,205 **1962** (to Dupont).

3.	Marks, B. M., U.S. Patent 3,441,538 **1969.**

4.	Colquhoun, H. W. and Lewis, D. F., British Patent 2,116,990 **1983.**

5. '	Jansons, V., U.S. Patent 4,361,693 **1982.**

6.	Dahl, K. J., U.S. Patent 3,956,240 **1976.**

7.	Jansons, V., Gors, H. C., *WO*, 84 03, 892 **1984.**

8.	Effenberger F. and Epple, *G. Angew. Chem. Int. Ed.*, *11*, 299, **1972.**

9.	Goodman, I, McIntyre, J. E. and Russell, W., British Patent 971,227 **1964.**

10.	Allinger, N. L., Cava, M. P., DeJongh, D. C., Johnson, C. R., Lebel, N. A., Stevens, C. L., Organic Chemistry, 2nd ed., Worth Publishers, Inc., New York, **1976.**

11.	Jennings, B. E.M Jones, M. E. B., Rose, J. B., *J. Polym. Sci. Part C.*, 715, **1967.**

12.	Rose, J. B., *Chem. Ind. (London)*, 461, **1968.**

13.	Johnson, R. N., Farnham, A. G., Clendinning, R. A., Hale, W. F., Merriam, C. N., *J. Polym. Sci. Part A-1*, *5*, 2375 **1967.**

14.	Johnson, R. N., Farnham, A. G., British Patent 1,078,234 **1967.**

15.	Johnson, R. N., Farnham, A. G., U.S. Patent 4,108,837 **1978.**

16.	Taylor, I. C., German Patent 2,635,101 **1977.**

17.	Gerd, B. Claus, C., German Patent 2,749,645 **1978.**

18.	Viswanathan, R., Johnson, B. C., McGrath, J. E., *Polymer*, *25*, 1827, **1984.**

19. Mohanty, D. K., Sachdeva, Y., Hedrick, J. L., Wolfe, J. F., McGrath, J. E., *Polym. Prepr.*, *25*(2), 19, **1984**.

20. Jensen, B. J., Hergenrother, P. M., Havens, S. J., *Polym. Prepr.*, *26*(2), 174, **1985**.

21. Hergenrother, P. M., Havens, S. J., Jensen, B. J., *Intl. SAMPE Tech. Conf. Series*, *18*, 454, **1986**.

22. Connell, J. W.; Hergenrother, P. M., *Polym. Mat. Sci. and Eng. Proceedings*, *60*, 527-531, **1989**.

23. Connell, J. W.; Hergenrother, P. M., *High Performance Polymers*, *2*(4), **1991**.

24. Connell, J. W.; Hergenrother, P. M., *J. Polym. Sci. Part A: Polymer Chem.*, *29*, **1990**.

25. Connell, J. W.; Hergenrother, P. M., *SAMPE Series*, *35*, 432, **1990**.

Chapter 3: Literature Review

3.1 Epoxy Resin Chemistry

The first commercial epoxy resin formulations were based on the reaction products of epichlorohydrin and bisphenol A to form a diglycidyl ether of bisphenol A (DGEBA). The formation of DGEBA is a two step reaction where: (1) a chlorohydrin intermediate is formed and (2) dehydrohalogenation of the intermediate to the glycidyl ether takes place (Figure 3.1). The sodium hydroxide catalyzes the formation of the chlorohydrin intermediate, serves as the dehydrohalogenating agent, and neutralizes the hydrochloric acid formed.

Because of the low cost and ready availability of phenol, acetone, propylene and chlorine, the raw materials used to synthesize bisphenol A and epichlorohydrin, bisphenol A type resins have been used extensively in composites. However, their uses are limited by an inherently low glass transition temperature (Tg).

A highly crosslinked system comprised of thermally stable coreactants is necessary to obtain optimum heat resistance. However, as a general rule the brittleness of a system is directly correlated to the degree of crosslinking. Therefore, as the thermal stability and Tg due to structural crosslinking increases, the flexibility of the system decreases[1].

An increase in crosslink density, and therefore, a higher Tg can be achieved
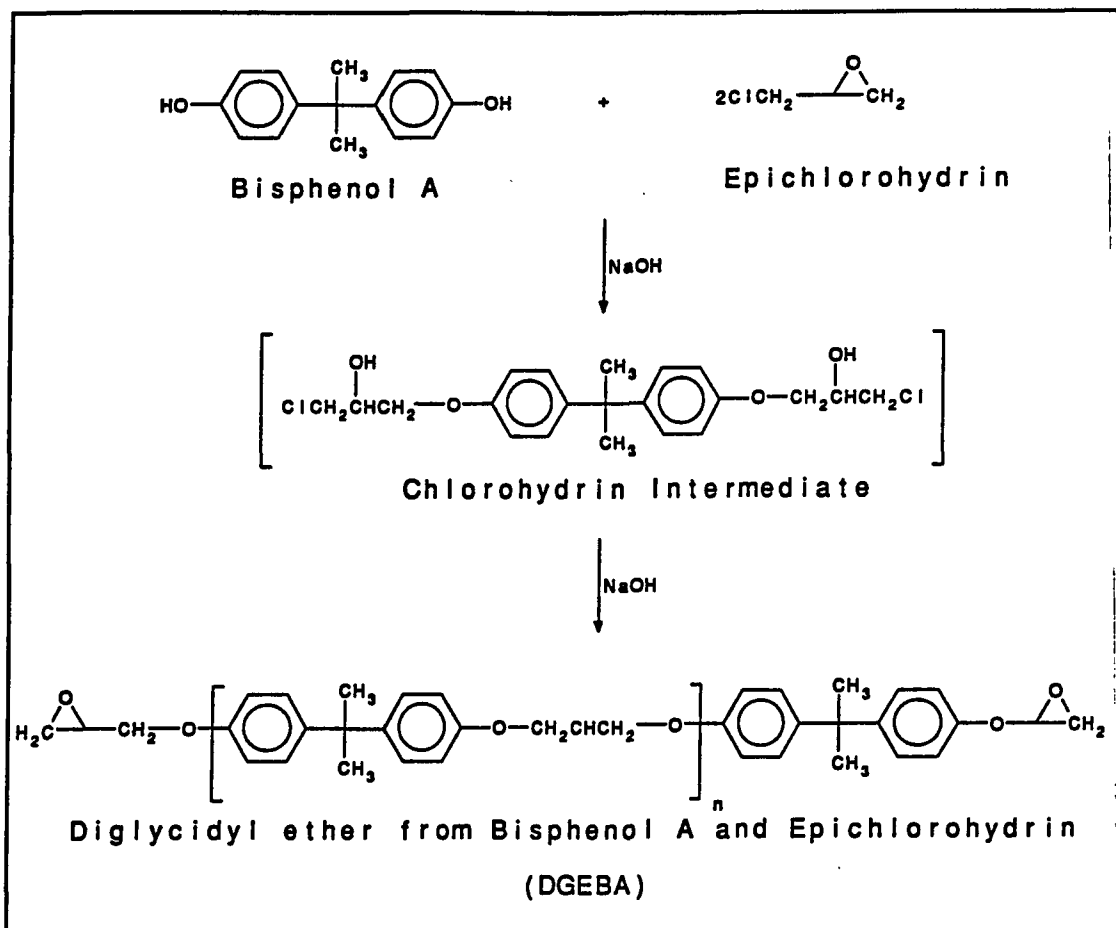
Figure 3.1 Synthesis of DGEBA

by employing a resin component of greater functionality. High Tg, high performance epoxies are generally based on a multifunctional aromatic backbone. TGMDA-diamino diphenyl sulphone based systems demonstrated the highest modulus (E) and glass transition temperature among the early epoxies[2]. This epoxy/curing agent combination has served as the basis for almost all epoxy

formulations used for advanced composites over the last 15 to 20 years. The first system to meet the requirements of the aerospace industry and the epoxy resin most often used in advanced composites is based upon N,N,N',N'-tetraglycidyl-4, 4'-diaminodiphenyl methane (TGMDA). Figure 3.2 illustrates an idealized synthetic scheme for TGMDA[3].
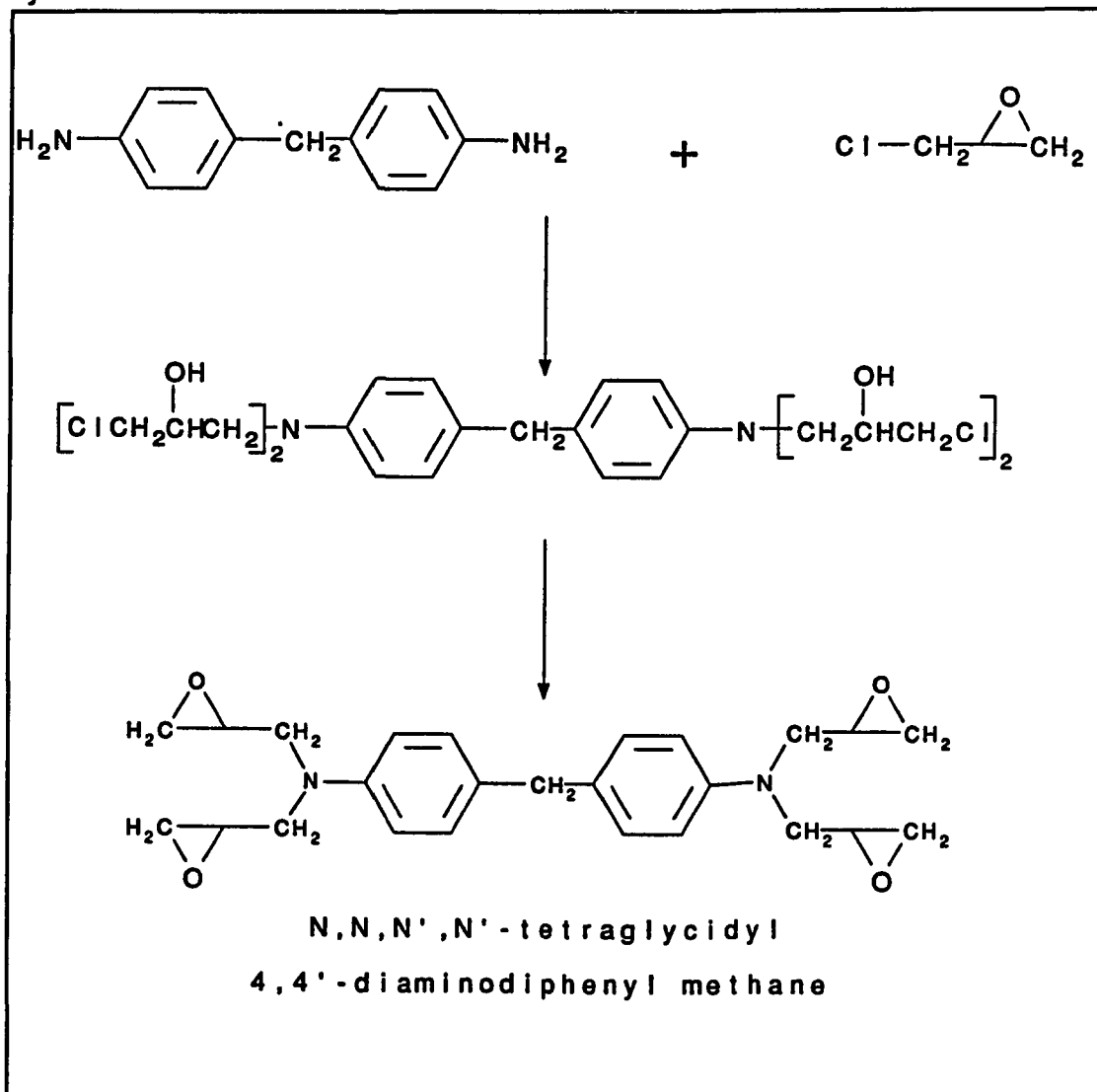
Figure 3.2 Synthesis of TGMDA

As early as 1970 it was discovered that the incorporation of a rigid aromatic structure into the backbone of a thermoplastic polymer imparted improved thermal stability and increased Tg's[4]. This observation has led to the development of epoxy resins based on the cardo group (i.e., fluorene), which offers improved high temperature properties, ductility, and very low moisture absorption due to the hydrophobic nature of the fluorene group. Based on these characteristics, research into further improvements on the mechanical properties using the diglycidyl ether of 9,9'-bis(4-hydroxyphenyl)fluorene resin (DGEHF) are currently being pursued. The structure for DGEHF is given in Figure 3.3, and its properties are compared to TGMDA and DGEBA in Table 3.1.
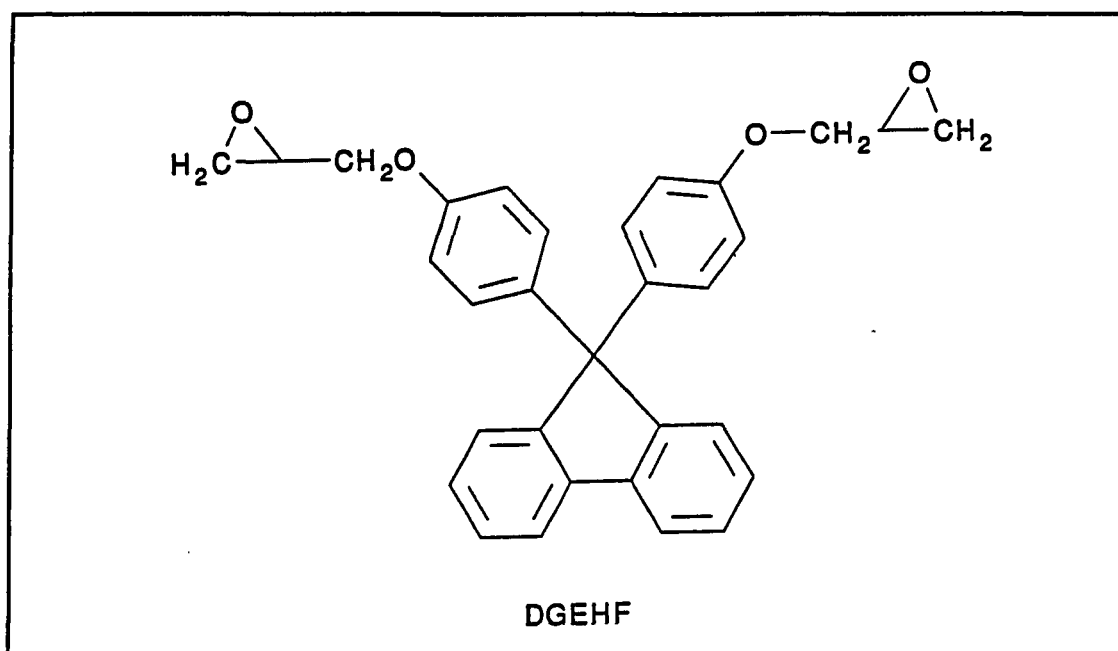
DGEHF

Figure 3.3 Diglycidyl-9,9'-bis(4-hydroxyphenyl)fluorene (DGEHF)

Table 3.1 Properties of DGEHF, TGMDA and DGEBA[5]

	DGEHF[a]	TGMDA[b]	DGEBA[c]
Tg(tan δ), °C	246	177	177
% Moisture[d]	2.8	5.7	3.4
Flex (RT/dry) Strength (ksi)	20	13	17
Flex (RT/dry) Modulus (ksi)	559	500	390
Flex (hot/wet)[e] Strength (ksi)	11	4.5	**
Flex (hot/wet)[e] Modulus (ksi)	361	277	**

a) Cure: 2 hrs @ 150 °C; 4 hrs @ 204 °C
b) Cure: 2 hrs @ 80 °C; 1 hr @ 100 °C; 4 hrs @ 150 °C; 7 hrs @ 200 °C
c) Cure: 1 hr @ 120 °C; 2 hrs @ 177 °C
d) 48 hours water boil
e) tested at 93 °C after 2 weeks immersion at 93 °C

3.2 Epoxy Curing

Epoxy resin systems are reactive intermediates that are converted into three dimensional networks by crosslinking with a curing agent. Many different functional groups can react with the epoxy moiety to form crosslinked systems. The basic curing agents employed in the epoxy resin technology fall under the

catagories of Lewis acids, inorganic bases, primary and secondary amines and amides[6]. Amines serve as the primary curing agent for industrial usage.
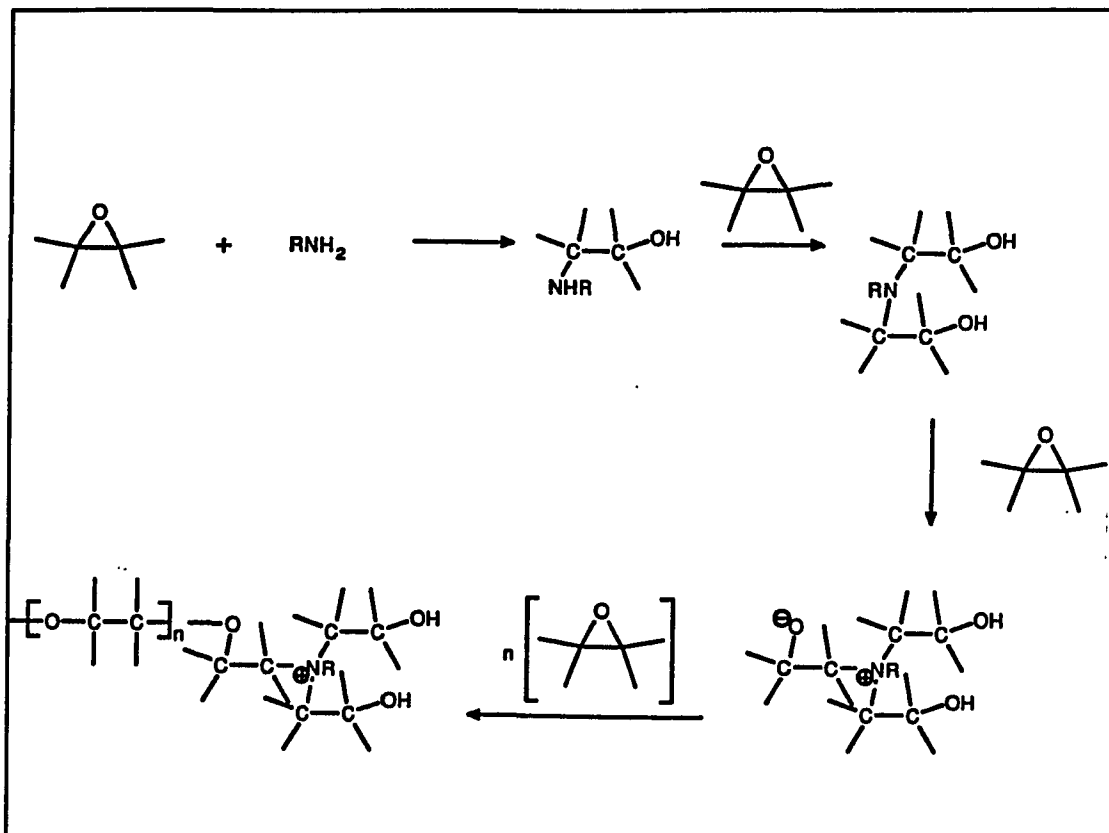
Figure 3.4 General reaction of an amine with an epoxy

The curing of epoxies with amines is represented in Figure 3.4[7,8]. The primary amine reacts with the epoxy to form the secondary amine which reacts with another epoxy to form a tertiary amine which then reacts with a third epoxy molecule to form a stable quarternary amine. This species is able to initiate homopolymerization of epoxy functionalities. With excess epoxide functionalities,

the hydroxyl groups of the zwitterion can react further to form products of higher molecular weight through chain branching and crosslinking (Figure 3.5). Hydroxy catalyzed reactions are observed only in cases where less than stoichiometric quantities of epoxy to amine groups are employed. Epoxy groups have been shown to react with the formed hydroxyl groups only after the amine hydrogens are consumed[9].
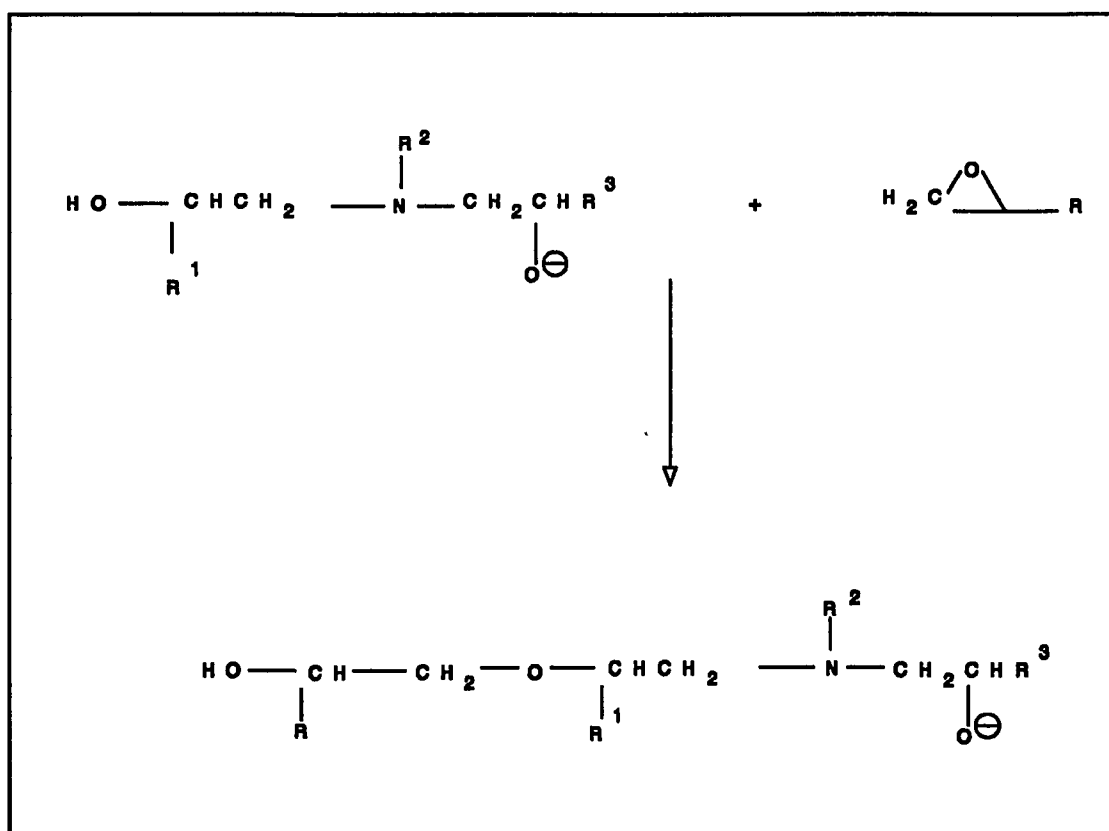
Figure 3.5 Epoxy reaction with hydroxyl group

As shown in Figure 3.6, the polymerization can terminate in several different ways, the most probable involves the decomposition of the quarternary ammonium salt under the influence of an alkoxide ion and heat to produce an olefin, a tertiary

amine and an alcohol via Hoffman elimination (reaction I). Dealkylation of the

quarternary amine complex by an adjacent alkoxide ion is also a probable route

(reaction II), along with the quarternary amine reacting with an alcohol to form an

ether and a tertiary amine[10] (reaction III).
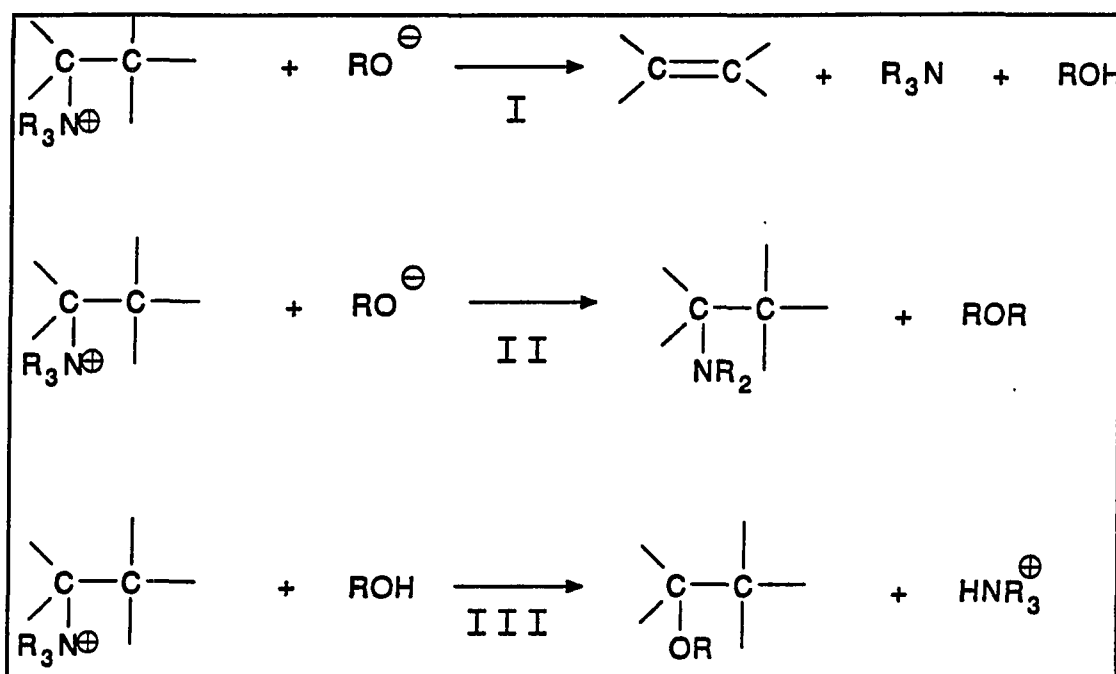
Figure 3.6 Termination of epoxy cure reaction

The structures given in Figure 3.7 represent some typical amine curing

agents. The curing agent studied with many model systems has been 4,4'-

diaminodiphenyl sulphone (DDS). 4,4'-diaminodiphenyl methane (MDA) and m-

phenylene diamine (MPA) have also been widely used in commercial products;

however, their use is declining because of their highly carcinogenic nature.

Research into resin matrices with improved hot\wet properties and ease of
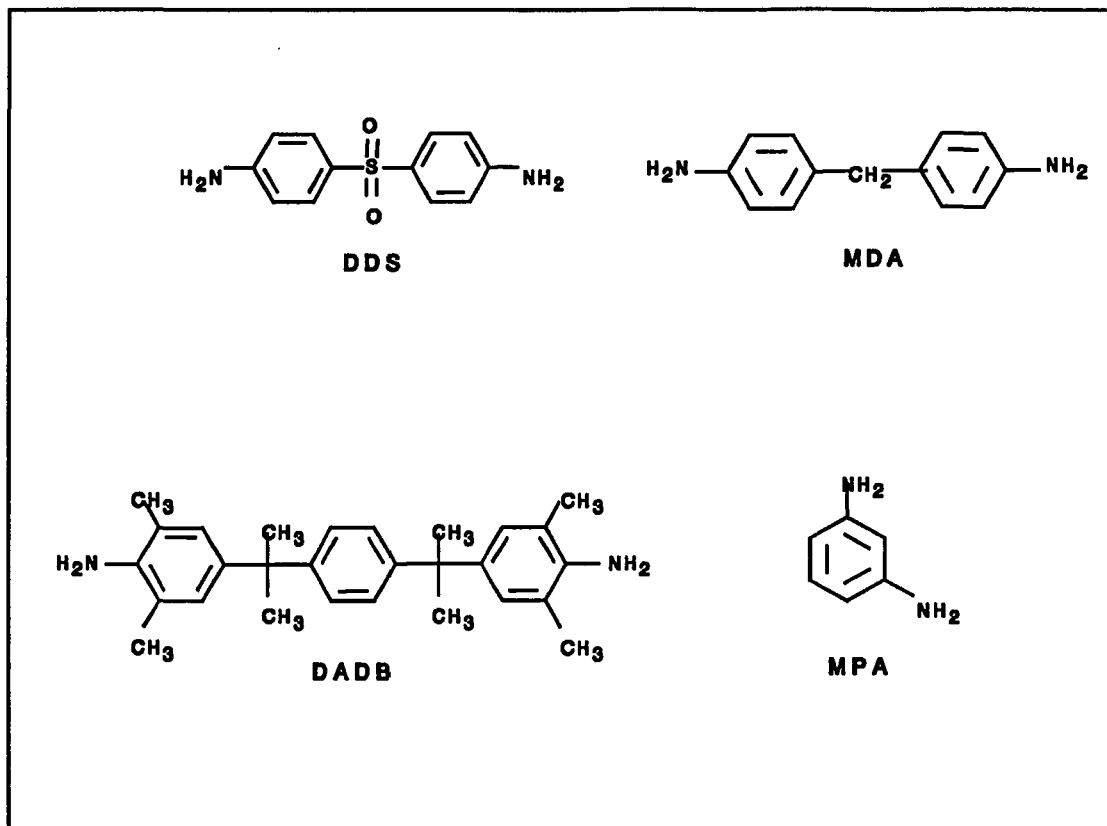
Figure 3.7 Typical Amine Curing Agents

processability has brought about improved curing agents for use with high performance epoxy resins. The aromatic diamine, α,α'-bis(3,5-dimethyl-4-aminophenyl)p-diisopropylbenzene (DADB) provides improved properties for many epoxy systems.

Imidazoles also cure epoxies, as illustrated in Figure 3.8. The first step in the imidazole polymerization is opening of the oxirane ring by reaction with the NH group of the imidazole ring. A second mole of epoxy then adds to the second ring nitrogen to form an equilibrium mixture, where the hydroxyl proton is undergoing rapid exchange. This alkoxide ion is an effective catalytic center, which can attack
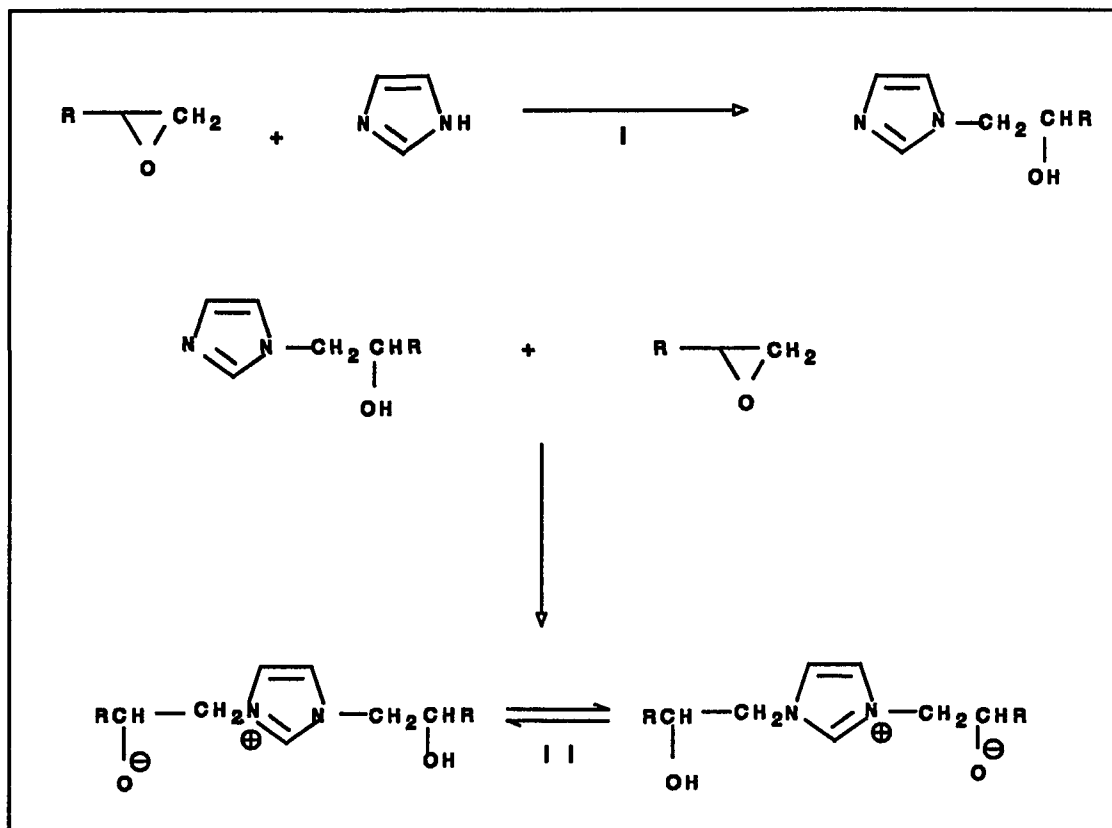
Figure 3.8 General reaction of an imidazole with an epoxy

another epoxy group and continue the polymerization reaction (Figure 3.9).

By this sequence the imidazole becomes part of the polymer, maintains its catalytic activity, and can cause extensive chain branching which leads to a highly crosslinked resin[11].
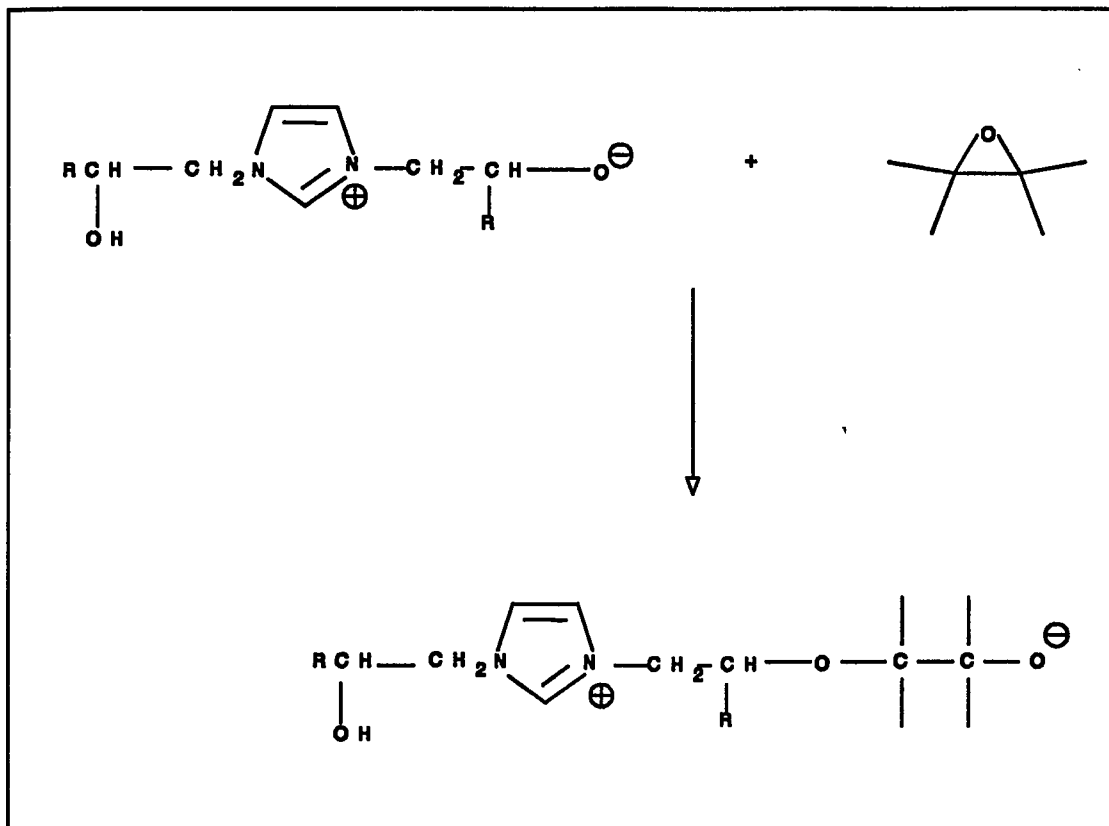
Figure 3.9 Reaction of an epoxy with an imidazole

3.3 Mechanical Properties of Polymers

The assessment of material strength and the need to determine the point of sudden or catastrophic failure is required for an ever increasing range of applications. A high ultimate strength has been obtained for many materials. However, the relatively low average strength of a material can be due to the presence of cracks or atomic deformation processes which nucleate cracks.

3.3.1 Fracture Behavior of Polymers

Fracture is an inhomogeneous deformation process where a crack passes through a region of the material. This creates a separation in the material and causes the load carrying capacity to decrease to zero. The critical stress intensity factor, K_c, represents the limit of a material where the crack becomes unstable. When the applied stress corresponds to plane strain conditions K_c becomes K_{Ic} may be determined. The subscript changes to IIc or IIIc depending on the direction of the stresses responsible for the crack opening. The crack extension force per unit length of crack is denoted by the parameter G. At the point of instability it becomes G_c. The relationship between K_c and G_c is approximated by the following equation[12] where E is the modulus:

$$K_c^2 \sim E\,G_c \qquad (3.1)$$

This approximation becomes exact under conditions of plane stress with entirely shear fracture which is perpendicular to the specimen faces, the plane strain critical stress intensity factor is given in equation 3.2:

$$K_{Ic}^2 = \frac{E\,G_{Ic}}{(1-v^2)}$$

(3.2)

Failure of a material takes place through the mode which requires the least amount of local strain at the tip of the advancing crack.

In addition to fracture there are two types of deformation in glassy and rubbery polymers: elastic and plastic deformation. Elastic deformation is recoverable in a finite period of time while plastic deformation which encompasses shear yielding, crazing and void formation is irrecoverable[13,14].

3.3.2 Deformation Behavior of Polymers:

Elastic behavior of polymers takes place through deformation of the structure on the molecular level. It is the dominant mechanism in isotropic polymer glasses where the amorphous material is frozen in the structure, coiled and randomly oriented. Here deformation is controlled by the internal energy of the polymer with elastic deformation in high modulus polymers taking place through higher energy forces of bending and stretching of the polymer backbone[15].

Elastic deformation in the rubbery state allows the coiled polymer chains to

reversibly translate past each other[16]. Elastic deformation of the polymer reduces the conformational entropy of the polymer chain, as the chains uncoil there are fewer conformations available and release of the stress allows the chain to increase entropy by returning to the uncoiled state. Since the deformation of a rubber is controlled by entropic changes instead of the internal energy forces of isotropic glasses or high modulus polymers, the equilibrium modulus increases with increasing temperature. In the case of crosslinked polymers, the equilibrium modulus of a rubber is given in equation 3.3[14]:

$$\zeta = \frac{\rho_d RT}{M_c} \tag{3.3}$$

where ρ_d is the density of the rubber, R is the molar gas constant and M_c is the average molar mass between crosslinks. Therefore, as the crosslink density of the rubber increases, the modulus increases.

3.3.2.1 Shear Yielding

Yielding is a plastic deformation under an applied stress while shear deformation is a permanent change in the specimen without a change in volume. Shear yielding, a deviatoric process, is an important mechanism in polymer fracture for two reasons. First, if brittle fracture can be suppressed, shear yielding

limits the ultimate strength of the polymer. Second, under plane strain conditions if brittle fracture cannot be suppressed, shear yielding is the major energy dissipating process in the vicinity of the crack tip, in the form of localized shear band formation[13,14,17]. This serves to increase tougheness by blunting the sharp crack tip.

One suggestion on the molecular theory of yielding is that under applied stress the mobility of the molecular chains increases until they are fully mobile allowing plastic flow to occur at yield. This reduces the Tg until the Tg at yield is equivalent to the test temperature[18,19]. Although there is translation of molecules past one another during deformation, they are anchored at entanglements which are not broken. Annealing the polymer above Tg returns it to its original conformation when there is sufficient mobility.

3.3.2.2 Crazing

The appearance of what seems to be small microcracks in stressed thermoplastics is known as crazing. Crazing or bridged microcracking is a cavitation process caused by the high hydrostatic stresses which are formed near a crack tip. It results in an increase in specimen volume. The cavitation produces a thin sheet of microvoids normal to the applied load, usually within the plane of fracture (Figure 3.10[20]). They typically migrate normal to the direction of the applied stress and reflect light, thus the stress-whitening in plastically deformed

thermoplastics.
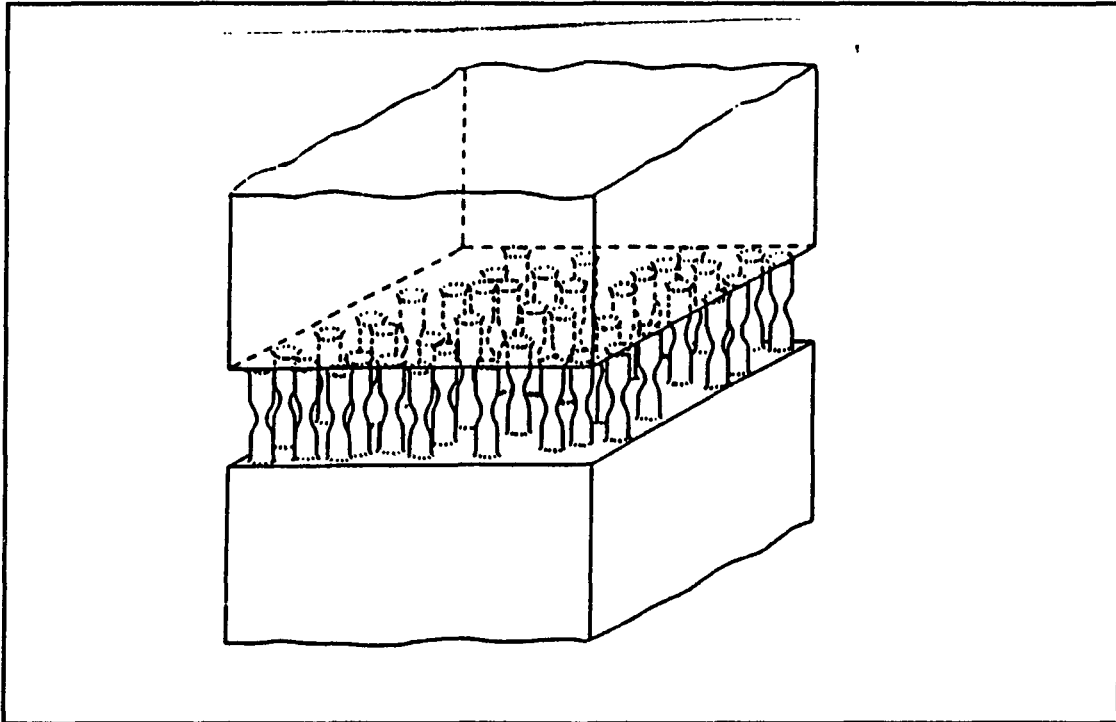
Figure 3.10 Cavitations, voids and fibrils produced from crazing

These voids lead to crack formation when the fibrils reach their maximum extension. As a sufficient number of microvoids combine, the crack grows and can ultimately lead to fracture when stressed. Crazes however differ from cracks in that they are load-bearing entities due to microfibrils stretched across the span of the area that would otherwise be considered a crack[21]. The ability of a craze to bear a load allows them to grow adjacent to each other as though the other were not there. A crack, on the other hand, tends to propagate towards and terminate perpendicular into the neighboring crack which ultimately leads to failure[17,22,23]. In multi-phase systems multiple crazing leads to general yielding and acts as a toughening mechanism. Crazing can be suppressed by lowering the yield stress

through an increase in temperature or pressure, which counterbalances the hydrostatic tensile stress[24,25].

Cracks propagate with crazes at their tips and molecular entanglements play an important role in controlling the geometry of crazing. The large extension ratios of the fibrils in the vicinity of a craze can only be achieved through interaction on the molecular level (i.e. chain scission or disentanglement of entangled polymer chains[26]).

Shear banding and crazing are considered competitive processes. A shear band is a thin planar region of high shear strain. Shear bands are initiated in areas where inhomogeneities of strain exist. These inhomogeneities may be due to internal or surface flaws, or to stress concentrators. Polymers with low yield stresses usually yield by shear banding before the critical hydrostatic stress for crazing is reached.

3.3.3 Deformation in Multiphased Systems

Combining adequate ductility through plasticization while maintaining strength leads to blunting of propagating cracks and improved fracture behavior. Ductile fracture can be promoted in a glassy polymer through plasticization by a low molecular weight liquid which serves to lower the material's yield stress, but this also lowers the Tg and modulus of the polymer. Incorporation of a second phase of dispersed rubbery particles into a matrix polymer toughens by providing

localized energy absorbing mechanisms such as crazing and shear yielding. This involves the entire sample, not merely the region at the immediate crack tip.

Several mechanisms have been proposed for the increased toughness observed in such multiphase systems. These include: particle deformation, crazing, shear yielding, simultaneous crazing with shear yielding, and voiding. Kunz and co-workers[27,28] have proposed a particle deformation toughening mechanism for rubber-toughened epoxies where the rubber particles are considered to bridge a crack as it propagates through the material[27]. They developed a quantitative model in which the toughness was equated to a simple rule of mixtures:

$$G_{Ic}(system)(1-\upsilon_{fp}) + \Delta G_{Ic}(rubber) \ (\upsilon_{fp}) \qquad (3.4)$$

where G_{Ic} is the fracture energy of the matrix system, υ_{fp} is the volume fraction of the rubber particles, and $G_{Ic}(rubber)$ is the toughening contribution from the rubber particles. Here the increase in toughness is expressed in terms of the amount of elastic energy stored in the rubber particles during the stretching which is irreversibly dissipated upon rupture. The model agrees somewhat with observations; however, it does not adequately explain the stress whitening or the large amount of plastic deformation observed in most rubber-toughened epoxy resins[29,30,31,32]. Therefore, it was hypothesized that, although ligaments of rubber spanning a crack serve to reduce the stress concentration at the crack tip, this mechanism is only of secondary importance to the increased toughness of

multiphase systems[33].

Shear yielding, a major mechanism in the fracture of single phase polymers can be greatly enhanced by the presence of a second particulate phase, especially if it is rubbery. Haaf et al.[34] and Donald and Kramer[35] concluded that the dispersed rubber phase initiates microshear bands which could explain the observed stress whitening in modified epoxy systems. This also suggests that multiple shear yielding deformations accompanied by the initiation of cavities could occur without crazing.

Many toughened polymers exhibit multiple deformation mechanisms. Simultaneous shear yielding and crazing have been observed. Shear yielding is often the dominant mechanism in an unmodified epoxy system, and this is reflected in the modified epoxy resin. Riew et al.[36] observed that particle size plays an important role in determining which toughening mechanism is dominant. Shear deformations prevail in networks toughened with small rubber particles (< 0.5 μm) while crazing dominates in networks toughened with large rubber particles (1-5 μm), and maximum toughening is obtained when both large and small particles are present with combined shear and craze deformations operating. In tests where simultaneous initiation of shear bands and crazes have been observed, it has been suggested that in addition to increasing the energy absorption, shear bands serve as effective craze terminators for growing crazes[37].

Plastic flow combined with dilation and void formation has been proposed by Bascom et al.[38,30] and Hunston et al.[39] as a mechanism of rubber toughening.

Void formation is speculated to occur either in the particle or at the particle matrix interface. The sharp crack is blunted by an increase in the size of the plastic zone ahead of the crack tip due to cavitation of the rubbery particles. They also proposed that both shear yielding of the matrix and elongation of the rubber particle contribute to toughening. This theory was supported by Kinloch et al.[40] through TEM and SEM micrographs, who further proposed that the primary energy dissipating mechanism at work was that of shear yielding of the epoxy resin matrix.

Bucknall and co-workers[13,41,42] have suggested that rubber particles serve as craze terminators which prevent the growth of large crazes and results in a large number of small crazes. Multiple crazing throughout a large volume of the rubber-modifed material could explain the high energy absorption in fracture test and the extensive stress whitening observed in deformation and failure.

Investigators are currently debating the actual existence of crazing in highly crosslinked materials such as epoxies. It has been suggested that crazing in materials of high crosslink density is questionable since the short chain lengths between crosslinks should inhibit craze deformation[40]. Donald and Kramer[35] have shown that a transition from crazing to shear yielding exists in glassy thermoplastics as the length of the polymer chain between physical entanglements increases. Therefore, theories involving crazing mechanisms are offered only as a possible toughening mechanism in modified epoxy resin networks since the evidence is not conclusive.

3.4 Modified Epoxy Systems

Thermosets have a reputation of being very brittle, intractable highly crosslinked materials and many methods of maximizing and improving their toughness have been investigated. The use of epoxies as structural materials requires rigidity, resistance to creep, high Tg, and high impact strength. But damage tolerance and high impact strength are qualities of rubbery materials or thermoplastics rather than thermosets. This is currently the major problem in designing commercially viable high performance resins. Blends of thermosets and rubbers, glassy thermoplastics or reactive thermoplastics are currently being evaluated as potential toughening matrices, wherein specific attributes of several polymers are combined into a single material.

3.4.1 Control of Phase Separation

Modification of an epoxy through the introduction of a rubbery phase leads to different phase-separated morphologies which serve to improve the mechanical properties of the material[43,44]. The amount of modifier incorporated, cure kinetics, thermodynamics, polymerization rate and the nature of the thermoset/modifier employed all influence the phase behavior in these systems[45,46,47,48]. At the onset of gelation, phase separation is halted and the morpholgy fixed. Phase behavior of thermosetting systems is complicated by both molecular weight and viscosity

increases with conversion of the network. The effects of chemical composition of the modifier, temperature of the cure and the gelation time on the resulting morpholgy and mechanical properties of the toughened epoxy resin networks have been investigated[45,49,50].

Compatibility of the modifier with the epoxy is critical since this is the primary factor for determining the type and extent of phase separation. An ideal system initially forms a homogeneous mixture with the epoxy resin and then undergoes *in situ* phase separation during curing. For instance, increasing the acrylonitrile content of a carboxyl-terminated butadiene/acrylonitrile copolymer (CTBN) system, increases the polarity of the system which increases compatiblity with the epoxy; smaller phase domains are produced since precipitation is achieved at a later stage of cure[45].

3.4.2 Polymer Morphology

Homogeneous, particulate, bi-continuous and more complex morphologies have all been observed in modified epoxy matrices[51]. The different phase structures give rise to different energy absorbing mechanisms, thereby contributing differently to fracture toughness values.

A modified epoxy resin resulting in a multiphase system can be organized in a variety of morphologies. If the modifier is immersed in the matrix of the epoxy resin, the continuous phase dominates the properties. This is the case for many

of the matrices generated by rubber toughening of epoxies.

A phase inverted morphology is obtained when the thermoplastic forms the continuous phase and the epoxy the particulate. This type of morphology offers enhanced toughness through tearing of the ductile matrix and debonding at the phase boundary.

A system where both epoxy and thermoplastic polymers are continuous simultaneously results in the formation of an interpenetrating network (IPN). Here each phase contributes properties in proportion to its concentration in the blend. There appears to be no abrupt interface, but areas of higher concentration of epoxy or modifier have been observed for some systems[52,53].

The development of a bi-continuous morphology where the two networks exist seperately with attachments at crosslink points would give improved fracture toughness over the unmodified matrix, and remove the necessity for interfacial adhesion between the two phases. This is a distinct advantage to a modified system that develops a bi-continuous morphology upon curing.

In one comprehensive study into the optimum thermoset/thermoplastic morphology for improved fracture toughness, the thermoplastic backbone was varied to control the nature of the interactions between the epoxy network and the thermoplastic[54]. Thermoplastics of similar molecular weight, hydroxy end group, concentration (30% w/w), and the same epoxy resin formulation (DEN 431/DGEBA/DDS) were compared. The systems investigated all had similar moduli and fracture toughness values, but resulted in differing morphologies. It

was concluded that the modulus of the blend is determined solely by the properties of the pure components; however, the fracture toughness is crucially dependent on the resultant morphology. The morphology providing the optimum mechanical properties in this study was a complex two phase semi-interpenetrating network. The mechanism for toughening of this type of morphology, however, was not apparent.

3.4.3 Crosslinking Modifications

Several researchers have established that reducing the crosslink density of the cured resin renders the matrix more toughenable[55,56,57,58]. The toughening by second phase elastomer particles depends upon deformation in the resin matrix, which is often accompanied by cavitation of the rubber particle. As the crosslink density increases, the capability of the resin matrix to deform is reduced and G_{Ic} decreases to that of unmodified systems. The data in Table 3.2 illustrate the enhanced toughening effect of a poly(ether sulfone) (PES) thermoplastic modifiers when the ductility of the epoxy resin matrix is increased. The trifunctional resin shown in Figure 3.11, triglycidyl tris(hydroxyphenyl)methane, was replaced with the more ductile difunctional DGEBA resin resulted in a net increase in ultimate elongation, fracture energy and tensile strength with a slight decrease in modulus.

**Table 3.2 Neat Resin Properties of PES Modified
Epoxy Resins** [57]

Epoxy Resin	% PES	Tensile Strength (ksi)	Tensile Modulus (ksi)	Ultimate Elongation (%)	Tg (°C)
TGMDA 30% TGHPM 70%	0 8	10.6 11.9	551 537	2.2 2.6	238 243
TGMDA 30% DGEBA 70%	0 8	12.5 12.0	595 551	2.5 3.0	235 225

Figure 3.11 Triglycidyl tris(hydroxyphenyl) methane (TGHPM)

Kinloch *et al.*[59] investigated toughening as a function of increasing molecular weight between crosslinks (M_c) in the epoxy matrix phase for a rubber toughened epoxy resin. M_c was controlled by utilizing different cure schedules which changed the degree of crosslinking without altering the morphology. The molecular weight between crosslinks was varied from ~600 g/mole to 5000 g/mole and was determined from the equilibrium rubbery modulus of DMA curve. A two fold increase in fracture toughness was realized for both modified and unmodified systems as the molecular weight was increased. The enhanced toughness was attributed to an increase in ductility with the greater chain length between crosslinks allowing the system to undergo plastic deformation.

3.4.4 Rubber Modifications

The most widely used method of thermoset modifications has been the dispersion of a ductile second phase into the thermoset. Preparing blends by the introduction of a low-modulus, second component has been the focus of epoxy resin modification research for some 30 years[60]. A low molecular-weight liquid rubber, end capped with functional groups that react with the epoxy (see Table 3.3) and initially miscible with the resin, functions to toughen the matrix by forming discrete particles upon curing. A certain degree of incompatibility between the rubber and resin must exist in order to obtain a discrete rubber phase, while maintaining some molecular interaction between phases in order to insure sufficient energy transfer. The particles initiate energy dissipating deformation in

the resin matrix by cavitation within the rubber. Phase separated particles of 10^2-10^3 nm in diameter are apparently necessary for a substantial increase in fracture energy.

Table 3.3 Liquid Rubber Modifiers

Liquid Rubber	Symbol
Carboxyl-terminated butadiene/acrylonitrile copolymers	CTBN
Amine-terminated butadiene/acrylonitrile copolymers	ATBN
Polycaprolactone	PCL
Poly(propylene oxide)	PPO
n-Butyl acrylate	n-BA
Carboxyl-terminated polyisobutylene	CTPIB
Carboxylated butadiene/acrylonitrile copolymers	ABAN
Carboxyl terminated poly(n-butyl acrylate)	CTPnBA
Hydroxy-terminated polybutadienes	HTPB
Carboxyl-terminated polybutadienes	CTPB

A major factor in the toughening ability of the rubber is the crosslink density of the epoxy matrix. Therefore direct comparisons of results from the liquid rubber modifiers in epoxy matrices of differing ductility should be avoided.

3.4.5 Thermoplastic Modifiers

Thermoplastic modifies offer the advantage of higher modulus and higher Tg over liquid rubber modifiers, while improving mechanical properties. In

comparison to thermosets, many thermoplastics can tolerate higher strains prior to failure and exhibit better fracture toughness and fatigue endurance[61]. These features have been incorporated in epoxies by mixing thermoplastic oligomers of varying molecular weights which have been endcapped with a reactive group (i.e., hydroxy, epoxy or amino) into the unreacted epoxy. The system is then cured and the thermoplastic is incorporated chemically via this reactive end group by the same type of reactions seen for the curing agents. The majority of these systems have a multi-phase morphology which may phase separate or undergo morphological changes at elevated temperatures under stress[62]. The degree of toughening is dependent on modifier type, endgroup functionality, heterophase distribution, heterophase/matrix interface adhesion, resin and curing agent types, curing conditions, and molecular weight between crosslinks in the matrix resin.

Table 3.4 summarizes the thermoplastics that have been incorporated into epoxy resin systems as reactive modifiers to increase flexibility and fracture toughness.

Table 3.4 Thermoplastics Modifiers

Polymer	Symbol	Ref
Poly(butylene terephthalate)	PBT	63
Poly(ethylene terephthalate)	PET	63
Polysulfone	PSF	64,65
Poly(phenylene sulfide)	PPS	62,66
Poly(ether sulfone)	PES	57,65,67,68
Poly(ether ketone)	PEEK	66
Polyimides	PI	64
Polyhydantoin	PH	69
Poly(aryl ether ketone)	PAEK	58
Poly(arylene ether)	PAE	70
Poly(ether imide) (ULTEM®)	PEI	70,71,72,73
Poly(ethylene oxide)	PEO	71
Blendex 311®	---	71
Polyurethane	PU	74
Polycyanate	PC	75
Fluoroelastomer (Vitron® GF)	FE	76
Perfluoroalkyl ether diacyl fluoride	PEDF	52,53
Poly(butylene isophthalate)	PBuI	77
Poly(ethylene phthalate)	PEP	77
Poly(butylene phthalate)	PBP	77
Poly(hexylene phthalate)	PHP	77
Poly(hexylene isophthalate)	PHI	77
Polysiloxane	PS	78

Research in the area of additive contributions a particular group imparts

to a given polymer[79] has led to the development of thermoplastics that may contribute desirable properties to epoxy resins. For example: incorporation of ether or sulphide groups in a polymer lowers the Tg and renders the polymer more processable; inclusion of sulphone substituents increases Tg and melt temperature[68] and incorporation of silicon and certain phosphorus containing groups increases resistance to oxygen plasma erosion in polymers for space applications[80,81,82,83]. Utilization of these polymer properties has allowed for improved modified resins properties based on the nature of the substituents in the backbone of the modifier. The data in Table 3.5 demonstrates the effect of variations in sulphone content on the fracture toughness of the thermoplastic.

Table 3.5 Sulphone content and its effect on fracture toughness of PES[68]

Thermoplastic	% Sulphone in Polymer	Tg (°C)	G_{Ic} (resin) (psi)
Victrex® (PES)	27.55	225	196
	26.40	225	169
	25.07	213	196
	23.55	208	224
	21.79	208	251
	19.73	160	335
Udel® (PES)	14.48	180	196

The relationship between molecular weight and the toughening ability of the poly(ether sulphone) modifiers on K_{Ic} (Table 3.6), gives evidence that the K_{Ic} of the blend increases with increasing PES molecular weight without significantly affecting the modulus or Tg of the system.

Table 3.6 Modified DGEBA/DDS/PES 15% w/w[65]

M$_n$ of PES	K$_{Ic}$ (psi√in)	Flexural Modulus (ksi)	Tg (°C)
Control	582	46.4	192
4,360	637	45.0	194
8,910	646	46.4	---
14,100	646	46.4	196
20,000	755	45.0	194

Because of variations in manufacturers, molecular weight, substituent concentrations used in modifiers and the thermoset matrix studied, one must be cautious of making direct comparisons of experimental results even when it appears that the same type of modifier has been studied. This may serve to explain why several research groups have evaluated poly(ether sulfone) as an epoxy resin modifier with varying results. In the above study, addition of PES to a TGMDA/DDS resin system did not effect the modulus (E) of the blend, but increases in ultimate elongation and fracture toughness (K$_{Ic}$) were noted. The modulus and thermal properties were not affected at thermoplastic levels below 15% w/w. However, increasing modifier concentrations above this level adversley affected these properties.

Phase separation of the modified system was not observed using a high multiple scanning electron microscope (SEM) to observe fracture surfaces. Other studies have shown that PES modifiers in a DGEBA/DDS system also resulted in

a homogeneous system, as observed by SEM and dynamic mechanical properties[57].

A third study using PES as a modifier to a DGEHF/DADB resin system, resulted in only a minimal change to the flexural properties of the modified system, in PES concentrations as high as 30% w/w[70] (Table 3.7).

Table 3.7 Properties of PES Modified Resin (DGEHF/DADB)

Property	Control	10%w PES	20%w PES	30%w PES
Tg (tan δ, °C)	250	235	235	242
Fracture Toughness Kq, (psi√in)	525	434	688	1031
Fracture Energy G_{Ic}, (psi)	5.9	4.1	10.2	21.3
Room Temperature Elongation, %	4.16	4.22	3.94	6.21

Due to the miscibility properties of some thermoplastics, several of the modifiers in Table 3.4 are ineffective in maintaining thermal stability while improving fracture toughness. Blendex 311® (a PVC toughener), was ineffective with the test TGMDA/DDS system because of incompatibility between phases resulting in macrophase separation where large particles of thermoplastic were observed by optical microscopy after curing. Poly(ethylene oxide) is also ineffective because of miscibility with the matrix, which

Table 3.8 Neat Resin Properties of modified TGMDA/DDS system

Modifier	Ultem® Poly(ether imide)	Blendex® ABS Copolymer	Poly(ethylene oxide) $M=5x10^6$
Wt%	10	5	3
K_{Ic} Ksi√in	1.09	0.62	0.57

Various levels of success in improving fracture toughness by incorporating poly(ether imide)s such as Ultem®, into epoxy matrices have been reported. A 22% increase in fracture toughness for a DGEHF/DADB resin modified with Ultem® 1000 (ca. 10%w/w) over that of the unmodified resin was reported with little or no adhesion between phases[70].

Table 3.9 Properties of thermoplastic modified resin
(DGEHF/DADB)

Property	Control	10%w Ultem®	20%w Ultem®	30%w Ultem®
Tg (tan δ, °C)	250	238	235	233
Fracture Toughness Kq, (psi√in)	525	638	1112	1249
Fracture Energy G_{Ic}, (psi)	5.9	8.6	26	33
Room Temperature Elongation, %	4.16	2.66	3.00	2.51

A TGMDA/DDS resin matrix modified with 16.6 vol. % of PEI provided improvements in fracture toughness in terms of G_{Ic} by a factor of 8, with no

crosslinking between the phases (Table 3.9). Another report states that the thermoplastics do not seem to significantly alter the mechanical and thermal properties of the TGMDA/DDS blends, and in fact lead to a depression in Tg due to plasticization[71]. The decrease in Tg due to PEI has also been supported by research that concluded that the Tg in modified epoxies decreased with increasing PEI content[73].

The introduction of fluoroelastomers into DGEBA/DDS resin systems has met with moderate success. Vitron GF® was modified to incorporate polar substituents in the backbone. The introduction of polar groups allowed for compatibility in the partially cured resin which phase separated upon complete curing. The net effect was a decrease in thermal stability but a fourfold increase in fracture energy in the blends containing 15% w/w polar elastomer[76]. Copolymerization of perfluoroalkyl ether diacyl fluoride (EDAF) with this epoxy resin resulted in an increase in strength, modulus, and toughness, both flexural and tensile (Table 3.10). A net increase in Tg for the blend was also observed. This effect was attributed to an increase in crystallinity via hydrogen bonding which offset the expected losses due to the energy absorbing dampening effect of the elastomer. The morphology of the system was described as a simultaneous interpenetrating polymer network, where there is no abrupt interface. However, areas of higher concentration of elastomer or epoxy copolymer were observed. The net result seems to be that this system afforded both chemical reinforcement via a crosslinked, hydrogen bonded elastomer-epoxy copolymer matrix and

physical reinforcement via a rubber phase/brittle polymer interface[52,53].

Table 3.10 EDAF modified DGEBA resins

Sample (% EDAF)	TGA 5% wt loss (°C)	Tg (°C)	Tensile strength (ksi)	Tensile modulus (ksi)
0	395	160	13.9	2029
3	385	168	23.3	352
5	385	173	11.6	199
8	380	178	11.4	187

Studies utilizing a poly(arylene ether), (Figure 3.12), as a modifier to a DGEHF/DADB system resulted in modified systems with lower glass transition temperatures, but served as an effective toughening modifier at 20% w/w[70] (Table 3.11).
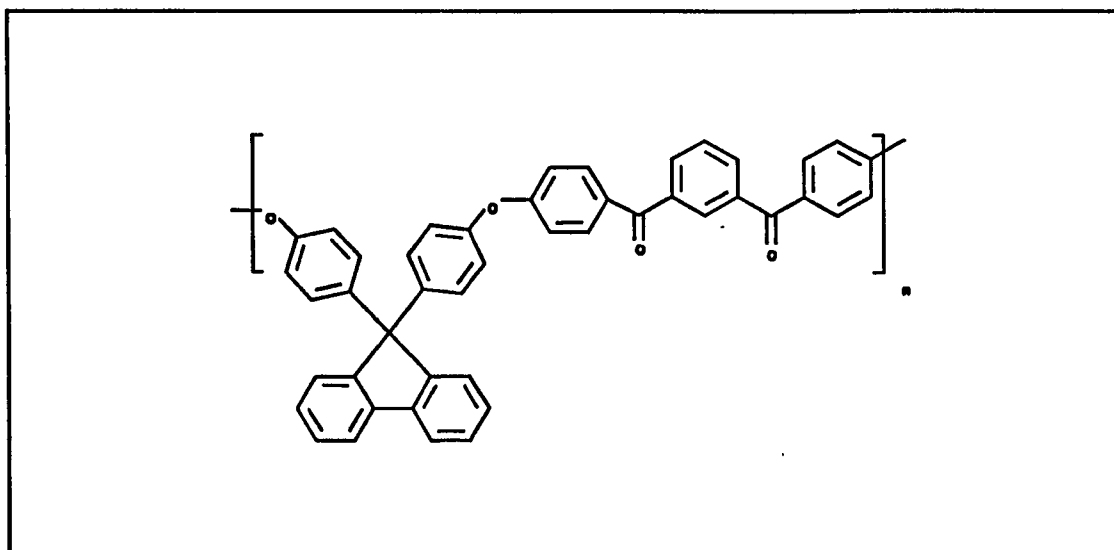
Figure 3.12 PAE modifier for DGEHF/DADB system

Table 3.11 PAE modified DGEHF/DADB system

Property	Control	10%w PAE	25%w PAE
Tg (tan δ, °C)	250	230	231
Fracture Toughness Kq, (psi√in)	525	536	701
Fracture Energy G_{Ic}, (psi)	5.9	6.1	9.9
Room Temperature Elongation, %	4.16	2.49	2.87

Another epoxy resin modification utilizing a poly(aryl ether) (Figure 3.13), yielded a multi phase morphology which exhibited improvement in break elongation and fracture energy. These properties increased with an increasing thermoplastic content. The epoxy value of a resin represents the fractional number of epoxy groups contained in 100 grams of resin. Increasing the ductility of the epoxy matrix by replacing the DGEBA resin of epoxy value 0.51 with one of epoxy value 0.44, greatly enhanced the toughening ability of the PAE thermoplastic with only minimal decreases in Tg and modulus (Table 3.12).
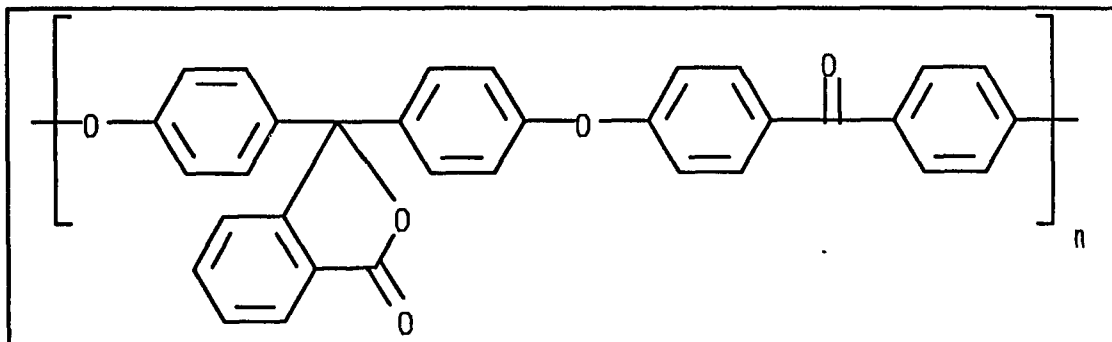
Figure 3.13 PAE modifier for TGMDA/DGEBA system

Table 3.12 Neat Resin properties of epoxy modified with PAEK, cured with DDS[58]

Resin System	PAE (%)	Tensile Strength (ksi)	Tensile Modulus (ksi)	Elongation (%)	Tg (°C)
TGMDA DGEBA-51	0	12.5	60	2.5	235
	2	12.9	57	2.8	236
	10	12.5	61	3.1	240
TGMDA DGEBA-44	0	12.1	57	3.0	235
	2	14.0	55	3.4	233
	10	13.3	60	4.0	235

Aromatic polyesters have also been used to reduce the brittleness of DGEBA resins. Aromatic polymers prepared from phthalic or isophthalic acids and α,ω-alkanediols and incorporated into the thermoset matrix resulted in lower thermostability compared to the parent resin. The effectiveness of the modifiers introduced in Table 3.13, decreased with increasing chain length of the alkylene units of the polymer, i.e. PEP>PBP>PHP. Of the aromatic polyesters listed in Table 3.4, (PBuI; PEP; PBP; PHP; PHI) the most effective blend, from inclusion of 20% w/w of PEP (MW 7200), resulted in a 150% increase in fracture toughness

(K_{Ic}) at no expense to the modulus and strength properties. Increasing the molecular weight of polyesters decreased the modulus and strength properties and lowered K_{Ic} because of macrophase separation[77].

Table 3.13 Properties of Poly(alkylene Isophthalate) modified DGEBA/DDS epoxy resin[77]

Modifier	MW	Tensile Strength (psi)	Elong ation (%)	Tensile Modulus (psi)	K_{Ic} (ksi√in)	Tg (°C)
PEP	3000	130	3.4	52.8	1.03	82
	6300	122	4.0	48.0	1.25	87
	7200	125	4.3	49.0	1.38	91
	10100	102	3.0	46.4	1.33	92
PBP	3100	129	4.7	49.3	0.97	70
	4900	121	4.5	49.0	1.02	71
	7000	124	4.7	47.9	0.98	71
	8700	104	4.4	43.4	1.17	70
	10200	98	6.9	37.3	1.17	92
	15600	84	9.4	32.0	1.74	99
PHP	2600	114	4.1	45.4	0.82	68
	6300	101	7.1	39.4	0.96	73
	9200	83	6.2	32.8	1.02	82
PBuI	7000	116	4.9	47.7	0.93	74
	12500	91	5.5	39.4	1.19	91
PHI	6500	85	6.5	38.6	1.04	70
	13200	62	10.3	28.0	1.70	85
DGEBA		120	6.6	41.3	0.55	99

Several other modes of modification exist for epoxy resin matrices. It is possible to obtain a matrix resin with better comprehensive properties by mixing two or more kinds of epoxies in proper ratios. Modification of the chemical

structure by introducing "flexible segments" into the crosslinked network or using curing agents with a flexible molecular structure can also result in improved mechanical properties.

3.5 Poly(arylene ether)s and Poly(arylene ether imidazole)s

Poly(arylene ether)s and poly(arylene ether imidazole)s have good mechanical properties, as well as low melt viscosities and good processing characteristics. Many PAEs are currently available commercially such as Udel[®] a polysulfone, Kadel[®] a polyketone[85], PEEK[®] a poly(ether ether ketone)[86], and Victrex[®] PES a polysulfone[86]. These high performance thermoplastics have found use in a large variety of applications such as adhesives, composites, coatings and toughening agents.

The first reports of poly(arylene ether)s prepared through Friedel-Crafts reactions were reported in the late 1950's[87] and early 1960's[88]. Friedel-Crafts acylation polymerizations have received a great deal of attention over the last two decades. Initially the solvent-catalyst system of choice was either hydrogen fluoride/boron trifluoride or trifluoromethanesulfonic acid. For example Marks[89] prepared a high molecular-weight crystalline poly(aryl ketone) utilizing the anhydrous hydrogen fluoride/boron trifluoride as both a catalyst and solvent. Marks[90] also prepared a high molecular-weight, two-component system utilizing trifluoromethanesulfonic acid as a solvent. Jansons[91] successfully prepared a high

molecular-weight, two-component system using anhydrous hydrogen fluoride/boron trifluoride and terephthalic acid. He also prepared a high molecular weight polymer using trifluoromethanesulfonic acid with isophthaloyl chloride and diphenyl ether[92]. Other representative one-component and two-component systems prepared by this method are given in Figures 3.14[90], 3.15[92] and 3.16[93].
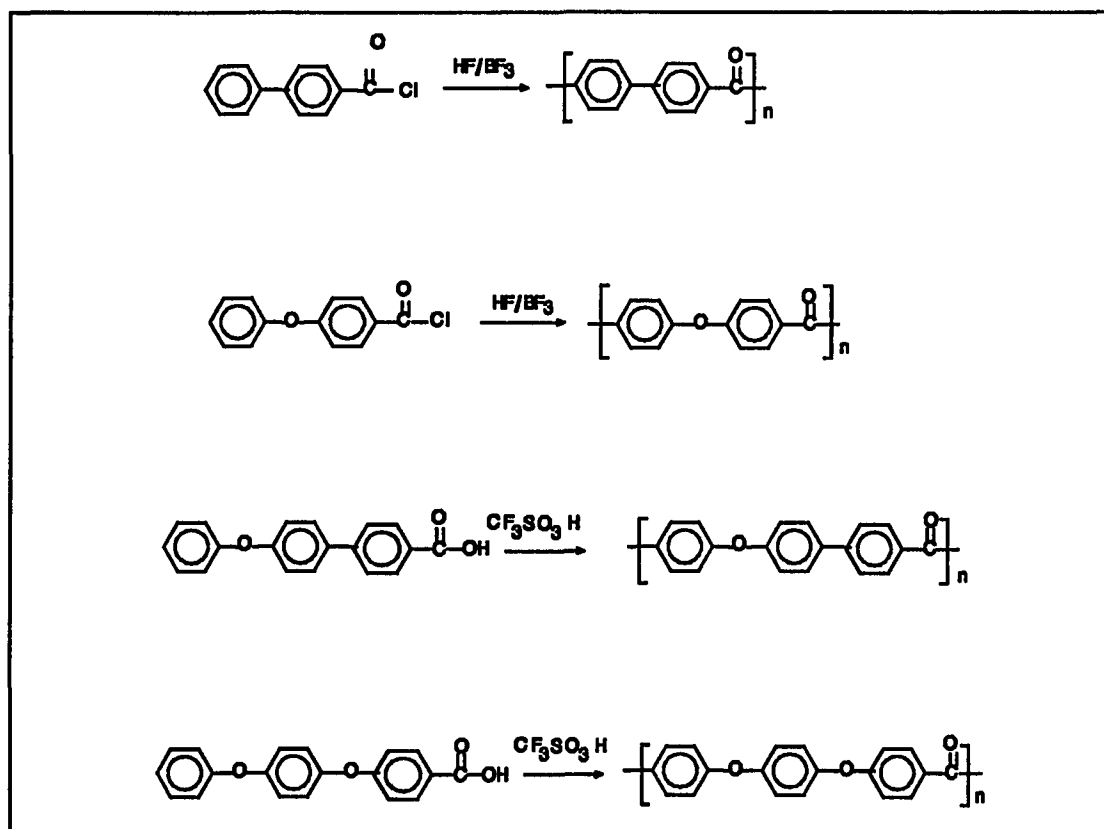
Figure 3.14 Synthesis of one component systems by Friedel-Crafts Acylation
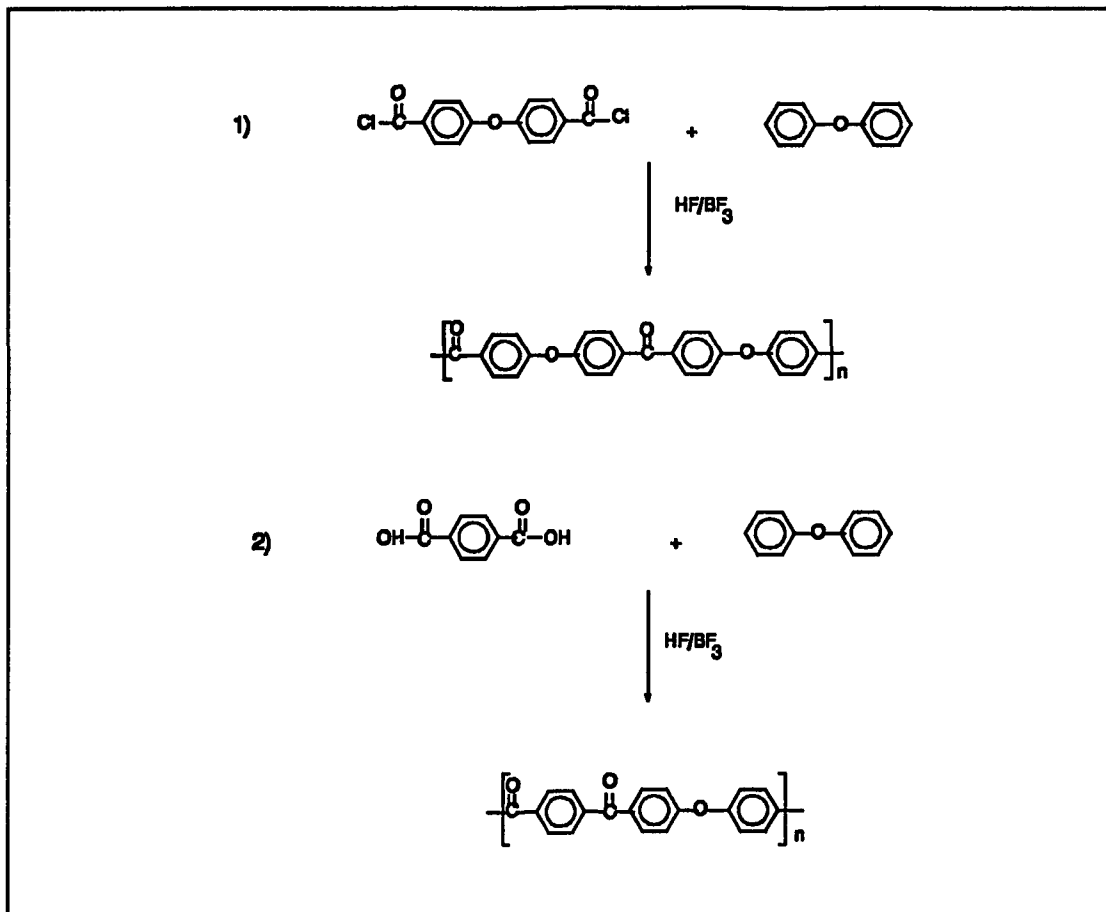
Figure 3.15 Synthesis of two component systems by Friedel-Crafts acylation

Although successful on the laboratory scale, HF/BF$_3$ and CF$_3$SO$_3$H solvent-catalyst systems are not suitable for industrial use, owing to inhibitive cost and handling problems.

Jansons and Gor (1984) reported a method which employed aluminum chloride (AlCl$_3$) in chlorinated solvents in conjunction with a Lewis base to synthesize high molecular weight polymers[94]. Figure 3.17 gives a representative synthetic scheme for two early poly(aryl ketone)s synthesized by this method[95,96].
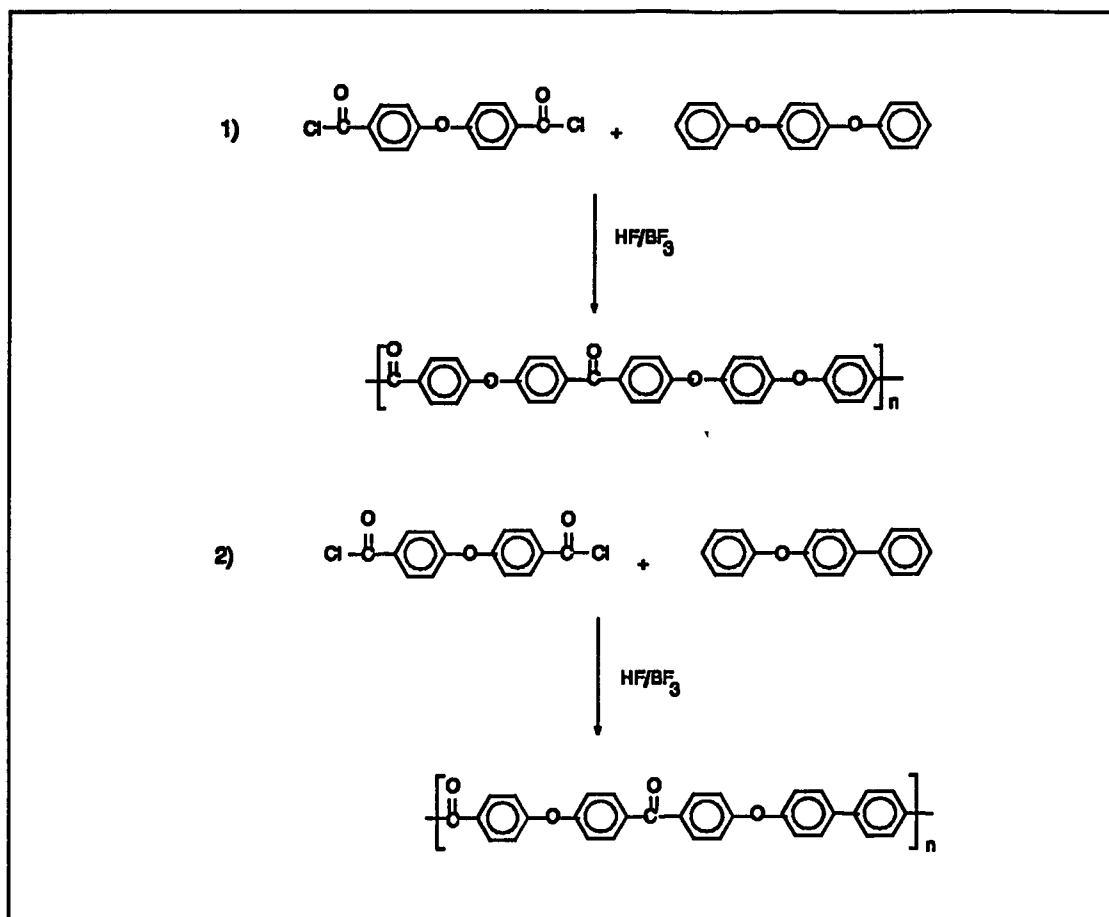
Figure 3.16 Synthesis of two component systems by Friedel-Crafts Acylation

Poly(arylene ether)s and poly(arylene ether imidazole)s have also been prepared through nucleophilic substitution of an activated aromatic halide by alkali metal phenolates to give a high molecular-weight product. A poly(arylene ether) has been prepared by reacting a dihalide with the disodium salt of bisphenol A in dimethylsulfoxide (DMSO) with a catalytic amount of copper oxide[97,98]. A second research group used 4,4'-difluorobenzophenone in DMSO to prepare a high molecular weight poly(arylene ether) in 30 minutes at 135 °C[99].
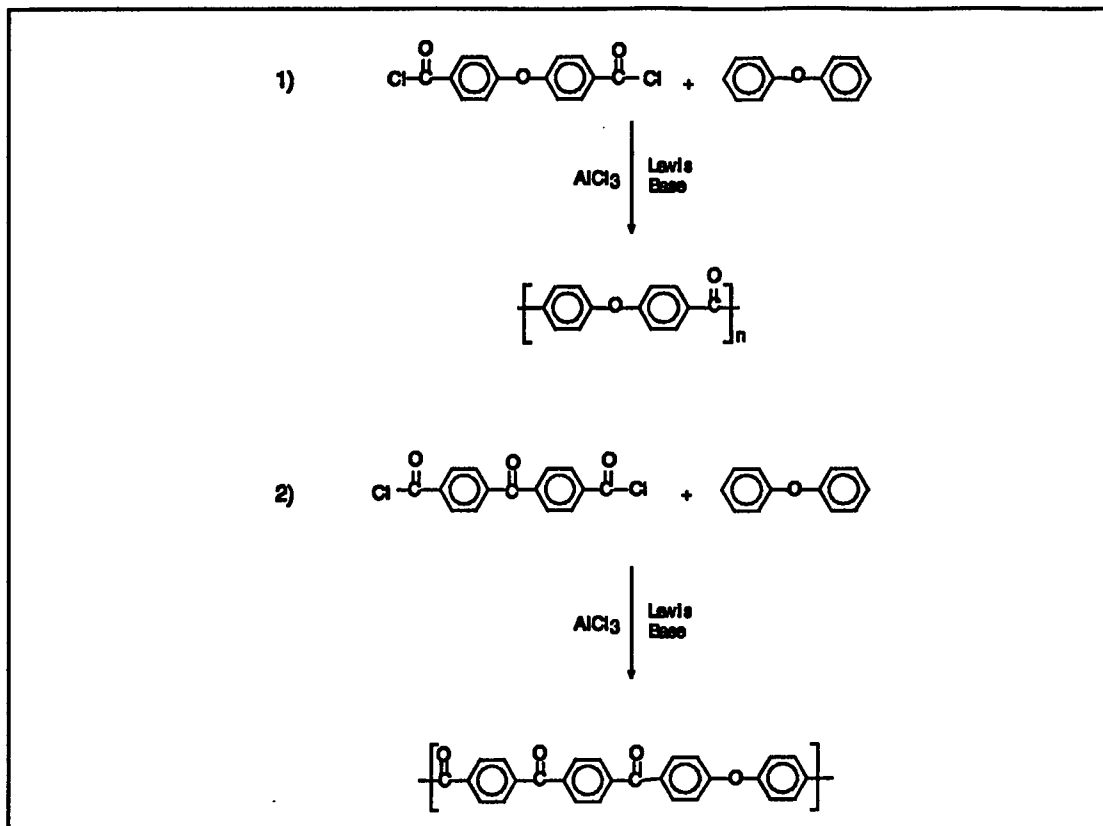
Figure 3.17 Synthesis of early Poly(aryl ketone)s

The general mechanism for nucleophilic aromatic substitution, shown in Figure 3.18, proceeds through an anionic intermediate. Electron withdrawing groups in the ortho and para positions enhance the reactivity of the leaving groups and stabilize the intermediate through induction and delocalization of the negative charge through resonance. Substitution at the meta position results in little activation because of the lack of resonance stabilization at the meta position. Halogens are typically utilized as leaving groups, and have the following order of reactivity, F > Cl > Br > I. Preparation of high molecular weight polymers from this
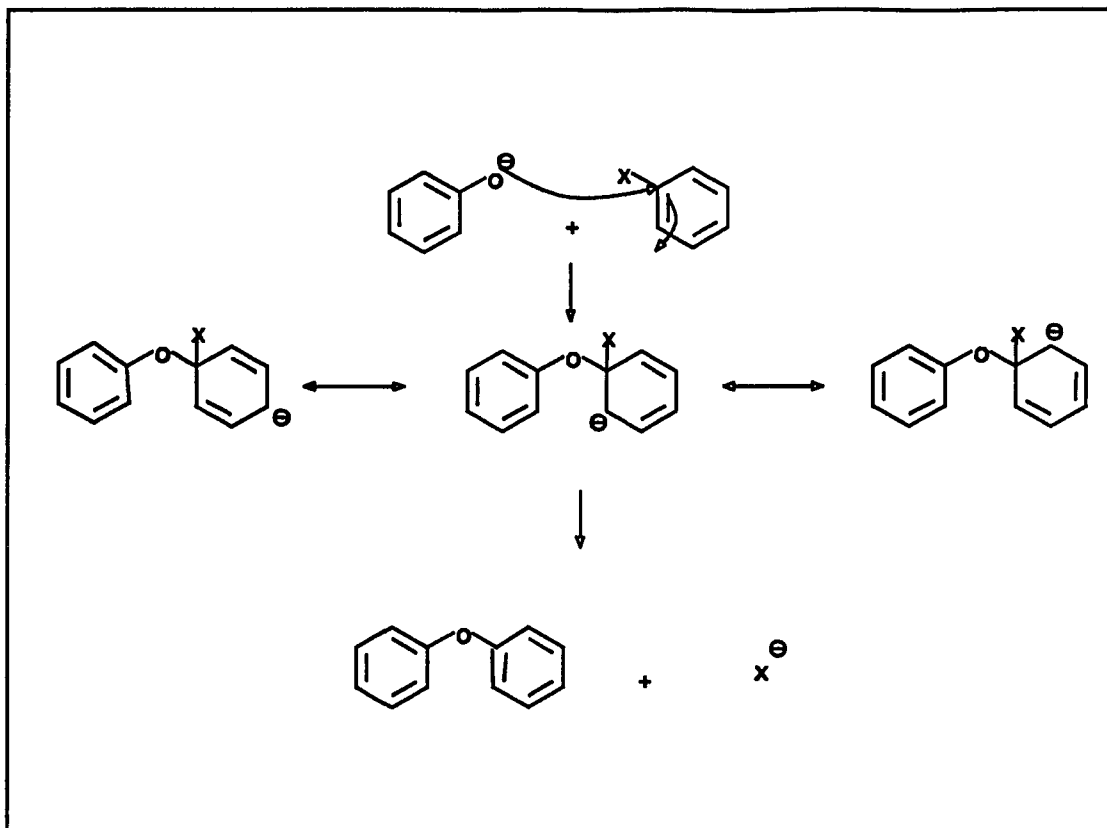
Figure 3.18 Nucleophilic aromatic substitution of poly(aromatic ether)s

method with bisphenols and dihalides requires the dihalide to be sufficiently activated and be a good leaving group (F or Cl). The bisphenol must also be a good nucleophile and attack the dihalide at the electron deficient aromatic carbon. Additionally, the alkali metal phenolates as well as the propagating polymer chain must be soluble. Anhydrous and anaerobic conditions are required because phenoxides are easily oxidized by oxygen at elevated temperatures, and they are readily hydrolyzed by water. Additionally, any hydroxide ion present can react with the activated aromatic dihalide effectively changing the stoichiometry.

The base (sodium hydroxide) must be present in stoichiometric amounts

since an excess leads to degradation of the dihalide or chain scission of the polymer and deficiencies lead to incomplete reaction. An improved synthetic method utilizing anhydrous potassium carbonate in a polar aprotic solvent such as (N,N-dimethylacetamide or N-methylpyrrolidinone) was developed in the late 1970s[100,101]. Since potassium carbonate is only sparingly soluble in organic solvents, excesses can be used without interferring with the prodution of high molecular weight polymer. It is also a strong enough base to react with phenols at elevated temperatures and the limited solubility results in the slow generation of potassium bisphenoxide and water during the reaction (Figure 3.19).

$$K_2CO_3 + HO-Ar-OH \rightleftharpoons K^{\oplus}O^{\ominus}-Ar-OH + KHCO_3$$

$$KHCO_3 + K^{\oplus}O^{\ominus}-Ar-OH \rightleftharpoons K^{\oplus}O^{\ominus}-Ar-O^{\ominus}K^{\oplus} + H_2O \ CO_2$$

$$2KHCO_3 \longrightarrow K_2CO_3 + CO_2\uparrow + H_2O$$
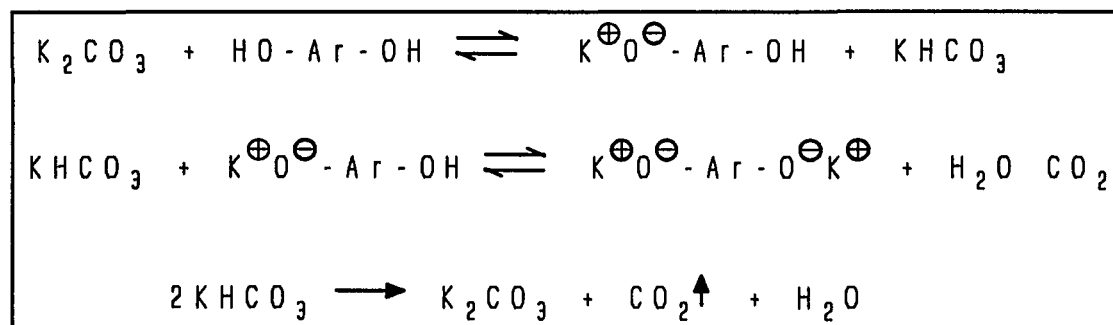
Figure 3.19 Potassium carbonate participation in nucleophilic substituion

Anhydrous conditions are maintained by adding toluene and refluxing, thereby forming an azeotropic mixture with the water generated during the reaction and removed by distillation into a Dean-Stark moisture trap.

This system requires higher temperatures than the dimethylsulfoxide/aqueous sodium hydroxide system since the reaction rate is

approximately ten times slower. This has been attributed to several factors: 1) the initial heterogeneous state of the potassium carbonate, 2) the lower dielectric constant of the reaction medium because of the toluene, and 3) the possibility of hydrogen bonding between the phenoxide and unreacted phenols. Viswanathan *et al.* observed after 10 hours at 140 °C the reaction yielded only trimers and oligomers while at 157 °C high molecular weight polymers resulted[102].

Many other high molecular weight poly(arylene ether)s have been synthesized by this alternative method[103,104,105], and complete discussions of the synthesis, characterization, chemical and physical properties of these materials are also available[106,107].

Little attention has been paid to poly(imidazole)s because of the difficulties encountered in synthesizing high molecular weight systems via conventional methods. Low molecular weight systems have been prepared utilizing aromatic dialdehydes with bis(phenyl-α-diketone)s in the presence of ammonia[108]. Recently, however, poly(arylene ether imidazole)s which are similar in structure to the poly(imidazole)s, have been prepared utilizing nucleophilic aromatic substitution[109,110,111,112]. The reaction represented in Figure 3.20, of a bisphenol imidazole with an activated aromatic dihalide in the presence of potassium carbonate, yields polymers of high molecular weight, high glass transition temperature, and good mechanical properties. Figure 3.21, gives some of the poly(arylene ether imidazole)s that have been prepared along with representative properties.
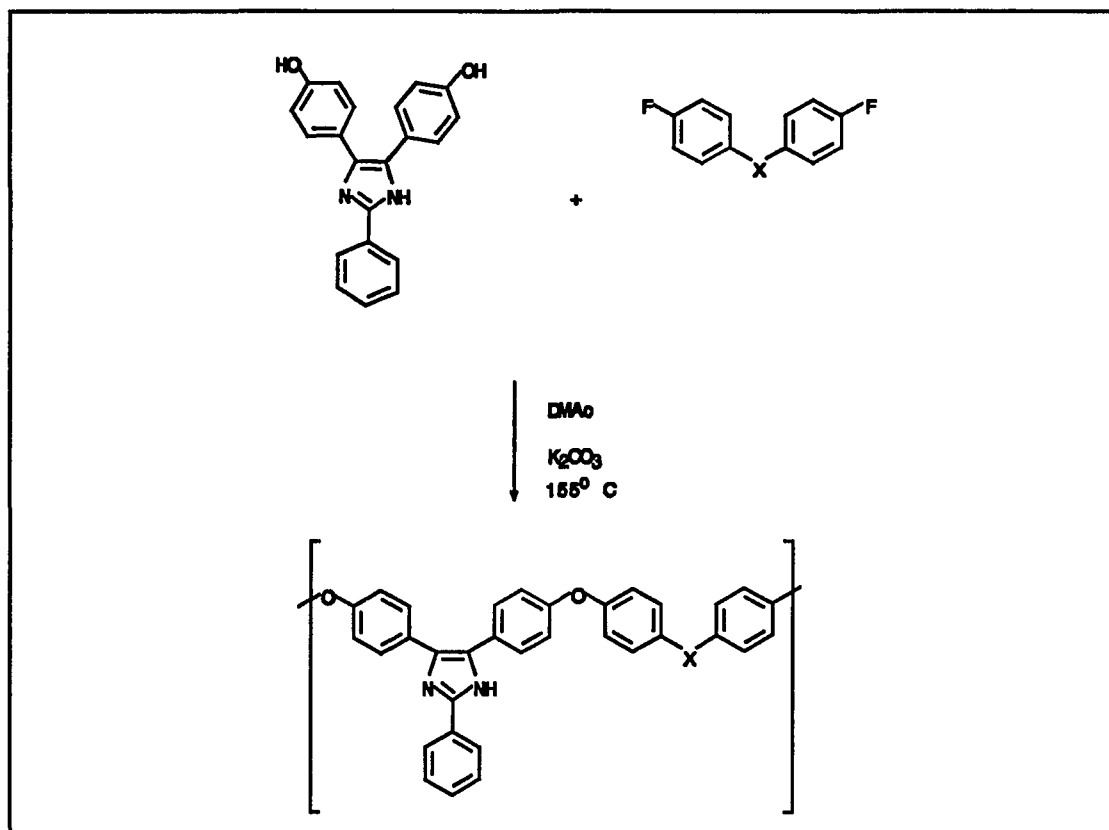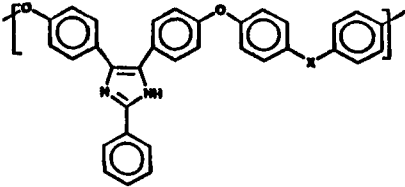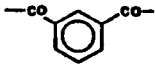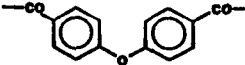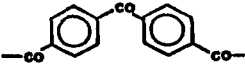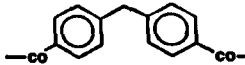
Figure 3.20 Preparation of high molecular weight PAEIs
(X is given in Figure 3.21)
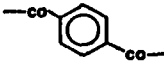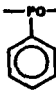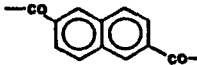
Inherent Viscosity	X	Tg, °C
0.55		230
0.64		230
0.49		239
0.58		231
0.53		258

1) 0.5% solutions in DMAc at 25°C
2) Heated at 20°C/min, DSC

Figure 3.21a (X) Component of dihalide in PAE synthesis and representative properties of PAEIs

Poly(arylene ether)s and poly(arylene ether imidazole)s are both high performance engineering thermoplastics with attractive properties for a variety of applications. Incorporation of functionalized moieties along the backbone of poly(arylene ether)s have been synthesized as random, block and graft copolymers[113,114,115,116,117,118], however, copolymer PAE/PAEI systems have not been

Inherent Viscosity	X	Tg, °C
0.41	SO₂	277
0.61	CO	259
0.89	—CO—C₆H₄—CO—	248
0.24	—PO—C₆H₅	318
0.40	—CO—naphthalene—CO—	248

1) 0.5% solutions in DMAc at 25°C
2) Heated at 20°C/min, DSC

Figure 3.21b (X) Component of dihalide in PAE synthesis and representative properties of PAEIs

investigated. Tgs of some PAEs have been reported to range from 110 to 310 °C, with fracture toughness values ranging from 2400 to 3800 psi√in. PAE thin film tensile strengths ranging from 10 to 14 ksi and modulus values from 350 to 400 ksi have also been reported. Tgs of PAEIs have been reported to range from 230 to 300 °C, with room temperature thin film tensile strengths ranging from 13 to 18

ksi and modulus values from 400 to 460 ksi.

It is envisaged that random copolymers containing these moieties may combine to give synergistic toughening when incorporated as a modifier for epoxy resins. The arylene ether portion should impart toughness while the reactivity of the imidazole moiety with the oxirane ring of the epoxy allows for the the distance between crosslinks of the epoxy/thermoplastic to be controlled by the concentration of the reactive group. This combination may result in an excellent overall combination of properties.

3.6 References

1. Allcock, H. R.; Lampe, F. W., *Contemporary Polymer Chemistry*, 2nd ed., Prentice Hall, Englewood Cliffs, New Jersey, **1990**.

2. Busso, N., Technical Report No. AFML-TR-68-286, Part I, Sept. **1968**, AFML-TR-69-238, Part II, Jan **1970**.

3. Wang, H. T.; Chaudhari, M. A.; Cobuzzi, C., *SAMPE*, 484-493, **1988**.

4. Korshak, V. V., *J. Macromol. Sci. Rev. Macromol. Chem*, *C11*(1), 45-142, **1974**.

5. Shell Chemical Co., Tech. Bulletin, March **1990**.

6. Lee, H.; Neville, K., in *Ency. of Polym. Sci. and Tech.*, *6*, 209-271, **1967**.

7. Byrne, C. A.; Hagnauer, G. L.; Schneider, N. S.; Lenz, R. W., *Polym. Composites*, *1*(2), 71-76, **1980**.

8. Dusek, K.; Bleha, M., *J. Polym. Sci.*, *15*, 2393-2400, **1977**.

9. Dusek, K., Bleha, M., Lunak, S., *J. Polymer Sci., Polymer Chem Ed.*, *15*, 2393 **1977**.

10. Lee, H.; Neville, K.; *Handbook of Epoxy Resins*, McGraw-Hill **1967**.

11. Farkas, A.; Strohm, P., *J. App. Polym. Sci.*, *12*, 159-168, **1968**.

12. Berry, B. W., *Fracture Toughness*, The Iron and Steel Inst., **1968**.

13. Bucknall, C. B., *Toughened Plastics*, Wiley, New York **1977**.

14. Kinloch, A. J., Young, R. J., *Fracture Behavior of Polymers*, Applied Science, New York **1983**.

15. Crist, B., Ratner, M. A., Brower, A. L., Savin, J. R., *J. Appl. Phys.*, *50*, 6047, **1979**.

16. Treloar, L. R. G., *The physics of rubber elasticity*, Clarendon Press, Oxford **1958**.

17. Haward, R. N., _The Physics of Glassy Polymers_, John Wiley and Sons, New York **1973**.

18. Andrews, R. D., Kazama, Y., _J. Appl. Phys._, _38_, 4118 **1967**.

19. Bryant, G. M. _Text. Res. J._, _31_, 399 **1961**.

20. Passaglia, E., _J. Phys. Chem. Solids_, _48_(11), 1075 **1987**.

21. Aziz, A. W., Ab-el-Nour, K. N., _J. Appl. Polym. Sci._, _31_, 2267 **1986**.

22. Kambour, R. P., _J. Polym. Sci.:Macromol. Rev._, _7_, 1 **1973**.

23. Kramer, E. J., Berger, L. L., in _Crazing in Polymers, Vol. 2_, Adv. Polym. Sci. 91/92, Springer-Verlag, New York, pp. 1-68, **1990**.

24. Young, R. J., Beaumont, P. W. R., _Polymer_, _17_, 717 **1976**.

25. Ting, R. Y., Cottington, R. L., _J. Appl. Polym. Sci._, _25_, 1815 **1980**.

26. Aharoni, S. M., _Macromolecules_, _18_, 2624 **1985**.

27. Kunz-Douglas, S., Beaumont, P. W. R., Ashby, M. F., _J. Mater. Sci._, _15_, 1109 **1980**.

28. Kunz, S., Beaumont, P. W. R., _J. Mater. Sci._, _16_, 3141, **1981**.

29. Sultan, J. N., McGarry, F. J., _Polym. Eng. Sci._, _13_, 29, **1973**.

30. Bascom, W. D., Ting, R. Y., Moulton, R. J., Riwe, C. K., Siebert, A. R., _J. Mater. Sci._, _16_, 2657, **1981**.

31. Bascom, W. D., Cottington, R. L., _J. Adhesion_, _7_, 333 **1976**.

32. Bitner, J. R., Rushford, J. L., Rose, W. S., Hunston, D. L., Riew, C. K., _J. Adhesion_, _13_, 3 **1982**.

33. Yee, A. F., Pearson, R. A., _J Mater. Sci._, _21_, 2462 **1986**; _21_, 2475 **1986**.

34. Haaf, F., Breuer, H, Stabenow, J., _J. Macromol. Sci. Phys._, _B14_, 387 **1977**.

35. Donald, A. M., Kramer, E. J., _J. Mater. Sci._, _17_, 1765, **1982**.

36. Riew, C. K., Rowe, E. H., Siebert, A. R., in _Toughness and Brittleness of Plastics_, Eds. R. D. Deanin and A. M. Crugnola, Adv. Chem. Ser. 154, American Chemical Society, Washington D. C., pp. 326-343, **1976**.

37. Bucknall, C. B., Clayton, D., Keast, W. E., *J. Mater. Sci.*, *7*, 1443, **1972**.

38. Bascom, W. D., Cotting, R. L., Jones, R. L., Peyser, P., *J. Appl. Polym. Sci.*, *19*, 2545 **1975**.

39. Hunston, D. L., Bitner, J. L., Rushford, J. L., Oroshnik, J., Rose, W. S., *Elast. Plast.*, *12*, 133 **1980**.

40. Kinloch, A. J., Shwa, S. J., Tod, D. A., Hunston, D. L., *Polymer*, *24*, 1341 **1983**; *24*, 1355 **1983**.

41. Bucknall, C. B., *Adv. Polym. Sci.*, *27*, 121 **1978**.

42. Haward, R. N., Bucknall, C. B., *Pure and Appl. Chem.*, *46*, 227 **1976**.

43. McGarry, F. J.; Willner, A. M., *Research Report, School of Engineering*, MIT, Cambridge, MA, **1966**.

44. McGarry, F. J.; Willner, A. M., *Research Report, School of Engineering*, R68-8, MIT, Cambridge, MA, **1968**.

45. Manzione, J. K., Gillham, J. K., McPherson, C. A., *J. Appl. Polym. Sci.*, *26*, 889 1981; *26*, 907 **1981**.

46. Williams, R. J. J., Borrajo, J., Adabbo, H. E., Rojas, A. J., in <u>Rubber Modified Thermoset Resins</u>, C. K. Riew and J. K. Gillham, Eds., Adv. Chem. Ser. 208, American Chemical Society, Washington D.C., pp. 195-213, **1984**.

47. Verchére, D., Sautereau, H., Pascault, J. P., Moschiar, S. M., Riccardi, C. C., Williams, R. J. J., *Polymer*, *30*(1), 107 **1989**.

48. Bucknall, C. B., Yoshii, T., *Brit. Polym. J.*, *10*, 53 **1978**.

49. Yamanaka, K., Inoue, T., *J. Mat. Sci.*, *25*, 241 **1990**.

50. Yamanaka, K., Takagi, Y., Inoue, T., *Polymer, 30*, 662 **1989**; *30*, 1839 **1989**.

51. Woodward, A. E., <u>Atlas of Polymer Morphology</u>, Oxford Univ. Press, New York **1989**.

52. Rosser, R. W.; Chen, T. S.; Taylor, M., *Polym. Comp.*, *5*(3), 198-201, **1984**.

53. Rosser, R. W.; Taylor, M. S.; *NASA Tech Briefs, 9*(1), 86-88, **1985**.

54. Sefton, M. S.; McGrail, P. T.; Peacock, J. A.; Wilkinson, S. P.; Crick, R. A.; Davies, M.; Almen, G., *SAMPE*, Oct. 13-15, 700-710, **1987**.

55. Pearson, R. A.; Yee, A. E, Tough Comp. Mat. Rec. Dev., Noyes Publishing, Park Ridge NJ, 157-177, **1987**.

56. Pearson, R. A.; Yee, A. F., *J. Mat. Sci., 24*(7), 2571-2580, **1989**.

57. Youqing, H.; Huiqong, W.; Xiping, Z., *SAMPE*, May 8-11, 875-883, **1989**.

58. Wang, H.; Hua, Y.; Zhang, X.; Zhang, Y.,*SAMPE, 35*, 2035-2042, **1990**.

59. Kinloch, A. J., Finch, C. A., Hashemi, S., *Polym. Comm., 28*, 322 **1987**.

60. Nir, Z.; Gilwee, W. J.; Kourtides, D. A.; Parker, J. A., *Polym. Composites, 6*(2), 65-71, **1985**.

61. Muzzy, J. D.; Kays, A. C., *Polym. Composites, 5*(3), 169-172, **1984**.

62. Paul, D. R.; Newman Ed, S., Polymer Blends, Vol. 1; Academic Press, New York, **1978**.

63. Rodriguez, F., Principles of polymer systems, 2nd ed., Mcgraw Hill, New York **1982**.

64. Pritchard, G., Developments in reinforced plastics, Applied Science, London **1980**.

65. Fu, Z.; Sun, Y.,*Polym. Prepr., 29*(2), 177-178, **1988**.

66. Hartness, J. T., Thermoplastic matrix composites, SPE. NATEC Pro., Bal Harbour, Fla., Oct., **1982**.

67. Amoco Corp., European Patent Application 89201878.9, **1989**.

68. Almen, G. R.; Mackenzie, P.; Malhotra, V.; Maskell, R. K.; McGrail, P. T.; Sefton, M. S., *SAMPE*, Sept. 27-29, 46-59, **1988**.

69. Kubel Jr., E. J.; *Adv. Materials & Processes, 136*(2) **1989**.

70. Bauer, R. S.; Stenzenberger, H. D.; Romer, W., *SAMPE*, April 2-5, 395-407, **1990**.

71. Diamont,J.; Moulton, R. J., *SAMPE*, Apr. 3-5, 422-436, **1984**.

72. Bucknall, C. B.; Gilbert, A. H., *Polymer, 30*(2), 213-217, **1989**.

73. Chen, H. H.; Schott, N. R., *Polym. Preprints, 31*(1), 457-459, **1990.**

74. Hsieh, K. H.; Han, J. L., *J. Polym. Sci.: Pt. B: Physics, 28*, 783-794, **1990.**

75. Shimp, D. A.; Hudock, F. A.; Ising, S. J., *SAMPE,* March 7-10, 754-766, **1988.**

76. Mijovic, J.; Pearce, E. M.; Foun, C. C., *Adv. Chem. Ser., 208*,293-307, **1983.**

77. Iijma, T.; Tomoi, M,; Tochimoto, T.; Kakiuchi, H., *J. of App. Polym. Sci., 43*, 463-474, **1990.**

78. Riffle, J. S.; Yorkgitis, E. M., , <u>TLSP: Final Report</u>, **1986.**

79. Van Krevelen, <u>Properties of Polymers</u>, published by Elsevier Scientific Publishing Co.

80. Smith, J. E., Connell, J. W., Hergenrother, P. M., (submitted for publication) **1994.**

81. Arnold, C. A., Summers, J. D., Chen, Y. P., Bott, R. H., Chen, D. H., McGrath, J. E., *Polymer, 30*(6), 986 **1989.**

82. Connel, J. W., Working, D. C., St. Clair, T. L., Hergenrother, P. M., in <u>Polyimides: Materials, Chemistry, and Characterization</u>, C. Feger, Ed., Technomic Pub. Co., Lancaster, PA., **1992.**

83. Young. P. R., Slemp, W. S., LDEF Materials Workshop '91, <u>NASA Conf. Pub. 3162 Part 1</u>, 376-378 **1991.**

84. Diamont, J.; Moulton, R. J., *SAMPE Quarterly, 16*(1),, 13-21, **1984.**

85. Amoco Performance Products Inc. Bound Brook, NJ, 08805

86. ICI Americas Inc., Wilmington, DE 19897.

87. Kreuchumas, A. U.S. Patent 2,822,351 **1958.**

88. Bonner, W. H., U.S. Patent, 3,065,205 **1962** (to DuPont).

89. Marks, B. M., U.S. Patent 3,441,538 **1969.**

90. Colquhoun, H. W., Lewis, D. F., British Patent 2,116,990 **1983.**

91. Janson, V., U.S. Patent 2,822,351 **1958.**

92. Janson, V., U.S. Patent 4,361,693 **1982.**

93. Dahl, K. J., U.S. Patent 3,956,240 **1976.**

94. Jansons, V., Gors, H. C., WO 84 03, 892 **1984.**

95. Effenberger, F., Epple, G., *Angew. Chem. Int. Ed., 11,* 299 **1972.**

96. Goodman, I., McIntyre, J. E., Russell, W., British Patent 971,227 **1964.**

97. Jennings, B. E., Jones, M. E. B., Rose, J. B., *J. Polym. Sci. Part C, 715* **1967.**

98. Rose, J. B., *Chem. Ind. (London), 461* **1968.**

99. Allinger, N. L., Cava, M. P., DeJongh, D. C., Johnson, C. R., Lebel, N. A., Stevens, C. L., Organic Chemistry, 2nd ed., Worth Publishers, Inc., New York, **1976.**

100. Taylor, I. C., German Patent 2,635,101 **1977.**

101. Gerd, B., Claus, C., German Patent 2,749,645 **1978.**

102. Viswanathan, R., Johnson, B. C., McGrath, J. E., *Polymer, 25,* 1827 **1984.**

103. Jensen, B. J., Hergenrother, P. M., Havens, S. J., *Polym. Prepr., 26*(2), 174 **1985.**

104. Hergenrother, P. M., Havens, S. J., Jensen, B. J., *Intl. SAMPE Tech. Conf. Series, 18,* 454 **1986.**

105. Hergenrother, P. M., Jensen, B. J., Hadvens, S. J., *Polymer, 29,* 358 **1988.**

106. Mullins, M. J., Woo, E. P., *J. Macromol. Sci. Revs. Macromol. Chem. Phys. C27*(2), 313 **1987.**

107. Rose, J. B., *Polymer, 15,* 456 **1974.**

108. Krieg, V. B., Manecke, G., *Makromol. Chem., 108,* 210 **1967.**

109. Connell, J. W., Hergenrother, P. M., *Polym. Mat. Sci. and Eng. Proc., 60,* 527 **1989.**

110. Connell, J. W., Hergenrother, P. M., *SAMPE Series, 35,* 432 **1990.**

111. Connell, J. W., Hergenrother, P. M., *High Perf. Polym., 2*(4), 211 **1990**.

112. Connell, J. W., Hergenrother, P. M., J. Polym. Sci.: Pt. A: Polym. Chem., 29, 1667 **1991**.

113. Jensen, B. J., Hergenrother, P. M., Bass, R. G., *High Performance Polym., 3*(1), 3, **1991**; *3*(1), 13, **1991**.

114. Jensen, B. J., Hergenrother, P. M., Bass, R. G., Proc. *Polym. Matl. Sci. and Eng., 60*, 294 **1989**.

115. Jensen, B. J., Hergenrother, P. M., Bass, R. G., *Polym. Prepr., 30*(2), 132 **1989**.; *31*(1), 618 **1990**.

116. Pak, S. J., Lyle, G. D., McGrath, J. E., Proceedings from 37th SAMPE Symp., March 9-12, 667 **1992**.

117. Pak, S. J., Lyle, G. D., Mercier, R., McGrath, J. E., *Polymer, 34*(4), 885 **1993**.

118. Hedrick, J. L., Yilgor, I, Jurek, M., Hedrick, J. C., Wilkes, G. L., McGrath, J. E., *Polymer, 32* (11), 2020 **1991**.

Chapter 4: Experimental

4.1 Chemicals

4.1.1 Solvents

A variety of slovents were employed in the preparation and characterization of polymers and oligomers. The following list contains general data on the solvents used, suppliers and method of purification. Density of liquids are given at 20 °C ±5 °C.

Glacial Acetic Acid

Boiling Point:	116-118°C
Supplier:	Corco Chemicals Corp.
Purification:	Used as received

Methanol

Boiling Point:	64°C
Supplier:	Fisher Chemical Co.
Purification:	Used as received

Tetrahydrofuran (THF)

Density (g/cm^3):	0.8892
Boiling Point:	67°C
Supplier:	Aldrich Chemical Co.
Purification:	Used as received

Chloroform

Density (g/cm^3):	1.4460
Boiling Point:	60.5-61.5°C
Supplier:	Aldrich Chemical Co.
Purification:	Used as received

Dichloromethane

Density (g/cm^3):	1.4460
Boiling Point:	40°C
Supplier:	Fluka Chemika
Purification:	Used as received

N,N-Dimethylacetamide (DMAc)

Density (g/cm^3):	0.937
Boiling Point:	164.5-166°C
Supplier:	Fluka Chemika

Purification: Used as received

Toluene

Boiling Point: 111°C

Supplier: Aldrich Chemical Co.

Purification: Used as received

N-Methyl-2-Pyrrolidinone (NMP)

Boiling Point: 81-82°C/10mm

Density (g/cm^3):   1.033

Supplier: Fisher Chemical Co.

Purification: Vacuum distilled

4.1.2 Monomers

Some monomers were used as received. Others were recrystallized with an appropriate solvent according to the following procedure. The monomer was dissolved in a warm solution with stirring. Activated charcoal was added and the dark solution was stirred for 20 minutes then filtered hot through a porcelain Buchner funnel using Celite® to remove the charcoal. The solution was slowly cooled to room temperature to yield crystals. The crystals were isolated by

filtration and then dried under vacuum.

The list below contains general data on the monomers used to synthesize polymers and oligomers. The structures for the dihalide monomers are presented in Table 4.1 and the bisphenol monomers are presented in Table 4.2.

Table 4.1 Structure of Various Dihalide Monomers utilized to prepare the functionalized Poly(arylene ether)s and Poly(arylene ether-co-imidazole)s

DIHALIDE	NAME	ABBREVIATION
	1,3-Bis(4-fluorobenzoyl)benzene	1,3-FBB
	1,4-Bis(4-fluorobenzoyl)benzene	1,4-FBB
	Bis(4-fluorophenyl)ketone	4-FPK

1,3-Bis(4-fluorobenzoyl)benzene (1,3-FBB)

Empirical Formula:	$C_{20}H_{12}O_2F_2$
Molecular Weight:	322.31 g/mol
Supplier:	Daychem Laboratories Inc.
Purification:	Recrystallized in toluene

1,4-Bis(4-fluorobenzoyl)benzene (1,4-FBB)

Empirical Formula:	$C_{20}H_{12}O_2F_2$
Molecular Weight:	322.31 g/mol
Supplier:	Daychem Laboratories Inc.
Purification:	Recrystallized in toluene

Bis(4-fluorophenyl)ketone (4-FPK)

Empirical Formula:	$C_{13}H_8OF_2$
Molecular Weight:	218.20 g/mol
Supplier:	Aldrich Chemical Co.
Purification:	Recrystallized in toluene
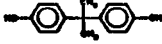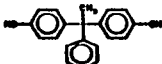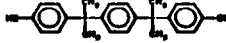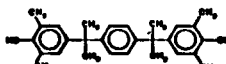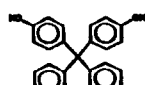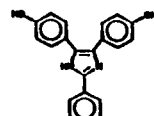
BISPHENOL	NAME	ABBREVIATION
	Bisphenol A	Bis A
	1-Methyl-1-phenyl-[4-hydroxyphenyl]methane	Bis AP
	1,4-Bis[(4-hydroxyphenyl)2-propyl]benzene	1,4-HPB
	1,4-Bis[(4-hydroxy-3,5-dimethyl phenyl)-2-propyl]benzene	1,4-HDMPB
	Bis(4-hydroxyphenyl)methane	4-HPM
	9,9-Bis(4-hydroxyphenyl)fluorene	9,9-HPF
	2-Phenyl-4,5-bis(4-hydroxyphenyl imidazole	DHI

Table 4.2 Bisphenol Monomers utilized to prepare the functionalized Poly(arylene ether)s and Poly(arylene ether-co-imidazole)s

Bisphenol A (Bis A)

Empirical Formula:	$C_{15}H_{16}O_2$
Molecular Weight:	228.27 g/mol
Melting Point:	154-155°
Supplier:	Aldrich Chemical Co.
Purification:	Recrystallized in toluene

1-Methyl-1-phenyl bis(4-hydroxyphenyl)methane (Bis AP)

Empirical Formula:	$C_{20}H_{18}O_2$
Molecular Weight:	290.36 g/mol
Supplier:	Kennedy and Klim Inc.
Purification:	Recrystallized in toluene

1,4-Bis[(4-hydroxyphenyl)-2-propyl]benzene (1,4-HPB)

Empirical Formula:	$C_{24}H_{26}O_2$
Molecular Weight:	346.47 g/mol
Supplier:	Shell Chemical Co.
Purification:	Recrystallized in Ethanol/H_2O

1,4-Bis[(4-hydroxy-3,5-dimethylphenyl)-2-propyl]benzene (1,4-HDMPB)

Empirical Formula:	$C_{28}H_{38}O_2$
Molecular Weight:	406.61 g/mol
Supplier:	Shell Chemical Co.
Purification:	Recrystallized in Ethanol/H_2O

Bis(4-hydroxyphenyl)methane (4-HPM)

Empirical Formula:	$C_{13}H_{12}O_2$
Molecular Weight:	200.24 g/mol
Supplier:	Aldrich Chemical Co.

Purification: Used as recieved

9,9-Bis(4-hydroxyphenyl)fluorene (9,9-HPF)

Empirical Formula: $C_{25}H_{18}O_2$

Molecular Weight: 350.42 g/mol

Supplier: Kennedy and Klim Inc.

Purification: Recrystallized in toluene

2-Phenyl-4,5-bis(4-hydroxyphenyl imidazole) (DHI)

Empirical Formula: $C_{21}H_{16}O_2N_2$

Molecular Weight: 328.37 g/mol

Supplier: Daychem Laboratories Inc.

Purification: Recrystallized in Ethanol/Water

4.1.3 Other Chemicals

The following list contains general data on the other chemicals used in monomer or polymer synthesis and characterization including suppliers and methods of purification.

Potassium Carbonate

Molecular Weight: 138.21 g/mol

Supplier: Fisher

Purification: Used as received

4,4'-Dimethoxy benzil (anisil)

Empirical Formula: $C_{16}H_{14}O_4$

Molecular Weight: 270.28 g/mol

Supplier: Midori Kagaku Co.

Purification: Used as recieved

Benzaldehyde

Empirical Formula: C_7H_6O

Molecular Weight: 106.12 g/mol

Supplier: Fisher Chemical Co.

Purification: Vacuum Distilled

Hydrobromic Acid (48 %)

Supplier: Aldrich Chemical Co.

Purification: Used as received

Anhydrous Ammonium Acetate

Molecular Weight: 77.08 g/mol

Supplier: Aldrich Chemical Co.

Purification: Used as received

1,4-Dioxane

Molecular Weight: 88.11 g/mol

Supplier: Fisher Chemical Co.

Purification: Used as received

Trimethylaminesilane

Empirical Formula: $Si(CH_3)_3NH$

Molecular Weight: 88.09 g/mol

Purification: Used as received

Trimethylchlorosilane

Empirical Formula: $Si(CH_3)_3Cl$

Molecular Weight: 108.45 g/mol

Purification: Used as received

Triethylamine

Empirical Formula: $(CH_3CH_2)_3N$

Molecular Weight: 101.19 g/mol

Supplier: Aldrich Chemical Co.

Purification: Used as received

4,4'-Diaminodiphenyl sulphone (DDS)

Empirical Formula: $C_{12}H_{12}N_2O_2S$

Molecular Weight: 248.30 g/mol

Supplier: Aldrich Chemical Co.

Melting Point: 175-177 °C

Purification: Used as received

4.1.4 Epoxies

N,N,N',N'-Tetraglycidyl-4,4'-methylenebisbenzenamine (TGMDA)

Manufacture Name: Araladite® MY 720

Supplier: Ciba-Geigy

Weight per epoxide: 117

Purification: Used as received

N,N,N',N'-Tetraglycidyl-4,4'-methylenebisbenzenamine (TGMDA)

Manufacture Name: Araladite® MY 721

Supplier: Ciba-Geigy

Weight per epoxide: 110

Purification: Used as received

N,N,N',N'-Tetraglycidyl-4,4'-methylenebisbenzenamine (TGMDA)

Manufacture Name:	Araladite® XU 722
Supplier:	Ciba-Geigy
Weight per epoxide:	125
Purification:	Used as received

Diglycidyl ether of 4-aminophenol

Manufacture Name:	Araladite® MY 0510
Supplier:	Ciba-Geigy
Weight per epoxide:	95-107
Purification:	Used as received

Diglycidyl-9,9'-bis(4-hydroxyphenyl)fluorene (DGEHF)

Manufacture Name:	Epon HPT® Resin 1079
Supplier:	Shell Chemical Co.
Weight per epoxide:	240-270
Purification:	Used as received

N,N,N',N'-tetraglycidyl-α,α'-bis(4-aminophenyl)-p-diisopropylbenzene(TGAI)

Manufacture Name:	Epon HPT® Resin 1071
Supplier:	Shell Chemical Co.
Weight per epoxide:	150-185

Purification: Used as received

N,N,N',N'-tetraglycidyl-α,α'-bis(4-amino-3,5-dimethylphenyl)-p-diisopropylbenzene (TGAMI)

Manufacture Name: Epon HPT® Resin 1072

Supplier: Shell Chemical Co.

Weight per epoxide: 150-185

Purification: Used as received

Triglycidyl tris(hydroxyphenyl) methane (TGHPM)

Manufacture Name: Tactix® 742 Resin

Supplier: Dow Plastics

Weight per epoxide: 150-170

Purification: Used as received

4.2 Synthesis

4.2.1 Bis(imidazole phenol) Monomers

4.2.1.1 2-Phenyl-4,5-bis(4-methoxyphenyl)imidazole

The reaction is outlined in Figure 4.1 (reaction A). Into a 3L, three-neck round bottom flask, equipped with a mechanical stirrer was charged 4,4'-dimethoxybenzil (94.4 g, 0.35 mol) and acetic acid (750 mL). The mixture was stirred and warmed to give a yellow solution. Freshly distilled benzaldehyde (50 g, 0.47 mol), ammonium acetate (500 g, 6.5 mol) and acetic acid (500 mL) were subsequently added. The mixture was heated to reflux (~ 120 °C) overnight (16 hr). The orange solution was cooled and poured into water to give a white solid. The solid was collected, washed in water and dried at 125 °C for 3.5 hr. The solid was recrystallized from ethanol (1000 mL) and water (500 mL) and air dried: yield 239.2 g (96%); mp 202 °C (lit.[1] mp 197.5 -198 °C.)

4.2.1.2 Demethylation

Figure 4.1 (reaction B) outlines the demethylation of 2-phenyl-4,5-bis(4-methoxyphenyl)imidazole. 2-Phenyl-4,5-bis(4-methoxyphenyl)imidazole (66.2 g, 0.185 mol), acetic acid (250 mL) and 47-49% aqueous hydrobromic acid solution

(1000 mL) were placed into a 2L, three-neck round bottom flask equipped with a

mechanical stirrer, nitrogen inlet, thermometer, reflux condenser and HBr gas trap.

The mixture was heated to reflux (~120 °C) overnight (~ 16 hr) under nitrogen.

The mixture was cooled and the solid collected, dissolved in sodium hydroxide

solution and the pH adjusted to neutral using concentrated hydrochloric acid. The

resulting white precipitate was collected, washed in water and dried 4 hr at 125 °C:

yield 57.8 g (87%); mp 318-320 °C. The solid was recrystallized from N,N-

dimethylacetamide (DMAc) (300 mL) and water (250 mL) using activated charcoal.

The crystals were collected and dried for 12 hr at 150 °C under vacuum: yield 38.9

g (67%); mp 326-328 °C (lit.[2] 327-330 °C).
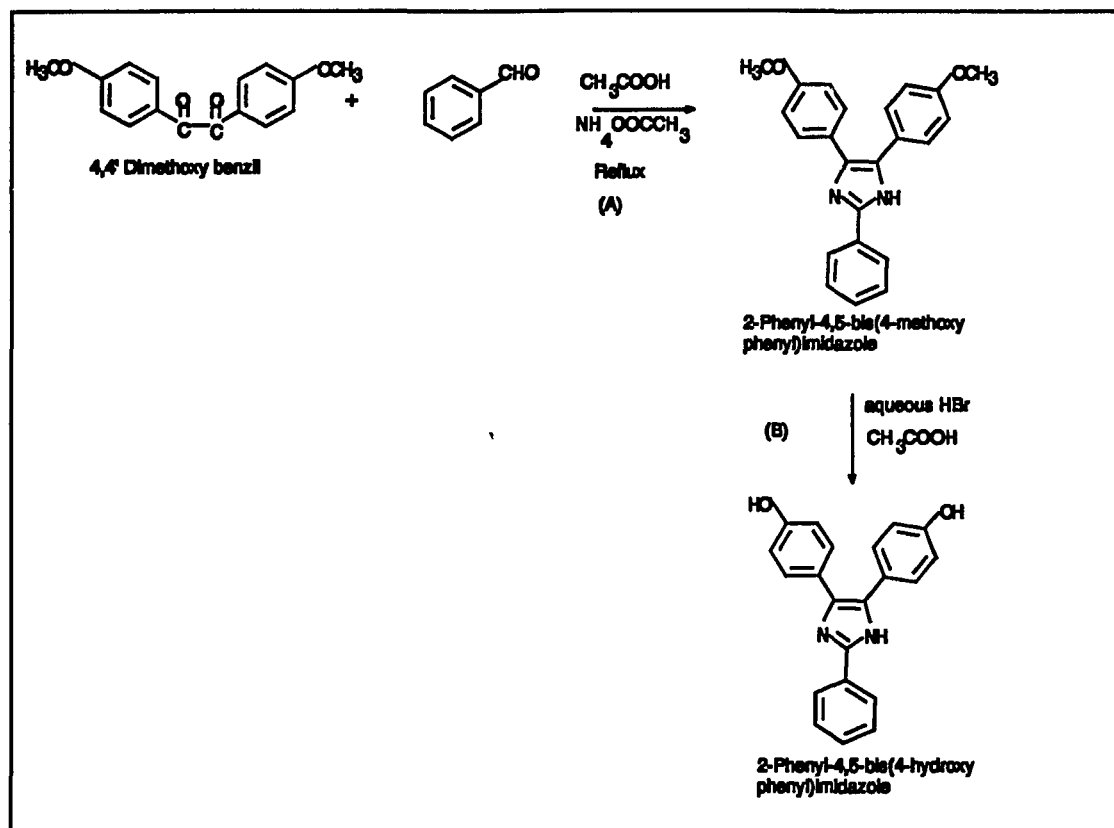
Figure 4.1 Synthesis of 2-Phenyl-4,5-bis(4-hydroxyphenyl) imidazole

4.3 2-Phenyl-4,5-bis(4-trimethylsilyloxy phenyl)imidazole

Procedure 1:

2-Phenyl-4,5-bis(4-hydroxy phenyl)imidazole (DHI; 10 g; 0.03 mol) and trimethylaminesilane (5.37 g; 0.06 mol) were charged into a 100 mL round bottom three-neck flask equipped with a mechanical stirrer, thermometer, N_2 inlet, and reflux condenser. 1,4-dioxane (100 mL) was added and the solution was heated

overnight under nitrogen, using an oil bath (Figure 4.2 reaction A). The insoluble material was separated by filtration through a sintered glass funnel. 1,4-Dioxane was removed by rotary evaporation under vacuum and the solids washed with hot hexanes.
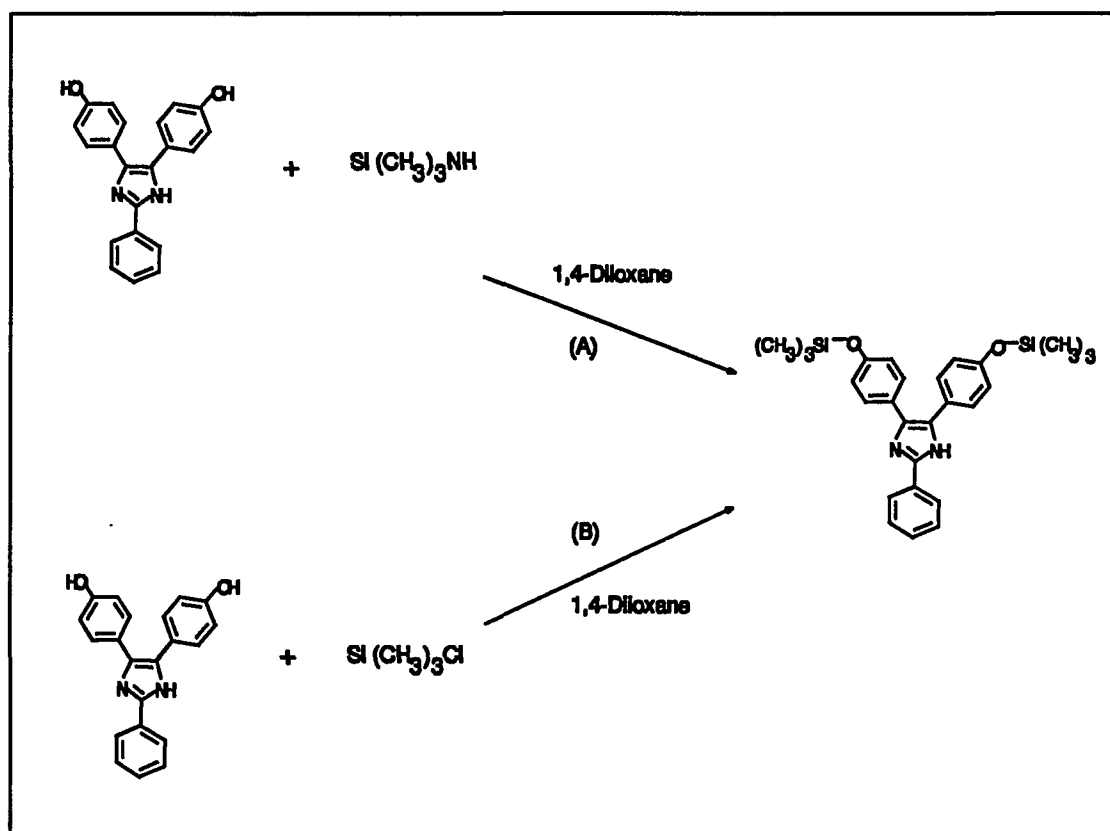
Figure 4.3 Synthesis of Silyated Diphenols

Procedure 2:

2-Phenyl-4,5-bis(4-hydroxy phenyl)imidazole (DHI; 5 g; 0.015 mol) and trimethylchlorosilane (3.31 g; 0.03 mol), and triethylamine (3.40 g; 0.03) were

charged into a 100 mL round bottom three-neck flask equipped with a mechanical stirrer, thermometer, N$_2$ inlet, and reflux condenser. 1,4-dioxane (100mL) was added and the solution was heated to reflux in an oil bath overnight (Figure 4.2 reaction B). The insoluble material was separated by filtration through a sintered glass funnel. 1,4-Dioxane was removed by rotary evaporation under vacuum and the solids washed with hot hexanes.

4.4 Synthesis of Poly(arylene ether)s from Silyated Diphenols

2-Phenyl-4,5-bis(4-trimethylsilyloxy phenyl)imidazole (1.93 g; 0.004 mol) and bis(4-fluorophenyl)ketone (0.89 g; 0.004 mol) were charged into a three-neck flask equipped with a mechanical stirrer, nitrogen inlet, thermometer, condenser and Dean-Stark moisture trap. The reactants were dissolved in 10 mL of N,N'-dimethylacetamide (DMAc; 20% solids) and 45 mL toluene. Potassium carbonate (K$_2$CO$_3$; 1.3 g; 0.009 mol) was added. The mixture was heated using an oil bath and purged with nitrogen until the toluene began to reflux (approximately 110 to 120 °C). The solution was refluxed 4 hours. Toluene was removed from the system via the Dean-Stark trap and the temperature increased to 140-150 °C. Heating was continued for an additional 16 hours, resulting in a light brown solution. The polymer was precipitated in a water/glacial acetic acid mixture in a blender. The light brown polymer was isolated by filtration, stirred in hot water (90-95 °C) for 1-2 hours then stirred in hot methanol (55-60 °C) for 1-2 hours to

remove any trapped salts, collected, and dried under vacuum 10 hours at 150-175 °C.

4.5 2,4,5-Triphenyl Imidazole
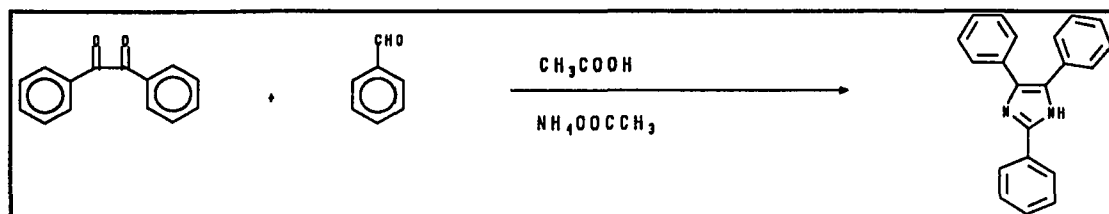
Figure 4.4 Synthesis of 2,4,5-Triphenylimidazole

Benzil (35.51 g; 0.17 mol) and acetic acid (283 mL; 15 % solids) were charged into a 1L three-neck flask equipped with a mechanical stirrer, nitrogen inlet, thermometer, and reflux condenser. The mixture was stirred and warmed via a heating mantle until all solids had dissolved into a bright yellow solution. Benzaldehyde (18.82 g; 0.18 mol) and solid anhydrous ammonium acetate (235 g; 3.05 mol) were added to the flask and rinsed in with an additional 190 mL acetic acid. The flask was wrapped in glass wool to retain heat and refluxed approximately 16 hours under nitrogen at 120 °C. The yellow solution was cooled, filtered through sintered glass and poured into ice water to yield a white solid. The solid was isolated by filtration, washed in water, collected and dried under vacuum at 175 °C for 8 hours: yield 45.97 g (92 %). The crude solid was recrystallized in methanol to yield shiny white crystals: yield 23.71 g (52%); mp 278 °C. lit. [lit.

275-278 °C].

4.6 Synthesis of Poly(arylene ether)s and Poly(arylene ether-co-imidazole)s
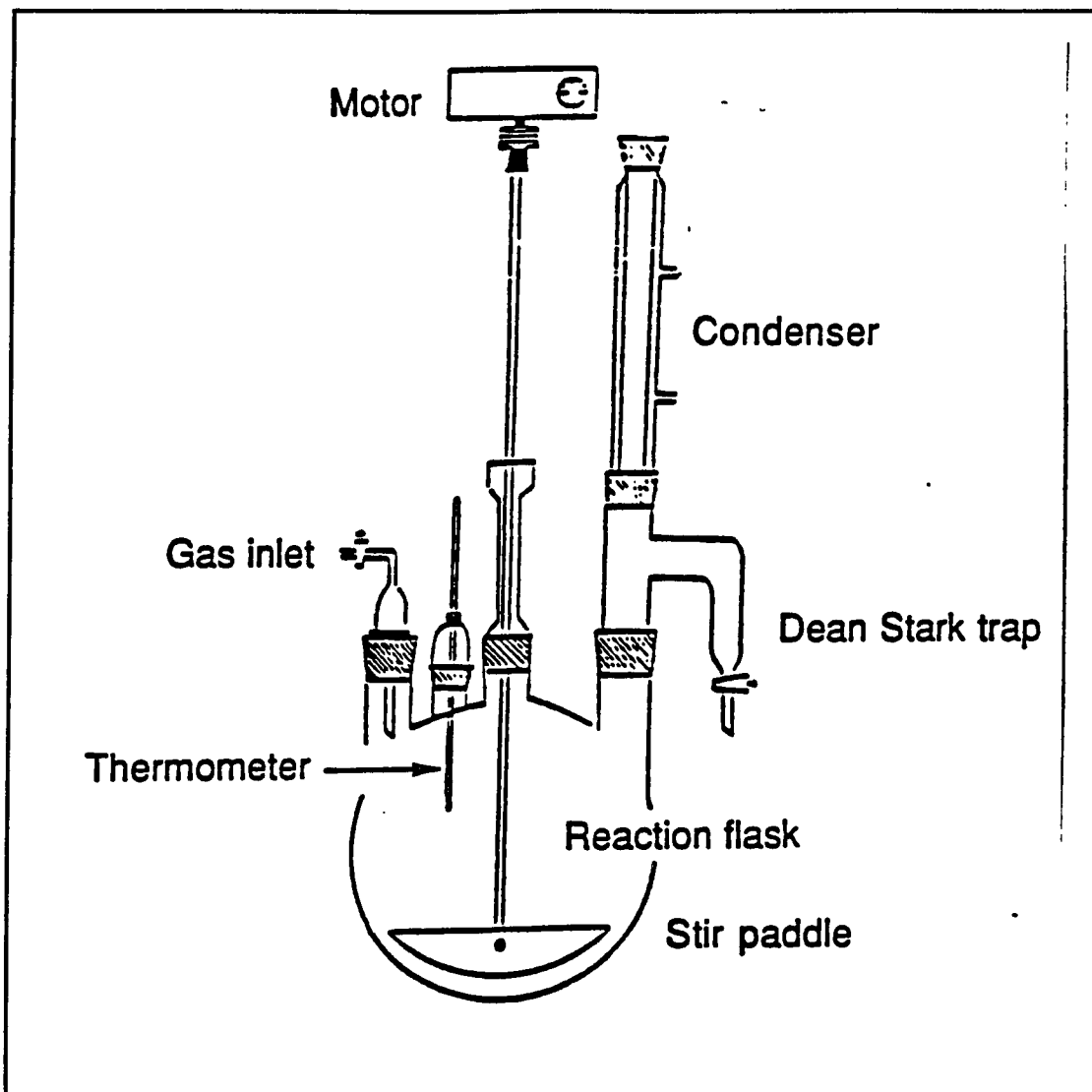
Figure 4.5 Reaction Apparatus for Polymer Synthesis
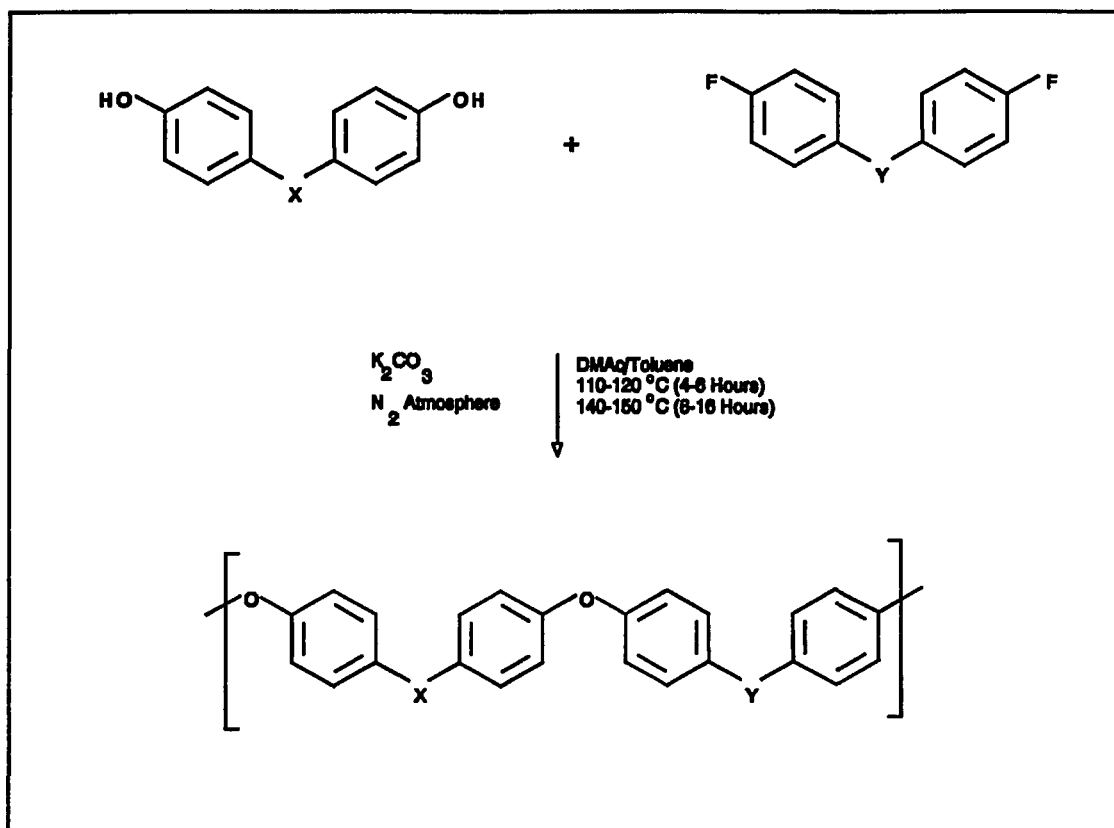
Figure 4.6 Synthetic Scheme for Poly(arylene ether)s

4.6.1 9,9-HPF/4-FPK (PAE-1)

Into a 100 mL three-neck flask equipped with a mechanical stirrer, nitrogen inlet, thermometer, condenser and Dean-Stark moisture trap (Figure 4.5) were placed 9,9-bis(4-hydroxylphenyl)fluorene (9,9-HPF; 3.3145 g; 9.5 x 10^{-3} mol); bis-(4-fluorophenyl)ketone (4-FPK; 2.0639 g; 9.5 x 10^{-3} mol); pulverized anhydrous potassium carbonate (3.00 g; 0.02 mol); toluene (45 mL) and N, N-dimethylacetamide (DMAc; 20 mL; 20% solids). The mixture was heated in an oil

bath and purged with nitrogen until the toluene began to reflux (approximately 110 to 120 °C). The solution was refluxed 4 hours, toluene was removed from the reaction medium via the Dean-Stark trap and the temperature increased to 140-150 °C. Heating was continued for an additional 16 hours, resulting in a viscous, orange solution. The reaction mixture was precipitated in water/glacial acetic acid mixture in a blender. The precipitated white polymer was isolated by filtration, stirred in hot water (90-95 °C) for 1-2 hours then, stirred in hot methanol (55-60 °C) for 1-2 hours to remove trapped salts, collected, and dried under vacuum for 8 hours at 150-175 °C: yield 4.86 g (97%); Tg 250 °C; η_{inh} 0.61 dL/g, $CHCl_3$, 35°C

.

4.6.2 Bis-A/1,3-FBB (PAE-2)

Into a 100 mL three-neck flask equipped with a mechanical stirrer, nitrogen inlet, thermometer, condenser and Dean-Stark moisture trap were placed bisphenol A (Bis A; 2.2829 g; 0.0100 mol); 1,3-bis(4-fluorobenzoyl)benzene (1,3-FBB; 3.2231 g; 0.0100 mol); pulverized anhydrous potassium carbonate (3.18 g; 0.02 mol); toluene (45 mL) and N, N-dimethylacetamide (DMAc; 20 mL; 20% solids). The mixture mixture was heated in an oil bath and purged with nitrogen until the toluene began to reflux (approximately 110 to 120 °C). The solution was refluxed 4 hours, toluene was removed from the reaction medium via the Dean-Stark trap and the temperature increased to 140-150 °C. Heating was continued for an

additional 16 hours, resulting in a viscous, orange solution. The reaction mixture was precipitated in water/glacial acetic acid mixture in a blender. The precipitated white polymer was isolated by filtration, stirred in hot water (90-95 °C) for 1-2 hours, then stirred in hot methanol (55-60 °C) for 1-2 hours to remove trapped salts, collected, and dried under vacuum for 8 hours at 150-175 °C: yield 4.21 g (84%); Tg 150 °C; η_{inh} 1.38 dL/g, CHCl$_3$, 35 °C.

4.6.3 1,4-HDMPB/1,3-FBB (PAE-3)

Into a 100 mL three-neck flask equipped with a mechanical stirrer, nitrogen inlet, thermometer, condenser and Dean-Stark moisture trap were placed 1,4-bis[(4-hydroxy-3,5-dimethylphenyl)-2-propyl]benzene (1,4-HDMPB; 2.9391 g; 7.3 x 10^{-3} mol); 1,3-bis(4-fluorobenzoyl)benzene (1,3-FBB; 2.3531 g; 7.3 x 10^{-3} mol); pulverized anhydrous potassium carbonate (2.32 g; 0.02 mol); toluene (45 mL) and N, N-dimethylacetamide (DMAc; 20 mL; 20% solids). The mixture was heated in an oil bath and purged with nitrogen until the toluene began to reflux (approximately 110 to 120 °C). The solution was refluxed 4 hours, toluene was removed from the reaction medium via the Dean-Stark trap and the temperature increased to 140-150 °C. Heating was continued for an additional 16 hours, resulting in a viscous, yellow solution. The reaction mixture was precipitated in water/glacial acetic acid mixture in a blender. The precipitated white polymer was isolated by filtration, stirred in hot water (90-95 °C) for 1-2 hours, then stirred in hot

methanol (55-60 °C) for 1-2 hours to remove trapped salts, collected, and dried under vacuum for 8 hours at 150-175 °C: yield 2.92 g (58%); Tg 192 °C; η_{inh} 1.14 dL/g, $CHCl_3$, 35 °C.

4.6.4 1,4-HPB/1,4-FBB (PAE-4)

Into a 100 mL three-neck flask equipped with a mechanical stirrer, nitrogen inlet, thermometer, condenser and Dean-Stark moisture trap were placed 1,4-bis[(4-hydroxyphenyl)-2-propyl]benzene (1,4-HPB; 5.5103 g; 0.0159 mol); 1,4-bis(4-fluorobenzoyl)benzene (1,4-FBB; 5.1261 g; 0.0159 mol); pulverized anhydrous potassium carbonate (5.06 g; 0.04 mol); toluene (45 mL) and N, N-dimethylacetamide (DMAc; 40 mL; 20% solids). The mixture was heated in an oil bath and purged with nitrogen until the toluene began to reflux (approximately 110 to 120 °C). The solution was refluxed 4 hours, toluene was removed from the reaction medium via the Dean-Stark trap and the temperature increased to 140-150 °C. Heating was continued for an additional 16 hours, resulting in a viscous, yellow solution. The reaction mixture was precipitated in water/glacial acetic acid mixture in a blender. The precipitated white polymer was isolated by filtration, stirred in hot water (90-95 °C) for 1-2 hours, then stirred in hot methanol (55-60 °C) for 1-2 hours to remove trapped salts, collected, and dried under vacuum for 8 hours at 150-175 °C: yield 4.54 g (45%); Tg gel; η_{inh} gel.

4.6.5 Bis-AP/4-FPK (PAE-5)

Into a 100 mL three-neck flask equipped with a mechanical stirrer, nitrogen inlet, thermometer, condenser and Dean-Stark moisture trap were placed 1-methyl-1-phenyl bis(4-hydroxyphenyl)methane (Bis AP; 6.4161 g; 0.0220 mol); bis-(4-fluorophenyl)ketone (4-FPK; 4.8217 g; 0.0220 mol); pulverized anhydrous potassium carbonate (7.02 g; 0.05 mol); toluene (45 mL) and N, N-dimethylacetamide (DMAc; 40 mL; 20% solids). The mixture was heated in an oil bath and purged with nitrogen until the toluene began to reflux (approximately 110 to 120 °C). The solution was refluxed 4 hours, toluene was removed from the reaction medium via the Dean-Stark trap and the temperature increased to 140-150 °C. Heating was continued for an additional 16 hours, resulting in a viscous, yellow solution. The reaction mixture was precipitated in water/glacial acetic acid mixture in a blender. The precipitated white polymer was isolated by filtration, stirred in hot water (90-95 °C) for 1-2 hours, then stirred in hot methanol (55-60 °C) for 1-2 hours to remove trapped salts, collected, and dried under vacuum for 8 hours at 150-175 °C: yield 4.86 g (49%); Tg 160 °C; η_{inh} 1.79 dL/g, $CHCl_3$, 35 °C.

4.6.6 1,4-HPB/1,3-FBB (PAE-6)

Into a 100 mL three-neck flask equipped with a mechanical stirrer, nitrogen

inlet, thermometer, condenser and Dean-Stark moisture trap were placed 1,4-bis[(4-hydroxyphenyl)-2-propyl]benzene (1,4-HPB; 5.5103 g; 0.0159 mol); 1,3-bis(4-fluorobenzoyl)benzene (1,3-FBB; 5.1261 g; 0.0159 mol); pulverized anhydrous potassium carbonate (7.58 g; 0.05 mol); toluene (45 mL) and N, N-dimethylacetamide (DMAc; 40 mL; 20% solids). The mixture was heated in an oil bath and purged with nitrogen until the toluene began to reflux (approximately 110 to 120 °C). The solution was refluxed 4 hours, toluene was removed from the reaction medium via the Dean-Stark trap and the temperature increased to 140-150 °C. Heating was continued for an additional 16 hours, resulting in a viscous, yellow solution. The reaction mixture was precipitated in water/glacial acetic acid mixture in a blender. The precipitated white polymer was isolated by filtration, stirred in hot water (90-95 °C) for 1-2 hours, then stirred in hot methanol (55-60 °C) for 1-2 hours to remove trapped salts, collected, and dried under vacuum for 8 hours at 150-175 °C: yield 8.33 g (83%); Tg 157 °C; η_{inh} 1.23 dL/g, CHCl$_3$, 35 °C.

4.6.7 DHI/1,3-FBB (PAEI-1)

Into a 100 mL three-neck flask equipped with a mechanical stirrer, nitrogen inlet, thermometer, condenser and Dean-Stark moisture trap (Figure 4.5) were placed 2-phenyl-4,5-bis(4-hydroxyphenyl)imidazole (DHI; 2.6886 g; 8.2 x 10^{-3} mol); 1,3-bis(4-fluorobenzoyl)benzene (1,3-FBB; 2.6390 g; 8.2 x 10^{-3} mol); pulverized

anhydrous potassium carbonate (2.60 g; 0.02 mol); toluene (45 mL) and N, N-dimethylacetamide (DMAc; 20 mL; 20% solids). The mixture was heated in an oil bath and purged with nitrogen until the toluene began to reflux (approximately 110 to 120 °C). The solution was refluxed 4 hours, toluene was removed from the reaction medium via the Dean-Stark trap and the temperature increased to 140-150 °C. Heating was continued for an additional 16 hours, resulting in a viscous, dark orange solution. The reaction mixture was precipitated in water/glacial acetic acid mixture in a blender. The precipitated white polymer was isolated by filtration, stirred in hot water (90-95 °C) for 1-2 hours, then stirred in hot methanol (55-60 °C) for 1-2 hours to remove trapped salts, collected, and dried under vacuum for 8 hours at 150-175 °C: yield 4.93 g (99%); Tg 220 °C; η_{inh} 0.71 dL/g, DMAc, 35 °C.

4.6.8 DHI/4-FPK (PAEI-2)

Into a 100 mL three-neck flask equipped with a mechanical stirrer, nitrogen inlet, thermometer, condenser and Dean-Stark moisture trap were placed 2-phenyl-4,5-bis(4-hydroxyphenyl)imidazole (DHI; 3.2412 g; 9.9 x 10^{-3} mol); bis-(4-fluorophenyl)ketone (4-FPK; 2.1538 g; 9.9 x 10^{-3} mol); pulverized anhydrous potassium carbonate (3.14 g; 0.02 mol); toluene (45 mL) and N, N-dimethylacetamide (DMAc; 20 mL; 20% solids). The mixture was heated in an oil bath and purged with nitrogen until the toluene began to reflux (approximately 110

to 120 °C). The solution was refluxed 4 hours, toluene was removed from the reaction medium via the Dean-Stark trap and the temperature increased to 140-150 °C. Heating was continued for an additional 16 hours, resulting in a viscous, yellow solution. The reaction mixture was precipitated in water/glacial acetic acid mixture in a blender. The precipitated white polymer was isolated by filtration, stirred in hot water (90-95 °C) for 1-2 hours, then stirred in hot methanol (55-60 °C) for 1-2 hours to remove trapped salts, collected, and dried under vacuum for 8 hours at 150-175 °C: yield 4.84 g (97%); Tg 242 °C; η_{inh} 0.32 dL/g, DMAc, 35 °C.

4.6.9   4-HPM/DHI/4-FPK (PAE-co-I-1)

Into a 100 mL three-neck flask equipped with a mechanical stirrer, nitrogen inlet, thermometer, condenser and Dean-Stark moisture trap were placed 4-hydroxyphenyl)methane (4-HPM; 1.9021 g; 9.5 x 10^{-3} mol); 2-phenyl-4,5-bis(4-hydroxyphenyl)imidazole (DHI; 0.3466 g; 1.0 x 10^{-3} mol); bis-(4-fluorophenyl)ketone (4-FPK; 2.3031 g; 1.1 x 10^{-3} mol); pulverized anhydrous potassium carbonate (4.06 g; 0.03 mol); toluene (45 mL) and N, N-dimethylacetamide (DMAc; 20 mL; 20% solids). The mixture was heated in an oil bath and purged with nitrogen until the toluene began to reflux (approximately 110 to 120 °C). The solution was refluxed 4 hours, toluene was removed from the reaction medium via the Dean-Stark trap and the temperature increased to 140-150 °C. Heating was continued for an

additional 16 hours, resulting in a viscous, dark orange solution. The reaction mixture was precipitated in water/glacial acetic acid mixture in a blender. The precipitated white polymer was isolated by filtration, stirred in hot water (90-95 °C) for 1-2 hours, then stirred in hot methanol (55-60 °C) for 1-2 hours to remove trapped salts, collected, and dried under vacuum for 8 hours at 150-175 °C: yield 4.01 g (97%); Tg 146 °C; η_{inh} insoluble in THF, DMAc, NMP, $CHCl_3$, CH_2Cl_2.

4.6.10 Bis-AP/DHI/4-FPK (PAE-co-I-2)

Into a 100 mL three-neck flask equipped with a mechanical stirrer, nitrogen inlet, thermometer, condenser and Dean-Stark moisture trap were placed 1-methyl-1-phenyl bis(4-hydroxyphenyl)imidazole (Bis-AP; 1.5287 g; 5.3 x 10^{-3} mol); 2-phenyl-4,5-bis(4-hydroxyphenyl)imidazole (DHI; 0.1921 g; 5.8 x 10^{-4} mol); bis-(4-fluorophenyl)ketone (4-FPK; 1.2764 g; 5.9 x 10^{-3} mol); pulverized anhydrous potassium carbonate (1.86 g; 0.01 mol); toluene (45 mL) and N, N-dimethylacetamide (DMAc; 10 mL; 20% solids). The mixture was heated in an oil bath and purged with nitrogen until the toluene began to reflux (approximately 110 to 120 °C). The solution was refluxed 4 hours, toluene was removed from the reaction medium via the Dean-Stark trap and the temperature increased to 140-150 °C. Heating was continued for an additional 16 hours, resulting in a viscous, yellow orange solution. The reaction mixture was precipitated in water/glacial acetic acid mixture in a blender. The precipitated white polymer was isolated by

filtration through, in hot water (90-95 °C) for 1-2 hours, then stirred in hot methanol (55-60 °C) for 1-2 hours to remove trapped salts, collected, and dried under vacuum for 8 hours at 150-175 °C: yield 1.53 g (61%); Tg 186 °C; η_{inh} 0.91 dL/g, THF, 35 °C.

4.6.11 HPB/DHI/1,3-FBB (PAE-co-I-3)

Into a 100 mL three-neck flask equipped with a mechanical stirrer, nitrogen inlet, thermometer, condenser and Dean-Stark moisture trap were placed 1,4-bis[(4-hydroxyphenyl)-2-propyl]benzene (HPB; 12.4339 g; 0.0359 mol); 2-phenyl-4,5-bis(4-hydroxyphenyl)imidazole (DHI; 1.3094 g; 4.0 x 10^{-3} mol); 1,3-bis(4-fluorobenzoyl)benzene (1,3-FBB; 12.8522 g; 0.0399 mol); pulverized anhydrous potassium carbonate (19.01 g; 0.14 mol); toluene (45 mL) and N, N-dimethylacetamide (DMAc; 107 mL; 20% solids). The mixture was heated in an oil bath and purged with nitrogen until the toluene began to reflux (approximately 110 to 120 °C). The solution was refluxed 4 hours, toluene was removed from the reaction medium via the Dean-Stark trap and the temperature increased to 140-150 °C. Heating was continued for an additional 16 hours, resulting in a viscous, orange solution. Some gel particles adhered to the reaction vessel resulting in a lower yeild. The remaining reaction mixture was precipitated in water/glacial acetic acid mixture in a blender. The precipitated white polymer was isolated by filtration, stirred in hot water (90-95 °C) for 1-2 hours, then stirred in hot methanol (55-60

°C) for 1-2 hours to remove trapped salts, collected, and dried under vacuum for 8 hours at 150-175 °C: yield 22.14 g (89%); Tg 159 °C; η_{inh} 0.50 dL/g, CH_2Cl_2, 35 °C.

4.6.12 HPB/DHI/1,4-FBB (PAE-co-I-4)

Into a 100 mL three-neck flask equipped with a mechanical stirrer, nitrogen inlet, thermometer, condenser and Dean-Stark moisture trap were placed 1,4-bis[(4-hydroxyphenyl)-2-propyl]benzene (HPB; 2.5158 g; 7.3 x 10^{-3} mol); 2-phenyl-4,5-bis(4-hydroxyphenyl)imidazole (DHI; 0.2649 g; 8.1 x 10^{-4} mol); 1,4-bis(4-fluorobenzoyl)benzene (1,4-FBB; 2.6005 g; 8.1 x 10^{-3} mol); pulverized anhydrous potassium carbonate (2.54 g; 0.02 mol); toluene (45 mL) and N, N-dimethylacetamide (DMAc; 20 mL; 20% solids). The mixture was heated in an oil bath and purged with nitrogen until the toluene began to reflux (approximately 110 to 120 °C). The solution was refluxed 4 hours, toluene was removed from the reaction medium via the Dean-Stark trap and the temperature increased to 140-150 °C. Heating was continued for an additional 16 hours, resulting in a viscous, orange solution. The reaction mixture was precipitated in water/glacial acetic acid mixture in a blender. The precipitated white polymer was isolated by filtration, stirred in hot water (90-95 °C) for 1-2 hours, then stirred in hot methanol (55-60 °C) for 1-2 hours to remove trapped salts, collected, and dried under vacuum for 8 hours at 150-175 °C: yield 4.77 g (95%); Tg gel; η_{inh} gel.

4.6.13 9,9-HPF/DHI/4-FPK (PAE-co-I-5)

Into a 100 mL three-neck flask equipped with a mechanical stirrer, nitrogen inlet, thermometer, condenser and Dean-Stark moisture trap were placed 9,9-bis(4-hydroxylphenyl)fluorene (9,9-HPF; 2.9956 g; 8.5 x 10^{-3} mol); 2-phenyl-4,5-bis(4ydroxyphenyl)imidazole (DHI; 0.3119 g; 9.5 x 10^{-4} mol); bis-(4-fluorophenyl)ketone (4-FPK; 2.0726 g; 9.5 x 10^{-3} mol); pulverized anhydrous potassium carbonate (2.76 g; 0.02 mol); toluene (45 mL) and N, N-dimethylacetamide (DMAc; 20 mL; 20% solids). The mixture was heated in an oil bath and purged with nitrogen until the toluene began to reflux (approximately 110 to 120 °C). The solution was refluxed 4 hours, toluene was removed from the reaction medium via the Dean-Stark trap and the temperature increased to 140-150 °C. Heating was continued for an additional 16 hours, resulting in a viscous, dark orange solution. The reaction mixture was precipitated in water/glacial acetic acid mixture in a blender. The precipitated white polymer was isolated by filtration, stirred in hot water (90-95 °C) for 1-2 hours, then stirred in hot methanol (55-60 °C) for 1-2 hours to remove trapped salts, collected, and dried under vacuum for 8 hours at 150-175 °C: yield 4.65 g (93%); Tg 237 °C; η_{inh} 0.63, $CHCl_3$, 35 °C.

4.6.14 1,4-HDMPB/DHI/1,4-FBB (PAE-co-I-6)

Into a 100 mL three-neck flask equipped with a mechanical stirrer, nitrogen

inlet, thermometer, condenser and Dean-Stark moisture trap were placed 1,4-bis[(4-hydroxy-3,5-dimethylphenyl)-2-propyl]benzene (1,4-HDMPB; 10.7420 g; 2.6 x 10^{-3} mol); 2-phenyl-4,5-bis(4-hydroxyphenyl)imidazole (DHI; 0.9643 g; 2.9 x 10^{-4} mol); 1,4-bis(4-fluorobenzoyl)benzene (1,4-FBB; 9.4647 g; 2.9 x 10^{-3} mol); pulverized anhydrous potassium carbonate (9.33 g; 0.07 mol); toluene (45 mL) and N, N-dimethylacetamide (DMAc; 80 mL; 20% solids). The mixture was heated in an oil bath and purged with nitrogen until the toluene began to reflux (approximately 110 to 120 °C). The solution was refluxed 4 hours, toluene was removed from the reaction medium via the Dean-Stark trap and the temperature increased to 140-150 °C. Heating was continued for an additional 16 hours, resulting in a viscous, orange solution. The reaction mixture was precipitated in water/glacial acetic acid mixture in a blender. The precipitated white polymer was isolated by filtration, stirred in hot water (90-95 °C) for 1-2 hours, then stirred in hot methanol (55-60 °C) for 1-2 hours to remove trapped salts, collected, and dried under vacuum for 8 hours at 150-175 °C: yield 18.5 g (93%); Tg 207; η_{inh} 0.50 dL/g, CH_2Cl_2, 35 °C.

4.7 Molecular Weight Control in Condensation Polymerizations

All polymers and oligomers used in this study were prepared via step-growth polymerization reactions. End group functionality and molecular weight play a major role in the mechanical and thermal properties of a step-growth polymer. The

nucleophilic aromatic substitution reaction of an activated dihalide with the diphenolate salt of a bisphenol was used to prepare a variety of polymers with differing backbone structures and molecular weights. A stoichiometric imbalance of the difunctional monomers was employed in order to properly control molecular weight according to the Carothers equation which is presented below. For a more complete description of molecular weight and derivation of the Carothers equation, the reader is referred to most basic polymer texts[3,4] .

Molecular weight was controled by a calculated stoichiometric imbalance of the molar ratio of one difunctional monomer over the other. The Carothers equation relates the number of monomer residues per polymer molecule, X_n, to the extent of reaction, p. For difunctional monomers present in stoichiometric quantities:

$$X_n = \frac{1}{1-p} \qquad (4.1)$$

This illustrates that as p approaches 1, and the reaction reaches completion, the molecular weight approaches infinity.

The following equation relates X_n to p and to the stoichiometric imbalance, r, ($r=N_A/N_B$) where N_A and N_B are the moles of difunctional A and B monomers to:

$$X_n = \frac{1+r}{2r(1-p)+1-r}$$ (4.2)

In the limit of a complete reaction (p → 1),

$$X_n = \frac{1+r}{1-r}$$ (4.3)

The stoichiometric imbalance can be varied to control the number average degree of polymerization when r is equal to or less than unity. In the reactions in this study, there are two ways to imbalance the stoichiometry, (1) by varying the molar ratio of bisphenol to dihalide, or (2) by the incorporation of a monofunctional reagent which acts as step growth terminator in the polymerization reaction.

4.7.1 Arylene ether and Arylene ether-co-imidazole Oligomers

Arylene ether oligomers and oligomers containing imidazole units distributed randomly along the backbone of the chain were synthesized by varying the stoichiometry of the reactants according to the Carothers equation. Oligomers of 5 and 10 percent molar offsets were prepared. A representative synthetic procedure for offsetting in favor of either the dihalide or bisphenol is given below.

4.7.1.1 9,9-HPF/4-FPK (5% offset Olig-1)

Into a 100 mL three neck flask equipped with a mechanical stirrer, nitrogen inlet, thermometer, condenser and Dean-Stark moisture trap were placed 9,9-bis(4-hydroxylphenyl)fluorene (9,9-HPF; 3.3145 g; 9.5 x 10^{-3} mol); bis-(4-fluorophenyl)ketone (4-FPK; 1.9607 g; 9.0 x 10^{-3} mol); pulverized anhydrous potassium carbonate (3.01 g; 0.02 mol); toluene (45 mL) and N, N-dimethylacetamide (DMAc; 20 mL; 20% solids). The mixture was heated in an oil bath and purged with nitrogen until the toluene began to reflux (approximately 110 to 120 °C). The solution was refluxed 4 hours, toluene was removed from the reaction medium via the Dean-Stark trap and the temperature increased to 140-150 °C. Heating was continued for an additional in 16 hours, resulting in a viscous, orange solution. The reaction mixture was precipitated in water/glacial acetic acid mixture in a blender. The precipitated white polymer was isolated by filtration, stirred in hot water (90-95 °C) for 1-2 hours then, stirred in hot methanol (55-60 °C) for 1-2 hours to remove trapped salts, collected, and dried under vacuum for 8 hours at 150-175 °C: yield 4.80 g (96%); Tg 242 °C; η_{inh} 0.24 dL/g, THF, 35 °C.

4.7.1.2 9,9-HPF/4-FPK (5% offset Olig-2)

Into a 100 mL three neck flask equipped with a mechanical stirrer, nitrogen inlet, thermometer, condenser and Dean-Stark moisture trap were placed 9,9-bis(4-hydroxylphenyl)fluorene (9,9-HPF; 3.1488 g; 9.0 x 10^{-3} mol); bis-(4-

fluorophenyl)ketone (4-FPK; 2.0639 g; 9.0 x 10^{-3} mol); pulverized anhydrous potassium carbonate (2.86 g; 0.02 mol); toluene (45 mL) and N, N-dimethylacetamide (DMAc; 20 mL; 20% solids). The mixture was heated in an oil bath and purged with nitrogen until the toluene began to reflux (approximately 110 to 120 °C). The solution was refluxed 4 hours, toluene was removed from the reaction medium via the Dean-Stark trap and the temperature increased to 140-150 °C. Heating was continued for an additional 16 hours, resulting in a viscous, orange solution. The reaction mixture was precipitated in water/glacial acetic acid mixture in a blender. The precipitated white polymer was isolated by filtration through a sintered glass funnel of medium porosity. The polymer was stirred in hot water (90-95 °C) for 1-2 hours then, stirred in hot methanol (55-60 °C) for 1-2 hours to remove trapped salts, collected, and dried under vacuum for 8 hours at 150-175 °C: yield 4.86 g (97%); Tg 221 °C; η_{inh} 0.20 dL/g, THF, 35 °C.

4.8 Prepartion of Epoxy Blends

4.8.1 Stoichiometric Epoxy Curing

The following calculations allow one to determine the ratio required to achieve exact curing agent stoichiometry.

1. Calculate the amine hydrogen equivalent weight:

$$Amine \ H \ eq \ wt = \frac{MW \ of \ amine}{number \ of \ active \ hydrogens} \qquad (4.4)$$

Example:

$$Amine \ H \ eq \ wt \ of \ DDS = \frac{248.3}{4} = 62.08 \ g/eq \qquad (4.5)$$

2.   Calculate the parts by weight per 100 parts resins (phr):

$$phr = \frac{Amine \ H \ eq \ wt \ x \ 100}{Epoxide \ eq \ wt \ of \ resin} \qquad (4.6)$$

Example: phr of DDS to use with TGMDA epoxy resin having an epoxide equivalent weight of 125:

$$phr = \frac{62.08 \ x \ 100}{125} = 49.66 \qquad (4.7)$$

4.8.2 Sample Procedure
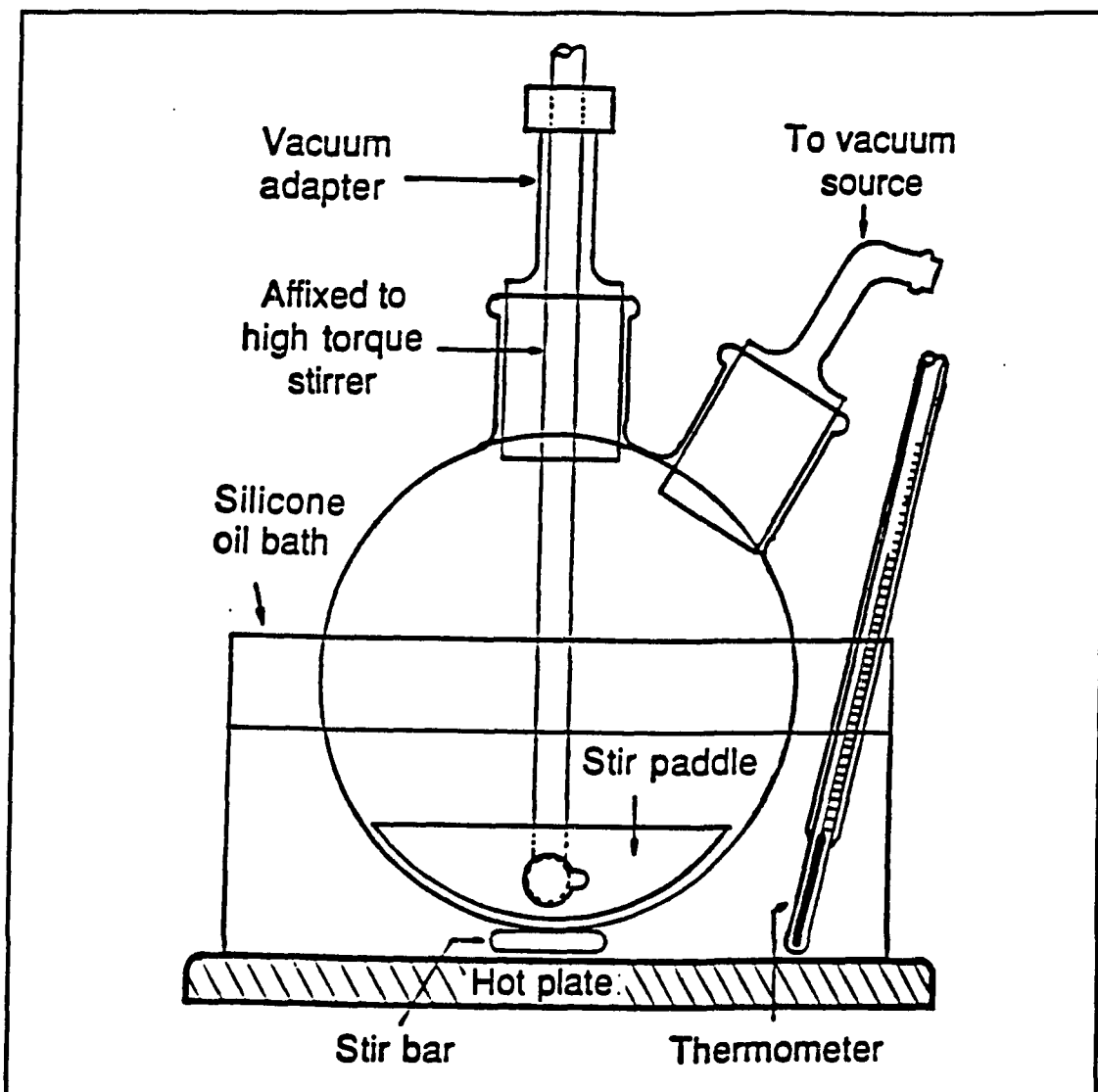
Figure 4.7 Reaction Apparatus for Polymer-Epoxy Blends

The following is a sample procedure for preparing a 10% w/w modified epoxy resin. The epoxy resin (45.06 g) and thermoplastic modifier (7.29 g) were weighed and added to the reaction vessel. A mechanical stirrer equipped with a glass paddle and a vacuum adapter were fitted to the vessel and placed in an oil bath heated to 120 °C (Figure 4.7). The mixture was heated and stirred for 8 hours until a homogeneous yellow solution was obtained. The temperature was

decreased to 100 °C and DDS (20.54 g) was added via a powder funnel. A vacuum was slowly applied to the stirring mixture in order to degas the resin and remove volatiles such as residual solvent and entrapped air. The system was degassed and stirred until the DDS dissolved (approximately 30 minutes) and a homogeneous hot-melt solution was obtained. The hot melt resin was poured into silicon molds specifically designed to the dimensions of fracture toughness and flex mechanical testing specimens. The epoxies were cured 1 hour at 80 °C, 1 hour at 100 °C, 4 hours at 150 °C, and 8 hours at 200 °C.

4.9 Model Imidazole Cure

2,4,5-Triphenylimidazole was added to 1,2-epoxy-3-phenoxypropane in an aluminum pan equipped with a magnetic stir bar. The viscous solution was warmed to approximately 50 °C and stirred approximately 20 minutes, until all solids had dissolved. The magnetic stir bar was removed and the epoxy was cured in an oven 18 hours at 50 °C, and 7 hours at 150 °C.

4.10 References

1. White, E. H., Harding, M. C., *Photocchem. Photobiol.*, **4** (6), 1129 **1965**.

2. Connell, J. W., Hergenrother, P. M., *J. Polym. Sci.: Pt. A: Polym. Chem.*, *29*, 1667 **1991**.

3. Odian, G., Principles in Polymerization, McGraw-Hill Book Co., **1970**.

4. Allcock, H. R.,; Lampe, F. W., Contemporary Polymer Chemistry, 2nd ed., Prentice Hall, Englewood Liffs, New Jersey, **1990**.

Chapter 5: Characterization

5.1 Molecular Weight Determinations

5.1.1 Gel Permeation Chromatographic Analysis

Gel permeation chromatographic (GPC) analyses were performed on a
Waters Associates high pressure liquid chromatograph. MicroStyragel HT®
columns with pore diameters of 10^3, 10^4, 10^5 and 10^6 angstroms were used with
a Waters Model 401 refractive index detector. A 1.0 mL/min flow rate was
employed for all GPC analysis. Columns were calibrated using narrow molecular
weight distribution polystyrene standards. Samples were dissolved in filtered and
degassed solvents and allowed to sit overnight, then filtered through a 0.2 μm
Teflon filter prior to injection into the chromatograph.

5.1.2 Intrinsic Viscosity Measurements

Intrinsic viscosity [η], measurements for some polymers and oligomers were
determined using Cannon viscometers immersed in a water bath maintained at
35 °C.

Intrinsic viscosities of some systems were determined from gel permeation chromatography by differential viscosity analysis. In this analysis, the Waters 150C GPC described in section □, was equipped with a differential refractive index detector and a Viscotek Model 150R differential viscosity detector connected in parallel configuration. Samples were dissolved in filtered and degassed solvents and allowed to sit overnight, then filtered through a 0.2 μm teflon filter prior to injection into the chromatograph. MicroStyragel HT® columns with pore diameters of 10^3, 10^4, 10^5 and 10^6 angstroms were used.

5.1.3 Multi-Angle Laser Light Scattering Photometry

Light scattering measurements were performed on a Wyatt Technologies Model Dawn-B Laser Photometer calibrated against toluene. Solvents were filtered through 0.2 μm fliters prior to dissolution of the polymers. Five polymer concentrations were measured for each sample. Polymers were dissolved and allowed to sit from 4 hours to overnight, and filtered through 0.2 μm filters prior to placement into the Wheaton disposable scintillation vials for testing. A detailed description of light scattering measurements for the polymers in this study may be found in Katzenberger, 1994[1].

5.1.4 Refractive Index Increment Measurements

Specfic refractive index increment measurements (dn/dc) were performed on a Chromatix Model KMX-16 Laser Differential Refractometer. Solution concentrations of approximately 0.002, 0.004, 0.006 and 0.008 g/mL were used. The refractometer was calibrated with $NaCl/H_2O$.

5.1.5 Inherent Viscosity Measurements

Inherent viscosity (η_{inh}) measurements were obtained on 0.5% solutions using Cannon viscometers in a water bath set at 25 °C or 35 °C.

5.2 Bulk Property Measurements

5.2.1 Molding

Fabrication involved the compression molding of the precipitated and dried polymer powder at elevated temperatures inside a metal mold. The temperature and pressure used depended on the particular sample and varied accordingly. Often, the process was complicated by the formation of bubbles caused by the vaporization of residual solvents trapped inside the polymer. When this occurred the material was broken up into numerous pieces and remolded.

5.2.2 Mechanical Testing

The American Society for Testing and Materials Specifications (ASTM) has established guidelines for measuring specific attributes of unreinforced plastic materials. Mechanical testing was performed on the Sintech model 2W screw driven test machine. Unless specifically stated all measurements adhered to ASTM standards D790 and E399.

5.2.2.1 Fracture Toughness Testing

The measure of a material's ability to resist fracture is given by the critical stress intensity factor (K_{Ic}). Fracture toughness of the blended epoxy resin specimens was determined from a 3-point bend test on a single-notch bend (SENB) specimen. Fracture toughness of the polymers and oligomers were determined from a compact tension test.

The fracture specimens were notched with a milling machine equipped with a 3 "-diameter, 1/16"-wide cutter with an 80° taper which resulted in a Chevron notch starter crack.

The ASTM standard requires that infinitesimately sharp cracks are needed for testing purposes. The more blunt the crack the tougher the material appears to be, thereby leading to improperly enhanced toughness values. One of the greatest experimental difficulties in performing fracture tests is to establish an
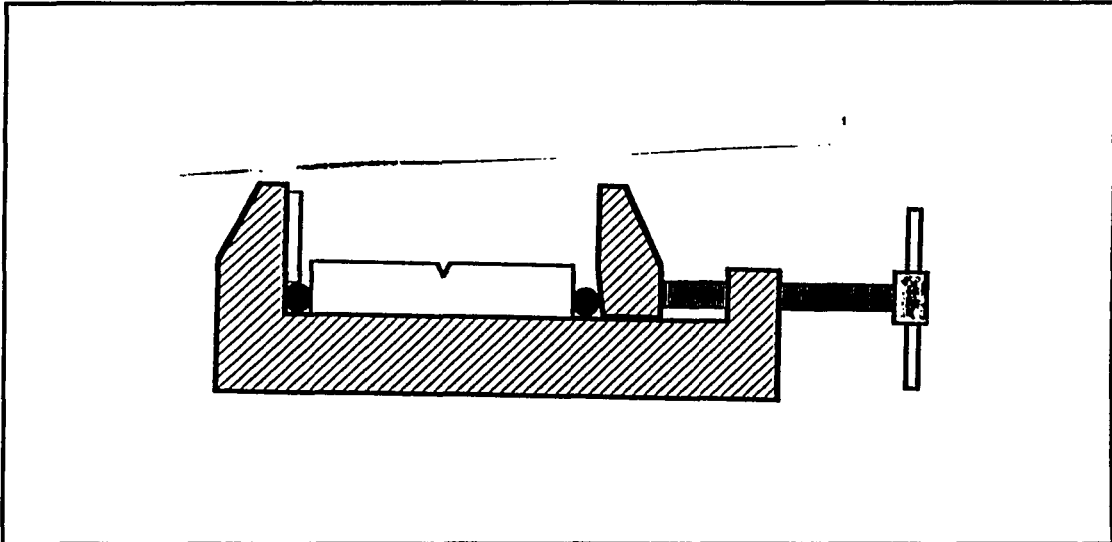
Figure 5.1 Eccentric Axial Load Technique for initiating infintesimately sharp starter cracks

appropriate initial flaw. A machined notch does not have a sufficiently small radius to act as an infinitesimately sharp crack, therefore a razor blade is driven into the notch to produce a sharp tipped crack. Fatigue, another method for sharpening starter cracks, is universally accepted as the preferred method in ductile metals. However, fatigue is unacceptable in certain situations[2]. ASTM recommends lightly tapping a new razor blade into a machined notch to produce a rapidly moving crack. For a SENB specimen, an axial compressive load can be applied to reduce the possibility of complete fracture resulting from a tapped razor blade[3]. A new method which applies the mechanics concept of a kern to determine the appropriate line of action for the applied compressive load was utilized in precracking the specimens[4] in this study. The samples were held in a modified vice arrangement (Figure 5.2) and a new sharp razor blade, cooled in liquid nitrogen, was tapped into the notch until a crack was generated. Care was taken

to ensure that the starter crack had propagated evenly through the specimen thickness with crack lengths approximately 0.45 to 0.55 of the sample width.

After the samples were fractured, the crack length, width and specimen thickness were all determined under a measuring microscope. Precracks were often meniscus shaped and Simpson's rule for a hyperbola (equation 5.1) was used to determine the average crack length.

$$a_{avg} = \frac{L + 4C + R}{6} \qquad (5.1)$$

Where a_{avg} is the average starter crack length, L is the left starter crack front, C is the center starter crack front, and R is the right starter crack front as illustrated in Figure 5.2.
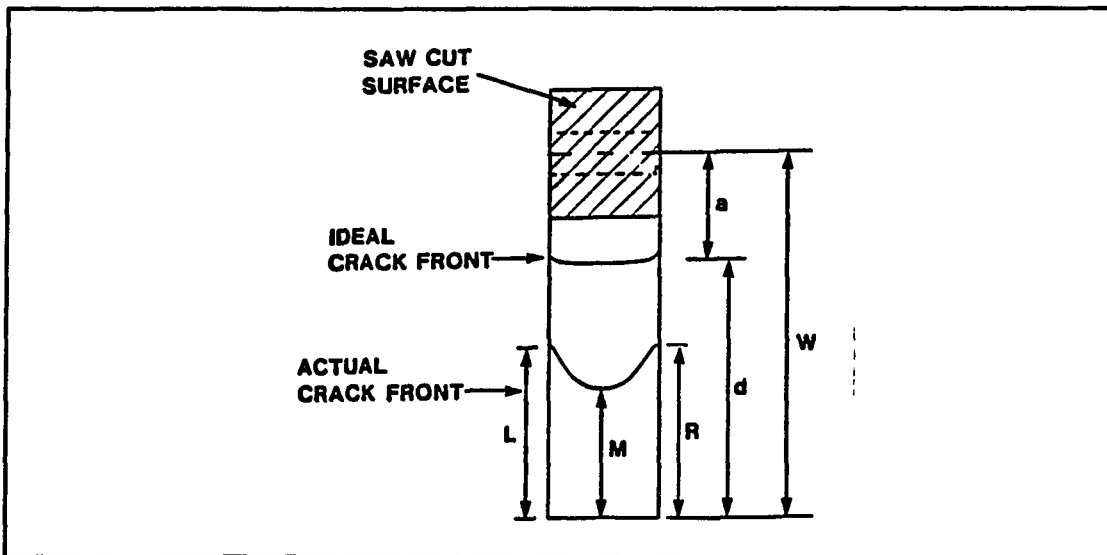

Figure 5.2 Illustration of Crack Front along Fracture Surface

5.2.2.1 3-Point Bend Testing

Specimens were prepared by casting the degassed hot-melt resin into silicon rubber molds of dimensions 2.5 x 0.5 x 0.25 inches. Tests were run under a compression mode in a three-point bend configuration.

The critical stress intensity (K_{Ic}), was calculated by equation 5.2[5].

$$K_{Ic} = \frac{P\,S}{B\,W^{3/2}} \; x \; f\left(\frac{a}{W}\right) \qquad (5.2)$$

where:

P = Load at failure; S = Span ; B = Thickness; W = Width and a = Crack Length and:

$$f\left(\frac{a}{W}\right) = \frac{3\left(\frac{a}{W}\right)^{1/2}\left[1.99-\left(\frac{a}{W}\right)\left(1-\frac{a}{W}\right) \; x \; \left(2.15-3.93\frac{a}{W} + 2.7\frac{a^2}{W^2}\right)\right]}{2\left(1 + 2\frac{a}{W}\right)\left(1 - \frac{a}{W}\right)^{3/2}}$$

5.2.2.3 Compact Tension Testing

Specimens samples were prepared by compression molding and were cut

into four specimens approximately 0.62 x 0.62 x 0.25 inches thick (Figure 5.3).

Force

0.62"

0.62"

Razor crack

Precut

Force

Figure 5.3 Compact Tension Fracture Toughness Specimen
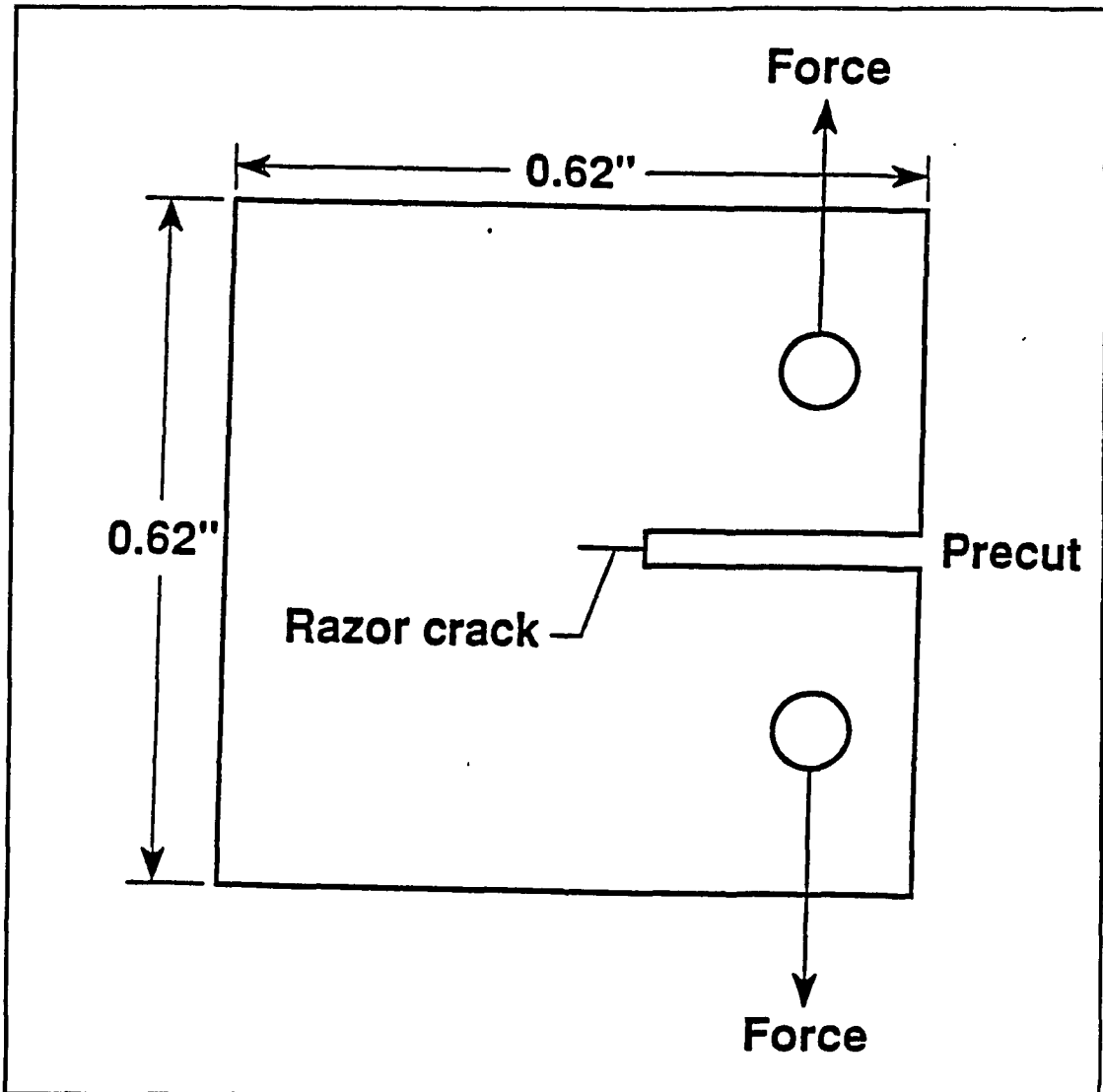
Tests were run under a tensile mode and the critical stress intensity (K_{Ic}), was calculated by equation 5.4[6].

$$K_{Ic} = \frac{P}{BW^{1/2}} \times f(\frac{a}{W})$$

(5.4)

$$f\left(\frac{a}{W}\right) = \frac{\left(2+\frac{a}{W}\right)\left(0.886+4.64\frac{a}{W}-13.32\frac{a^2}{W^2}+14.72\frac{a^3}{W^3}-5.6\frac{a^4}{W^4}\right)}{\left(1-\frac{a}{W}\right)^{3/2}}$$

5.2.2.4 Flexural Modulus Measurements

The ASTM specification (ASTM D790-84a) was followed for measuring the flexural properties of the polymers, oligomers and modified epoxy resin systems. Specimen dimensions were within a 16:1 length to depth ratio and were compression molded or formed in silicone molds.

Testing was performed in a three-point bend configuration and the cross-head speed was calculated by equation 5.6.

$$Cross\ Head\ Speed\ (inches/min) = 0.01\frac{L^2}{6d} \qquad (5.6)$$

where L is the span, and d is the sample thickness, both measured in inches.

Four types of information can be calculated from modulus measurements 1) Flexural Modulus; 2) Flexural Strength; 3) Strain at Failure; and 4) "Toughness" (area under a linear stress/strain plot).

The parameters can be calculated according to the following equations:

$$Flexural\ Modulus = E_B = \frac{L^3M}{4bd^3} \qquad (5.7)$$

$$Flexural \; Strength = \sigma_{max} = \frac{3LP}{2bd^2} \qquad (5.9)$$

$$Flexural \; Strain \; at \; Failure = \epsilon_{max} = \frac{6 dP_{max}}{L^2 M} \qquad (5.9)$$

$$Toughness = \tfrac{1}{2} \, \sigma_{max} \, \epsilon_{max} \qquad (5.10)$$

Where: P = Linear load at failure (brittle)

b = Width

d = Thickness

M = Slope from stress/strain plot

L = Span Length

5.2.2.5 Dynamic Mechanical Thermal Analysis

Dynamic mechanical thermal analysis of the polymers, oligomers and the blended materials was obtained with a Dupont Model 982. Samples (1.3 x 0.55 inches) were cut from compression molded specimens or obtained from hot melt molding into a RTV mold. Test were performed at a frequency of 1 Hz and a heating rate of 5 °C/min, between -150 and 500 °C, thus exceeding both the thermoset and thermoplastic modifier glass transition temperature. Samples were

mounted in a double cantilever clamp for mechanical perturbation. Storage modulus (E') and Tan δ were recorded.

5.2.3 Thermal Analysis

5.2.3.1 Differential Scanning Calorimetry

Glass transition temperatures for all systems were determined from a Shimadzu DSC-50 Differential Scanning Calorimeter, DSC. All reported glass transition temperatures were from the second scan, after heating to 400 °C. Tg was determined at the half point of the slope change from the baseline of the change in energy (Δmw) versus temperature curve. Temperature calibration was achieved by using Indium and Tin which have melting points of 156.6 and 231.9 °C, respectively. A heating rate of 10 or 20 °C/min was used.

5.2.3.2 Thermogravimetric Analysis

Thermogravimetric analyses of the samples were conducted on a Seiko Tg/DTA 200/220 at a heating rate at 50 °C/min from room temperature to 100 °C, held for 30 minutes and then ramped 2.5 °C/min to 650 °C in air at a flow rate of 15 cc/min. Thermal oxidative stability (TOS) was determined at the point of 5% weight loss.

5.3 Scanning Electron Microscopy

Morphologies of the neat resin were compared with that of the modified systems by examining scanning electron micrographs of fracture surfaces. SEMs were taken on a Hitachi S-510 SEM. Samples were cut to size then glued on the sampling base. The samples were sputter coated with gold using an Anatech Hummer VI sputter coater before placing inside the SEM. The SEM was operated at 15 kV.

5.4 Compatibility of Poly(arylene ether-co-imidazole)s with Commercial Epoxies

Poly(arylene ether-co-imidazole)s were screened for their compatability and miscibility with commercially available epoxy resins. Three percent by weight of polymers of various chemical compositions were weighed into aluminum pans containing a commercial epoxy. Each pan was equipped with a magnetic stir bar and warmed on a hot plate under low heat (50 to 75°C) for 1 to 4 hours. The temperature was increased to 100 °C and stirring was continued for an additional hour for any system that did not appear to be miscible. A stoichiometric amount of DDS was added, and stirring was continued until the DDS dissolved (approximately 15 to 20 minutes). Each sample was cured at a rate of 1 hour at 80 °C; 1 hour at 100 °C; 4 hours at 150 °C; and 6 hours at 200 °C. Samples were

evaluated in terms of visual polymer miscibility and processability.

5.5 Swelling

Swelling experiments were performed on cured modified epoxy resins. A sample was dried 72 hours at 150 °C, weighed and placed in a tightly sealed sample bottle with the sample immersed in THF. The sample's mass was checked periodically and recorded to ± 0.1 mg. The percentage of swelling was determined by equation 5.11.

$$Swelling\ \% = \frac{Swollen\ Mass\ -\ Initial\ mass}{Initial\ Mass} \times 100 \quad (5.11)$$

Sample weighing became increasingly difficult since a number of the specimens broke apart due to the internal stresses exerted on the sample by swelling.

Percentage swelling for various modified systems as a function of time were plotted and compared with swelling behavior from the unmodified network.

5.6 Moisture Uptake

An approach similar to that used for swelling was applied to monitor the moisture uptake for various modified epoxy resin systems. Samples were dried

72 hours at 150 °C, weighed, then placed in a boiling water bath. The samples were removed periodically, dried quickly with tissues and weighed to ± 0.1 mg. The moisture uptake was calculated using the following equation.

$$Weight \ \% \ Uptake = \frac{Sample \ Mass \ - \ Initial \ Mass}{Initial \ Mass} \ x \ 100$$

5.7 References

1. Katzenberger, A. T., Chemistry Honors Thesis, College of William and Mary (1994).

2. Marshall, G. P., Culver, L. E., and Williams, J. G., *Int. J. Fracture, 9,* 295 **1973.**

3. Williams, J. G., Cawood, M. J., Polym. Testing, 9, 15 (1990).

4. Dillard, D. A., Roberts-McDaniel, P., Hinkley, J. A., *J. of Mat. Sci. Letts., 12,* 1258 **1993.**

5. American Standard Test Method (ASTM D790).

6. American Standard Test Method (ASTM D790).

Chapter 6: Results and Discussion

6.1 2-Phenyl-4,5-bis(4-hydroxyphenyl)imidazole

2-Phenyl-4,5-bis(4-methoxyphenyl)imidazole was synthesized from 4,4'-dimethoxybenzil, benzaldehde and ammonium acetate in acetic acid. Demethylation was carried out in refluxing acetic acid using aqueous hydrobromic acid solution. This reaction was performed several times with varying degrees of success, in terms of obtaining high yields of pure product [i.e. 2-phenyl-4,5-bis(4-hydroxyphenyl)imidazole]. If only partial demethylation were occurring the resultant product would be a mixture of starting material, monohydroxy and desired product. Separation of the desired product by recrystallization was not achievable, presumably due to similar solubility characteristics. Synthesis of poly(arylene ether)s often resulted in low molecular weight polymers, in spite of repeated attempts at recrystallization of the monomer. Monofunctional monomers would cause chain termination during polymerization and decreased polymer molecular weights.

An alternative approach to purify the monomer was attempted through silylation of the hydroxy functionality. Successful silylation of the bisphenol functionality may result in a difference in solubility for the dihydroxy and the hydroxy/methoxy imidazole monomer. An attempt at the synthetic scheme outlined by Kricheldorf et al. 1983 resulted in a broad melting monomer. A second attempt

at silyation by the procedure outlined in section 4.3, also resulted in a broad melting monomer. Preparation of a stoichiometrically balanced poly(arylene ether) from 2-phenyl-4,5-bis(4-trimethylsilyloxy phenyl)imidazole resulted in a powdery low molecular weight polymer. The low molecular weight was attributed to the impurity of the imidazole monomer. High purity 2-phenyl-4,5-bis(4-hydroxyphenyl)imidazole monomer was subsequently obtained from Daychem corporation, and was used as received to yield high molecular weight polymers.

6.2 Model Cure Study

Alkyl substituted imidazoles are used to catalyze the cure of epoxies. A model cure reaction was performed to confirm that the aromatic substituted imidazole moeity serves as an effective crosslinking agent for epoxies and also becomes incorporated into the three dimensional epoxy network. A model imidazole compound similar in chemical composition to the imidazole substituent incorporated into the PAE-co-I's of this study was investigated. 2,4,5-Triphenylimdazole (MP. 278 °C) prepared from benzil, benzaldeyde and ammonium acetate in acetic acid solution was cured at a 1:1 stoichiometric ratio with 1,2-epoxy-3-phenoxypropane without additional curing agent. 1,2-epoxy-3-phenoxypropane was also cured at a 1:1 stoichiometric ratio with 4,4' DDS. Complete curing of the difunctional liquid epoxy with the imidazole and 4,4' DDS curing agents resulted in clear solid plaques (Tg 239 and 70 °C respectively). The

2,4,5-triphenylimdazole was not extractable from the cured plaque with methanol or THF. This served as confirmation that the imidazole had effectively cured the difunctional epoxy monomer, along with becoming incorporated into the thermoset network.

6.3 Poly(arylene ether)s, Poly(arylene ether imidazole)s and Poly(arylene ether-co-imidazole)s

Poly(arylene ether)s and poly(arylene ether imidazole)s were prepared from aromatic bisphenols and activated aromatic dihalides using potassium carbonate in DMAc at elevated temperatures. The polymers were characterized in terms of Tg, η_{inh}, and a good solvent system for solution characterization, the homopolymer structures are presented in Figures 6.1 and polymer characterization is summarized in Table 6.1.
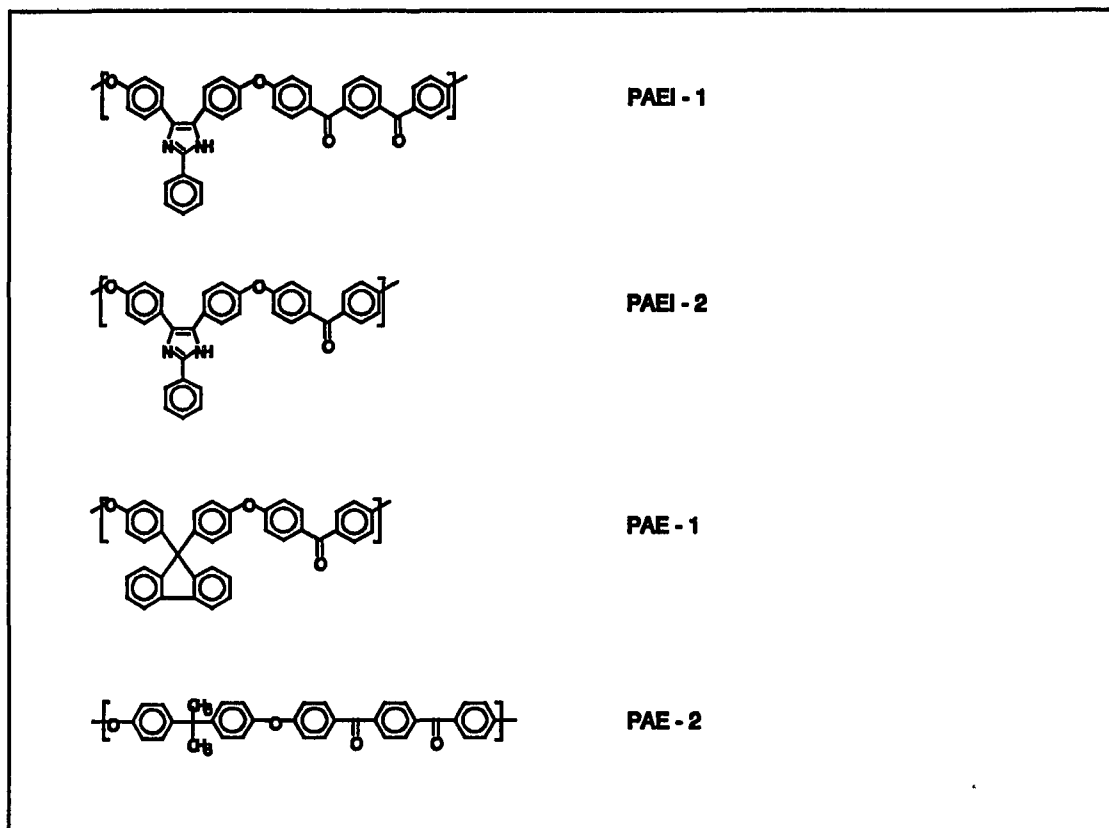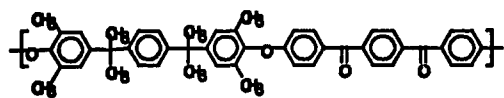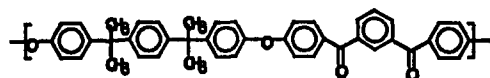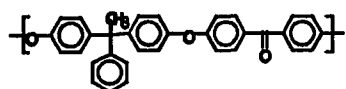
PAEI - 1

PAEI - 2

PAE - 1

PAE - 2

Figure 6.1 PAE and PAEI Homopolymers

PAE - 3

PAE - 4

PAE - 5
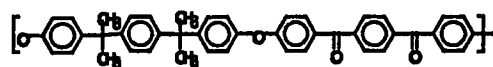
PAE - 6

Table 6.1 PAE AND PAEI Homopolymers Characterization

Polymer Name	Tg (°C)	η_{inh} (dL/g)	Solvent
PAEI-1	220	0.71	DMAc
PAEI-2	242	0.32	DMAc
PAE-1	250	0.61	$CHCl_3$
PAE-2	150	1.38	$CHCl_3$
PAE-3	192	1.14	$CHCl_3$
PAE-4		gel	
PAE-5	160	1.79	$CHCl_3$
PAE-6	157	1.23	$CHCl_3$

Poly(arylene ether-co-imidazole)s of varying chemical composition were prepared according to the method previously described in section 4.6. The imidazole content of the random copolymers was held constant at 10 mole percent of the total diol units in all copolymers presented in this section. The polymers were characterized in terms of Tg, η_{inh}, and a good solvent system for solution characterization, the structures are presented in Figure 6.2 and polymer characterization in Table 6.2.
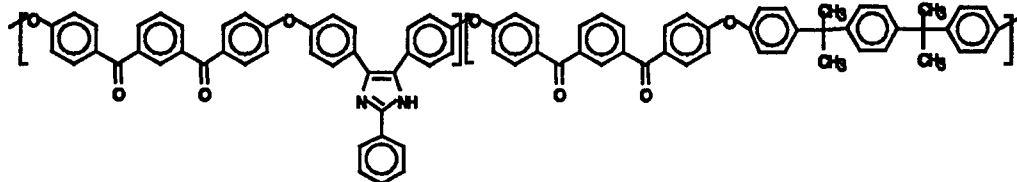
PAE - co - I - 1

PAE - co - I - 2

PAE - co - I - 3

PAE - co - I - 4

PAE - co - I - 5

PAE - co - I - 6

Figure 6.2 PAE-co-I Copolymers
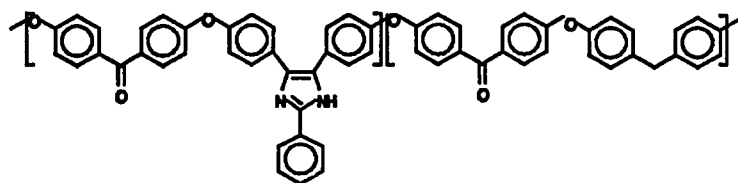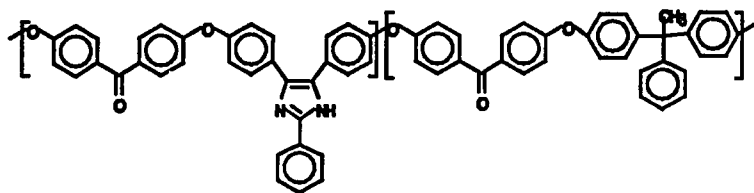
Table 6.2 PAE-co-I with 10% Imidazole Characterization

Polymer Name	Tg (°C)	η_{inh} (dL/g)	Solvent
PAE-co-I-1	146	**	insoluble
PAE-co-I-2	186	0.91	THF
PAE-co-I-3	159	0.50	CH_2Cl_2
PAE-co-I-4		gel	
PAE-co-I-5	237	0.63	$CHCl_3$
PAE-co-I-6	207	0.50	CH_2Cl_2

6.4 Epoxy Modification

6.4.1 Polymer Processability

The poly(arylene ether)s, poly(arylene ether imidazole)s and poly(arylene ether-co-imidazole)s were tested for solubility and processability as modifiers for the commercially available high performance epoxy resins represented in Figure 6.3. It is critical to obtain homogeneous blends prior to curing to assure uniform distribution of the toughening agent (i.e. PAE, PAEI, PAE-co-I) in the matrix.
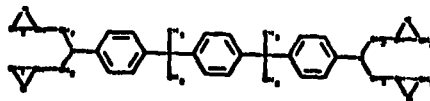
N,N,N',N'-tetraglycidyl-a a'bis(4-aminophenyl)-p-diisopropylbenzene

(TGAI, Shell Epon 1071)
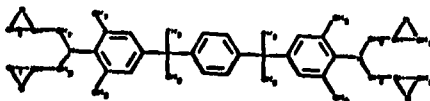
N,N,N',N'-tetraglycidyl-a a'bis(4-amino-3,5-dimethylphenyl)

(TGAMI, Shell Epon 1072)
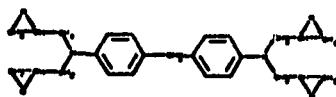
N,N,N',N'-tetraglycidyl-4,4'-diaminodiphenyl methane

(TGMDA, Ciba Geigy 720;721;722)
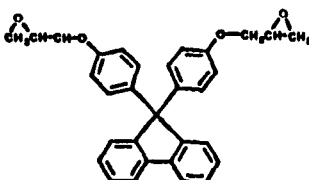
Diglycidyl-9,9'-bis(4-hydroxyphenyl)fluorene

(DGEHF, Shell Epon 1079)
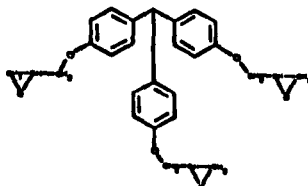
Triglycidyl tris(hydroxyphenyl)methane

Figure 6.3 Commercially available high performance epoxy
resins screened as possible toughening matrices

Solubility was determined by mixing 3 percent by weight polymer with a resin while heating (Table 6.3). Very soluble (VS) systems dissolved within 1 hour requiring only minimal stirring and heating at 50 °C. Soluble (S) systems dissolved within a 1 to 4 hour time period requiring heating to approximately 75 °C. Slightly soluble (SS) systems required the temperature to be increased to 100 °C and 1 hour of additional heating. Slightly soluble systems often displayed visual signs of unincorporated polymer after complete curing. Insoluble systems did not dissolve in the resin system even after additional heating at a higher temperature, and were clearly apparent as discrete polymers after curing.

Table 6.3 Polymer Solubility in Commercial Epoxies

Polymer	TGMDA 720	TGMDA 721	TGMDA 722	DGEHF	TGAI	TGAMI	TGHPM
PAEI-1	IS	IS	IS	IS	IS	IS	IS
PAEI-2	IS	SS	SS	IS	IS	IS	IS
PAE-1	SS	S	S	SS	IS	IS	SS
PAE-2	IS	IS	IS	IS	IS	IS	IS
PAE-3	IS	IS	IS	IS	IS	IS	IS
PAE-4	IS	SS	S	IS	IS	IS	IS
PAE-5	IS	IS	IS	IS	IS	IS	IS
PAE-6	IS	SS	S	IS	IS	IS	IS
PAE-co-I-1	SS	S	VS	S	SS	SS	IS
PAE-co-I-2	IS	SS	SS	IS	IS	IS	IS
PAE-co-I-3	SS	S	VS	S	SS	SS	IS
PAE-co-I-4	IS	IS	IS	IS	IS	IS	IS
PAE-co-I-5	SS	S	VS	S	IS	IS	S
PAE-co-I-6	SS	SS	S	SS	SS	SS	IS

The commercially available epoxy resins that were supplied in a solid or semisolid state , TGAI, TGAMI, and TGHPM resulted in the lowest number of soluble polymers and were eliminated as possible toughening matrices. Although DGEHF is supplied as a solid, it still resulted in a high number of soluble or slightly soluble mixtures and was further investigated as a toughening matrix. The polymer systems that ARE very soluble or soluble in the highest number of commercial resins were chosen for further investigation. PAE-co-I-3 through PAE-co-I-6 polymers exhibited the highest degree of solubility in the resins. These polymers were prepared in larger quantites of ~40 g each and studied for their processablity with the commercial resins.

Modified polymer-resin systems containing 5 and 7% w/w were evaluated for solubility and handling in terms of viscosity and relative ease of molding.

The processability for a system was rated in terms of pre-cure viscosity and post-cure consolidation. Viscosity was determend by the relative ease of pouring pre-cured resin-polymer-curing agent mixtures into the specimen molds. Samples were rated as (1) low viscosity-void free (2) medium viscosity-void free (3) medium viscosity-moderate voids (4) high viscosity-high voids. Table 6.4 summarizes polymer processability with the epoxy resins.

Table 6.4 Processability of Uncured

Epoxy-Polymer Systems 5 and 7% w/w

Polymer	TGMDA 720	TGMDA 721	TGMDA 722	DGEHF	Total
PAE-co-I-1 (5%)	3	2	2	3	10
PAE-co-I-1 (7%)	3	3	3	3	12
PAE-co-I-3 (5%)	3	2	1	2	8
PAE-co-I-3 (7%)	3	3	1	3	10
PAE-co-I-5 (5%)	3	2	1	2	8
PAE-co-I-5 (7%)	3	3	1	2	9
PAE-co-I-6 (5%)	3	3	2	3	11
PAE-co-I-6 (7%)	4	4	3	4	15
TOTAL	25	22	14	22	

Several of the polymers were soluble at the initial 3% and the 5% w/w concentrations. However, many systems became increasingly difficult to process as the concentration of polymer was increased to 7%. Processing difficulties consisted of highly viscous systems which broke the glass stirring paddles during mixing or systems that were too viscous to degas adequately and resulted in samples with high void content upon curing.

The epoxy resin and polymer systems with the lowest total score were

selected for further investigation. The TGMDA based resins offered the best polymer solubility and the best processing conditions. Of the three TGMDA resins evaluated, TGMDA-722 offered the most promise due to its extremely low viscosity. The polymer-epoxy system that resulted in a low to medium viscosity mixture and also yielded a void free sample upon curing was chosen for further evaluation.

The PAE-co-I-3 and PAE-co-I-5 systems were chosen as the most soluble and easiest to process systems. A 135-g batch of the PAE-co-I-3 polymer was prepared and evaluated. Epoxy-polymer samples of 3, 5 and 10 weight percent were prepared. The precured 3 and 5 weight percent samples were semi-viscous prior to curing and resulted in void free mechanical test specimens. However, the 10 weight percent samples were extremely viscous prior to curing and required constant application of heat, via a heat gun, in order for them to be poured into the RTV molds. Cured samples of the 10% w/w modified resin had high void content, probably due to inadequate degassing, and were not suitable for mechanical testing.

6.4.2 PAE-co-I-3 Modifications

Table 6.5 lists the K_{Ic} and Tg values for the 3, 5 and 10 percent samples. No appreciable difference in fracture toughness was realized with this polymer. A higher proportion of thermoplastic to thermoset may be required in order to

affect the fracture toughness of the epoxy resin.

Table 6.5 TGMDA-722/PAE-co-I-3
Modified Resins Characterization

Weight % Polymer	Tg (°C)	K_{Ic} (psi/√in)
0	208	437 ± 60
3	202	436 ± 40
5	197	457 ± 42
10	185	**

The effect of imidazole concentration on thermal oxidative stability of PAE-co-Is, viscosity and Tg were also investigated at this time. A series of polymers represented in Figure 6.4 were synthesized where the mole percent of imidazole (X) randomly distributed along the backbone was varied from 0 to 100. The properties are summarized in Table 6.6.
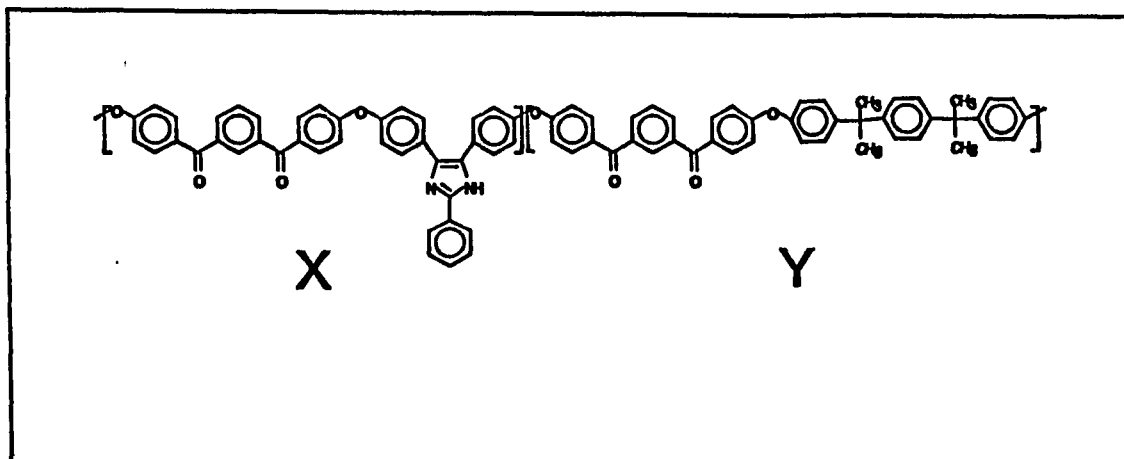
Figure 6.4 PAE-co-I of various mole percent imidazole

Table 6.6 Effect of Imidazole Concentration on Polymer Properties

Polymer	X:Y	TOS (° C, TGA)	[η]$_{THF}$ (dL/g)
PAE-6	0:100	402	0.70
PAE-co-I-3	10:90	404	0.44
PAE-co-I-7	30:70	367	0.44
PAE-co-I-8	50:50	425	0.42
PAE-co-I-9	70:30	387	0.42
PAE-co-I-10	90:10	367	insoluble
PAEI-1	100:0	374	0.55

The thermal oxidative properties of the polymer decrease with increasing imidazole

concentration. The anomaly is the 50:50 PAE-PAEI copolymer which exhibited the highest TOS as determined by 5% weight loss by TGA, of all systems studied. This property was reproducible between different TGA runs and polymer batches.

There is a preferential solvation of the polymer depending on which portion of the copolymer predominates. The PAE homopolymers tend to be more soluble in chlorinated solvents such as $CHCl_3$ or CH_2Cl_2, while the PAEI homopolymers prefer polar aprotic solvents like DMAc. This complicated the determination of dilute solution properties where it is desirable to make comparisons between polymers in the same solvent. All polymers in this series were completely soluble in THF except PAE-co-I-10. This insolubility was reproducable for different polymer batches.

Figure 6.5 illustrates the relationship between Tg and mole percent imidazole in the polymer backbone. This linear relationship allows one to establish the desired Tg of the PAE-co-I prior to synthesis.
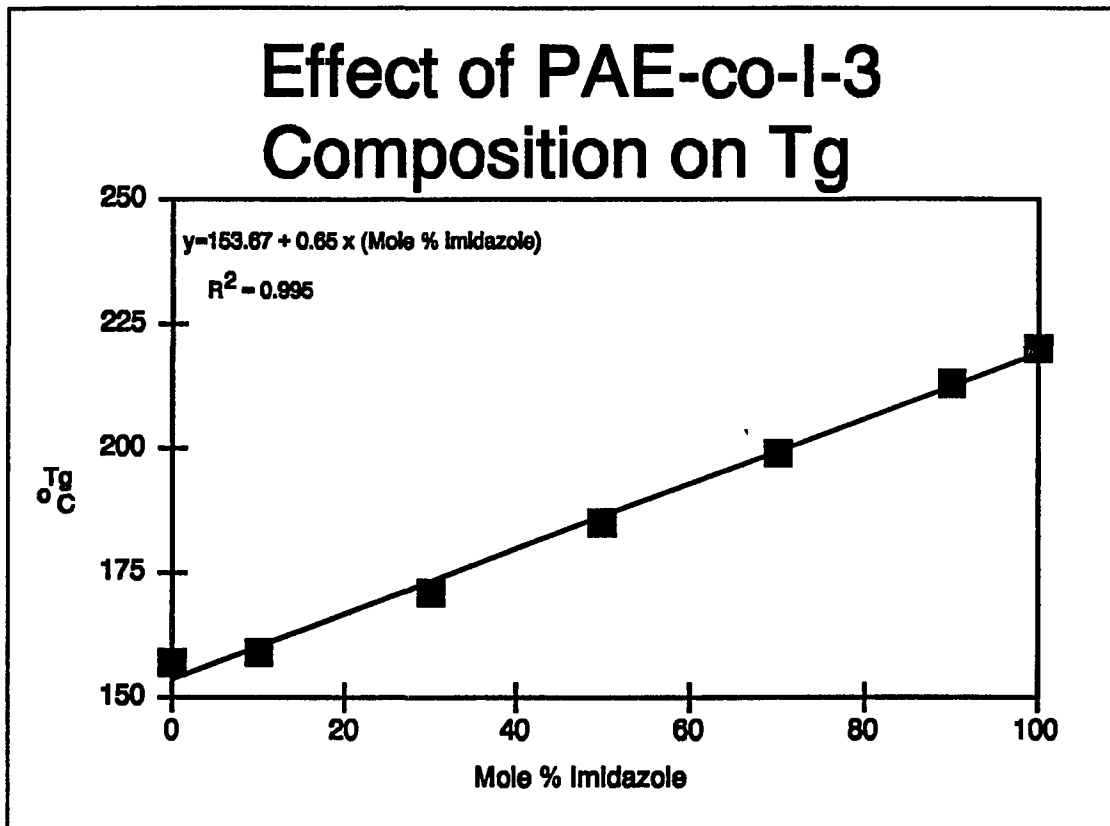
Effect of PAE-co-I-3 Composition on Tg

$$y = 153.67 + 0.65 \, x \, (\text{Mole \% Imidazole})$$

$$R^2 = 0.995$$

Figure 6.5 Effect of PAE-co-I-3 composition on Tg

6.4.3 PAE-co-I-5 Modifications

The PAE-co-I-5 polymer based on the fluorene ring system was selected as a possible epoxy modifier due to its high solubility in the epoxy resins and the ineffectivness of PAE-co-I-3 as a toughness modifier at less that 10% w/w concentration. Modified epoxy resins of 5, 7 and 10 w/w percent polymer were evaluated in terms of their fracture toughness. Figure 6.6 summarizes the effect of increasing polymer content on fracture toughness.
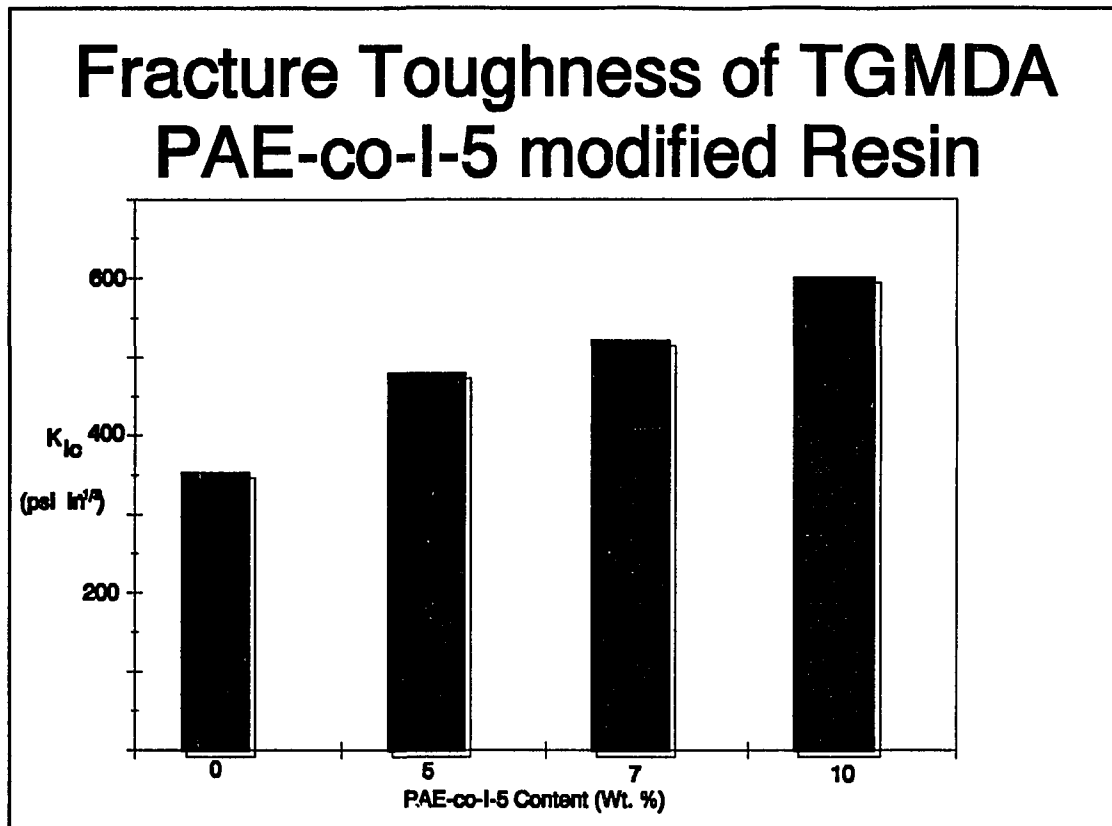
Fracture Toughness of TGMDA PAE-co-I-5 modified Resin

Figure 6.6   Fracture Toughness of TGMDA/PAE-co-I-5 modified resin

The fracture toughness of the neat polymer was 1666 psi. The simple rule of mixtures predicts the fracture toughness of the 10 percent w/w modified resin should be approximately 520 psi√in. The fracture toughness value for this modified resin was 16% greater than expected at 601 psi√in, which is 1.7 times that of the unmodified epoxy.

Significant fracture toughness improvements have been found for bismaleimides modified with 20% PAE. Further improvements in epoxy resin fracture toughness might be realized if higher PAE-co-I weight loadings were possible. Samples containing 20% w/w could not be prepared with this

polymer/resin combination due to the high viscosity of the precured mixtures.

6.4.4 TGMDA 722-0510-HPB modified resins

Diglycidyl ether of 4-aminophenol (MY 0510), a low viscosity epoxy, was investigated as a possible diluent for the PAE-co-I/TGMDA based systems. A decrease in epoxy resin viscosity accompanied with a higher degree of solubility in the diluent would lead to improved processing conditions for the polymer-resin systems. The diluent was effective in decreasing the viscosity of the TGMDA resins (Figure 6.7). However, the PAE-co-I was less soluble in the diluent than the TGMDA 722. Therefore a net increase of viscosity resulted with increasing ratios of diluent (Figure 6.8). Based on these data, attempts of diluting the TGMDA 722 resin with MY 0510 were suspended.
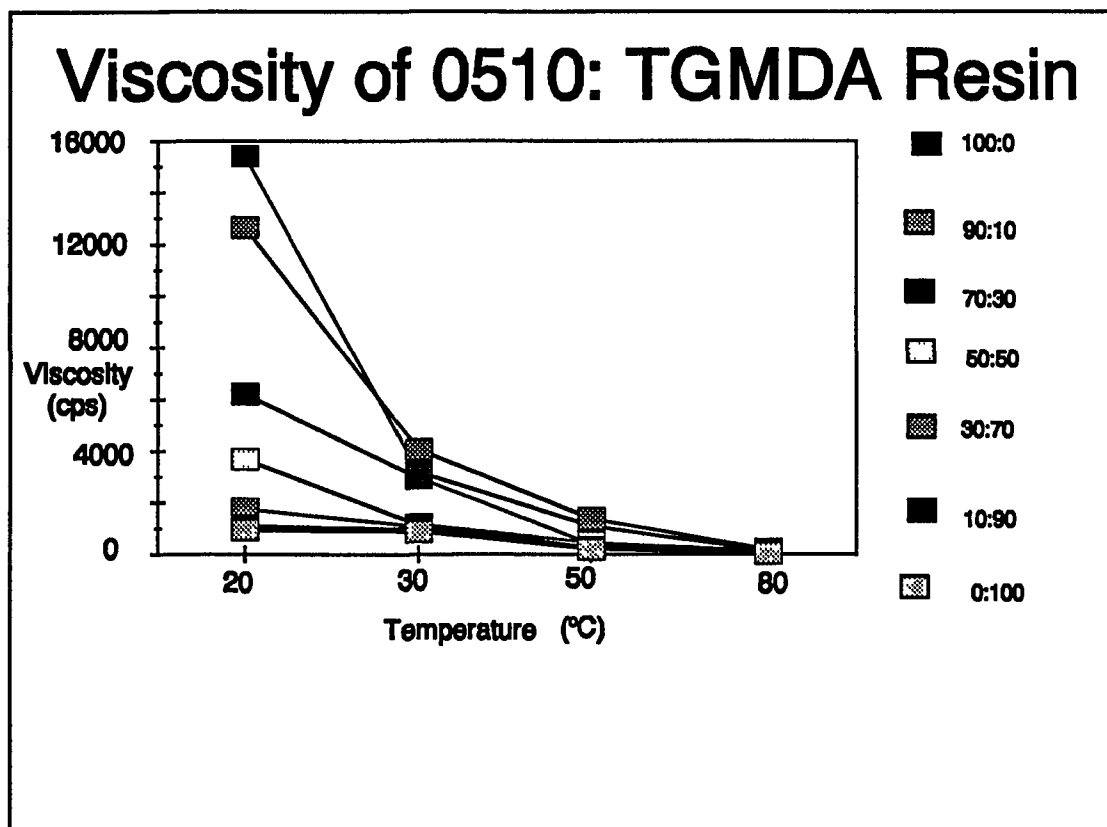
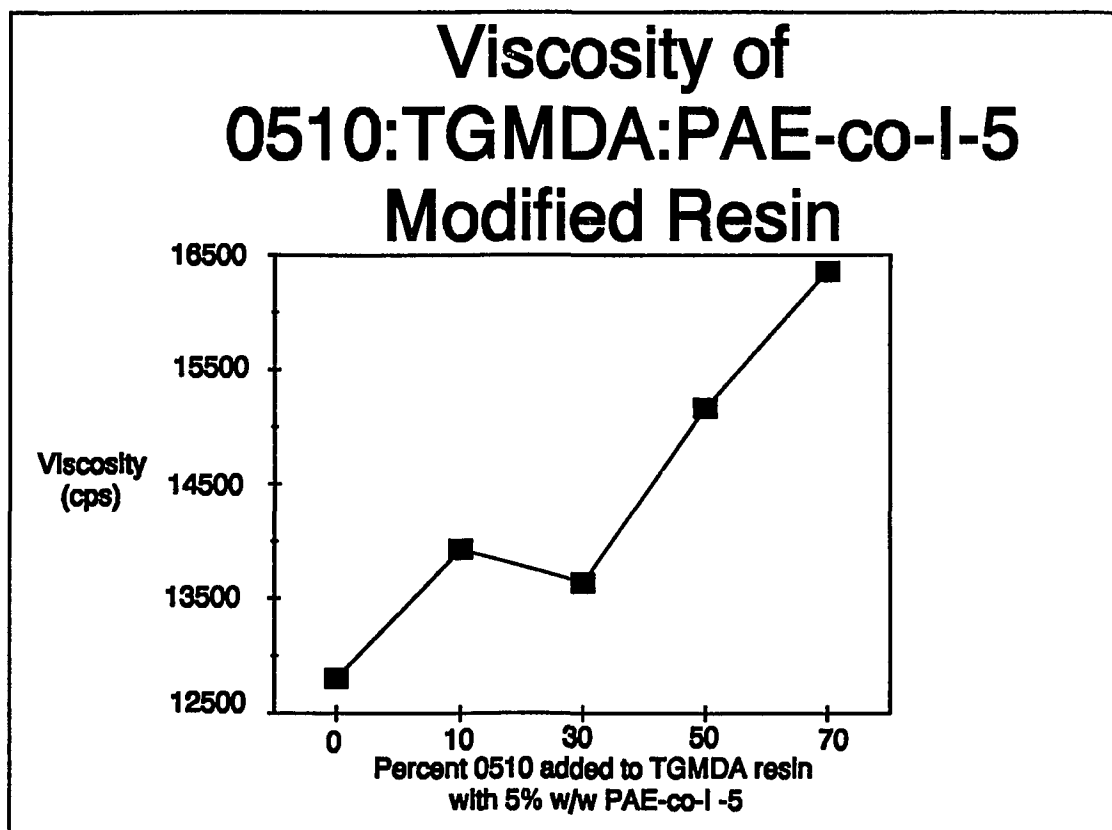**Figure 6.7** Viscosity of 0510:TGMDA resin

Viscosity of 0510:TGMDA:PAE-co-I-5 Modified Resin

Figure 6.8 Viscosity of 0510:TGMDA:PAE-co-I-5 modified resin

6.4.5 Arylene ether and Arylene ether-co-imidazole Oligomers as Epoxy Modifiers

High molecular weight PAE-co-Is have limited solubility in the epoxy resin. As a result, PAE-co-I oligomers were investigated as tougheners. Stoichiometric imbalance of the monomers was employed to properly control molecular weight according to the Carothers equation by varying the molar ratio of bisphenol to dihalide. All polymers designated Olig-1 and Co-Olig-1 possess phenol endgroups

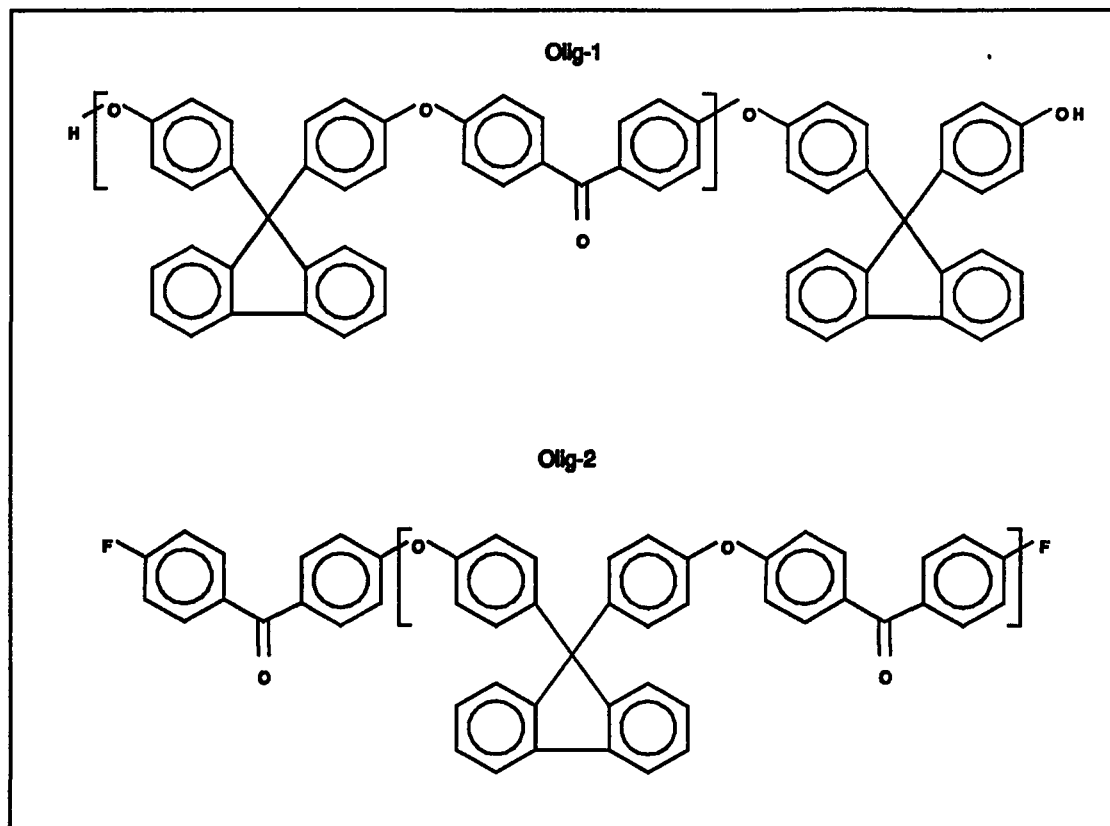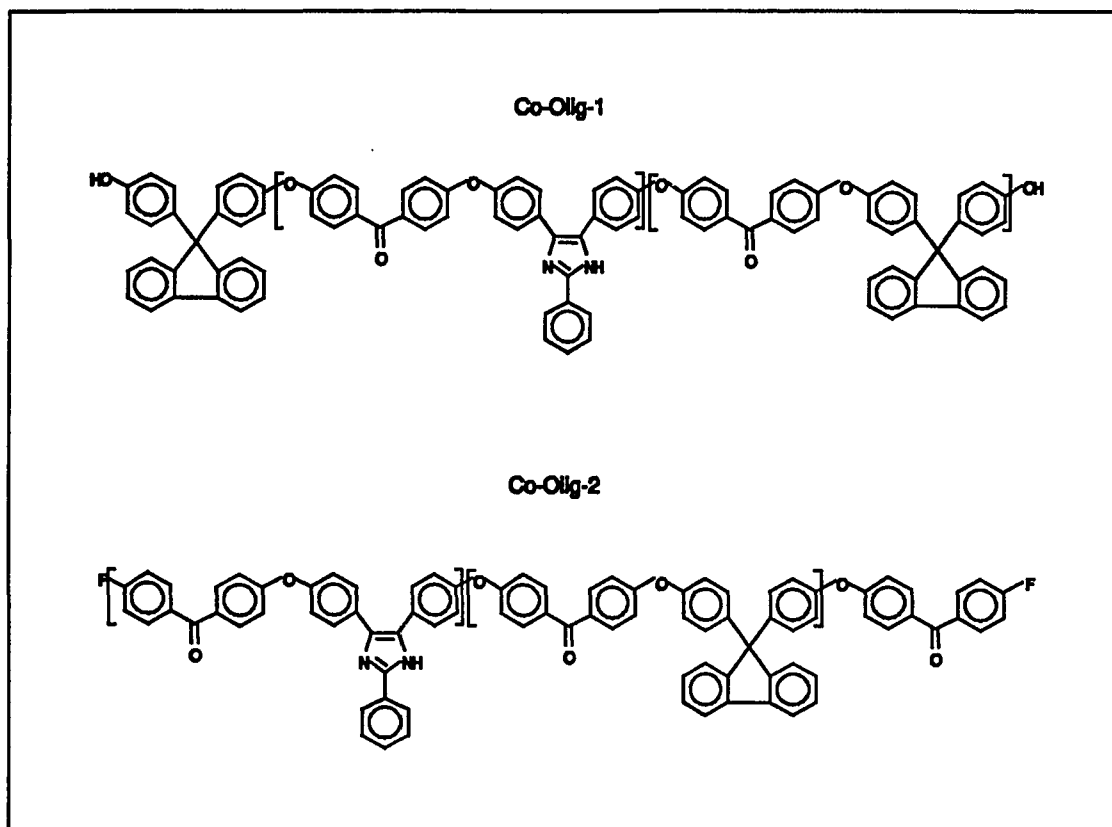and Olig-2 and Co-Olig-2 possess fluoro endgroups Figures 6.9.

Figure 6.9 Arylene ether and Arylene ether-co-imidazole Oligomers

Co-Olig-1

Co-Olig-2

End group functionality and molecular weight play a major role in the mechanical and thermal properties of a polymer. Stoichiometric imbalance results in polymer chains predominated by one endgroup or the other depending on the system favored. To assess the effects of stoichiometric offsetting and possible interaction of the endgroup with the epoxy resin, polymer systems were prepared offsetting in favor of both the dihalide and bisphenol, holding the imidazole concentration distributed along the polymer backbone constant at 10 mole percent.

A second parameter investigated was the capability of PAEs without the imidazole moiety to serve as toughness modifiers for epoxy resins. PAE homopolymers and oligomers were also blended with the TGMDA 722 epoxy resin

and the solubility and toughness characteristics of the systems were determined.

The influence of the imidazole moiety on the solubility and incorporation of the polymer into the cured epoxy resin network is dramatically demonstrated in Figure 6.10. The appearance of a 7 % w/w modified specimen of the 1:1 stoichiometric homopolymer without the imidazole moiety (PAE-1) is distinctly different than that of a 7 % w/w modified specimen of the 1:1 stoichiometric copolymer with 10 % imidazole (PAE-co-I-5) randomly distributed along the polymer backbone. Upon initial mixing, both polymers appeared to be miscible with the uncured epoxy resin, giving clear yellow solutions. However, as illustrated in the photograph, the homopolymer system is not compatible in the cured state, and actually appears to be excluded from the cured epoxy network, while the copolymer system is incorporated into the network. This solubility effect was also exhibited in the preparation of modified epoxy resins. Generally the solubility of the tougheners decreased with decreasing imidazole content.

(a) 7% w/w PAE-1/TGMDA

(b) 20% w/w PAE-co-I-5/TGMDA
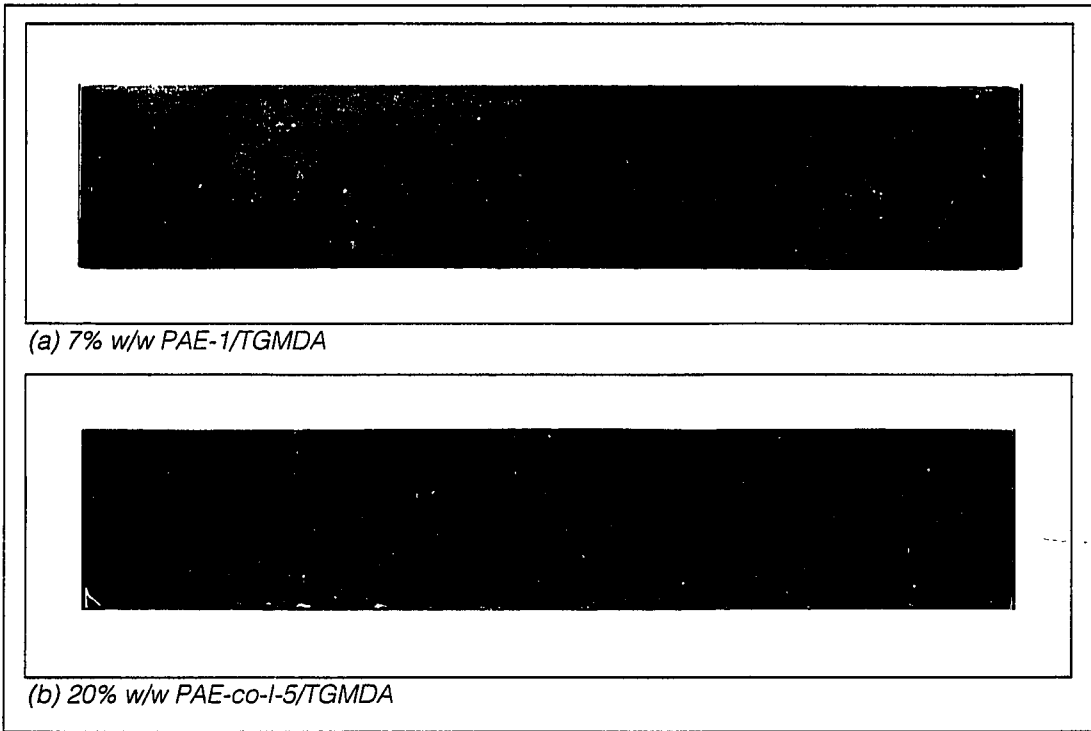
Polymer modified TGMDA samples   *Figure 6.10*

Table 6.7 summarizes the solubility of the polymer/oligomer systems along with the times required to obtain homogeneous mixtures.

Table 6.7 Solubility of Modifiers in TGMDA-722 Prior to Cure

Description	Temp. °C	Solubility	Mixing Time
Homopolymers			
PAE-1	120	slightly soluble	24 hours
10% offset Olig-1	120	slightly soluble	24 hours
10% offset Olig-2	120	slightly soluble	24 hours
5% offset Olig-1	140	insoluble	48 hours
5% offset Olig-2	120	slightly soluble	24 hours
10% Imidazole Copolymers			
PAE-co-I-5	100	soluble	8 hours
10% offset Co-Olig-1	100	soluble	10 hours
10% offset Co-Olig-2	100	soluble	4 hours
5% offset Co-Olig-1	100	soluble	18 hours
5% offset Co-Olig-2	100	soluble	7 hours

The PAE oligomers required extended mixing times at elevated temperatures to dissolve in the epoxy resin. The 5% offset Olig-1 was insoluble

Table 6.8 Mechanical Properties of Neat Polymers

Description	Flexural Modulus (ksi)	Flexural Strength (ksi)	K_{lc} (psi√in)
Homopolymers			
PAE-1	624 ± 6	19.3 ± 1	1870 ± 170
10% offset Olig-1	555 ± 3	4.9 ± 0.4	**
10% offset Olig-2	493 ± 3	2.2 ± 0.3	**
5% offset Olig-1	633 ± 6	18.5 ± 1	1490 ±124
5% offset Olig-2	584 ±22	4.5 ± 0.1	**
10% Imidazole Copolymers			
PAE-co-I-5	598 ± 11	18.4 ± 2	1666 ± 100
10% offset Co-Olig-1	591 ± 16	3.4 ± 0.5	**
10% offset Co-Olig-2	**	**	**
5% offset Co-Olig-1	383 ± 8	1.4 ± 0.1	1177 ± 74
5% offset Co-Olig-2	587 ± 20	4.4 ± 1	474 ± 165

** Neat Polymers to brittle to characterize

Fracture toughness values for the neat polymers ranged from 474 to 1870 psi√in, with flexural modulus values from approximately 400 to 600 ksi, and flexural strength values from approximately 1 to 20 ksi. The fracture toughness value of the 5% offset Co-Olig-2 is low at 474 psi√in, however the modulus and strength

values for this oligomer are in line with the other oligomers in this study. These modulus and strength values compare well with thin film properties of PAEIs previously reported[1]

As previously stated, the epoxy/PAE-1 modified system was immiscible in the cured state and 5% Olig-1 was insoluble in the epoxy resin; therefore, mechanical properties of these systems could not be determined. The mechanical properties of the modified epoxy resins are presented in Table 6.9.

Table 6.9 Mechanical Properties of Modified TGMDA 722
with of 7% w/w Polymer

Description	Flexural Modulus (ksi)	Flexural Strength (ksi)	K_{lc} (psi√in)
Neat TGMDA 722	516 ± 31	11 ± 5.1	353 ± 17
Homopolymers			
PAE-1	**	**	**
10% offset Olig-1	556 ± 36	5.1 ± 0.7	326 ± 22
10% offset Olig-2	397 ± 90	1.3 ± 0.4	***
5% offset Olig-1	**	**	**
5% offset Olig-2	547 ± 46	2.6 ± 0.8	372 ± 5
10% Imidazole Copolymers			
PAE-co-I-5	680 ± 22	14.2 ± 0.5	522 ± 29
10% offset Co-Olig-1	515 ± 23	9.5 ± 0.3	395 ± 37
10% offset Co-Olig-2	505 ± 40	7.9 ± 3.5	444 ± 59
5% offset Co-Olig-1	407 ± 29	5.6 ± 0.7	422 ± 49
5% offset Co-Olig-2	510 ± 64	7.7 ± 0.1	411 ± 36

** Nonviable modified system

*** System too brittle to characterize

Fracture toughness values for the modified resins ranged from 326 to 522 psi√in. The greatest improvement in fracture toughness was realized for the PAE-

co-I-5 resin, which also had the highest fracture toughness in the neat polymer state. The second highest modified system in terms of fracture toughness was the 10% offset Co-Olig-2, with a 25% increase in fracture toughness over the unmodified resin. Both of these systems exhibited toughening greater than that predicted by a rule of mixtures relationship. Flexural modulus values ranged from approximately 400 to 700 ksi and flexural strength from 1 to 14 ksi. Except for the 10% offset Olig-2 and 5% offset Co-Olig-1 modulus values of the modified resins are approximately equal to or greater than the neat epoxy. Strength values of the modified resins are lower than the unmodified epoxy, except for the PAE-co-I-5 resin which has a higher strength. The lower strength values of the oligomers are attributed to the low molecular weight of these systems.

A second consideration in modifying high performance epoxy resins for improved fracture toughness is the effects of the modifier on the Tg and thermal oxidative stability of the resin. Tgs and 5% weight loss data of the neat polymers and oligomers are given in Table 6.10.

Table 6.10 Thermal Properties of Neat Polymers

Description	Tg (°C, DSC)	TOS (°C, TGA)
Homopolymers		
PAE-1	252	446
10% offset Olig-1	233	490
10% offset Olig-2	214	506
5% offset Olig-1	242	492
5% offset Olig-2	221	487
10% Imidazole Copolymers		
PAE-co-I-5	243	458
10% offset Co-Olig-1	223	431
10% offset Co-Olig-2	205	461
5% offset Co-Olig-1	251	431
5% offset Co-Olig-2	226	492

The Tgs of the neat polymers range from 205 to 252 °C, and the TOS as determined by TGA ranged from approximately 430 to 500 °C.

Thermal degradation of highly crosslinked epoxy systems occurs near the Tg, masking transitions by DSC. Therefore, the Tgs for the epoxy resins were determined by DMA. The glass transition temperatures for some neat polymers were also determined by DMA. The good agreement between the two methods, as summarized in Table 6.11, raises confidence in the DMA results for the epoxy resins. Determination of Tg by DMA for all neat polymers used in this study was not possible because of sample availability and the brittlness of some molded neat

polymer samples.

Table 6.11 Neat Polymer Glass Transition Temperature by DSC and DMA

Polymer	Tg (°C, DSC)	Tg (°C, DMA)
PAE-1	252	257
10% offset Olig-1	233	218
5% offset Olig-1	242	229
5% offset Olig-2	221	205
5% offset Co-Olig-2	226	223

Table 6.12 Thermal Properties for 7% Polymer Blends

Description	Tg (°C, DMA)	TOS (°C, TGA)
Neat Epoxy	243	322
Homopolymers		
PAE-1	**	**
10% offset Olig-1	213	311
10% offset Olig-2	***	322
5% offset Olig-1	**	**
5% offset Olig-2	***	294
10% Imidazole Copolymers		
PAE-co-I-5	224	330
10% offset Co-Olig-1	171	320
10% offset Co-Olig-2	188	323
5% offset Co-Olig-1	196	316
5% offset Co-Olig-2	164	323

** Nonviable modified system

*** Sample too brittle to characterize

The thermal oxidative stablity of the blends is dominated by the epoxy since it comprises 93% w/w of the modified system. The 5% weight-loss point for the modified resins is approximately equal to that of the unmodified resin. There is an

overall decrease in Tg with polymer modification. A decrease in Tg of over 80 °C was realized by incorporating 5% offset Co-Oig-2, while only a 20 ° C drop in Tg resulted from the incorporation of PAE-co-I-5. A net lowering in Tg is expected with modification of thermoset networks with thermoplastics due to the lowering of crosslink density.

Optimum increases in fracture toughness are realized through incorporation of the 1:1 stoichiometric copolymer PAE-co-I-5 for the systems examined in this study. However, the high viscosity and difficulties in processing limit the application of this system. In order to prepare modified resins containing higher weight percent thermoplastic, an oligomeric system of greater solubility and lower pre-cure viscosity was chosen. Based on the solubility of the oligomer, fracture toughness, thermal and thermal oxidative properties of the system, 10% offset Co-Olig-2 was chosen as a system likely to yield good modified epoxy resin specimens of higher polymer concentrations. Samples containing 10, 15, and 20 w/w were prepared and tested for fracture toughness, flexural modulus and flexural strength. A summary of the data is presented in Table 6.13.

Table 6.13 Mechanical Properties of Various Concentrations of Co-Olig-2

Concentration	Flexural Modulus (ksi)	Flexural Strength (ksi)	K_{Ic} (psi√in)
Neat Epoxy	516 ± 31	11 ± 5	353 ± 17
7 % w/w	505 ± 40	7.9 ± 3.5	444 ± 59
10% w/w	489 ± 16	9.7 ± 5	448 ± 42
15% w/w	540 ± 28	12.5 ± 3	439 ± 31
20% w/w	315 ± 11	6.4 ± 2	463 ± 21

Fracture toughness values ranged from 439 to 463 psi√in for the modified resins. Although the modified resins exhibit improvements in fracture toughness, increases in thermoplastic modifier concentrations as high as 20% w/w did not result in an additional increase in fracture toughness for the modified resin system.

Table 6.14 Thermal Properties of Various Concentrations of Co-Olig-2

Concentration	Tg (°C, DMA)	TOS (°C, TGA)
Neat Epoxy	243	322
7 % w/w	188	323
10% w/w	189	321
15% w/w	183	326
20% w/w	173	327

As expected, higher thermoplastic concentrations did not effect the dynamic thermal oxidative stablity of the epoxy, and an overall decrease in Tg resulted with the modified resins (Table 6.14).

6.4.6 PAE-co-Is of Varying Imidazole Concentrations as Epoxy Modifiers

The imidazole concentration of all copolymer systems discussed so far was held constant at 10 mole percent of the overall bisphenol concentrations. Increasing the amount of imidazole distributed along the polymer backbone decreases the molecular weight of polymer between crosslinking sites and changes the mechanical properties. High molecular weight PAE-co-I systems of the same chemical structure as PAE-co-I-5 containing 30 and 50 mole percent

imidazole were prepared and characterized as neat polymers and in 5% w/w

modified epoxy samples. The neat polymer data are summarized in Tables 6.15

and 6.16 and the modified epoxy data in Tables 6.17 and 6.18.

Table 6.15 Mechanical Properties of Neat Polymers
containing Various Mole Percents Imidazole

Description	Flexural Modulus (ksi)	Flexural Strength (ksi)	K_{Ic} (psi√in)
10% Imidazole	598 ± 11	18.4 ± 2.5	1666 ± 100
30% Imidazole	537 ± 44	4.0 ± 0.3	771 ± 43
50% Imidazole	587 ± 6.5	5.1 ± 0.4	644 ± 82

Fracture toughness values range from 644 to 1666 psi√in, with the 10%

imidazole polymer exhibiting K_{Ic} values twice as high as the other polymers.

Flexural modulus values ranged from 598 to 537 with the 30% imidazole having

the lowest value. The 10% imidazole also had far better flexural strength

properties than the other two polymers at 18 ksi in comparison to 4 and 5 ksi for

the 30 and 50% imidazole, respectively.

Table 6.16 Thermal Properties of Neat Polymers
containing Various Mole Percents Imidazole

Description	Tg (°C, DSC)	Tg (° C, DMA)	TOS (°C, TGA)
10% Imidazole	243	**	458
30% Imidazole	239	243	419
50% Imidazole	232	247	468

Increases in the imidazole concentration along the polymer backbone have only minimal effects on the glass transtion temperature and thermal oxidative stablity. It should be noted that the 50:50 PAE:PAEI copolymer's thermal stability by TGA is slightly higher than that of the other variations, as previously observed for other 50:50 PAE:PAEI random copolymers of different chemical composition (section 6.4.2).

Table 6.17 Mechanical Properties of 5% w/w Modified Resins containing Various Mole Percents Imidazole

Description	Flexural Modulus (ksi)	Flexural Strength (ksi)	K_{Ic} (psi√in)
Neat Epoxy	516 ± 31	11 ± 5	353 ± 17
10% Imidazole	487 ± 44	13.5 ± 3.3	522 ± 29
30% Imidazole	546 ± 31	11.6 ± 2.8	432 ± 41
50% Imidazole	567 ± 9.7	13.2 ± 2.5	401 ± 22

Increasing the imidazole concentration increased the flexural modulus from 487 ksi for 10% imidazole to 567 ksi for 50% imidazole. An increase in imidazole concentration increases the number of crosslinking sites between the thermoplastic modifier and the epoxy resin. Optimization of the percent of crosslinking between the epoxy resin and thermoplastic modifier must be accompanied with an optimization of crosslink density for the entire three dimensional network in order to afford improvements in fracture toughness. Increasing the imidazole concentration along the polymer backbone decreases fracture toughness. This is attributed to an overall increase in crosslink density.

Table 6.18 Thermal Properties of 5% w/w Modified Resins
containing Various Mole Percents Imidazole

Description	Tg (°C, DMA)	TOS (°C, TGA)
10% Imidazole	207	320
30% Imidazole	179	329
50% Imidazole	197	333

Increasing the concentration of imidazole from 10 to 30 % resulted in a 30 °C drop in Tg for the 5% w/w modified resin, but increasing it to 50% yields a resin with a Tg only 10 °C below the 10% system.

6.5 Copolymer Molecular Weight Characterization

Determination of homopolymer molecular weight by GPC is an acceptable method. However, random copolymer molecular weight characterization by this method may not be valid. The chemical composition of each polymer chain varies in a random system. For a homopolymer solution, the change in refractive index from that of the pure solvent can be used as a measure of the polymer concentration (mass/volume). However, for a solution of a copolymer the refractive index also varies with the chemical composition of the polymer chain. This non-uniformity in the chemical composition of a random copolymer may contribute to

the experimental error of the method. The effect is accentuated if the differences in refractive index between the two segments of the copolymer are large.

M_w determined by GPC will be compared to M_w determined by light scattering to validate the method as an acceptable means to determine random copolymer molecular weights for the PAE-co-Is.

6.5.1 GPC Molecular Weight Characterization

The molecular weights of the polymer systems were determined by gel permeation chromatography (GPC) in $CHCl_3$ and in NMP/LiBr. Varying degrees of difficulty were experienced in filtering the $CHCl_3$ solutions for GPC through 0.2 μm Teflon filters. The 5% offset Co-Olig-1 was the most difficult to filter. This solution was slightly cloudy and required 2 filters to yield 4 mls of solution. The PAE-1, 5 and 10% offset Olig-2, PAE-co-I-5 and 5% offset Co-Olig-2 were all intermediately difficult to filter. Each required 1 filter per 4 ml aliquot. The 5 and 10% offset Olig-1, the 10% offset Co-Olig-1 and 10% offset Co-Olig-2 were very easy to filter and required only one filter to obtain 8 mls of solution. Duplicate GPC runs were performed for each sample and reproducibility between runs was very good. However, there were discrepancies between the 5% offset Co-Olig-1 and PAE-co-I-5. The variation in samples may be due to inhomogeneity in the solutions injected as a result of the difficulty in the filtration step. The presence of more high molecular weight species in one sample compared to the duplicate

is most visible in the z average molecular weight (M_z). The M_z distribution is the most sensitive to the presence of the larger molecules. A second sample set of PAE-co-I-5 was run to confirm the results. The molecular weights and viscosity results are summarized in Table 6.19.

Table 6.19 Chloroform GPC Data

Description	M_n (g/mol) Theory	M_n (g/mol)	M_w (g/mol)	M_z (g/mol)	M_w/M_n
Homopolymers					
PAE-1		9,400	389,500	956,700	41.4
10% offset Olig-1	10,400	2,800	9,200	17,500	3.3
10% offset Olig-2	10,300	4,700	11,500	21,300	2.5
5% offset Olig-1	21,000	5,300	20,800	38,400	3.9
5% offset Olig-2	21,000	6,700	17,100	30,400	2.5
10% Imidazole Copolymers					
PAE-co-I-5		200	6,700	21,000	33.6
10% offset Co-Olig-1		200	3,700	17,600	17.9
10% offset Co-Olig-2		800	4,300	11,900	5.2
5% offset Co-Olig-1		600	6,800	7,300	11.4
5% offset Co-Olig-2		1,000	6,800	8,300	6.8

Except for the 1:1 stoichiometry polymers (PAE-1 and PAE-co-5) there is good agreement between the inherent viscosities determined in THF at 35 °C and the intrinsic viscosity determined by GPC in $CHCl_3$ (Table 6.20).

Table 6.20 Viscosities of PAE and PAE-co-I Modifiers

Description	η_{inh} dL/g	$[\eta]$ dL/g
Homopolymers		
PAE-1	0.63	1.70
10% offset Olig-1	0.17	0.16
10% offset Olig-2	0.15	0.16
5% offset Olig-1	0.24	0.26
5% offset Olig-2	0.20	0.21
10% Imidazole Copolymers		
PAE-co-I-5	0.52	0.30
10% offset Co-Olig-1	0.15	0.12
10% offset Co-Olig-2	0.13	0.11
5% offset Co-Olig-1	0.23	0.19
5% offset Co-Olig-2	0.20	0.18

The effects of offsetting the homopolymer by 5% and 10% towards the bisphenol and dihalide are shown in the GPC results in Figure 6.11 A and B. Offsetting in favor of either functional group resulted in a narrower molecular-weight distribution than the 1:1 stoichiometric homopolymer and as expected,

severely lowered the molecular weight. Figure 6.12 A and B compares the distributions of 5 and 10% Olig-1 and Olig-2. Offsetting in favor of the dihalide (Olig-2) resulted in the narrowest distribution for both 5 and 10% offsets. The presence of very low molecular weight species (molecular weights of several hundred) was also observed for both Olig-1 samples. It appears however, that the concentration of low molecular weight species was much lower for the 5% Olig-1 than the 10% Olig-1. This is probably expected due to the lower degree of stoichiometric imbalance.

Molecular Weight Distribution of PAE in CHCl$_3$

Figure 6.11a

Molecular Weight Distribution of PAE in CHCl$_3$

Figure 6.11b

Molecular Weight Distribution of PAE in CHCl₃

Figure 6.12a

Molecular Weight Distribution of PAE in CHCl₃
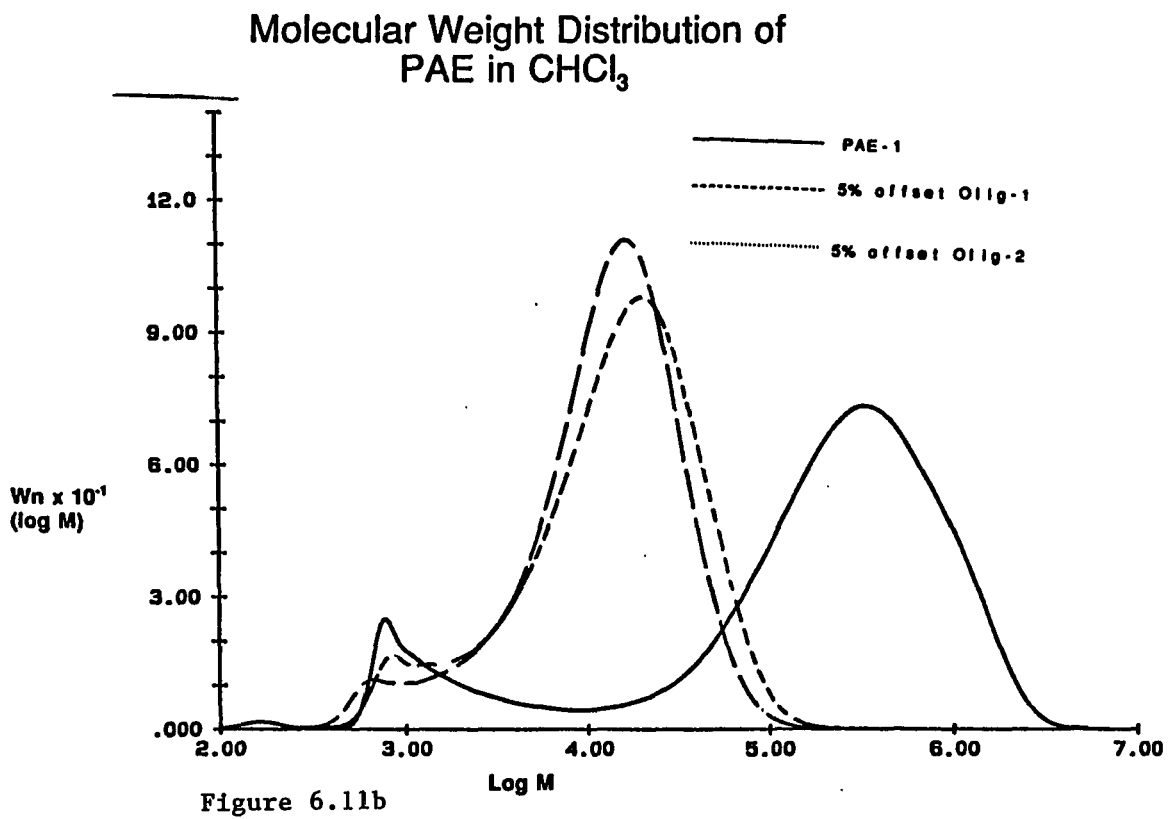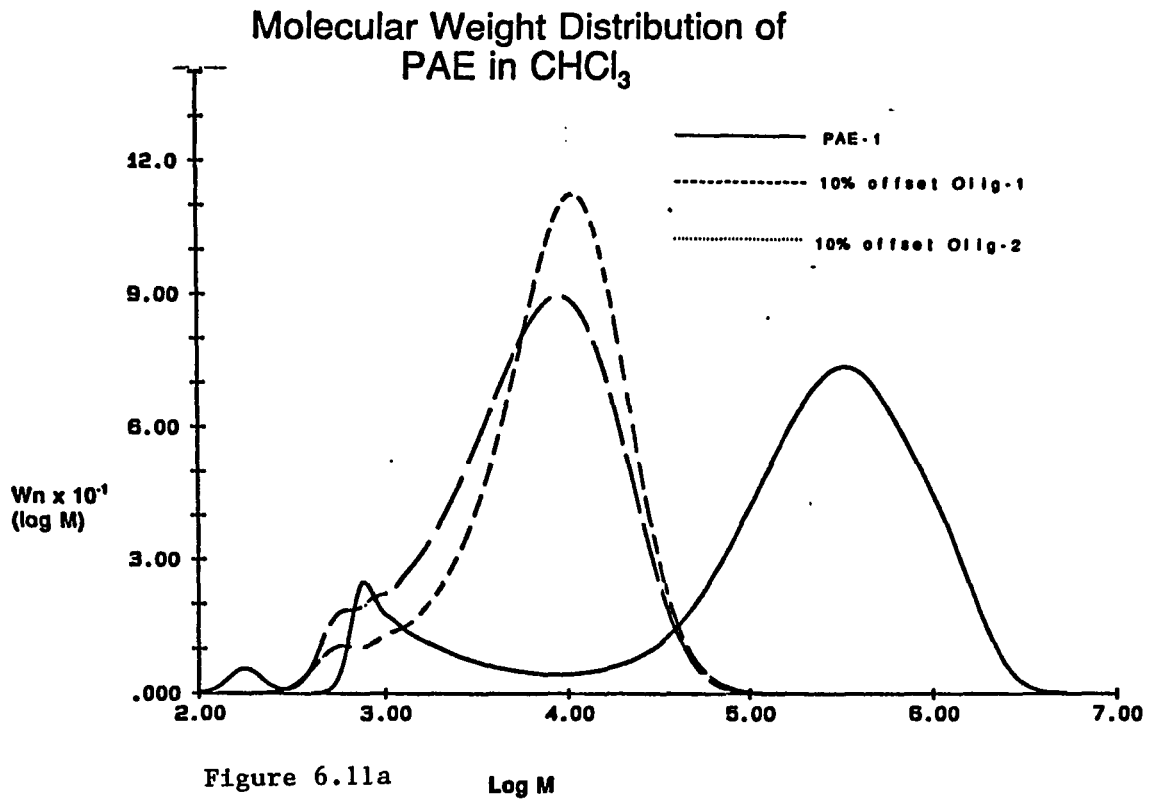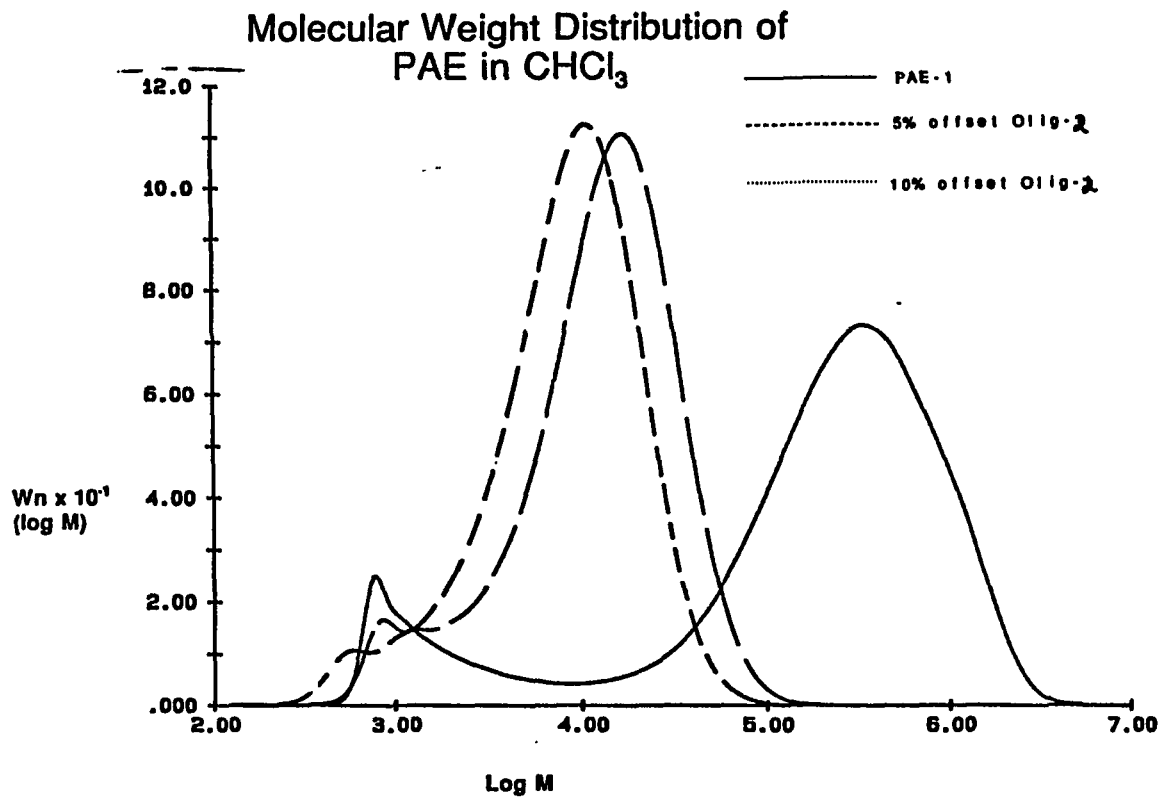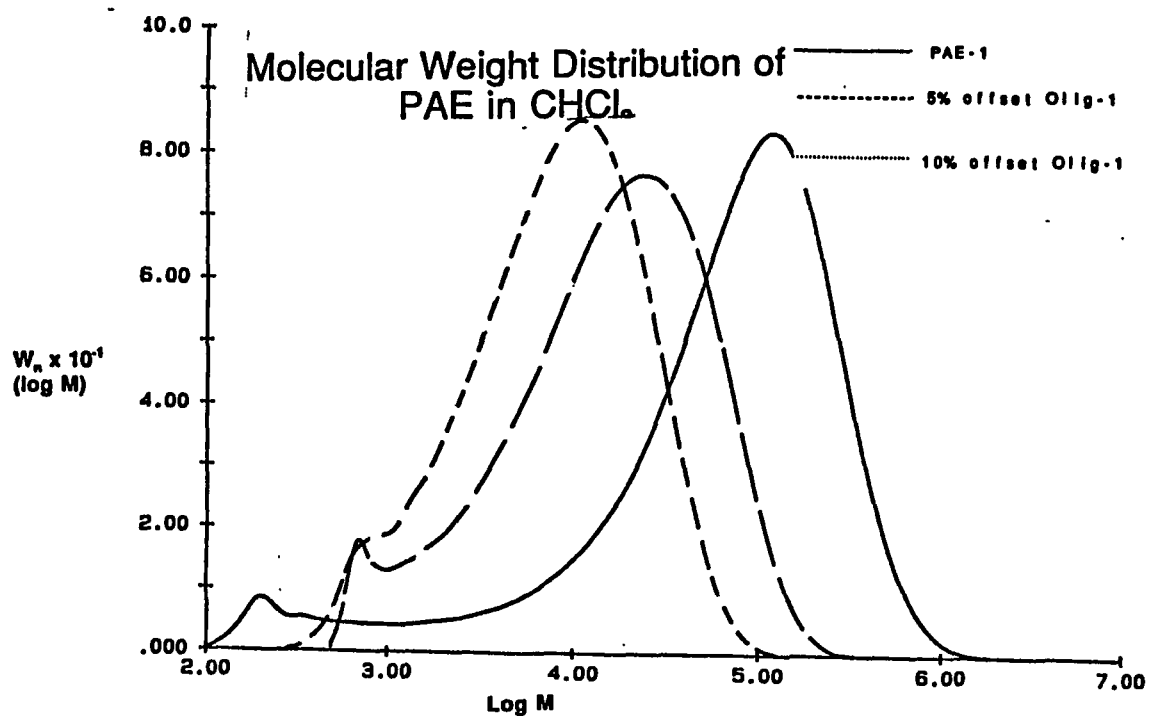
Figure 6.12b

Overlays of the distributions of the PAE-co-I-5 with the 5 and 10% Co-Olig 1 and 2 are shown in Figure 6.13 A and B. In both cases the stoichiometric imbalance did not produce as severe a difference as that noted for the homopolymers. It is possible that the difference between these polymers was erased by the prolonged retention of the samples on the columns. Figures 6.14 A and B are overlays of the distributions for 5 and 10% co-oligomers. The higher degree of offset resulted in a greater difference in the molecular weight distribution for Co-Olig-1. The prolonged retention time of the copolymers over the homopolymers becomes more apparent when one overlays the molecular weight distributions for PAE-1 and PAE-co-I (Figure 6.15).

The exact molecular weight averages of the copolymers may not be accurate due to differences in the distribution of chemical composition between chains for a random copolymer. The high variation in chemical composition may be responsible for the severe tailing in the lower molecular weight end of the copolymer. The copolymer may be interacting with the crosslinked polystyrene of the chromatographic column that would contribute to the tailing observed in the molecular weight distribution due to the polymer being retained much longer on the columns. This is evident in the very low number average molecular weights, as compared to theoretical values.

Figure 6.13a

Figure 6.13b

Molecular Weight Distribution of PAE-co-I in CHCl₃

Figure 6.14a
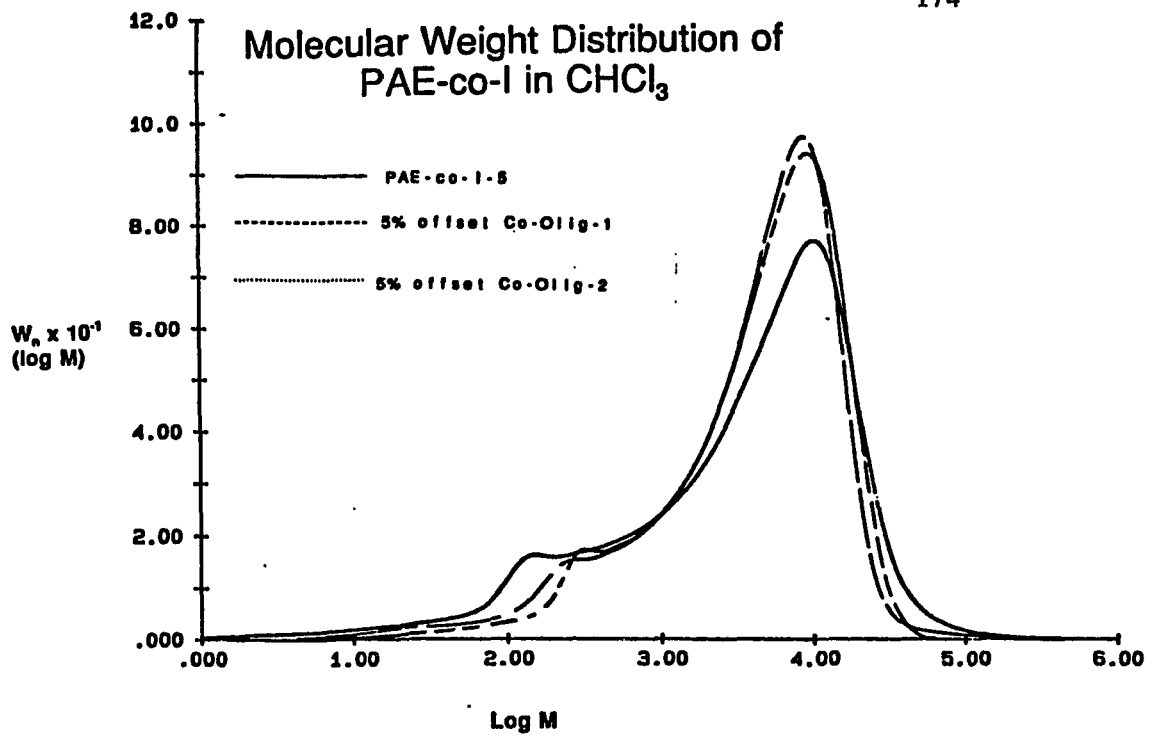
Molecular Weight Distribution of PAE-co-I in CHCl₃
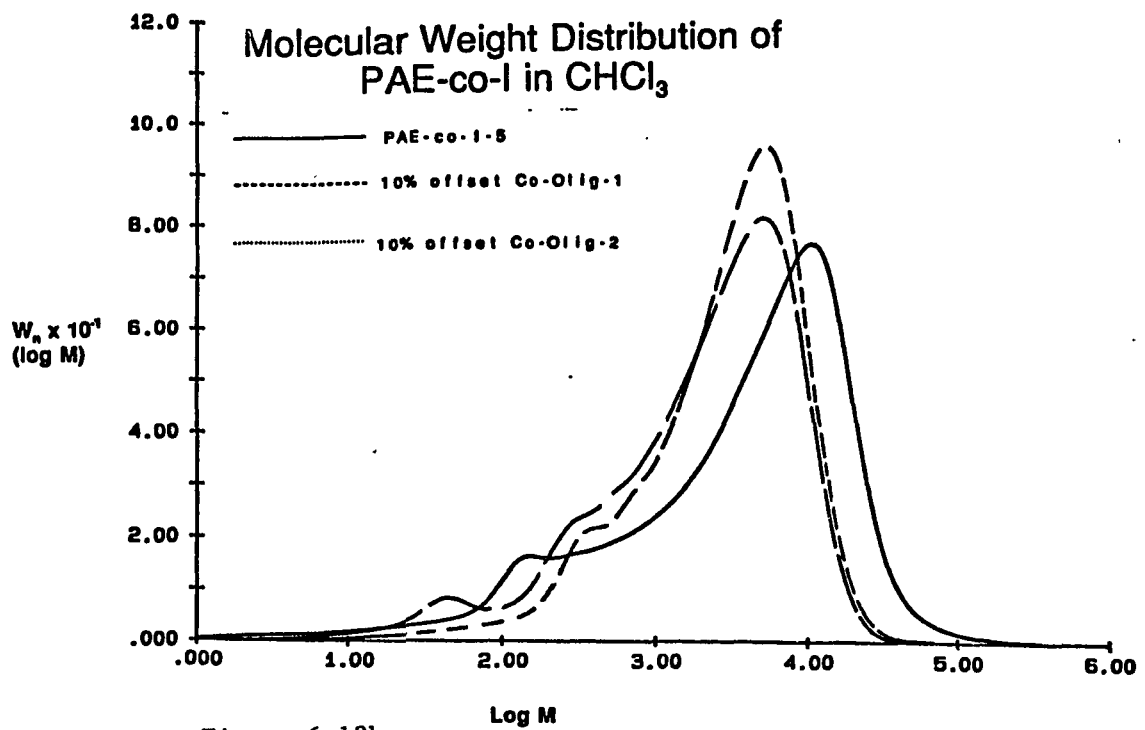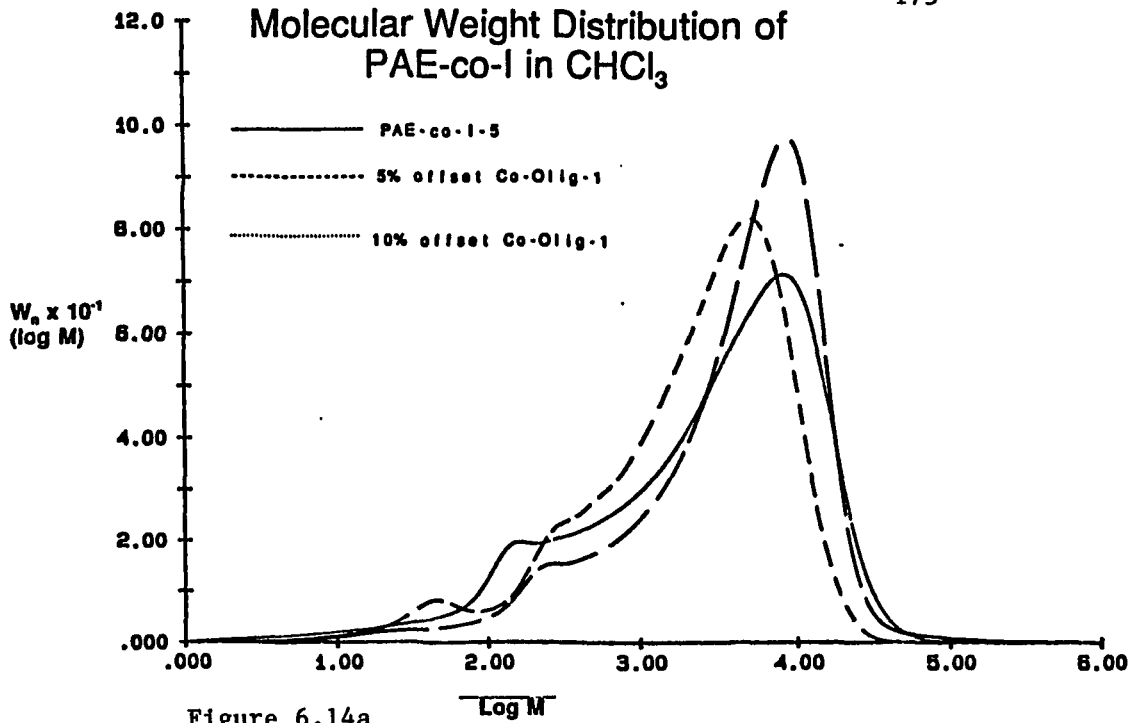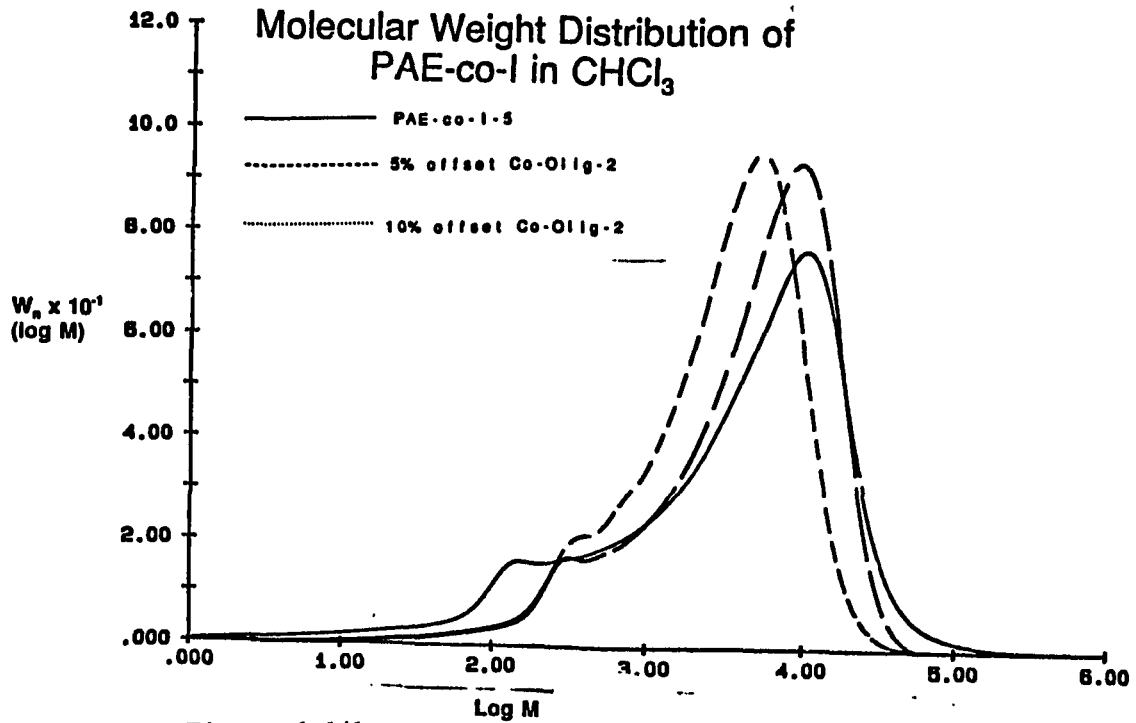
Figure 6.14b

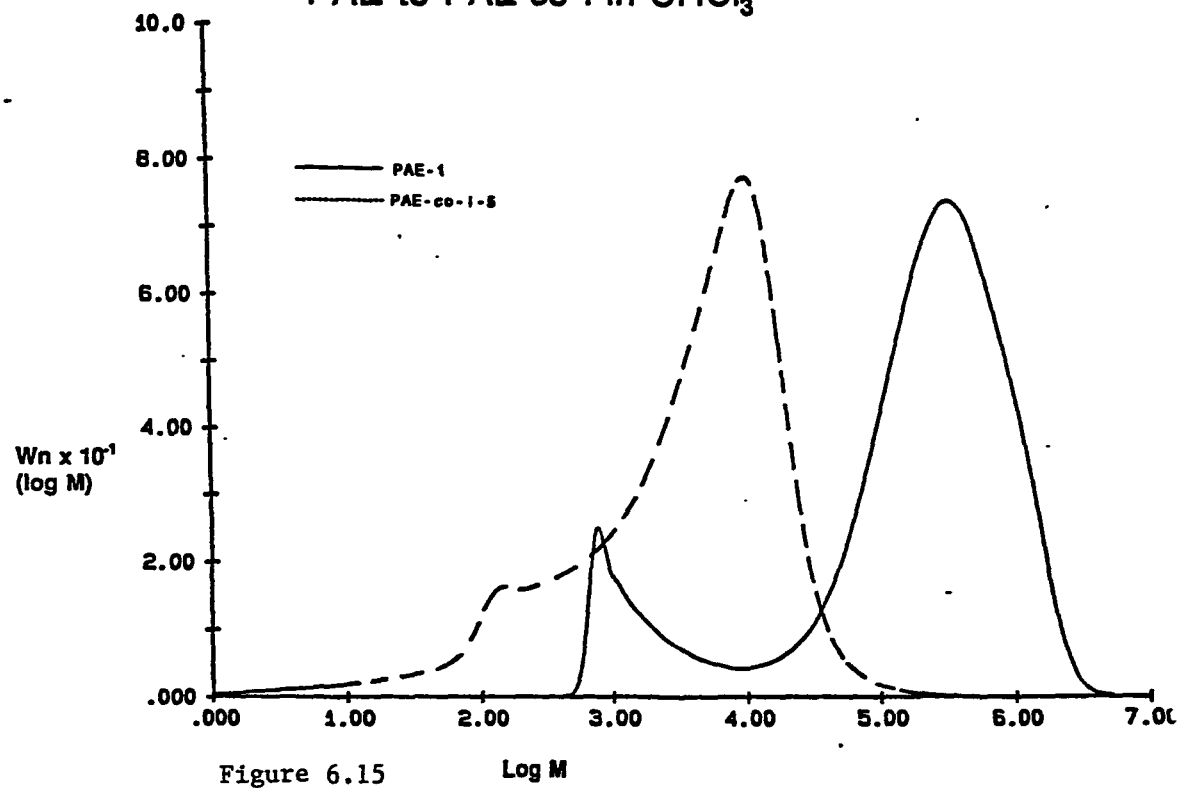# Comparison of Molecular Weight Distribution of
PAE to PAE-co-I in CHCl₃

Figure 6.15

The molecular weights of polymers of the same chemical composition as those listed in Table 6.21 were determined using freshly distilled NMP containing 0.02M LiBr as the mobile phase. NMP was chosen due to the solubility of the polymers and relative ease of filtration for all samples. All samples were filtered using one 0.2 μm filter to obtain 8 mls of solution. The LiBr was added to the solvent to reduce aggregation of chains which would lead to inflated molecular weights.

Table 6.21 NMP/LiBr GPC Data

Description	M_n (g/mol) Theory	M_n (g/mol)	M_w (g/mol)	M_z (g/mol)	M_w/M_n
Homopolymers					
PAE-1		5,300	119,500	257,400	22.5
10% offset Olig-1	10,400	4,000	12,380	23,900	3.1
10% offset Olig-2	10,300	3,900	12,800	20,100	3.3
5% offset Olig-1	21,000	6,200	26,800	55,200	4.3
5% offset Olig-2	21,000	5,300	18,400	38,800	3.5
10% Imidazole Copolymers					
PAE-co-I-5		4,900	109,800	312,100	22.5
10% offset Co-Olig-1		4,700	14,700	29,300	3.1
10% offset Co-Olig-2		3,700	10,200	19,100	2.7
5% offset Co-Olig-1		6,700	28,600	60,000	4.2
5% offset Co-Olig-2		5,800	20,800	44,500	3.6

The trend in molecular weights for the homopolymers follows the correct trend relative to their stoichiometric offsets. Similar to samples run in chloroform, the molecular weight distribution of the homopolymer is broader than the offset oligomers regardless of which monomer is favored, with a nominal portion being composed of low molecular weight species (Figure 6.16 A and B). A higher

molecular weight was obtained for the 5% Olig-1 than the 5% Olig-2 while the 10%

Olig-1 resulted in molecular weights approximately the same as the 10% Olig-2

(Figure 6.17 A and B). A slightly larger hydrodynamic volume is indicated for 10%

Olig-1 since the intrinsic viscosity determined in NMP/LiBr by GPC and the

inherent viscosiy determined in THF at 35 °C were slightly higher than the 10%

Olig-2 (Table 6.22). Unlike the viscosity data in $CHCl_3$ there is good agreement

between the two viscosity measurements for all polymers studied.

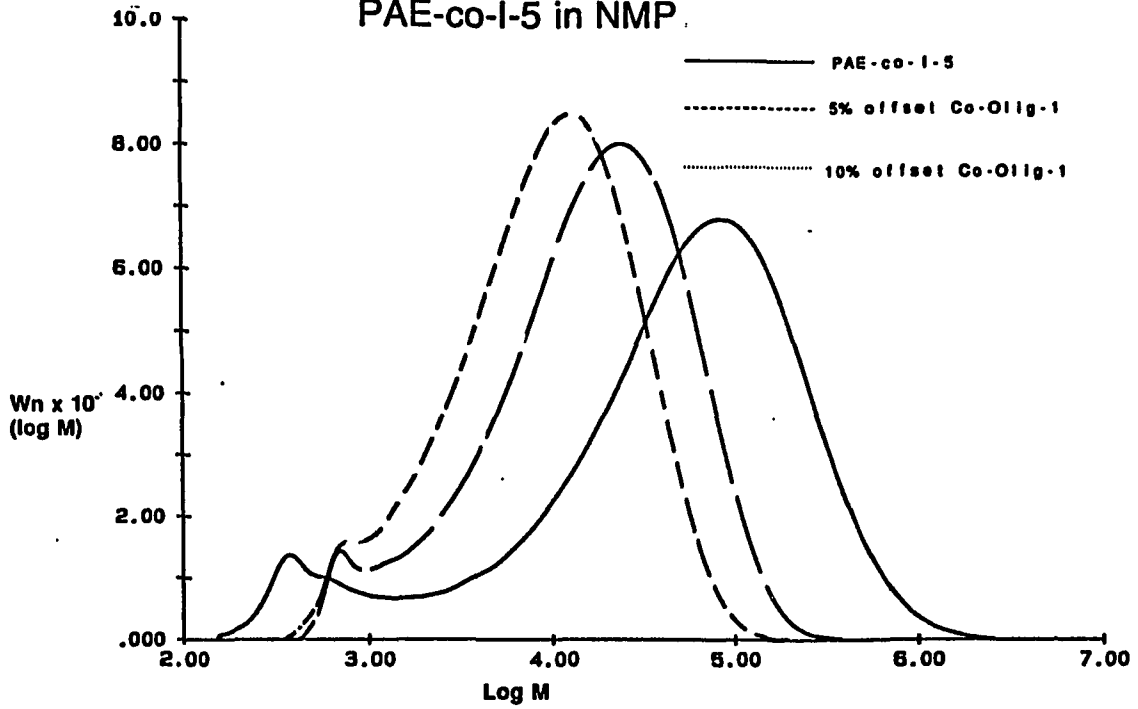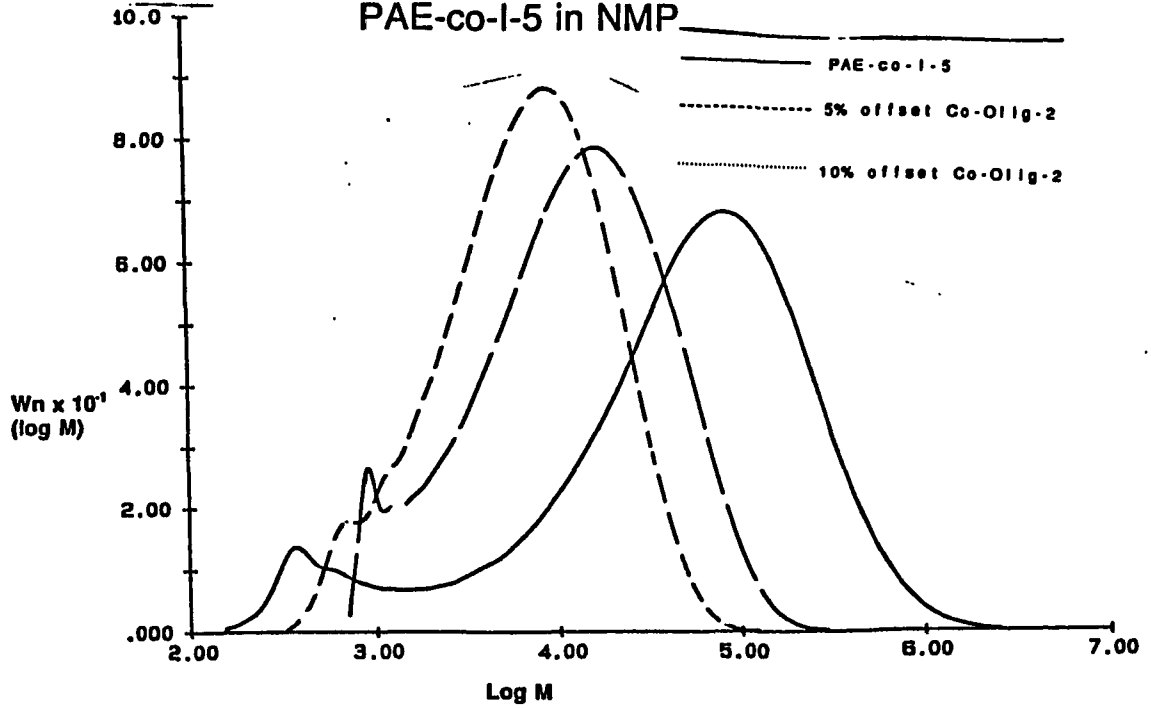# Molecular Weight Distribution of PAE in NMP/LiBr$_3$

Figure 6.16a

Comparison of Molecular Weight Distribution of PAE in NMP/LiBr

Figure 6.16b

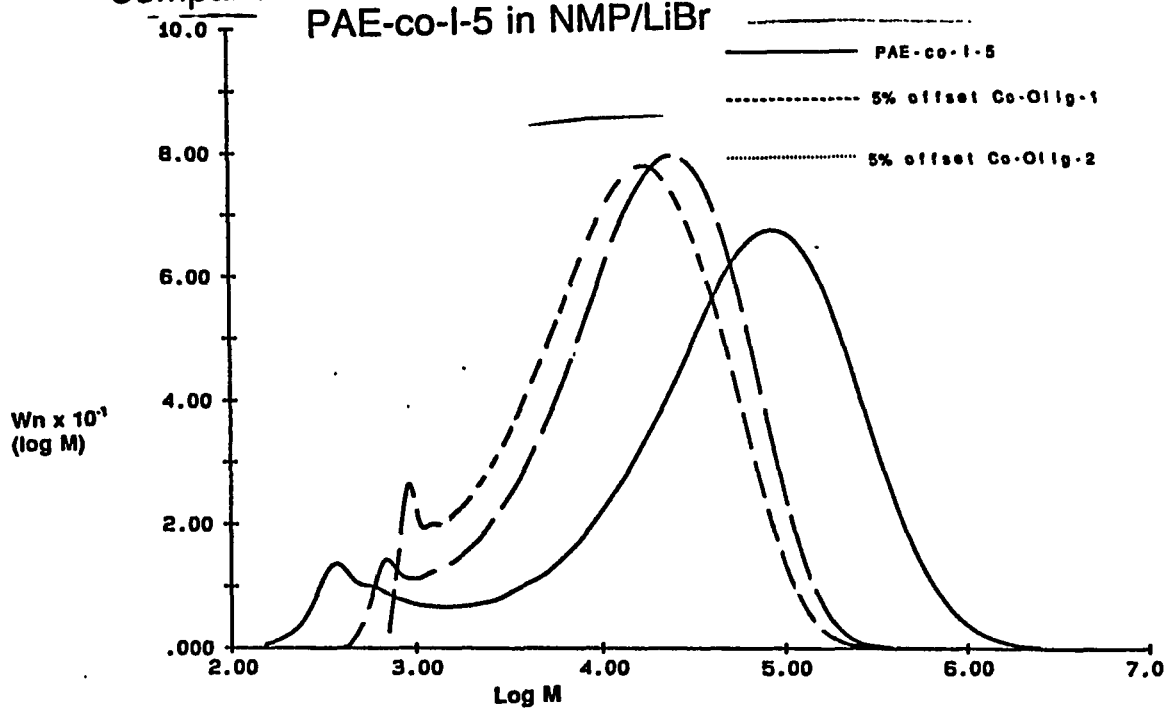## Comparison of Molecular Weight Distribution of PAE in NMP/LiBr

——————— PAE-1

------------ 5% offset Olig-1

·············· 5% offset Olig-2

Wn x 10⁻¹ (log M)

Log M

Figure 6.17a

Comparison of Molecular Weight Distribution of PAE-co-I-5 in NMP/LiBr

——————— PAE-1

------------ 10% offset Olig-1

·············· 10% offset Olig-2

Wn x 10⁻¹ (log M)

Log M
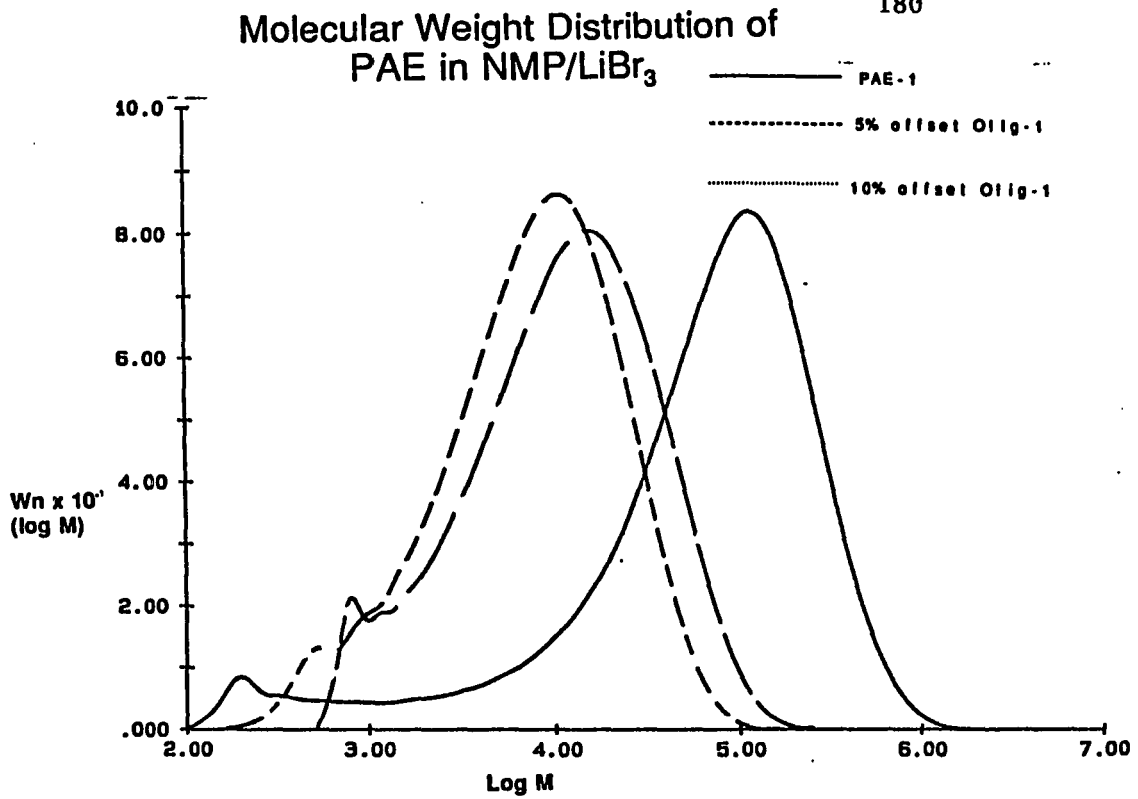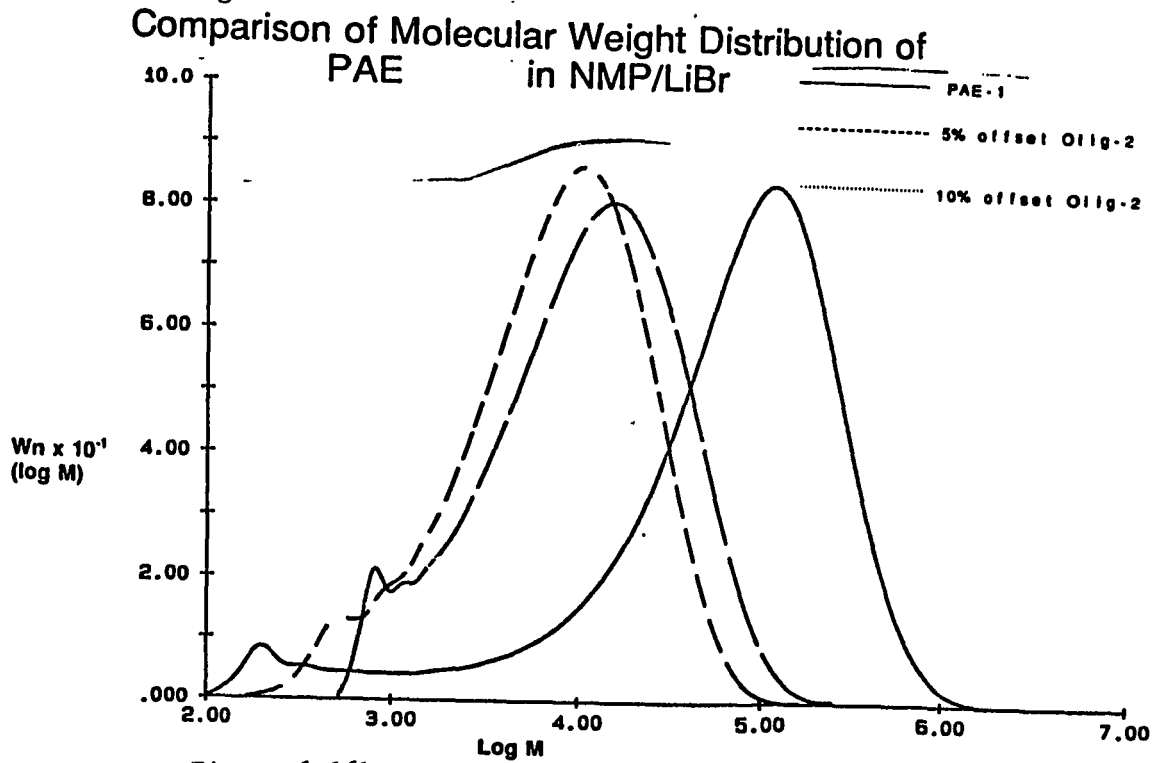
Figure 6.17b
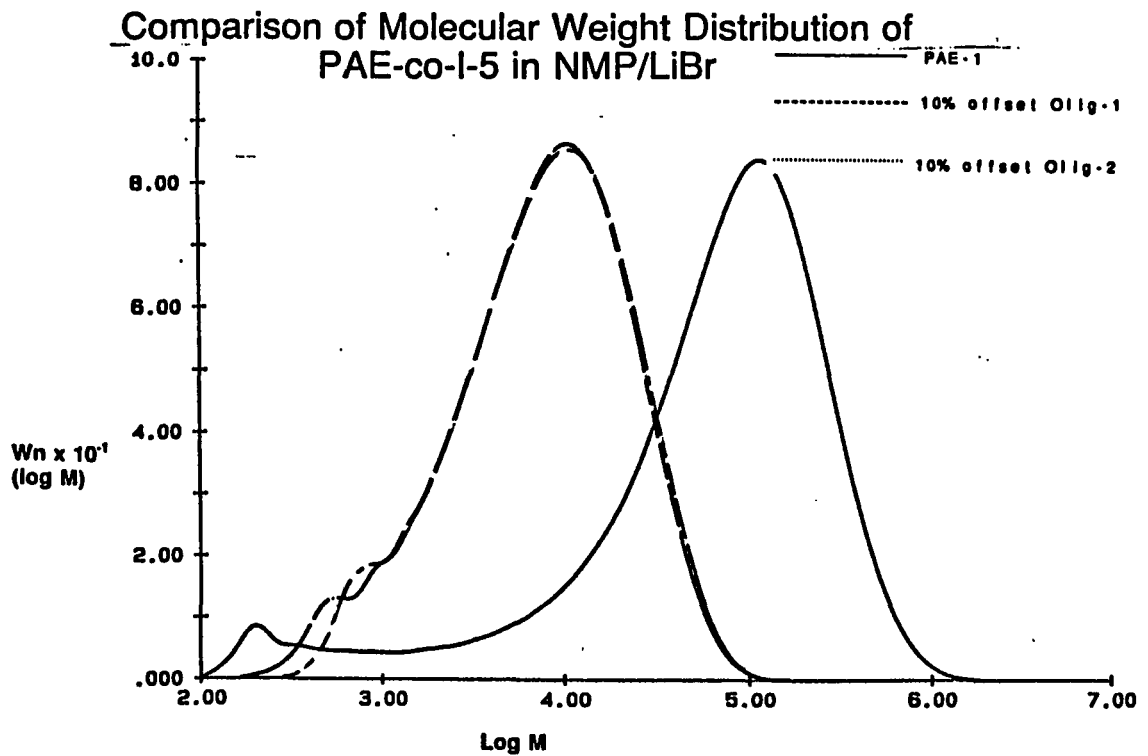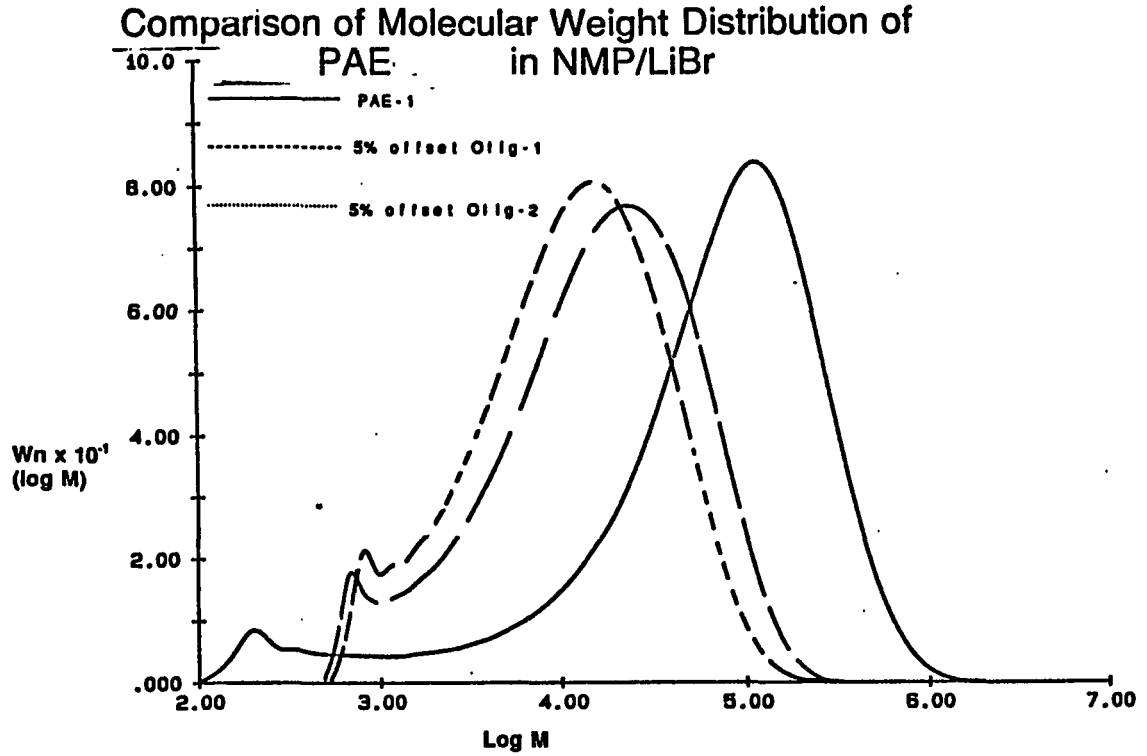
Table 6.22 Viscosities of PAE and PAE-co-I Modifiers

Description	η_{inh} dL/g	$[\eta]$ dL/g
Homopolymers		
PAE-1	0.63	0.71
10% Olig-1	0.19	0.16
10% Olig-2	0.15	0.16
5% Olig-1	0.24	0.26
5% Olig-2	0.18	0.20
10% Imidazole Copolymers		
PAE-co-I-5	0.54	0.54
10% Co-Olig-1	0.15	0.18
10% Co-Olig-2	0.13	0.13
5% Co-Olig-1	0.24	0.28
5% Co-Olig-2	0.21	0.22

Copolymer molecular weights also appear to be correct relative to their stoichiometric offset (Figure 6.18 A and B). Similar to PAE-1, the distribution is broader for PAE-co-I-5 and a nominal portion of low molecular weight species are also present. However, unlike Olig-1, Co-Olig-1 gives a slightly higher molecular weight than Co-Olig-2 for both the 5% and 10% offset (Figure 6.19 A and B).

Comparison of Molecular Weight Distribution of PAE-co-I-5 in NMP

Figure 6.18a

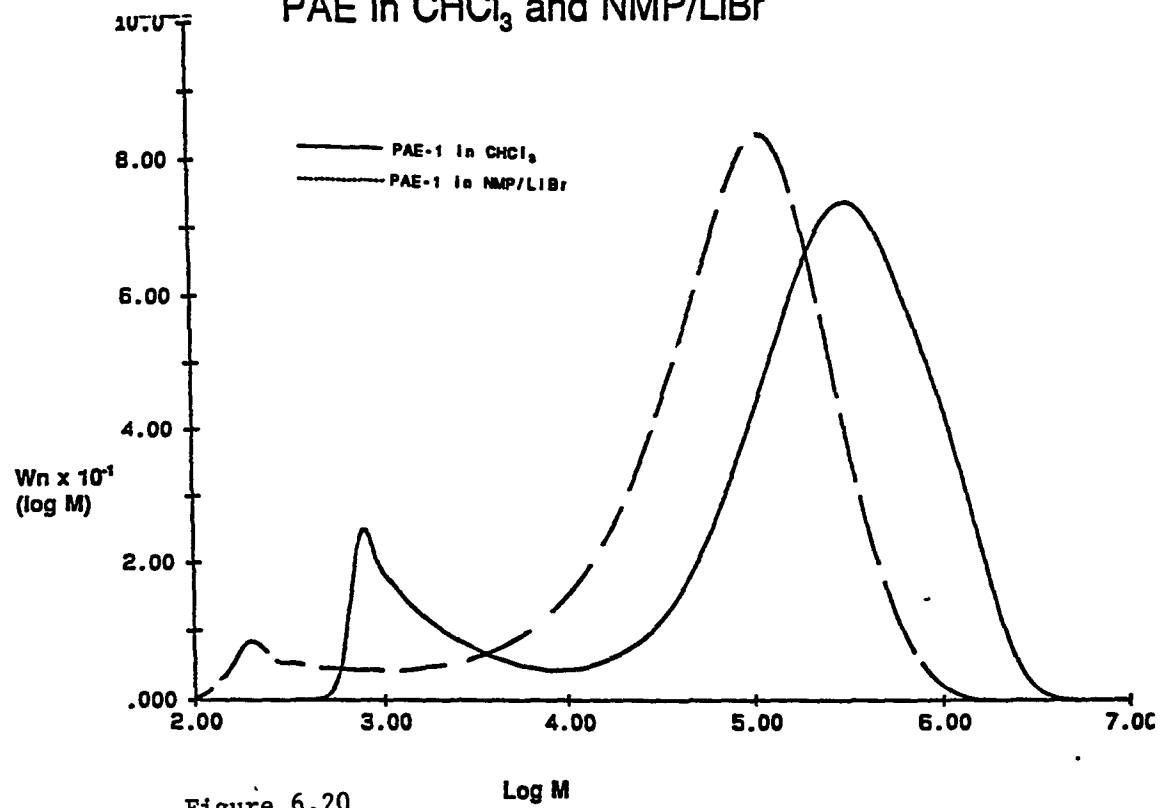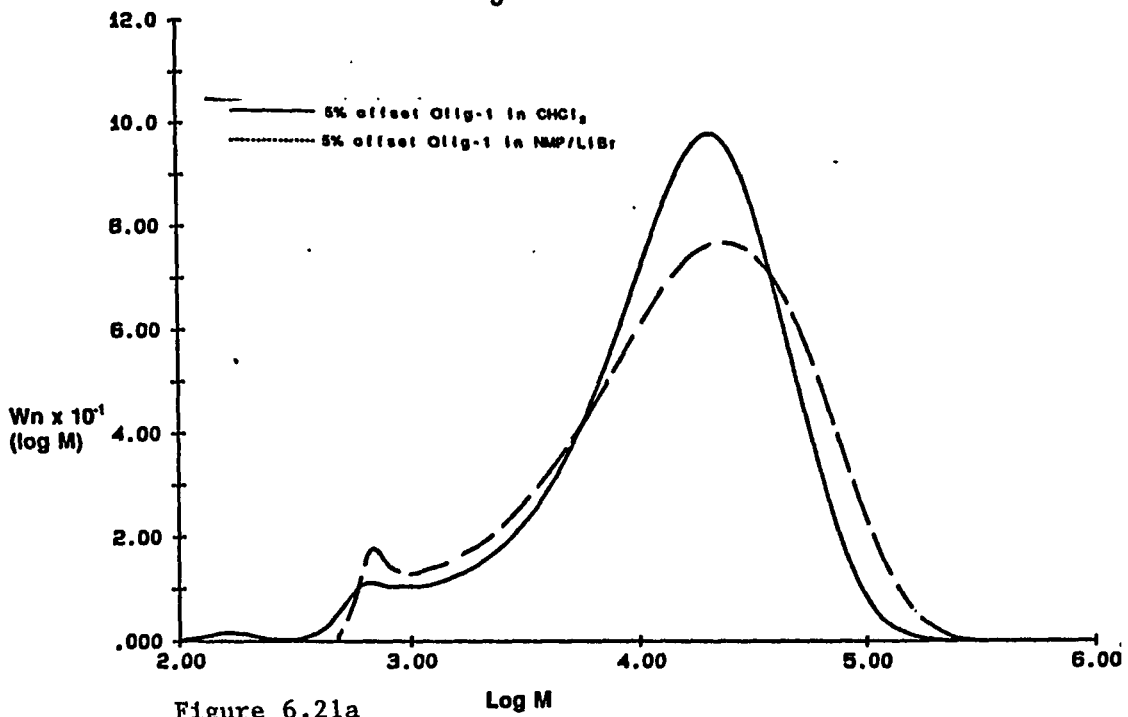## Comparison of Molecular Weight Distribution of PAE-co-I-5 in NMP

Figure 6.18b

Comparison of Molecular Weight Distribution of PAE-co-I-5 in NMP/LiBr

Figure 6.19a

Comparison of Molecular Weight Distribution of PAE-co-I-5 in NMP/LiBr
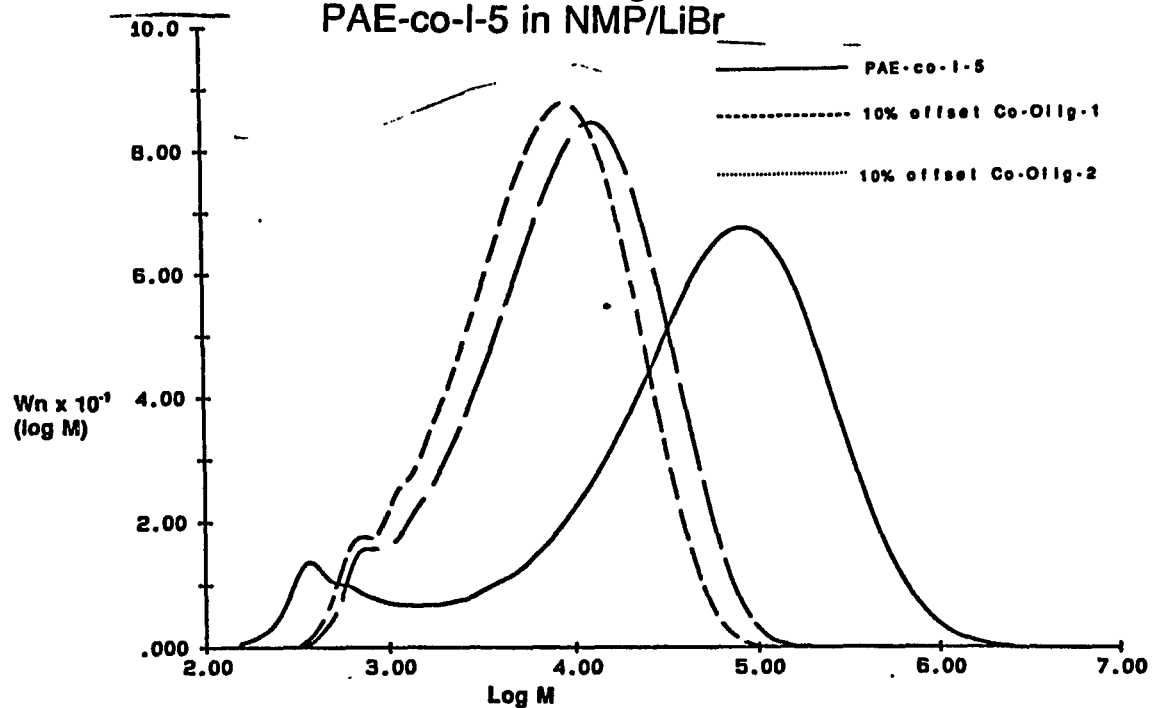
Figure 6.19b

Chromatographic behavior of a polymer may be very different depending on the solvent system employed. Comparison of the GPC molecular weight data for the polymers run in chloroform to those run in NMP/LiBr emphasizes the importance solvent interaction can have on the behavior of a system. Although a relatively large portion of low molecular weight species are present in both solvent systems, the tailing effect attributed to polymer-substrate interaction when the mobile phase was $CHCl_3$ is illustrated in Figure 6.20. This interaction resulted in a polydispersity of 41.4 in $CHCl_3$ and only 22.5 in NMP/LiBr for PAE-1. The molecular weight distribution of the oligomers are broader when run in NMP/LiBr (Figures 6.21 and 6.22), however the very low molecular weight species previously observed in Olig-1 are no longer present. The disappearance of the low molecular weight species may be attributed to the LiBr interupting the solute-column packing interaction thereby eliminating the prolonged retention of the samples on the column.

Comparison of Molecular Weight Distribution of PAE in CHCl₃ and NMP/LiBr

Figure 6.20

Comparison of Molecular Weight Distribution of [187]
PAE in $CHCl_3$ and NMP/LiBr

Figure 6.21a

Comparison of Molecular Weight Distribution of
PAE in $CHCl_3$ and NMP/LiBr

Figure 6.21b

Comparison of Molecular Weight Distribution of PAE in CHCl₃ and NMP/LiBr

Figure 6.22a

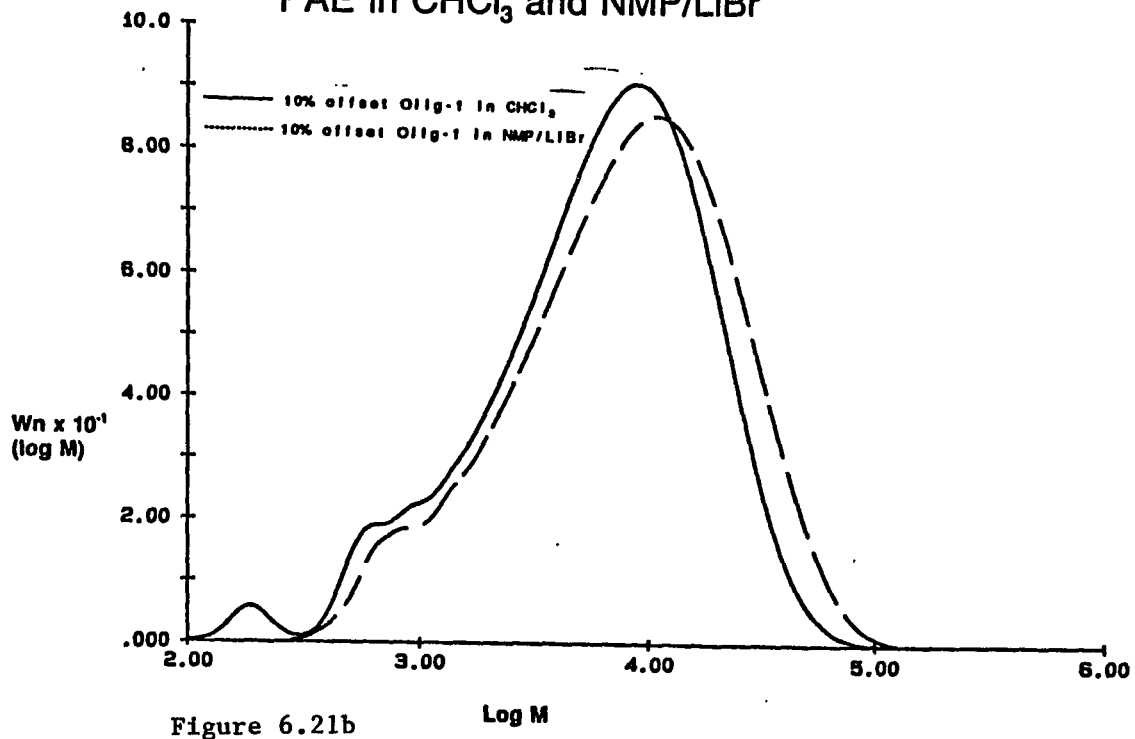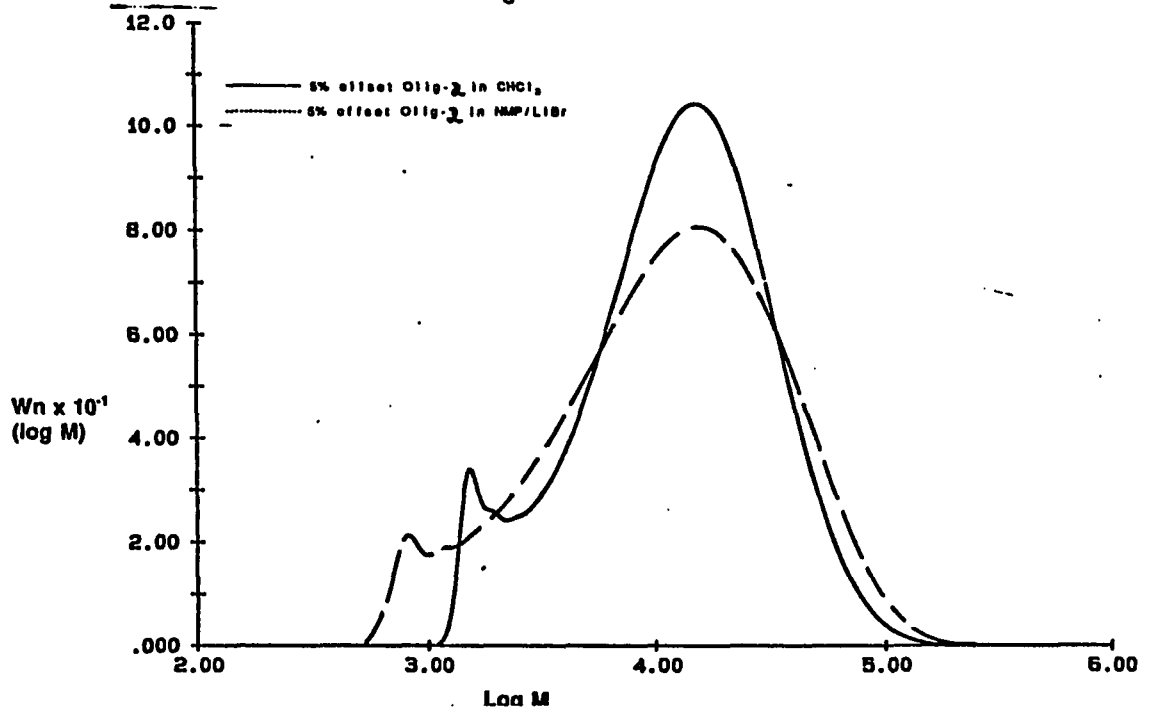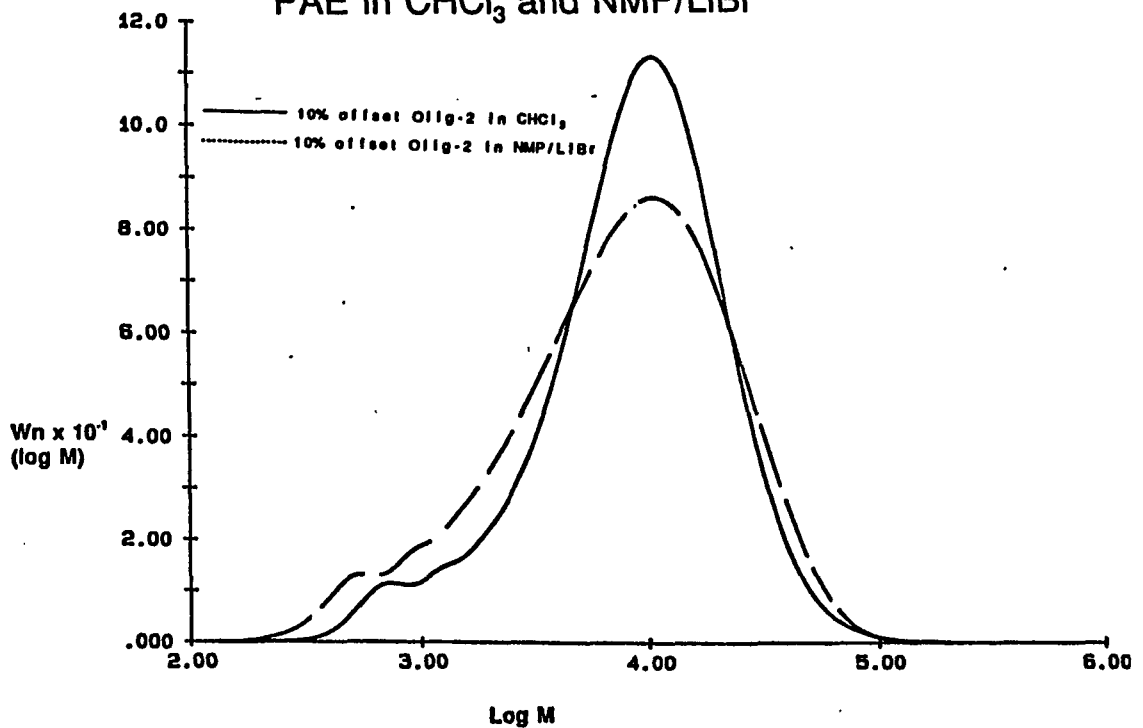## Comparison of Molecular Weight Distribution of PAE in CHCl₃ and NMP/LiBr

Figure 6.22b

The effects of solvent systems and GPC data are most apparent when one compares the copolymer systems (Figures 6.23 - 6.25). The M_n for PAE-co-I-5 in $CHCl_3$ was 200 g/mol while the M_n in NMP/LiBr was 4,900 g/mol. The higher molecular weight obtained in the NMP/LiBr is in better agreement with the physical properties of a solvent cast creasable film and a neat polymer K_{Ic} value of 1666 psi√in. Comparisons of the other copolymer systems do not exhibit the same disparity in the data, although, the severe tailing of the systems run in $CHCl_3$ versus those run in NMP/LiBr is very apparent. The chemical composition of the copolymer is such that the imidazole is capable of hydrogen bonding. Addition of LiBr to the NMP would serve to break up this type of interaction.

Comparison of Molecular Weight Distribution of PAE-co-I in CHCl₃ and NMP/LiBr
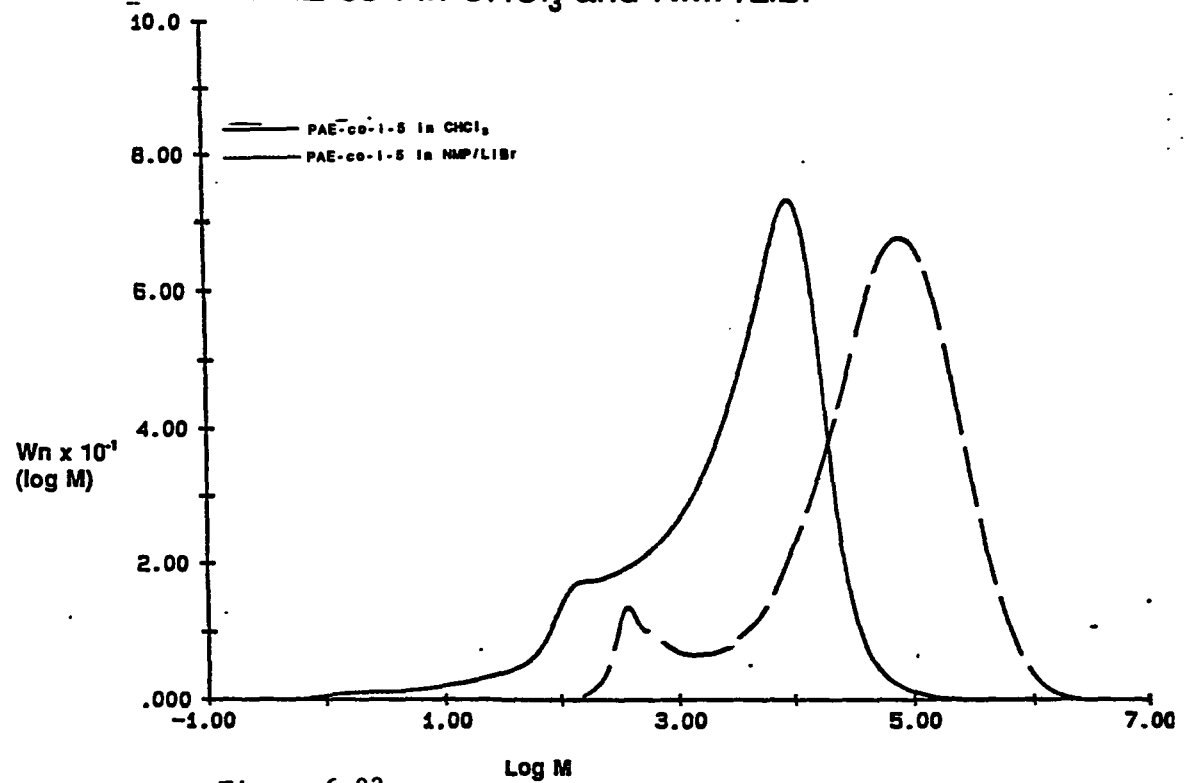

Figure 6.23

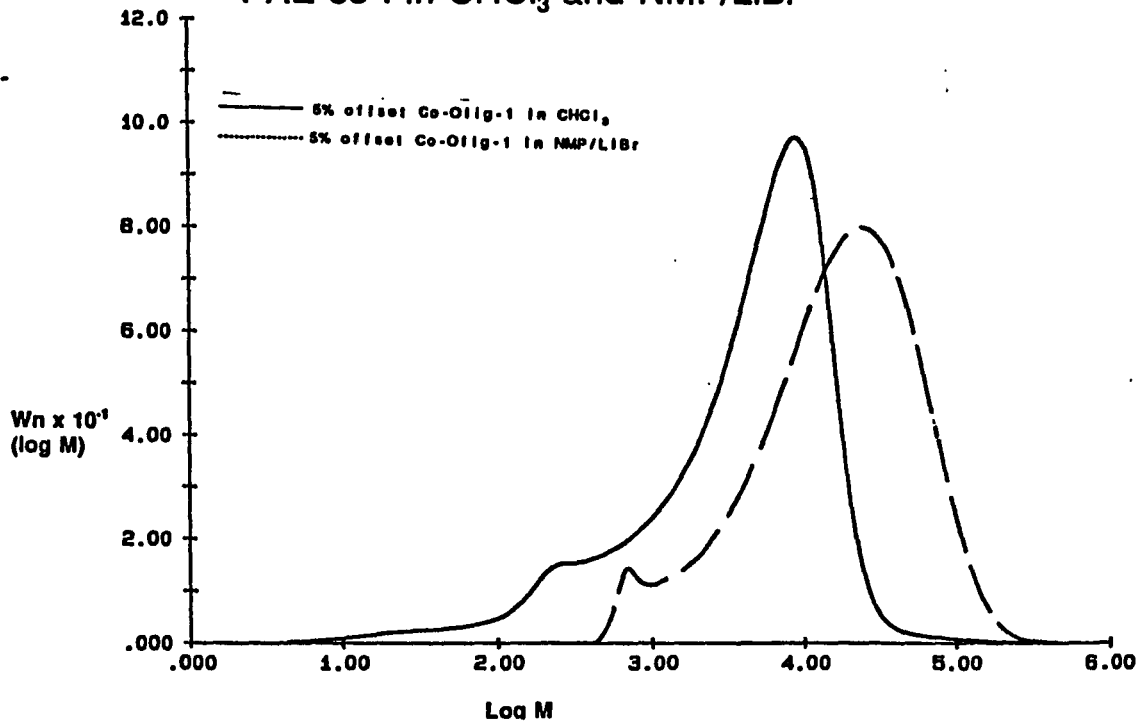# Comparison of Molecular Weight Distribution of PAE-co-I in CHCl$_3$ and NMP/LiBr

Figure 6.24a

Comparison of Molecular Weight Distribution of PAE-co-I in CHCl$_3$ and NMP/LiBr

Figure6.24b

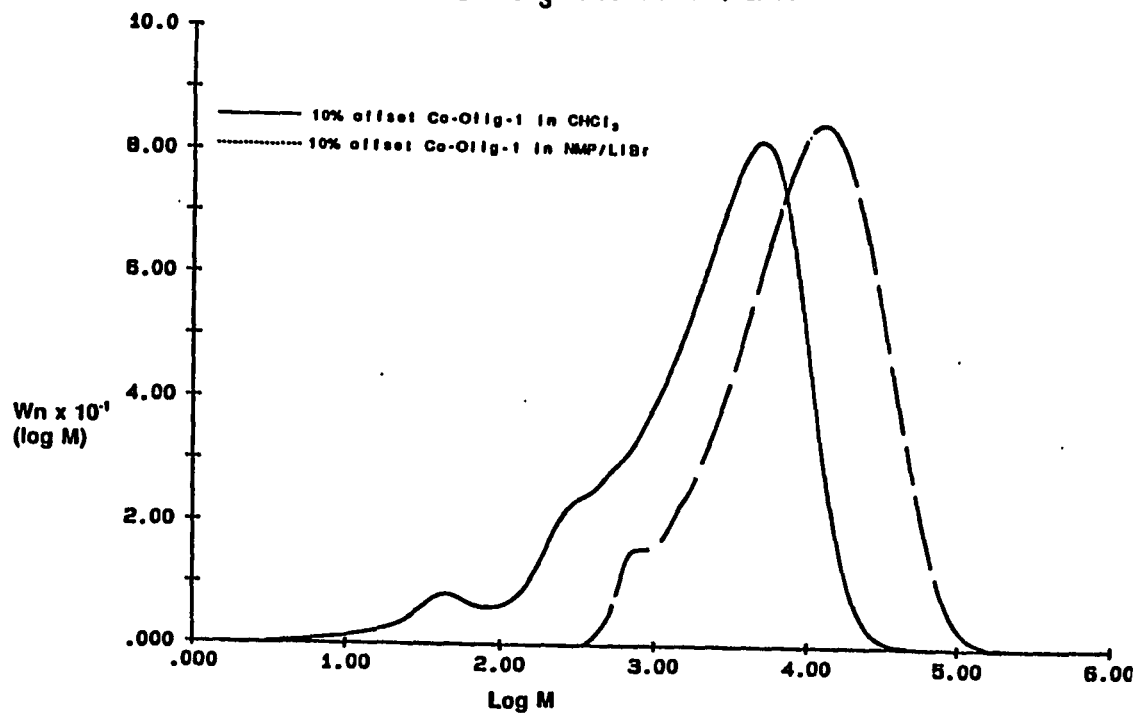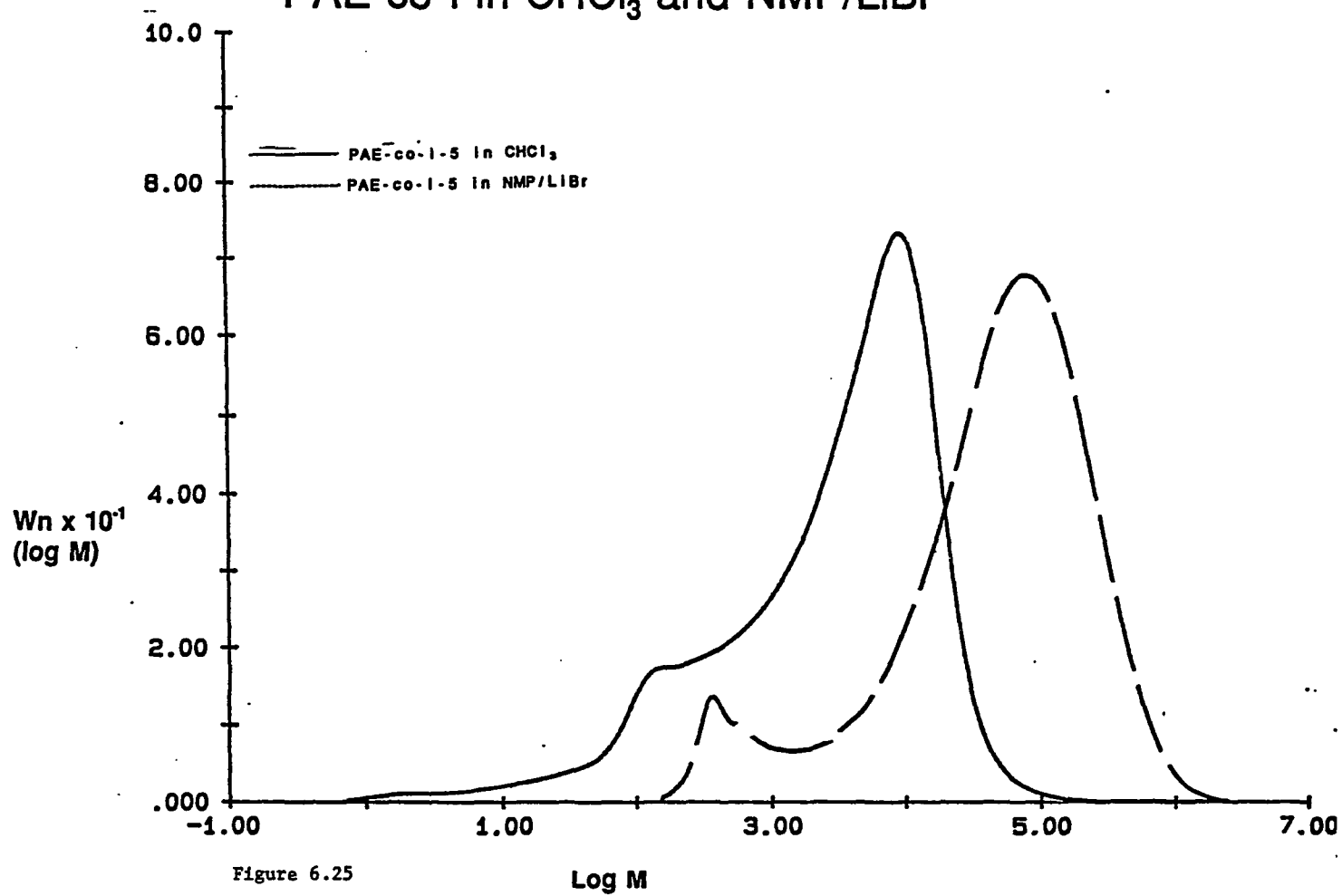Comparison of Molecular Weight Distribution of PAE-co-I in CHCl₃ and NMP/LiBr

Figure 6.25

6.5.2 Multi-angle Light Scattering Characterization

Although the molecular weight data of the polymers in NMP/LiBr appears to be more correct than those run in $CHCl_3$, the exact molecular weight averages are still influenced by the differences in chemical composition between chains for a random copolymer system. Multi-angle light scattering was performed on the ten polymers (Table 6.23) to validate the M_w determined by GPC. A complete description of this research is found in Katzenberger, 1994[2].

Table 6.23 Light Scattering Data

Description	°C	dn/dC (cm^3/g)	Solvent	M$_w$ (g/mol)
Homopolymers				
PAE	26	0.244	CHCl$_3$	144,000
10% offset Olig-1	26	0.239	THF	355,000
10% offset Olig-2	26	0.265	CHCl$_3$	13,000
5% offset Olig-1	26	0.237	THF	76,000
5% offset Olig-2	26	0.261	THF	22,700
10% Imidazole Copolymers				
PAE-co-I-5	24	0.297	THF	76,000
10% offset Co-Olig-1	26	0.256	THF	18,100
10% offset Co-Olig-2	26	0.251	THF	39,200
5% offset Co-Olig-1	28	0.263	THF	62,000
5% offset Co-Olig-2	28	0.270	THF	42,900

A graphical comparison of M$_w$ from both methods is given in Figures 6.26 and 6.27.

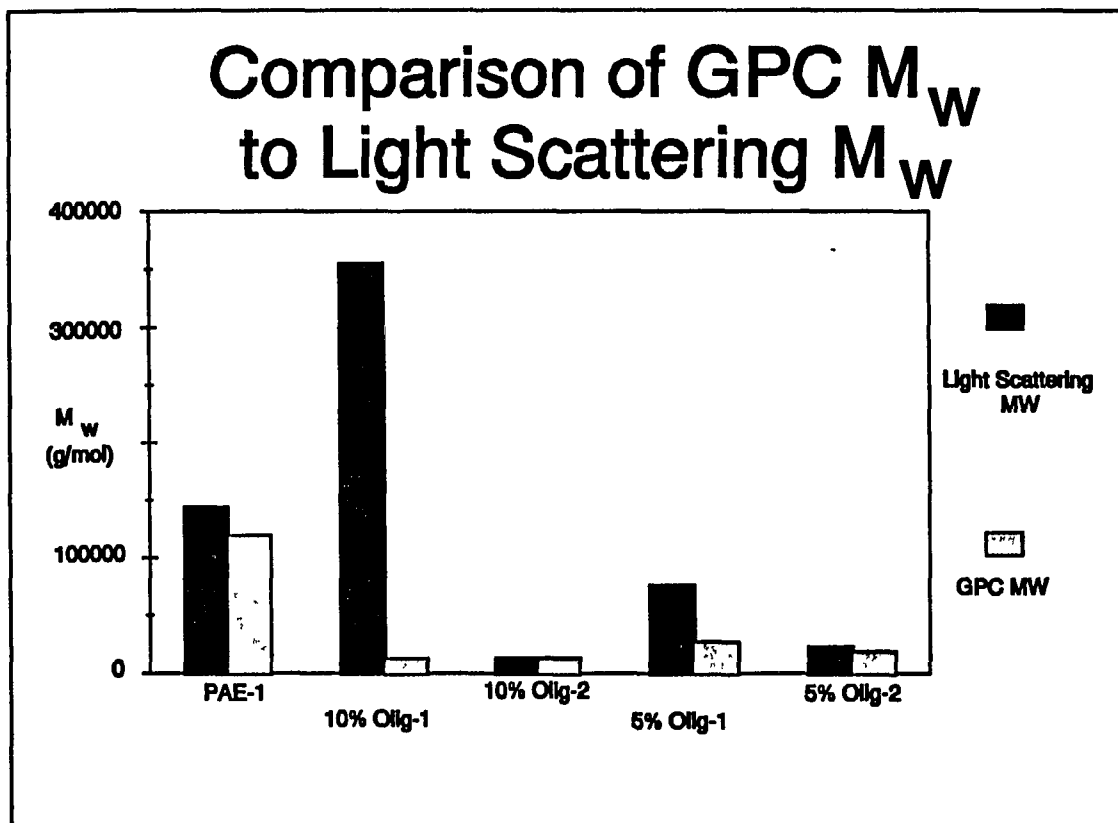**Comparison of GPC M$_W$ to Light Scattering M$_W$**

Figure 6.26 Comparison of homopolymer M$_w$ as determined by GPC and Light Scattering

There is relatively good agreement between the homopolymer data

except for the offsets favoring the bisphenol. PAE-1, 5 and 10% offset Olig-2

all agree within 20% for the two methods, and 5% offset Olig-2 agreeing within

2%. The oligomers offset in favor of the bisphenol disagree by almost 100% for

the 10% offset Olig-1 and 65% for the 5% offset Olig-1. Since light scattering

experiments were performed in THF there is the possibility that the bisphenol

chains are associating in solution. The second virial coefficient for 5% offset

Olig-1 is almost zero, this lends confirmation to the fact that THF is a poor

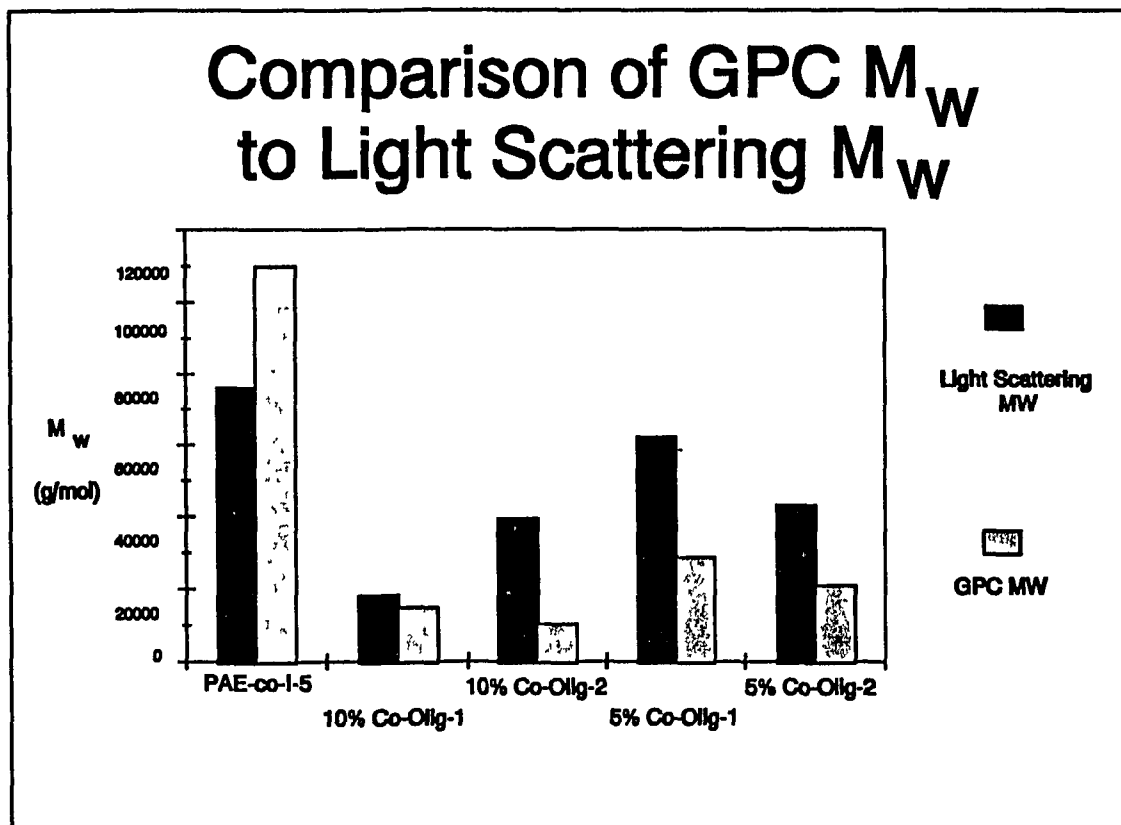solvent for the hydroxy terminated chains.

Figure 6.27 Comparison of copolymer M_w as determined by GPC and Light Scattering

The scatter in the copolymer data is much larger than that seen for the homopolymers. Variations between the two methods range from 19% for 10% offset Co-Olig-1 to 74% for 10% offset Co-Olig-2. As discussed previously, imidazoles are capable of hydrogen bonding. This would contribute to the experimental error of molecular weight determinations in THF.

Deviations from ideal behavior for dilute solution viscosities of

poly(arylene ether-co-imidazole)s have previously been cited[1]. A non-linear

concentration dependence in [η] was observed for PAE-co-I-3 (Figure 6.28).

This non-linear behavior improved with the introduction of LiBr to the DMAc but
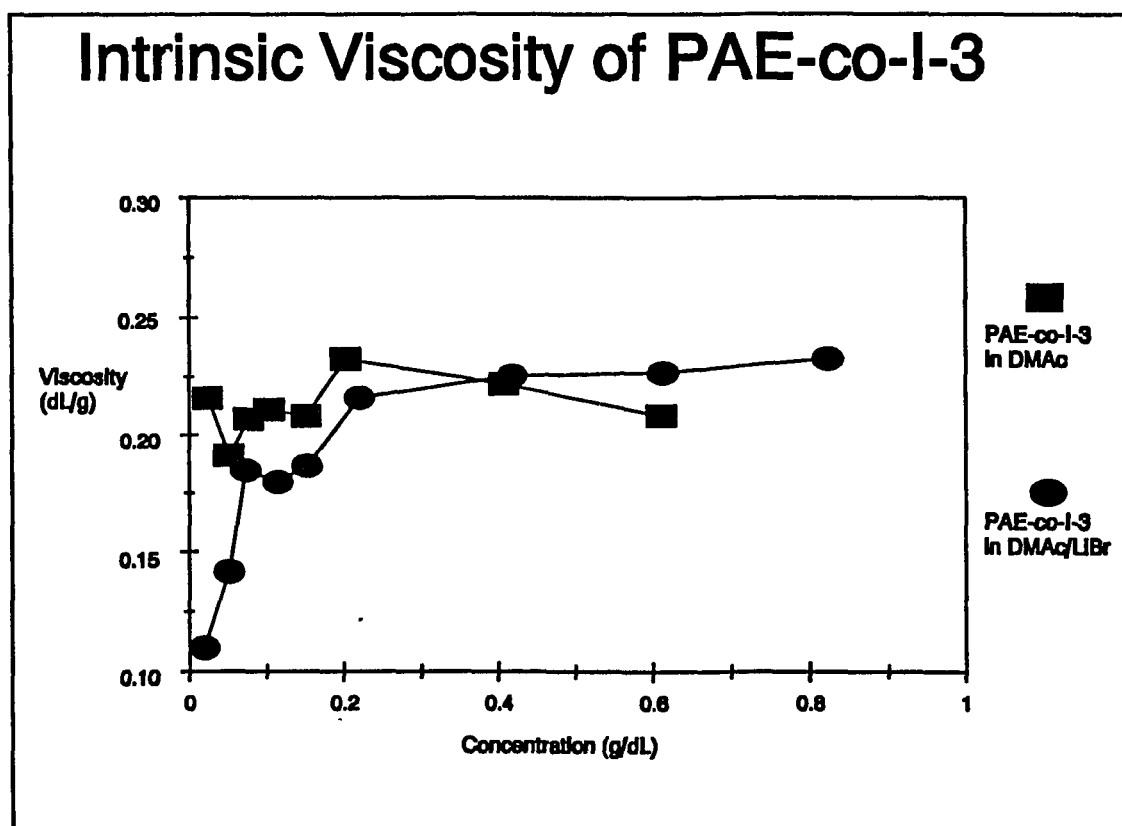
nonlinearity was still observed.

Intrinsic Viscosity of PAE-co-I-3

Figure 6.28   [η] behavior of PAE-co-I in DMAC and DMAc/LiBr

6.6 Moisture Absorption of Modified Epoxy Resins

Moisture absorption tests were run on all viable modified epoxy resins. Post mortem 3-point bend specimens were immersed in a warm water bath (90 °C) for the specified time period, removed, quickly towel dried and weighed. A measurement at 170 hours indicated that samples had reached equilibrium by 105 hours.
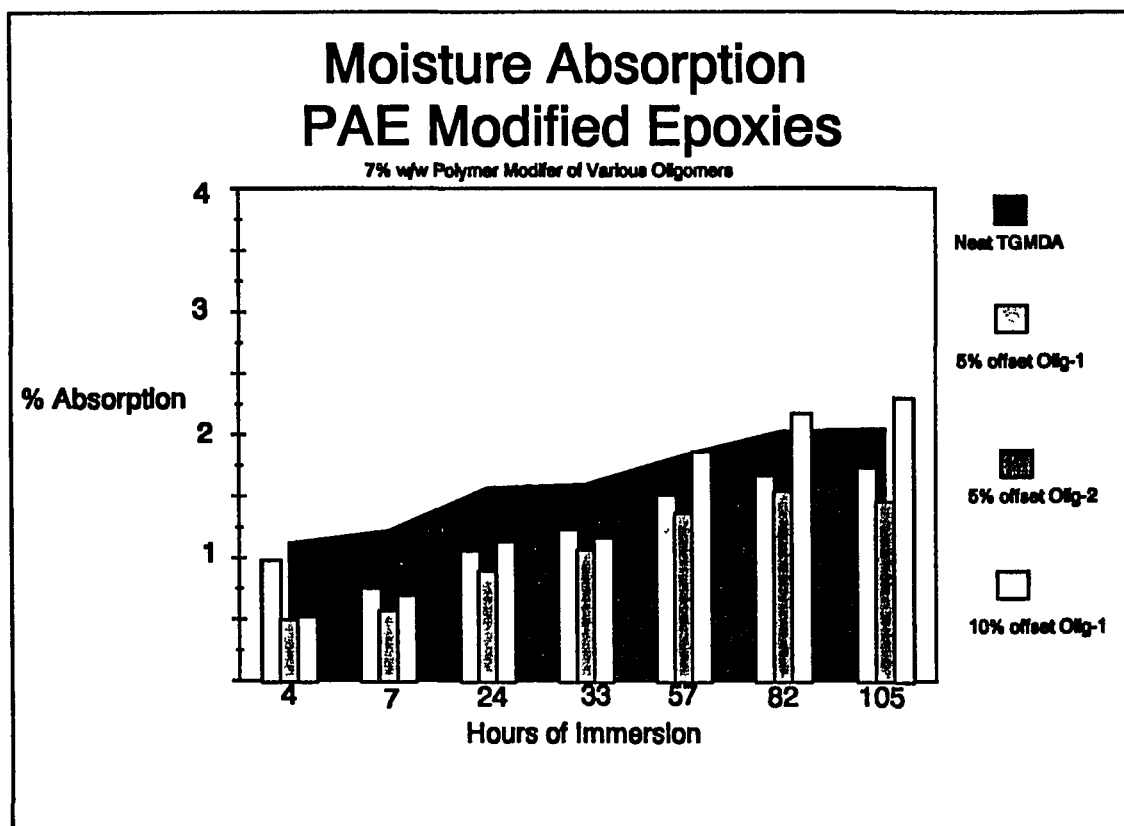

Figure 6.29 Moisture Absorption of PAE modified TGMDA resins

Figure 6.29 illustrates the moisture absorption of the PAE-1 modified

resins. The highest moisture absorption was exhibited by 10% offset Olig-1,

followed by the 5% Olig-1. These oligomers contain a high percentage of

hydroxy terminated chains and would be expected to have high moisture

absorption due to hydrogen bonding interactions. Olig-2 contains a higher

concentration of dihalide endgroups and modification with this oligomer resulted

in a decrease in moisture absorption of approximately 0.5% over the unmodified
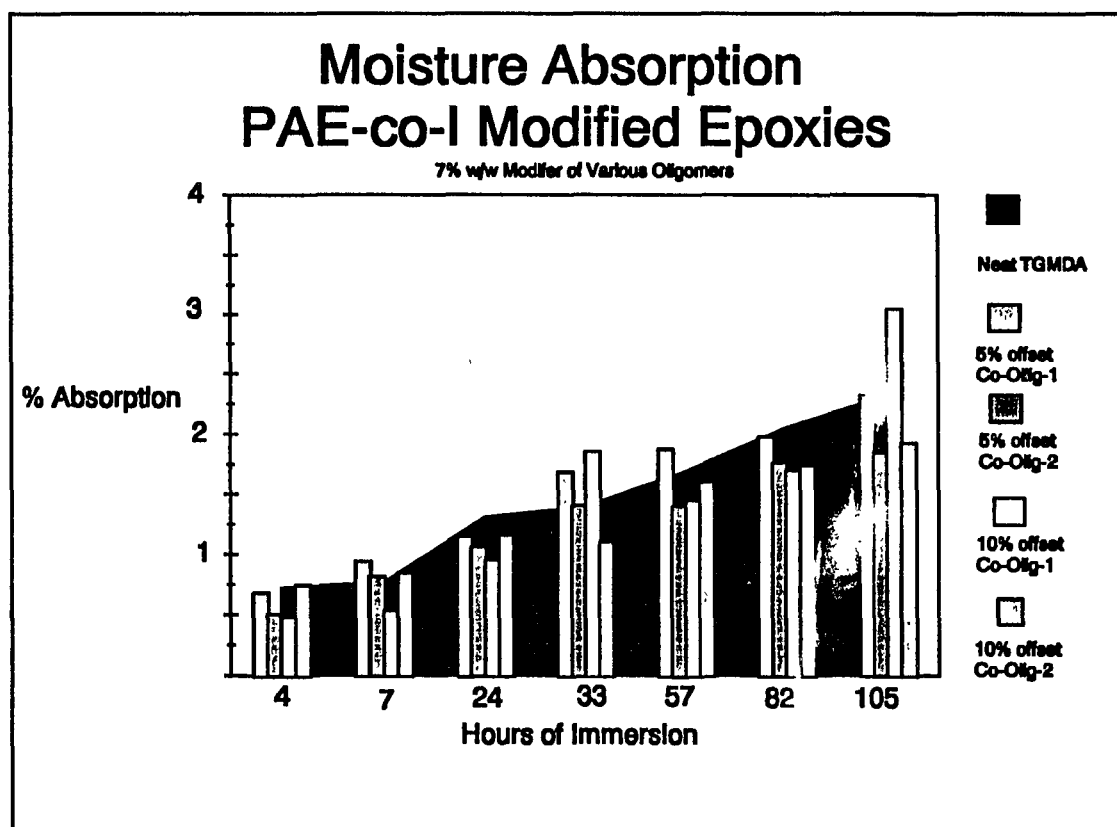
system.

Figure 6.30 Moisture Absorption of Co-Olig modified TGMDA resins

PAE-co-I oligomers offset in favor of the bisphenol (Co-Olig-1) also

exhibited higher moisture absorption. The 5 and 10% Co-Olig-1 moisture

absorption properties were approximately equal to or higher than the

unmodified epoxy. The oligomer offset in favor of the dihalide, 5 and 10% Co-

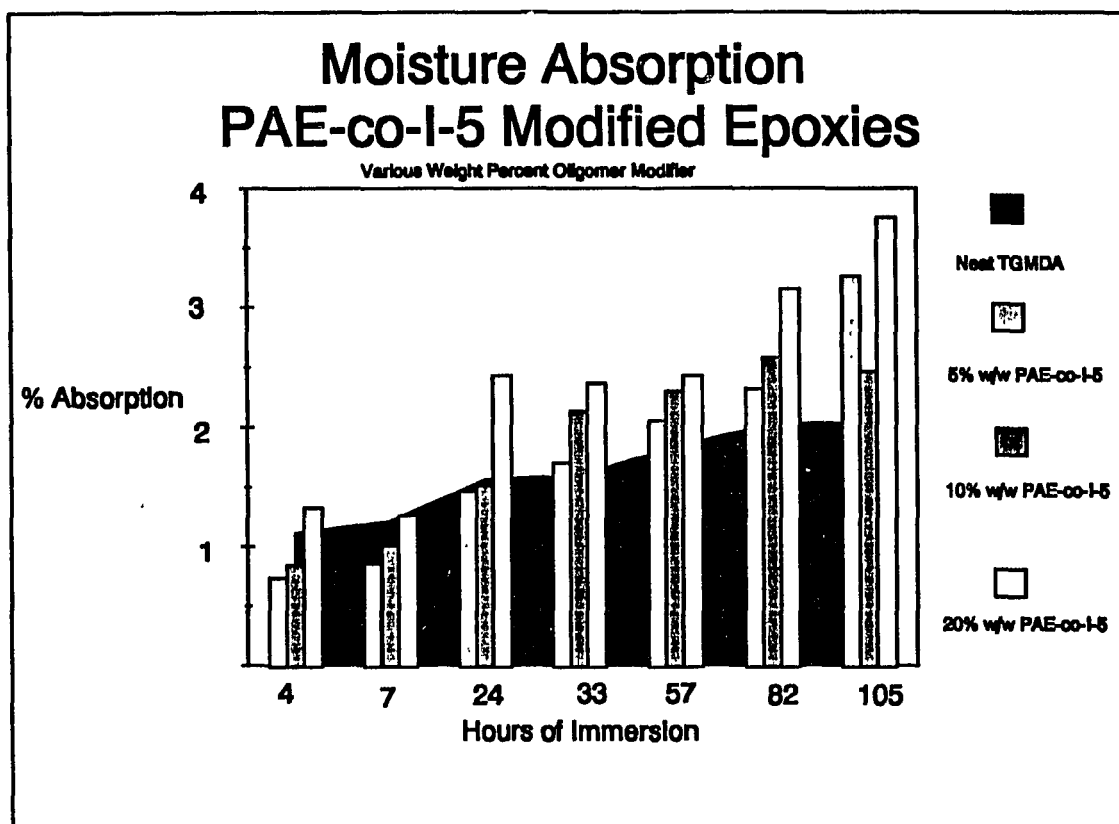Olig-2, had lower moisture absorption than the unmodified resin.

Figure 6.31 Moisture Absorption of PAE-co-I-5 modified
TGMDA resins

Moisture absorption increased with increasing PAE-co-I-5 content.

Initially properties were in line with or slightly less than the unmodified resin.

However within 24 hours the modified resins begin to exhibit higher moisture

absorption, with the 20% w/w sample absorbing 1% more moisture than the

unmodified resin. The hydrogen bonding capabilities of the imidazole moiety

contribute to the higher moisture absorption along with a higher void content for

resins with high polymer concentrations.

Moisture absorption also increased with increasing amounts of Co-Olig-2

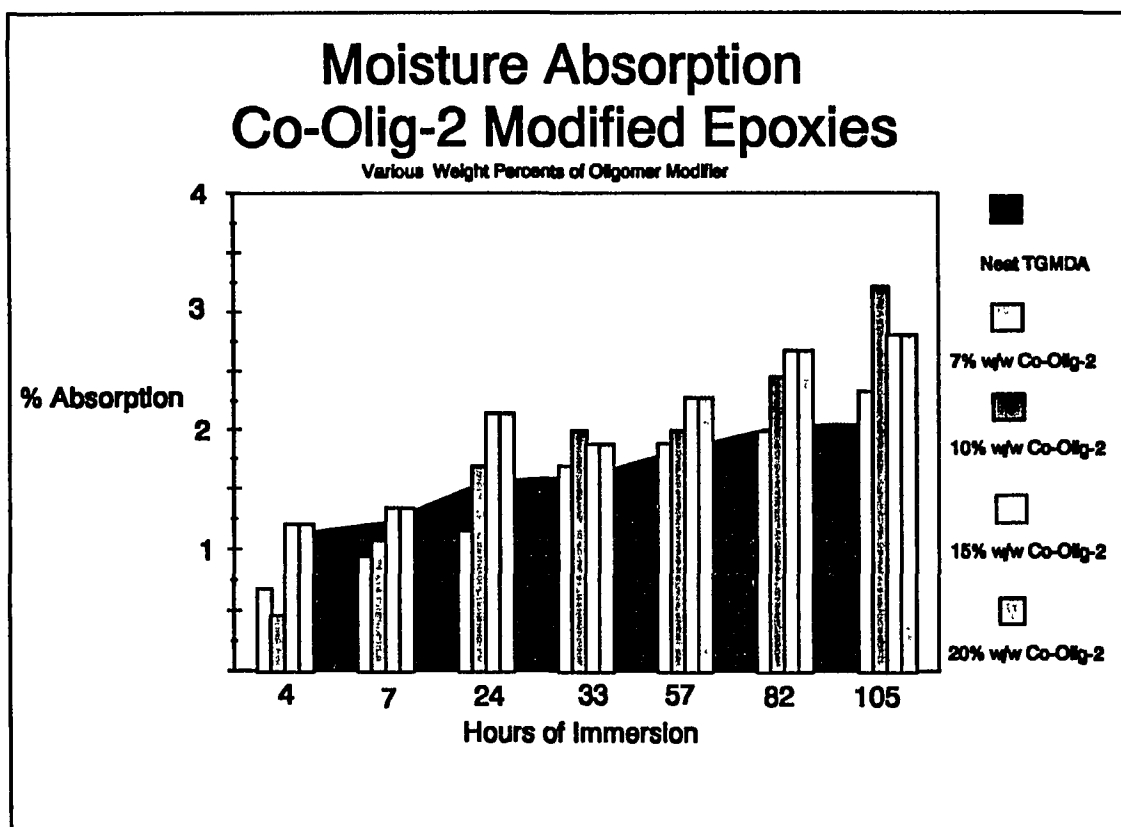modifier. Intially, modified resins are in line with the unmodifed epoxy with

Figure 6.32 Moisture Absorption of Co-Olig-2 modified TGMDA resins

increasing amounts of moisture absorption within 24 hours of immersion. The

hydrogen bonding properties of the imidazole and a higher void content would

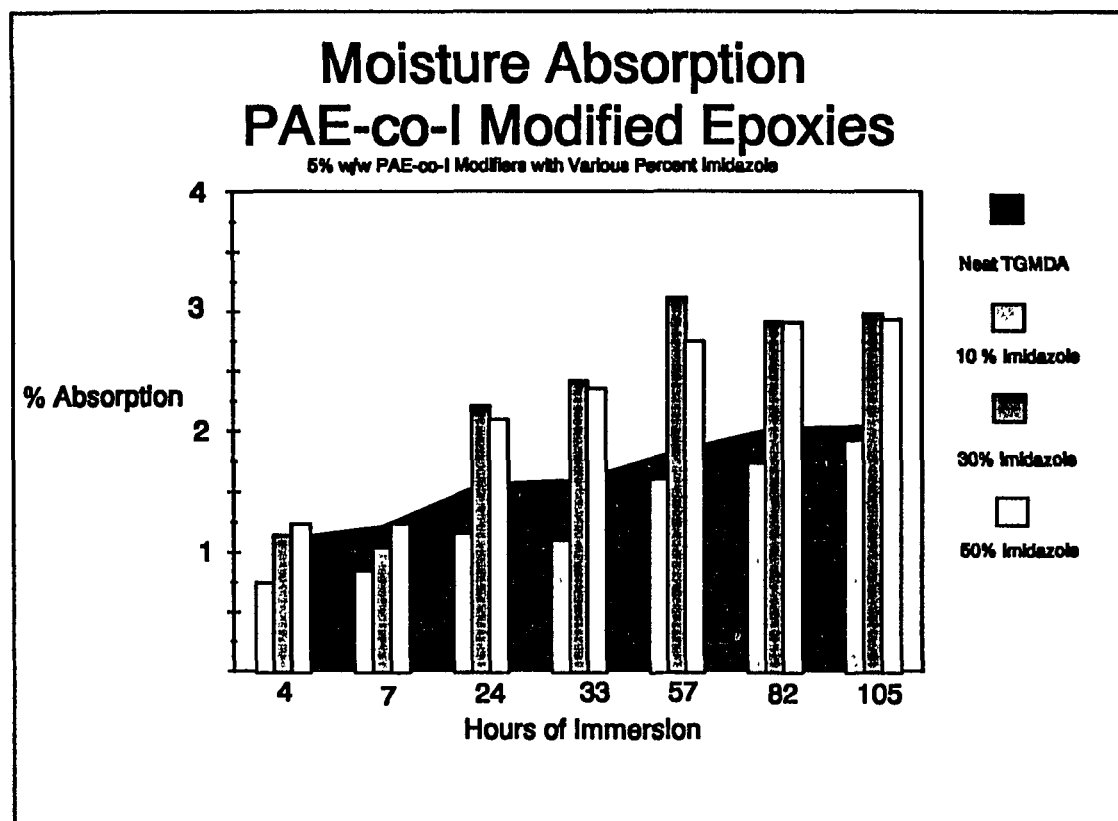also contribute to the moisture absorption properties for this polymer.

Moisture Absorption
PAE-co-I Modified Epoxies
5% w/w PAE-co-I Modifiers with Various Percent Imidazole

Figure 6.33 Moisture Absorption of PAE-co-Is (containing various mole percents imidazole) modified TGMDA resins

Increasing the imidazole concentration along the polymer backbone increased the moisture sensitivity of the modified resin. Since the imidazole moiety is capable of hydrogen bonding, increasing the imidazole concentration within the matrix should increase the moisture absorption of the modified system. The 10% imidazole PAE-co-I has lower moisture absorption properties than the unmodifed resin with very little difference between the 30% and 50%

imidazole copolymers. However, as expected both the 30 and 50% imidazole

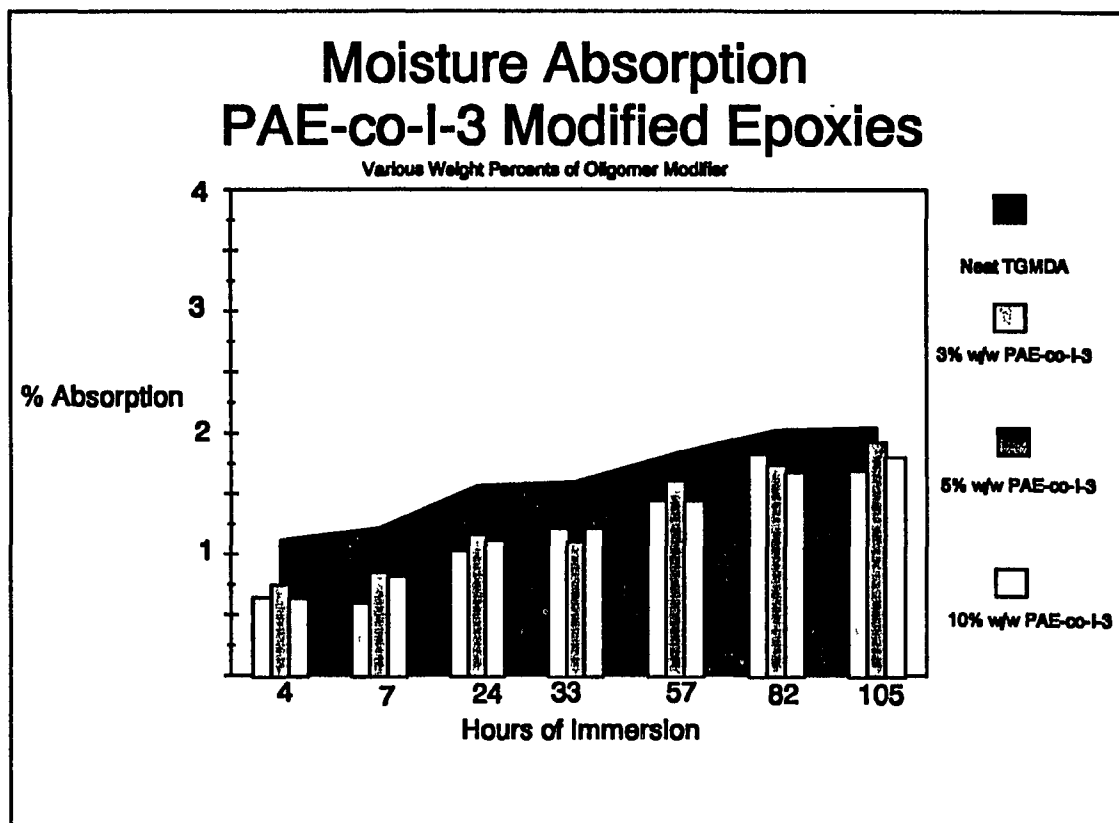polymers exhibited higher moisture absorption than the unmodified resin.

Figure 6.34 Moisture Absorption of PAE-co-I-3 modified TGMDA resins

PAE-co-I-3 modified epoxy resins exhibit lower moisture absorption properties than the unmodified resin for polymer concentrations up to 10% w/w. The moisture absorption properties of this polymer are less than the neat epoxy and similar polymer concetrations of PAE-co-I-5.

Epoxy resins modified with PAEs exhibit moisture absorption of less than or approximately equal to the unmodified resin. Hydroxy endgroups increase the moisture absorption of both PAEs and PAE-co-Is, and the hydrogen bonding ability of the imidazole increases the moisture absorption of the PAE-co-I to levels higher than the unmodified resin and PAE modified resins. Increasing polymer concetrations increases moisture absorption due to the higher imidazole concentration and the higher void content of the samples. Variations in the data may be attributed to nonuniformity in test specimens, differences in void content, and slight inconsistencies in drying samples prior to weighing.

6.7 Solvent Sensitivity of Modified Resins

Post mortem three-point bend samples of cured neat epoxies and systems modified with PAE-co-Is and PAEs were immersed in THF at room temperature and the weight gain was monitored. The samples were periodically removed from the sealed sample vial, quickly towel dried and

weighed. THF was chosen because both the polymer and uncured epoxy are soluble in it.

THF Sensitivity of PAE Modified Epoxies

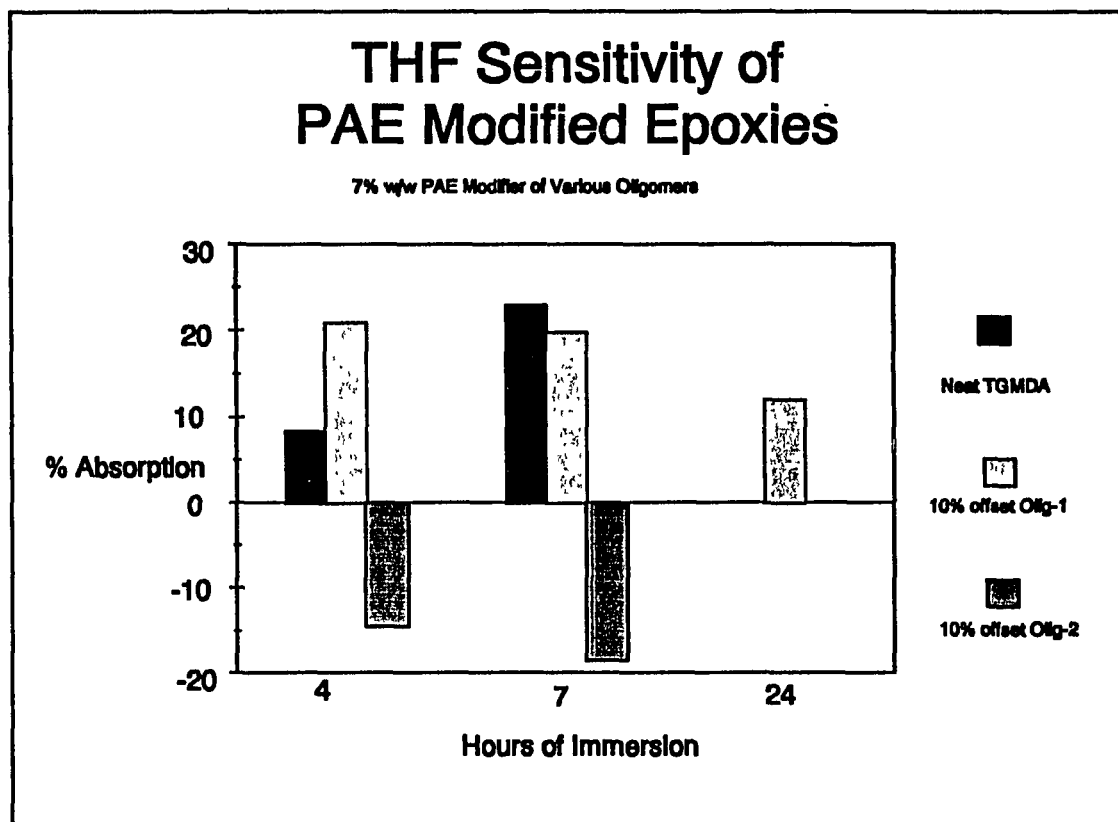7% w/w PAE Modifier of Various Oligomers

Figure 6.35   THF Sensitivity of PAE modified TGMDA resins

The sensitivity of the unmodified epoxy resin to THF was so severe that the sample broke apart after approximately 10 hours of immersion in the THF. The highly crosslinked, three-dimensional network of the unmodified resin allows little flexability for the polymer chains to accommodate infiltration of solvent molecules. The internal stresses applied by solvent absorption presumably caused a breakdown of the network. The 10% Olig-1 modified resin remained intact for approximately 24 hours but subsequently broke apart

due to severe solvent sensitivity. The sample registered a weight loss between 7 and 24 hours which is probably a result of the PAE modifier being extracted from the resin. The weight loss for the 5% Olig-2 resin was almost immediate and so that, after 7 hours, there was not enough solid for weighing. The 10% Olig-2 sample had a 14% weight loss after 7 hours of immersion. Olig-1 is dominated by hydroxy endgroups, while Olig-2 is dominated by dihalide endgroups. Hydroxyl functionalities can participate in epoxy curing reactions and therefore become chemically incorporated into the network. Dihalide functional groups do not participate in epoxy curing reactions. They apparently form a blended material but are not chemically incorporated into the epoxy matrix. Consequently, solvent immersion of such a system resulted in polymer extraction followed by resin fracture due to the severe solvent swelling of the resin.

All PAE-co-I modified resins exhibited lower THF sensitivity than the neat epoxy or PAE modified resins, as shown in Figure 6.36. The neat resin properties have been omitted from Figures 6.36 through 6.39 due to scaling limitations.
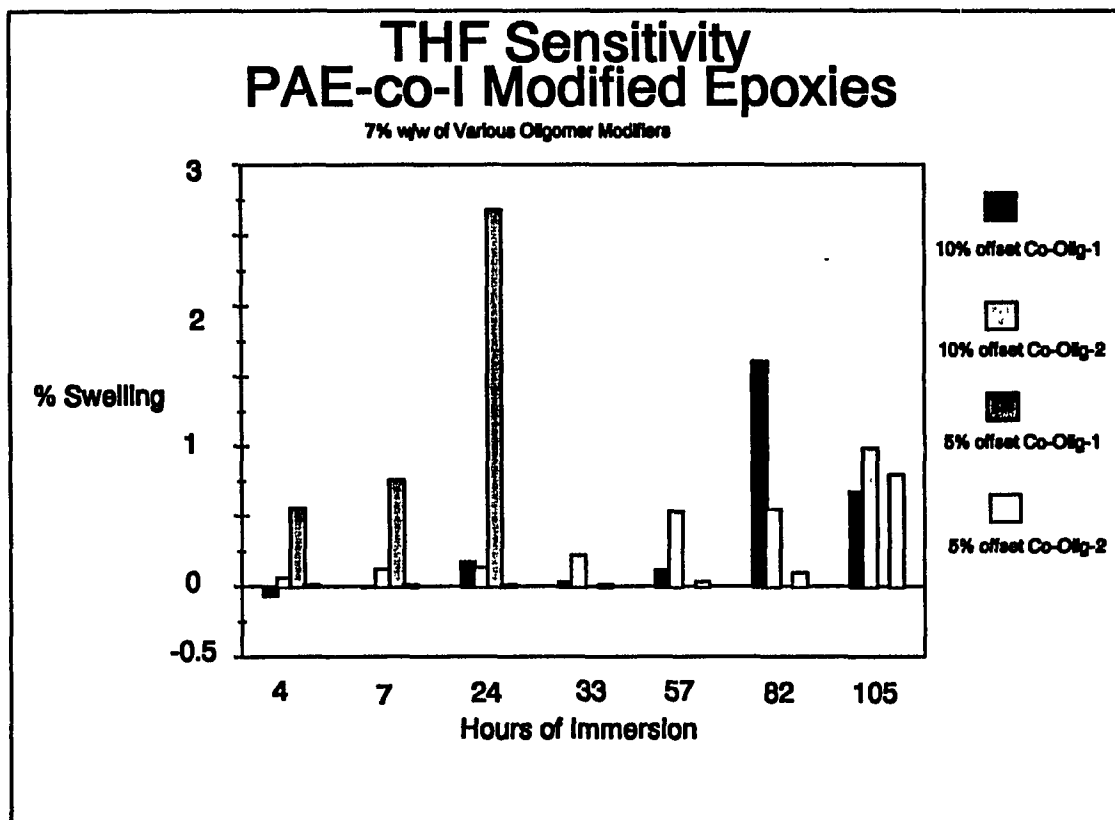
Figure 6.36 THF Sensitivity of Co-Olig modified TGMDA resins

The Co-Olig modified resins exhibited minimal solvent swelling for both the 5 and 10% Co-Olig-2 modified resins. Both exhibited less than 1% solvent sensitivity after 105 hours of immersion. The 5% Co-Olig-1 modified resin had swollen to 2.7% at 24 hours before the sample began to break apart presumably due to solvent stresses and sampling was discontinued. The 10% Co-Olig-1 modified resin exhibited maximum solvent swelling at 82 hours, the sample weight loss after this point is a result of solvent induced sample fracture.
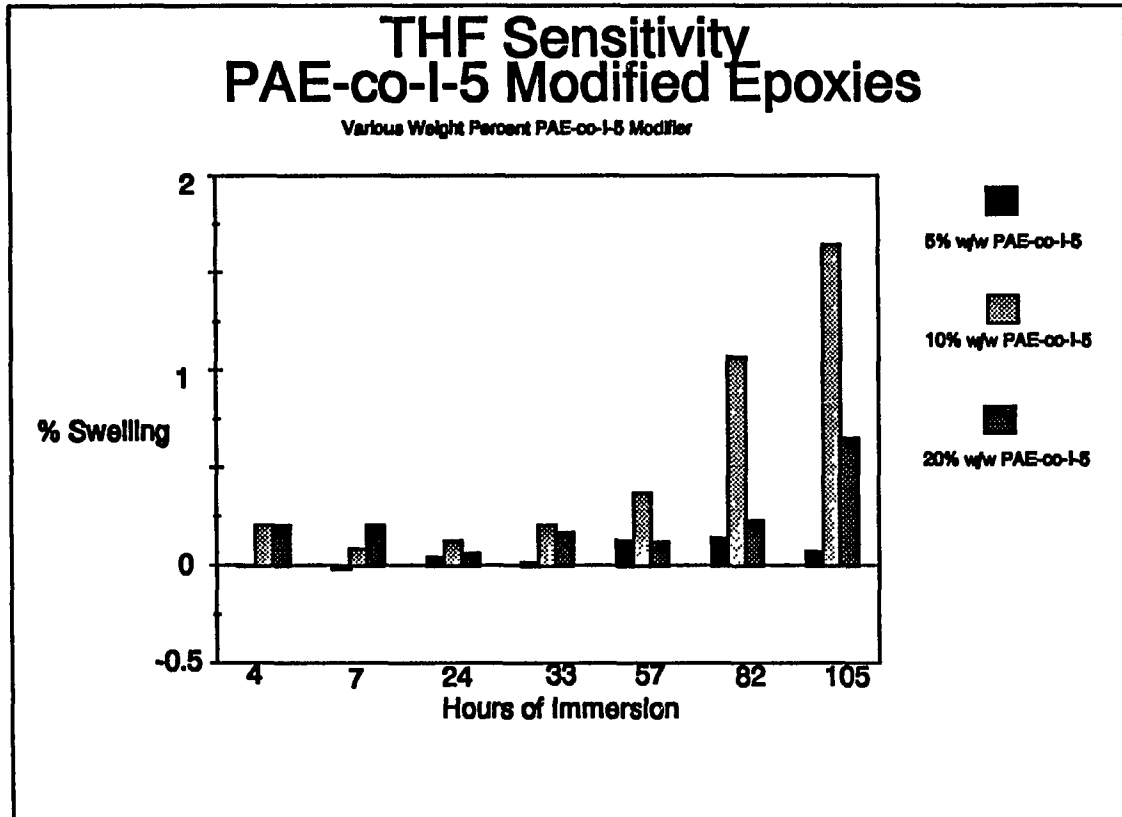
Figure 6.37 THF Sensitivity of PAE-co-I-5 modified TGMDA resins

Of the PAE-co-I-5 modified resins studied, the 10% w/w resin was the most solvent sensitive. However, only 1.6% solvent swelling resulted after 105 hours of immersion. A slight weight loss (0.01%) for the 5% w/w modified resin after 7 hours, this weight loss was negligible in comparison to the values for the PAE modified resins and may be the result of experimental error.

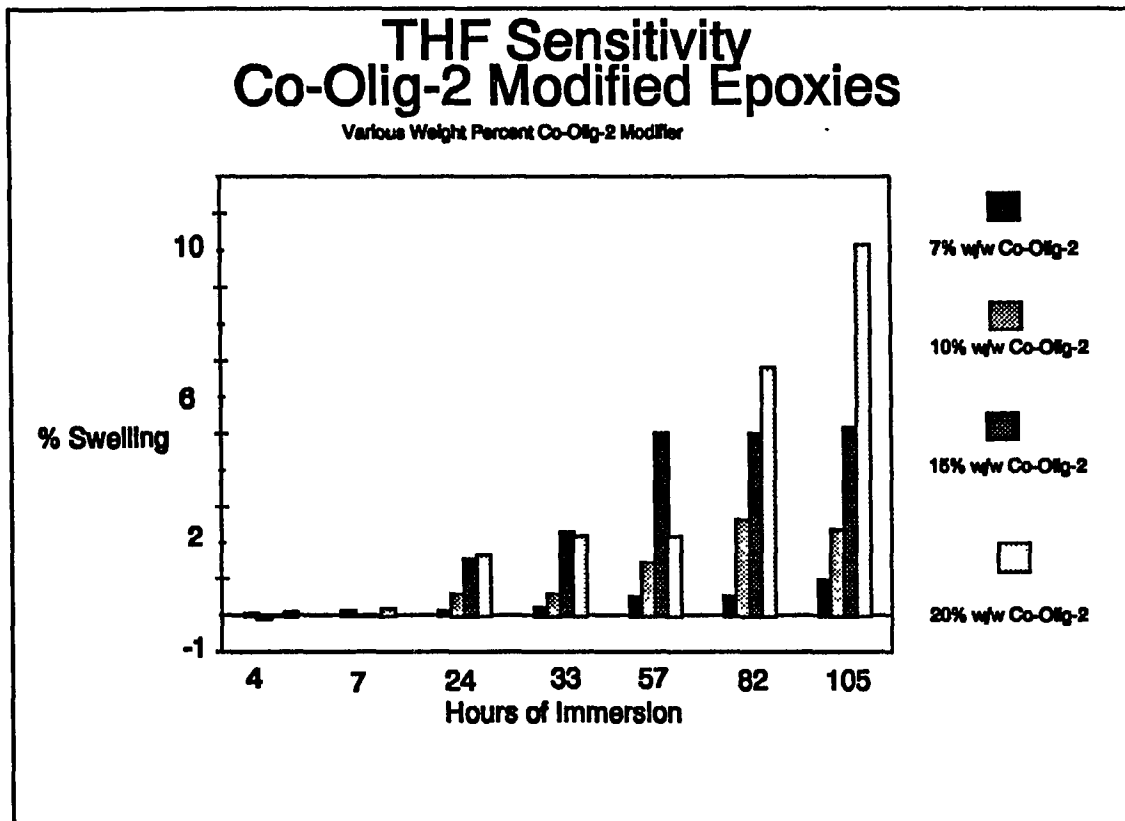Co-Olig-2 modified resins became more solvent sensitive with increasing

Figure 6.38 THF Sensitivity of Co-Olig-2 modified TGMDA resins

amounts of modifier. Increasing the reactive thermoplastic content of the resin allows for greater network flexability. This flexability allows the three dimensional network to accommodate more of solvent. This is illustrated in the 20% w/w modified resin which experienced 10.2% solvent absorption after 105 hours. This sample maintained its integrity without fracture and returned to within 0.2% of its pre-immersed weight upon drying.
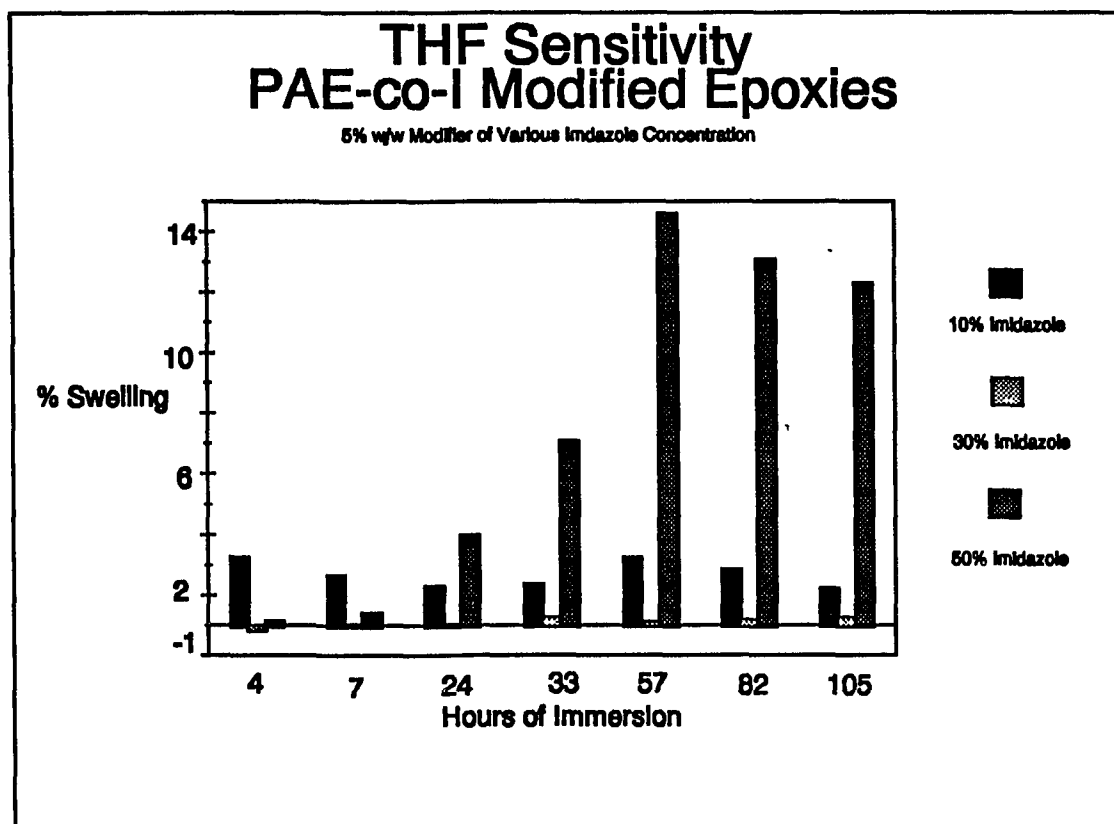
Figure 6.39 THF Sensitivity of PAE-co-I (containing various concentrations on imidazole) modified TGMDA resins

Of the PAE-co-Is modified with copolymer containing various

concentrations of imidazole in the polymer, the copolymer containing 30%

imidazole appears to be the least solvent sensitive. After 105 hours of

immersion 0.27% solvent swelling was recorded for this sample, and a slight

loss in sample weight (0.1%) at the end of 4 hours is presumably due to

experimental error. This sample returned to within 0.1% of its pre-immersed

sample weight upon drying, eliminating the possibility of polymer extraction

being accompanied with solvent incorporation. The 50% immidazole distributed

along the polymer backbone resulted in a maximum absorption of 13.6% after

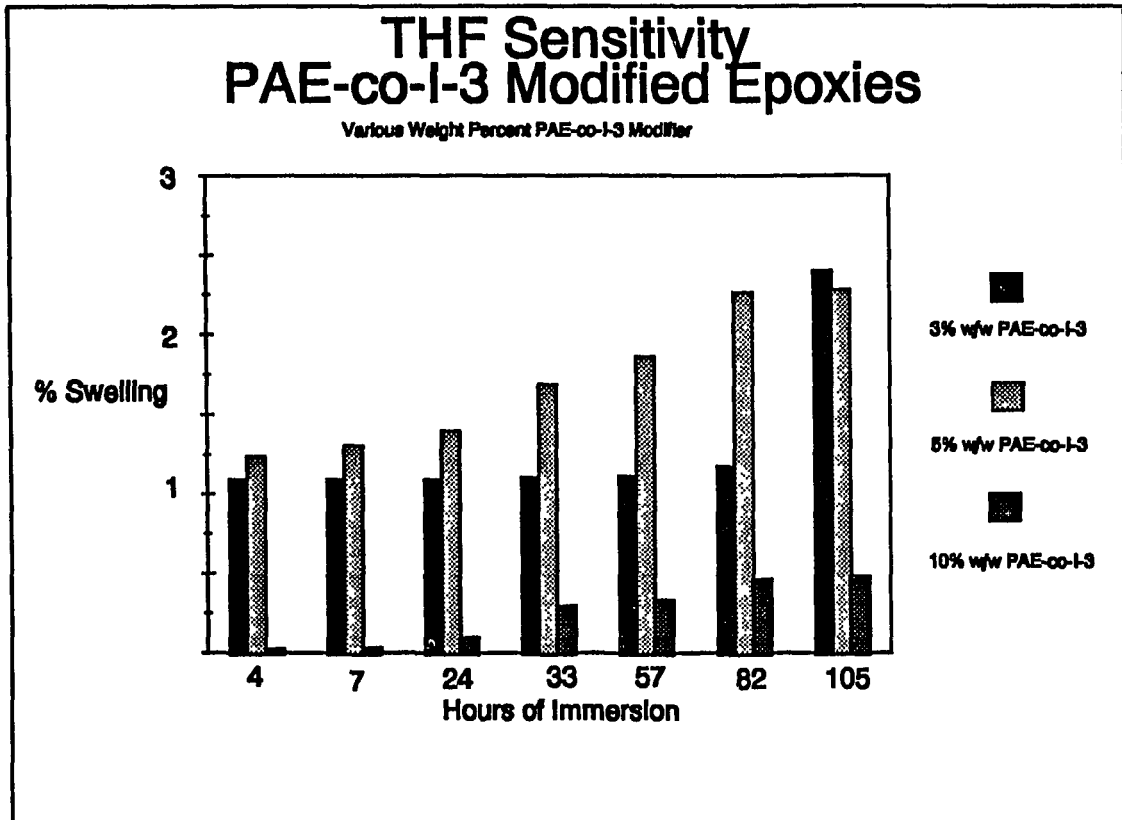57 hours followed by sample weight loss due to solvent induced sample

fracture.

THF Sensitivity
PAE-co-I-3 Modified Epoxies
Various Weight Percent PAE-co-I-3 Modifier

Figure 6.40 THF Sensitivity of PAE-co-I-3 modified TGMDA resins

Of the PAE-co-I resins studied, The PAE-co-I-3 (10% w/w) was the least

solvent sensitive with only 0.5% solvent swelling after 105 hours. However, 3

and 5% w/w samples only absorbed approximately 2% at the end of the

sampling time period, values far better than other PAE-co-I modified resins.

Incorporation of PAE-co-Is improve the THF sensitivity of epoxy resins.

Solvent sensitivity results reinforce that PAE-co-Is are chemically incorporated

into the epoxy matrix while PAEs without reactive endgroups are physical

blends. The solvent extraction of the PAE modified systems and the high solvent sensitivity of the unmodified resin was not observed for any PAE-co-I modified resin.

6.8 Fracture Surfaces and SEMs

Fracture toughness for the modified resins in this study was determined by 3-point bend test. When testing in this configuration the load rises linearly with strain and a stress-whitened zone develops (Figure 6.41). This process zone is directly related to the energy absorbing mechanism since it accounts for the total energy absorbtion prior to fast fracture[2]. The load then drops rapidly as the crack propagates. Matrix modifications lead to changes in the deformation behavior of a system. Changes that increase toughness often increase the stress whiteneing of the process zone. In order to assess the modified resin's fracture characteristics, SEMS of fracture surfaces were examined.
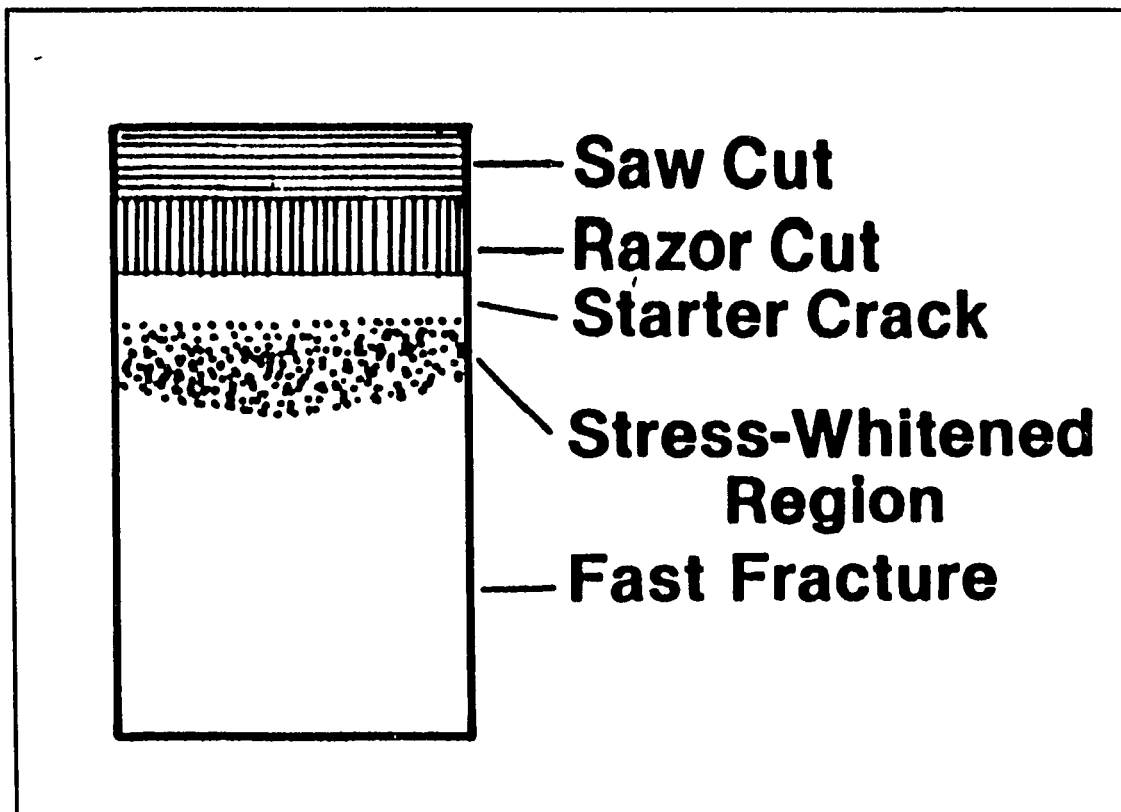
Figure 6.41 Illustration of Fracture Surface of 3-point bend Specimen

A classic example of a brittle fracture surface is illustrated in the SEMs of the unmodified epoxy resin (Figure 6.42). The fracture surface is basically featureless with very little evidence of striations, stress whitening or yielding at the boundary between the precrack and the process zone. This surface is representative of a material with low fracture toughness values.

SEMs for the PAE modified resins are shown in Figure 6.43 and 6.44. There is evidence of stress whitening at the process zone of both specimens. The higher magnifications show phase separation of the modified samples.

The fracture surface in Figure 6.43 is indicative of complete phase separation with evidence of discrete particle pull out and very low interfacial adhesion. This oligomer modifier (5% offset Olig-2) is dominated by the nonreactive dihalide endgroups, therefore there is no chemical interaction between the epoxy and thermoplastic. The Olig-1 exhibits some particle tearing along the fracture surface along with stress whitening, indicating more ductile fracture Figure 6.44. The reactivity of the hydroxyl endgroups allows Olig-1 to become incorporated into the epoxy network thereby allowing for some interfacial interaction rather than complete phase separation. However, the brittleness of the neat PAE due to its low molecular weight did not afford any increase in fracture toughness for the modified system.

PAE-co-I modified resins (7% w/w) did not show evidence of phase separation. However, there appeared to be more ductile fracture along the process zone as illustrated by the increase in stress whitening evident in Figure 6.45 and 6.46. This corresponds to an increase in fracture tougness obtained for the three point bend specimens.

Increasing the concentration of Co-Olig-2 from 7 to 20% w/w did not lead to an increase in fracture toughness. Examination of the fracture surfaces for these modified resins indicated an increase in stress whitening (Figures 6.47 through 6.49). Increased thermoplastic content led towards more ductile failure in the process zone. Close examination of the fracture surface of the 20% w/w modified resin shows the beginnings of a phase separated system (Figure 6.49

B).

A high degree of interface interaction results in a high degree of toughening when there is an energy absorbing mechanism such as crazing or interfacial interactions.   However the absence of a detectable phase separation does not eliminate the possibility of enhanced fracture toughness through thermoplastic modification. The presence of a bi-continuous network where 2 networks exist separately with attachments at the crosslink points or of a semi-interpenetrating network may also lead to increases in fracture toughness. The existence and toughening mode in operation for these types of systems is an area of debate. The absence of phase separation accompanied by an increase in fracture toughness for the PAE-co-I modified epoxy resin gives evidence that nontraditional morphologies may lend to increased fracture toughness although the mode of toughening is not fully understood.

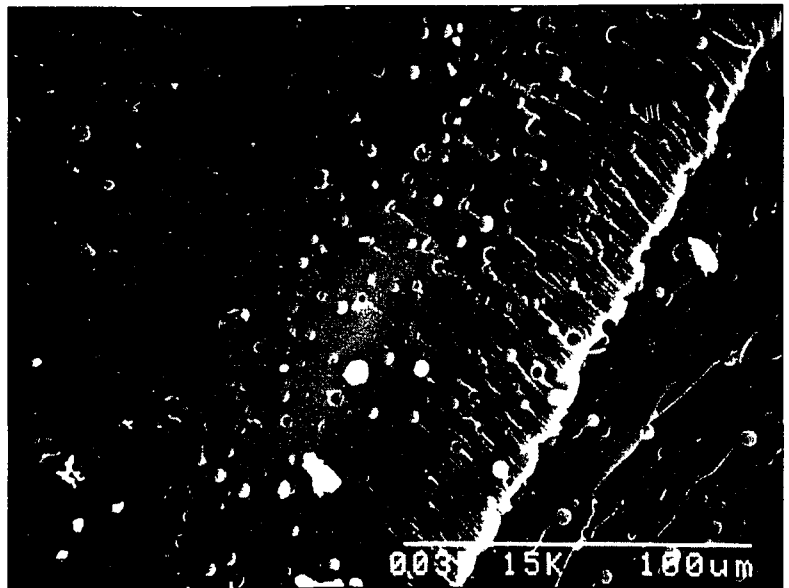N, N, N', N' - tetraglycidyl - 4, 4' - diaminodiphenyl methane
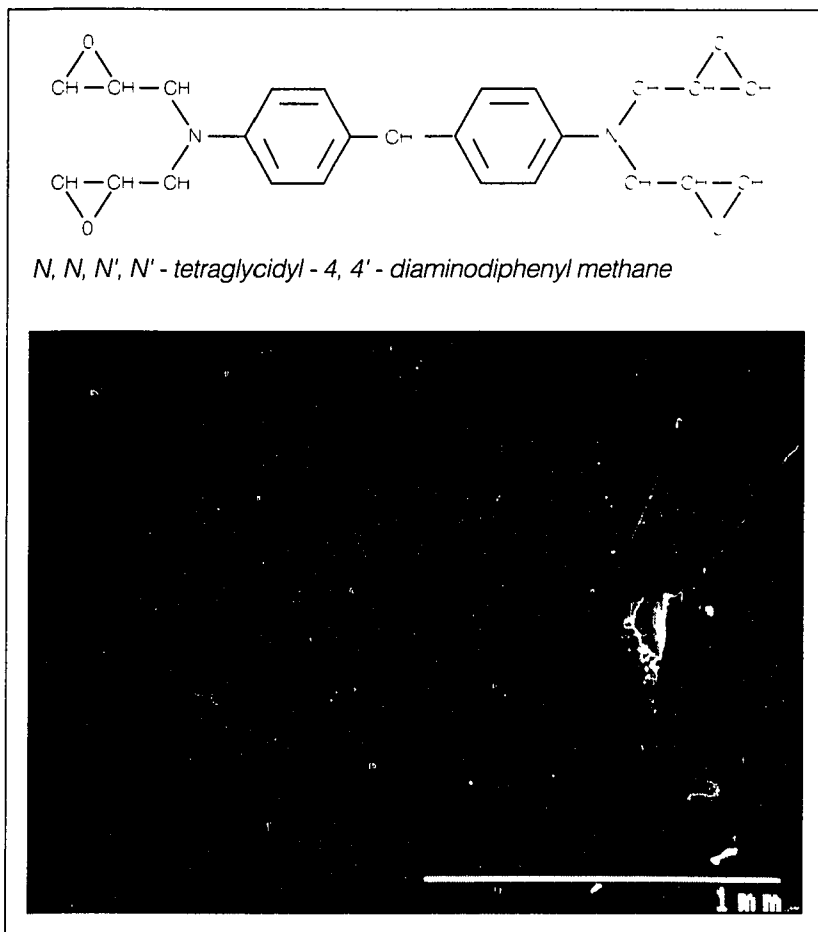
TGMDA

Figure 6.42

(a)

(b)

7% w/w 10% offset Olig-2/TGMDA

Figure 6.43

(a)

0009 15K   1 mm

(b)

.11 15K   100um
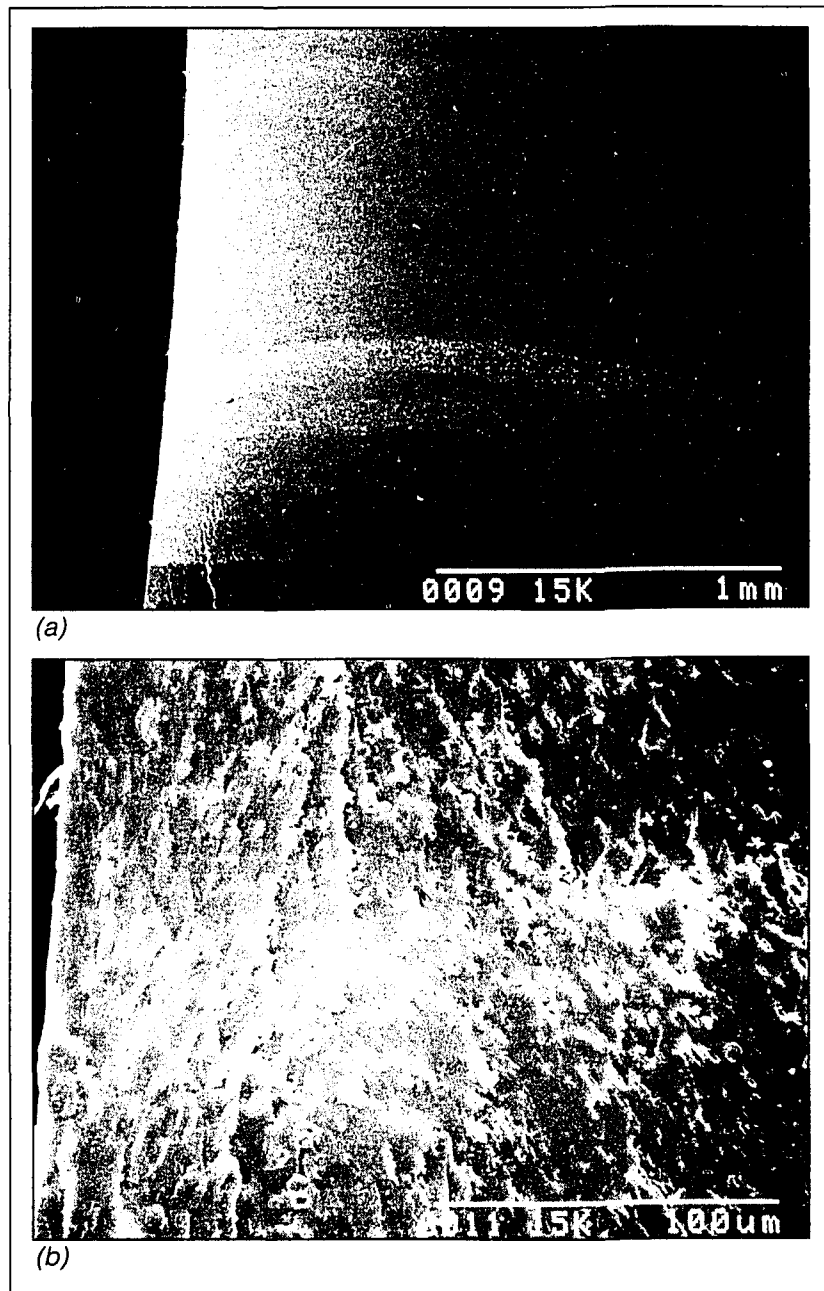
7% w/w 10% offset Olig-1/TGMDA   Figure 6.44
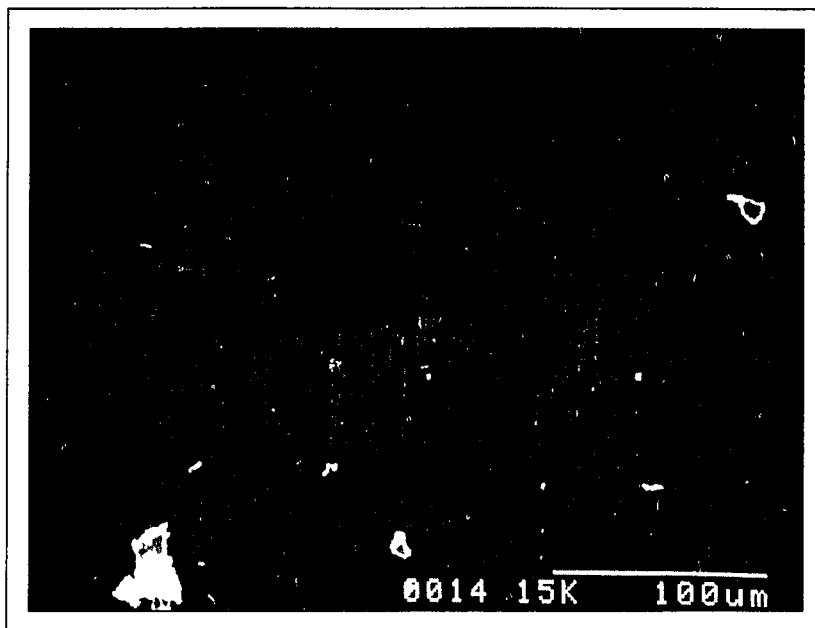
7% w/w PAE-co-I-5/TGMDA   *Figure 6 45*
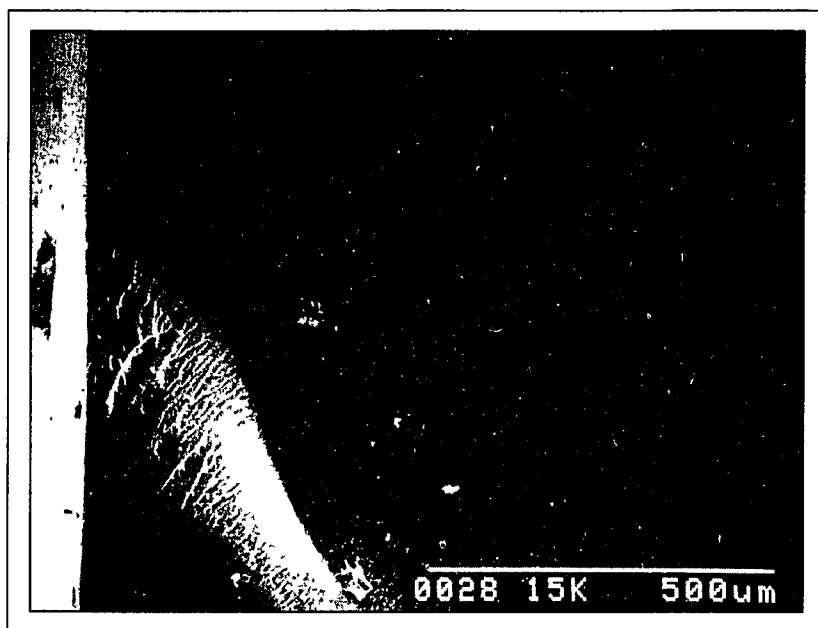
7% w/w 10% offset Co-Olig-2/TGMDA   *Figure 6.46*
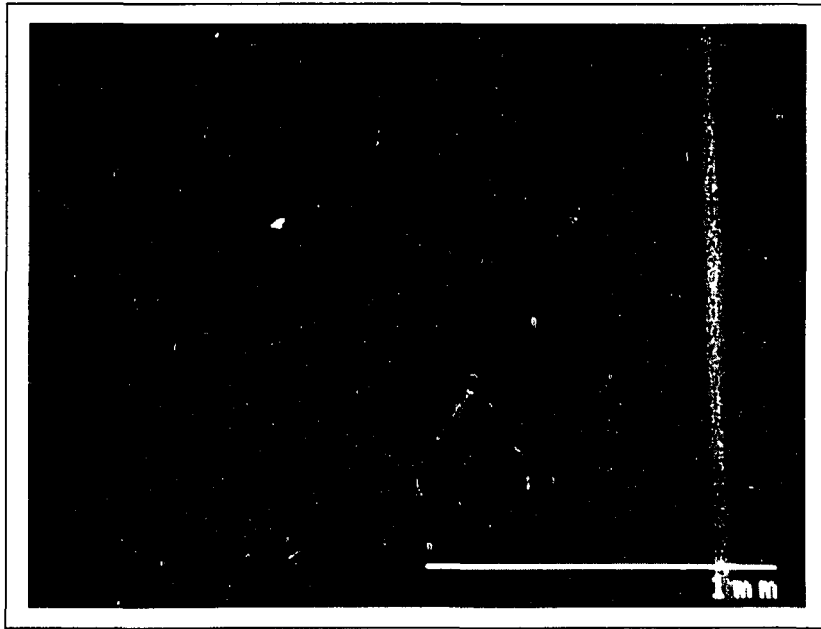
10% w/w 10% offset Co-Olig-2/TGMDA   *Figure 6.47*
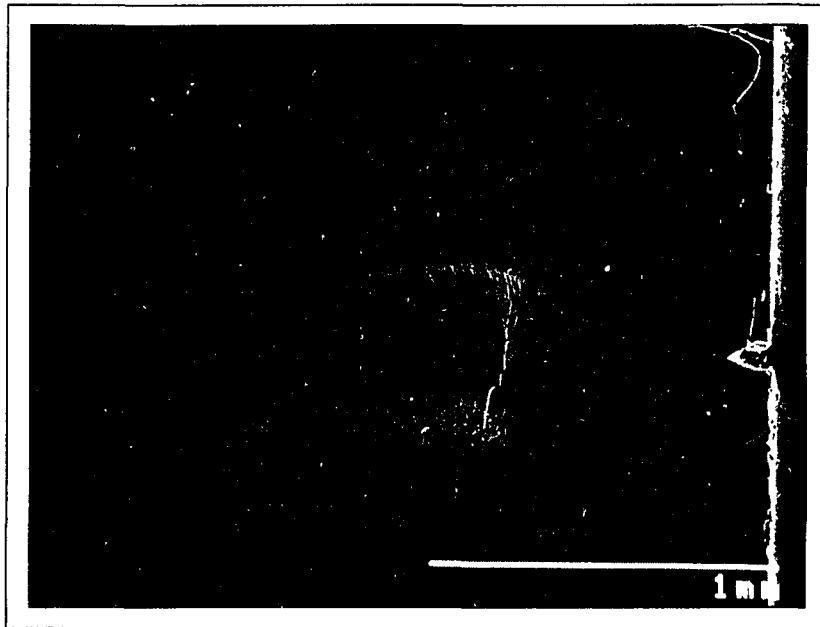
15% w/w 10% offset Co-Olig-2/TGMDA   *Figure 6.48*

(a)

(b)
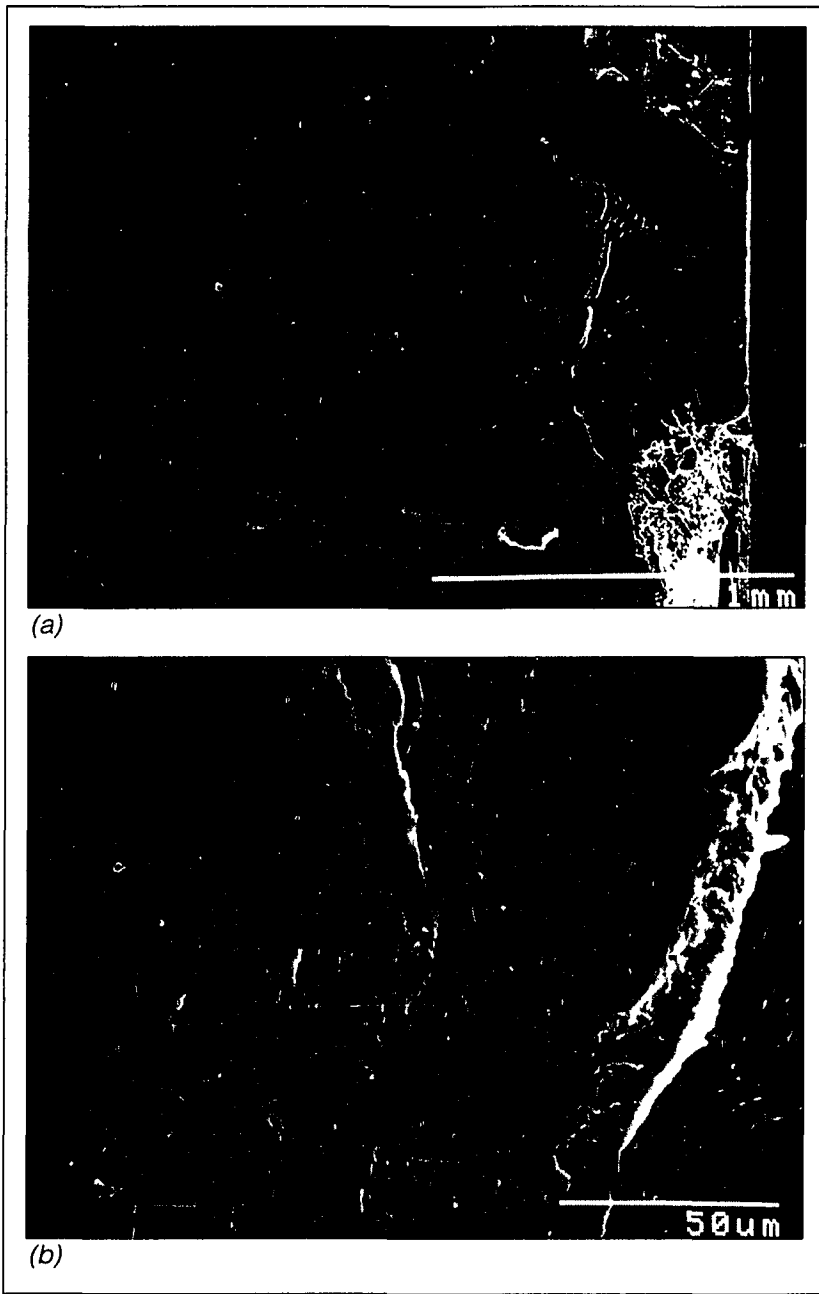
20% w/w 10% offset Co-Olig-2/TGMDA   Figure 6.49

6.9 References

1. Connell, J. W., Hergenrother, P. M., *SAMPE, 35*, 432, **1990**.

2. Katzenberger, A. T., Chemistry Honors Thesis, College of William and Mary **1994**.

3. Harrington, K., Senior Research, College of William and Mary, **1993**.

4. Yee, A. F., Pearson, R. A., NASA Contractor Report 3718 **1983**.

Chapter 7: Summary

A series of poly(arylene ether)s (PAE)s, poly(arylene ether imidazole)s (PAEI)s and novel poly(arylene ether-co-imidazole)s (PAE-co-I)s were prepared via aromatic nucleophilic displacement using 2-phenyl-4,5-bis(4-hydroxyphenyl) imidazole, various aromatic bisphenols and activated aromatic difluorides. The polymers were prepared using both exact and offset stoichiometric ratios resulting in high molecular weight polymers and controlled molecular weight oligomers with either phenol or fluoro endgroups. The polymerizations were performed in N,N-dimethylacetamide using potassium carbonate at elevated temperatures under nitrogen. The high molecular weight materials formed creasable films and exhibited glass transition temperatures ranging from 150 to 250 °C.

The polymers/oligomers were subsequently tested for solubility in seven different commercially available high performance epoxy resins. In addition, the effect of the polymer/oligomer on processability (i.e. melt flow characteristics) of the modified epoxy was assessed. The PAE-co-Is exhibited the highest degree of solubility in N,N,N',N'-tetraglycidyl-4,4'-diaminodiphenyl methane (TGMDA). In general, the PAE-co-Is also exhibited better solubility in the epoxies than either the PAEs or PAEIs. The high molecular weight polymers caused significant decrease in melt flow behavior of the modifed systems.

Modified systems were prepared using stoichiometric quantities of 4,4'-diaminodiphenyl sulphone and various amounts of polymer or oligomer. The mixtures were stirred at elevated temperature until they became homogeneous, degassed, poured into silicon-rubber molds, placed in a vacuum oven and thermally cured. The specimens were removed from the molds and subsequently tested for flexural and toughness properties.

One modified system with 10% w/w high molecular weight PAE-co-I exhibited improved fracture toughness (K_{Ic}) of 1.7 times that of the unmodified epoxy. Scanning electron photomicrographs of the fractured surface showed stress whitening and no clear phase separation. Oligomeric arylene ether-co-imidazoles resulted in only a 30% increase in fracture toughness at 20% w/w modifier concentrations and did not result in a phase separated morphology although an increase in stress-whitening was observed. Increasing the concentration of imidazole in the polymer backbone decreased the fracture toughness of the modified resin.

In general, molecular weight characterization of poly(arylene ether)s by gel permeation chromatography (GPC) compared well with characterization by multi-angle light scattering, except for the bisphenol terminated oligomers. Comparisons of characterization by GPC and multi-angle light scattering of the copolymers did not agree as well as the homopolymers.

Cured neat epoxies and systems modified with PAE-co-Is and PAEs were immersed in water at 90 °C and the moisture absorption was monitored over 170

hours. Arylene ether and arylene ether-co-imidazole oligomers terminated with hydroxyl groups exhibit higher moisture absorption than those terminated with fluoro groups. Modified system containing 7% w/w PAE-co-I exhibited weight gains comparable to that of the unmodified epoxy. Increasing the weight percent of poly(arylene ether-co-imidazole) modifier slightly increased the moisture absorption of the modifed resin.

Cured neat epoxies and systems modified with PAE-co-Is and PAEs were immersed in tetrahydrofuran (THF) at room temperature and the weight gain was monitored over 170 hours. Uncured epoxies and PAE-co-Is, PAEI, and PAEs are all soluble in THF. The unmodified TGMDA was highly sensitive to tetrahydrofuran exposure and resulted in greater than 20% solvent absorption after 7 hours. High molecular weight PAEs and oligomers terminated with hydroxy or fluoro groups were extracted from the modified resin with THF. The difluoro terminated oligomers were the most readily extracted. THF immersions of systems modified with PAE-co-Is exhibited substantially less solvent absorption than the unmodified resin. PAE-co-Is were not extractable from the modified matrix, further substantiating that they were chemically bound. Increasing the modifier content to 20% w/w increased the percent of solvent absorption to approximately 14%.

Bibliography

Aharoni, S. M., *Macromolecules, 18*, 2624 **1985**.

Allcock, H. R.; Lampe, F. W., Contemporary Polymer Chemistry, 2nd ed., Prentice Hall, Englewood Cliffs, New Jersey, **1990**.

Allinger, N. L., Cava, M. P., DeJongh, D. C., Johnson, C. R., Lebel, N. A., Stevens, C. L., Organic Chemistry, 2nd ed., Worth Publishers, Inc., New York, **1976**.

Andrews, R. D., Kazama, Y., *J. Appl. Phys., 38*, 4118 **1967**

Aziz, A. W., Ab-el-Nour, K. N., *J. Appl. Polym. Sci., 31*, 2267 **1986**.

Bascom, W. D., Ting, R. Y., Moulton, R. J., Riwe, C. K., Siebert, A. R., *J. Mater. Sci., 16*, 2657, **1981**.

Bascom, W. D., Cottington, R. L., *J. Adhesion, 7*, 333 **1976**.

Bascom, W. D., Cotting, R. L., Jones, R. L., Peyser, P., *J. Appl. Polym. Sci., 19*, 2545 **1975**.

Bauer, R. S.; Stenzenberger, H. D.; Romer, W., *SAMPE*, April 2-5, 395-407, **1990**.

Bitner, J. R., Rushford, J. L., Rose, W. S., Hunston, D. L., Riew, C. K., *J. Adhesion, 13*, 3 **1982**.

Bonner, W. H., U.S. Patent 3,065,205 **1962** (to Dupont).

Bryant, G. M. *Text. Res. J., 31*, 399 **1961**.

Bucknall, C. B., Toughened Plastics, Wiley, New York **1977**
Berry, B. W., Fracture Toughness, The Iron and Steel Inst., **1968**.

Bucknall, C. B., Clayton, D., Keast, W. E., *J. Mater. Sci., 7*, 1443, **1972**.

Bucknall, C. B., *Adv. Polym. Sci., 27*, 121 **1978**.

Bucknall, C. B., Yoshii, T., *Brit. Polym. J., 10*, 53 **1978**.

Busso, N., Technical Report No. AFML-TR-68-286, Part I, Sept. **1968**, AFML-TR-69-238, Part II, Jan **1970**.

Byrne, C. A.; Hagnauer, G. L.; Schneider, N. S.; Lenz, R. W., *Polym. Composites*, *1*(2), 71-76, **1980.**

Colquhoun, H. W. and Lewis, D. F., British Patent 2,116,990 **1983.**

Connell, J. W.; Hergenrother, P. M., *J. Polym. Sci. Part A: Polymer Chem.*, *29*, **1990.**

Connell, J. W.; Hergenrother, P. M., *SAMPE Series*, *35*, 432, **1990.**

Connell, J. W.; Hergenrother, P. M., *High Performance Polymers*, *2*(4), **1991.**

Connell, J. W.; Hergenrother, P. M., *Polym. Mat. Sci. and Eng. Proceedings*, *60*, 527-531, **1989.**

Crist, B., Ratner, M. A., Brower, A. L., Savin, J. R., *J. Appl. Phys.*, *50*, 6047, **1979.**

Dahl, K. J., U.S. Patent 3,956,240 **1976.**

Diamont, J.; Moulton, R. J., *SAMPE Quarterly*, *16*(1), 13-21, **1984.**

Donald, A. M., Kramer, E. J., *J. Mater. Sci.*, *17*, 1765, **1982.**

Effenberger F. and Epple, G. *Angew. Chem. Int. Ed.*, *11*, 299, **1972**

Farkas, A.; Strohm, P., *J. App. Polym. Sci.*, *12*, 159-168, **1968.**

Gerd, B. Claus, C., German Patent 2,749,645 **1978.**

Goodman, I, McIntyre, J. E. and Russell, W., British Patent 971,227 **1964**

Haaf, F., Breuer, H, Stabenow, J., *J. Macromol. Sci. Phys.*, *B14*, 387 **1977.**

Haward, R. N., Bucknall, C. B., *Pure and Appl. Chem.*, *46*, 227 **1976.**

Haward, R. N., The Physics of Glassy Polymers, John Wiley and Sons, New York **1973.**

Hergenrother, P. M., Havens, S. J., Jensen, B. J., *Intl. SAMPE Tech. Conf. Series*, *18*, 454, **1986.**

Hunston, D. L., Bitner, J. L., Rushford, J. L., Oroshnik, J., Rose, W. S., *Elast. Plast.*, *12*, 133 **1980.**

Jansons, V., Gors, H. C., *WO*, 84 03, 892 **1984.**

Jensen, B. J., Hergenrother, P. M., Havens, S. J., *Polym. Prepr.*, *26*(2), 174, **1985**.

Johnson, R. N., Farnham, A. G., U.S. Patent 4,108,837 **1978**.

Johnson, R. N., Farnham, A. G., British Patent 1,078,234 **1967**.

Johnson, R. N., Farnham, A. G., Clendinning, R. A., Hale, W. F., Merriam, C. N., *J. Polym. Sci. Part A-1*, *5*, 2375 **1967**.

Kambour, R. P., *J. Polym. Sci.:Macromol. Rev.*, *7*, 1 **1973**.

Kinloch, A. J., Young, R. J., Fracture Behavior of Polymers, Applied Science, New York **1983**.

Kinloch, A. J., Shwa, S. J., Tod, D. A., Hunston, D. L., *Polymer, 24*, 1341 **1983**; *24*, 1355 **1983**.

Korshak, V. V., *J. Macromol. Sci. Rev. Macromol. Chem, C11*(1), 45-142, **1974**.

Kramer, E. J., Berger, L. L., in Crazing in Polymers. Vol. 2, Adv. Polym. Sci. 91/92, Springer-Verlag, New York, pp. 1-68, **1990**.

Kreuchmas, A., U.S. Patent 2,2822,351 **1958**.

Kubel Jr., E. J.; *Adv. Materials & Processes, 136*(2) **1989**.

Kunz, S., Beaumont, P. W. R., *J. Mater. Sci., 16*, 3141, **1981**.

Kunz-Douglas, S., Beaumont, P. W. R., Ashby, M. F., *J. Mater. Sci., 15*, 1109 **1980**.

Lee, H.; Neville, K.; in, Ency. of Polym. Sci. and Tech., *6*, 209-271, **1967**.

Manzione, J. K., Gillham, J. K., McPherson, C. A., *J. Appl. Polym. Sci., 26*, 889 1981; *26*, 907 **1981**.

Marks, B. M., U.S. Patent 3,441,538 **1969**.

May, C. A. and Tanaka, G. Y., Eds. Epoxy Resin Chemistry and Technology, Marcel Dekker, New York, **1973**.

McGarry, F. J.; Willner, A. M., *Research Report, School of Engineering*, R68-8, MIT, Cambridge, MA, **1968**.

McGarry, F. J.; Willner, A. M., *Research Report, School of Engineering*, MIT, Cambridge, MA, **1966**.

Mohanty, D. K., Sachdeva, Y., Hedrick, J. L., Wolfe, J. F., McGrath, J. E., *Polym. Prepr.*, *25*(2), 19, **1984**.

Passaglia, E., *J. Phys. Chem. Solids*, *48*(11), 1075 **1987**.

Potter, W. G., Epoxide Resins, Springer-Verlag, New York, **1970**.

Riew, C. K., Rowe, E. H., Siebert, A. R., in Toughness and Brittleness of Plastics, Eds. R. D. Deanin and A. M. Crugnola, Adv. Chem. Ser. 154, American Chemical Society, Washington D. C., pp. 326-343, **1976**

Rose, J. B., *Chem. Ind. (London)*, 461, **1968**.

Shell Chemical Co., Tech. Bulletin, March **1990**

Sultan, J. N., McGarry, F. J., *Polym. Eng. Sci.*, *13*, 29, **1973**.

Taylor, I. C., German Patent 2,635,101 **1977**.

Ting, R. Y., Cottington, R. L., *J. Appl. Polym. Sci.*, *25*, 1815 **1980**

Treloar, L. R. G., The physics of rubber elasticity, Clarendon Press, Oxford **1958**.

Verchére, D., Sautereau, H., Pascault, J. P., Moschiar, S. M., Riccardi, C. C., Williams, R. J. J., *Polymer*, *30*(1), 107 **1989**.

Viswanathan, R., Johnson, B. C., McGrath, J. E., *Polymer*, *25*, 1827, **1984**.

Wang, H. T.; Chaudhari, M. A.; Cobuzzi, C., *SAMPE*, 484-493, **1988**.

Williams, R. J. J., Borrajo, J., Adabbo, H. E., Rojas, A. J., in Rubber Modified Thermoset Resins, C. K. Riew and J. K. Gillham, Eds., Adv. Chem. Ser. 208, American Chemical Society, Washington D.C., pp. 195-213, **1984**.

Yamanaka, K., Takagi, Y., Inoue, T., *Polymer*, *30*, 662 **1989**; *30*, 1839 **1989**.

Yamanaka, K., Inoue, T., *J. Mat. Sci.*, *25*, 241 **1990**.

Yee, A. F., Pearson, R. A., *J Mater. Sci.*, *21*, 2462 **1986**; *21*, 2475 **1986**

Young, R. J., Beaumont, P. W. R., *Polymer*, *17*, 717 **1976**.

Vita

Patricia D. Roberts-McDaniel

Born in Tokyo, Japan, July 1, 1959. Graduated from East High School in Akron, Ohio, June 1977. B.A. Chemistry 1981, Kent State University, Kent, Ohio. M.S. Chemistry 1988, Old Dominion University, Norfolk, Virginia. Entered the College of William and Mary in 1990, in the Applied Science Program.

Currently resides in Yorktown, Virginia with her husband, John and daughter, Alanna.